ORNL
MASTER COPY

[redacted]

OAK RIDGE NATIONAL LABORATORY

operated by

UNION CARBIDE CORPORATION

for the

U. S. ATOMIC ENERGY COMMISSION

ORNL - TM - 2877

14

APR 6 1970

[redacted]

DRAFT

TECHNICAL PROGRESS REVIEW

ISOTOPES AND RADIATION TECHNOLOGY

VOLUME 8, NO. 1

NOTICE This document contains information of a preliminary nature and was prepared primarily for internal use at the Oak Ridge National Laboratory. It is subject to revision or correction and therefore does not represent a final report.

[redacted]

LEGAL NOTICE

This report was prepared as an account of Government sponsored work. Neither the United States, nor the Commission, nor any person acting on behalf of the Commission:

A. Makes any warranty or representation, expressed or implied, with respect to the accuracy, completeness, or usefulness of the information contained in this report, or that the use of any information, apparatus, method, or process disclosed in this report may not infringe privately owned rights; or

B. Assumes any liabilities with respect to the use of, or for damages resulting from the use of any information, apparatus, method, or process disclosed in this report.

As used in the above, "person acting on behalf of the Commission" includes any employee or contractor of the Commission, or employee of such contractor, to the extent that such employee or contractor of the Commission, or employee of such contractor prepares, disseminates, or provides access to, any information pursuant to his employment or contract with the Commission, or his employment with such contractor.

OAK RIDGE NATIONAL LABORATORY
OPERATED BY
UNION CARBIDE CORPORATION
NUCLEAR DIVISION

POST OFFICE BOX X
OAK RIDGE, TENNESSEE 37830

ISOTOPES INFORMATION CENTER
AREA CODE 615 483-8611 EXT. 3-1742

April 6, 1970

To: Distribution Listed in ORNL-TM-2877

A draft copy of Isotopes and Radiation Technology, Vol. 8, No. 1, is being transmitted to DTI and DID, as well as to others concerned with the review for patent, classification, and administrative matters. If you have comments, criticisms, or suggestions concerning the contents of this issue, please send them immediately to Mr. Harold B. Atkinson of DTI, to Dr. Jack H. Kahn of Declassification, and to me. Mr. Atkinson's and Dr. Kahn's addresses are as follows:

Mr. Harold B. Atkinson
Scientific Publications Branch
Division of Technical Information
U. S. Atomic Energy Commission
Washington, D. C. 20545

Dr. Jack H. Kahn
Declassification Branch
Division of Classification
U. S. Atomic Energy Commission
Washington, D. C. 20545

Sincerely yours,

P. S. Baker

P. S. Baker, Editor
Isotopes and Radiation Technology

[redacted]

ORNL-TM- 2877

Contract No. W-7405-eng-26

DRAFT
TECHNICAL PROGRESS REVIEW
ISOTOPES AND RADIATION TECHNOLOGY
VOLUME 8, NO. 1

EDITORS:

P. S. Baker, Robert H. Lafferty, Jr., Martha Gerrard,

R. E. Greene, F. E. McKinney, F. J. Miller, Helen Raaen

ADVISER:

A. F. Rupp

APRIL 1970

Prepared for U.S. Atomic Energy Commission
by
Isotopes Information Center
OAK RIDGE NATIONAL LABORATORY
Oak Ridge, Tennessee
operated by
UNION CARBIDE CORPORATION
for the
U.S. ATOMIC ENERGY COMMISSION

[redacted]

[redacted]

Page

I. ISOTOPE PRODUCTION AND DEVELOPMENT..... 1

THE PRODUCTION OF RADIOISOTOPES BY SPALLATION (L. G. Stang, M. Hellman, E. Lebowitz)..... 1

Introduction..... 2

Advantages of the Spallation Process..... 2

Cross Sections of Spallation Reactions..... 2

Calculation of Product Activity..... 3

Some Additional Practical Considerations..... 4

Computer Calculation of Activities..... 5

References..... 6

II. ISOTOPE TECHNOLOGY DEVELOPMENT..... 9

RADIOISOTOPE METHODS OF ANALYSIS AND CHARACTERIZATION OF EL ELASTOMERS (D. R. Campbell and W. C. Warner)..... 9

Introduction..... 9

Diffusion and Dispersion..... 17

Adsorption and Coagulation..... 23

Radioreagent Methods..... 26

Applications of Special Radioisotope Techniques..... 28

References..... 33

FABRICATION OF SEMICONDUCTOR DEVICES AND SILICON MICROCIRCUITS BY NEUTRON-TRANSMUTATION DOPING (Summarized by Helen P. Raaen). 38

Introduction..... 38

Semiconductor Devices..... 39

Complex Microcircuits..... 58

Conclusions..... 89

References..... 91

DETECTION OF ART FORGERIES BY X-RAY-FLUORESCENCE SPECTROSCOPY.. (Richard Frankel) 92

Description of Instrument..... 92

Use in Detecting Art Forgeries..... 94

PORTABLE RADIOISOTOPE X-RAY ANALYZERS—TECHNIQUES AND APPLICATIONS (J. R. Rhodes)..... 99

Introduction..... 99

Description of the Instrument..... 100

Applications..... 101

References..... 101

A RADIOCHEMICAL STUDY OF THE DIFFUSION OF IONS THROUGH PROTECTIVE FILMS (A. L. Glass and Jack Smith)..... 108

Introduction..... 108

[redacted]

[redacted]

Page

Experimental Conditions..... 109
Results and Discussions..... 113
Conclusions..... 115
References..... 120
RADIOISOTOPIC GAGE FOR WIDTH CONTROL..... 122
PORTABLE NEUTRON RADIOGRAPHIC CAMERA USING ^{252}Cf
(C. B. Shaw and J. L. Cason)..... 123
Introduction..... 123
Analysis..... 125
Camera Design..... 129
Evaluation..... 131
References..... 135
III. FOOD IRRADIATION..... 136
THE TOUR OF THE PORTABLE CESIUM IRRADIATOR---PART II..... 136
Introduction..... 136
Results from 1967 Demonstrations..... 136
Demonstrations During January 2--March 23, 1968..... 138
Results of Demonstrations..... 139
Demonstrations During March 24--June 18, 1968..... 139
Results of Demonstrations..... 142
Demonstrations During June 18---August 10, 1968..... 144
Results of Demonstrations..... 145
Demonstrations During August 11---October 12, 1968..... 146
Results of Demonstrations..... 146
Demonstrations During October 13---December 19, 1968..... 147
Results of Demonstrations..... 148
Operations in 1969..... 148
References..... 149
IV. PROCESS RADIATION DEVELOPMENT..... 150
RADIATION GRAFTING ON COTTON TEXTILES AND FIBERS
(Allan S. Hoffman)..... 150
Introduction..... 150
Radiation Sources..... 150
Kinetic Considerations..... 151
Textile Modification with Radiation..... 156
Principles of Textile Finishing..... 165
Glossary..... 173
References..... 175

[redacted]

		Page
V.	ISOTOPIC HEAT AND POWER DEVELOPMENT	179
	FRENCH ISOTOPIC POWER GENERATOR "MARGUERITE 20"	179
VI.	APPLICATIONS IN LIFE SCIENCES	181
	RADIATION AND THE GREEN REVOLUTION	181
	Introduction	181
	FRENCH CARDIAC PACEMAKER	192
	SOME USES OF ISOTOPES IN METABOLIC STUDIES WITH SOIL MICRO-ORGANISMS (P. E. Stanley and D. J. D. Nicholas)	193
	Inorganic Nitrogen Metabolism	193
	Inorganic Sulfur Metabolism	197
	Transition Metals	206
	References	208
VII.	ISOTOPES AROUND THE WORLD	210
	FRENCH FACILITY FOR FABRICATION OF SEALED RADIOISOTOPIC SOURCES	210
	FRENCH X-RAY FLUORESCENCE ANALYZER	213
	ISOTOPES IN AUSTRALIA, JULY 1, 1968--JUNE 30, 1969 (Summarized by Martha Gerrard)	214
	ACTIVATION ANALYSIS WITH CHARGED PARTICLES AND GAMMA PHOTONS	219
	References	224
VIII.	MISCELLANEOUS	226
	AVAILABILITY OF ISOTOPES AND SERVICES	226
	AEC ACTIVITIES	236
	GENERAL	242

THE PRODUCTION OF RADIOISOTOPES BY SPALLATION* (2)

By L. G. Stang, Jr., M. Hellman, and E. Lebowitz**

Supplementary Key Words: (PRODUCTION, RADIOISOTOPE / PRODUCTION, ACCELERATOR / ACTIVATION, NEUTRON / ACTIVATION, CHARGED PARTICLE / ACCELERATOR / THEORY, APPLIED / DATA COMPILATION / DATA HANDLING / CROSS SECTION AND YIELD / FISSION PRODUCT)

Abstract:

This report is intended to provide a practical basis for planning to produce radioisotopes by spallation. For this purpose, it includes extensive tabulations of calculated yields of products from virtually every possible target element bombarded by 200-MeV protons. In addition, the effects of bombarding energy and choice of target on product yield are examined. Several advantages of the spallation process relative to fission are enumerated.

The work reported uses the thin-target spallation cross-section formula that was derived empirically by Rudstam. Examination of this formula shows that, for a given nuclide $_ZL^A$ (where Z = atomic number and A = mass number) produced from a given target of mass A_t, the spallation cross section goes through a maximum when the bombarding particle energy, E, is around 100 MeV. However, when thick targets are considered and the accompanying attenuation of beam intensity is taken into account, an incident particle energy of 200 MeV is shown to be a good practical compromise between the unmanageably thick targets that would be required for efficient use of much higher energy particles and the decreased product activity that would be encountered at lower bombarding energies. In this connection, the axial distributions of a typical product activity along the beam path in a thick target are shown graphically for 800- and 200-MeV incident protons. In addition, the yields of unwanted by-products are shown to be many times as great at 800 MeV as at 200 MeV. For a given E, the yield of $_ZL^A$ increases as A_t approaches A.

The yield in millicuries of $_ZL^A$ from a thick target is described by an equation that contains a suitable correction for the variation of spallation cross section with (decreasing) energy as the bombarding particle traverses the thick target. The equation applies to bombardments by protons, neutrons, deuterons, or alpha particles, provided that the appropriate ranges of the respective particles are used. The accuracy of the results is commensurate with that of the Rudstam formulation (i. e., within a factor of three of experimentally determined values, where such a comparison could be made). This equation was programmed for computer solution, and tabulated results show the independent yields produced by a 200- μA beam of 200-MeV incident protons bombarding for 24 hr targets that ranged from lithium to uranium. One table arranges the data by product desired, the other by target used. The latter table gives the activities of the radioactive products (with half-lives greater than one minute) as well as the production cross sections of both radioactive and stable products.

*The complete report on this work is USAEC Report BNL-50195 (T-547), The Production of Radioisotopes by Spallation, Brookhaven National Laboratory, Associated Universities, Inc., August 1969. The entire context of that report, only slightly edited, is given here. The report includes three supplementary tables: an auxiliary table (Table IV) which lists Z numbers with names of corresponding elements and vice versa, and two tables of computer-derived spallation-product data, one arranged by product desired (Table V) and the other by target used (Table VI). From these tables, only the explanatory notes and first entries of Tables V and VI are given here. They will show to the reader the comprehensive nature of the data given in the complete report—some 160 pages of data on elements from Z = 3 to Z = 92.

**Brookhaven National Laboratory, Upton, N. Y. 11973.

(Introduction)

The term spallation, meaning a process involving chipping something away, refers to a nuclear reaction in which the bombarding projectile has sufficient energy to cause the struck nucleus to eject several nucleons. Such reactions make a wide variety of products, many of which can be made in no other way, but until recently this type of reaction was not a source of significant quantities of radioactive material. However, the increasing availability of accelerators that produce high-current beams of high-energy particles is making spallation a practical route to useful quantities of otherwise unavailable nuclides. The purpose of this report is to provide a practical basis for future planning in the use of spallation to produce radioisotopes.

Advantages of the Spallation Process (3)

The spallation reaction resembles the fission process in that a given target isotope produces many nuclides of various masses and atomic numbers in yields that are a smooth function of the mass number. Therefore, the separation of one spallation product from another or from the target material is understandably similar to the separation of one fission product from another or from the fissile material, and the same technology and even the same equipment can be used for both kinds of work. Both fission and spallation provide products of very high specific activity.

However, there are important differences that, in some respects, make the spallation reaction even more attractive than the fission process, which has already been proven highly useful for producing copious quantities of radioactive products.

1. Fission products are limited to the region between mass 72 and mass 161, and nuclides producible in good yields are confined to the mass regions 81-108 and 126-154. (The use of plutonium, rather than uranium, as the fissile material and/or of fast, rather than thermal, neutrons to cause fission can increase the yields outside these limits, but practical considerations have prevented these measures from being used by isotope producers.) On the other hand, spallation can produce almost any nuclide of mass number lower than the mass number of the target nuclide.

2. Fission products are not only confined to the above mass regions, but they are also further limited to neutron-rich nuclides. However, spallation can produce both neutron-deficient and neutron-rich nuclides. For example, an antimony target would easily produce nuclides such as $In^{116-121}$, which can be produced in fission, in addition to nuclides such as $In^{<115}$, which can not be produced in fission.

3. The yield of any given fission product, as noted above, is determined by the mass number of the fission product, the nature of the fissile nuclide that produced it, and the neutron energy involved, and hence for practical purposes virtually nothing can be done to change the values. With spallation, the yield of a particular nuclide of interest can be maximized by proper choice of the target nuclide and of the energy used. These effects are discussed in detail below.

4. Spallation is induced by >50-MeV particles. Machine acceleration of such particles requires that they be charged. This charge allows beams of the particles to be steered, focused, and switched from one target to another appropriate electromagnets. This kind of flexibility is not found in reactor neutron irradiations and implies that selected areas of specially shaped targets can be irradiated. This could be of importance in maximizing the heat dissipation from the target without part of the beam; (i.e., one could irradiate a long flat target placed edgewise to a beam that has a long narrow transverse shape and use the high surface-to-volume ratio of the target to help dissipate the heat without wasting any of the beam by allowing it to miss the target).

5. By choosing the proper energy for the bombarding particle in the spallation process, one can not only maximize the yield of a particular nuclide from a given target but one can also minimize the relative amounts of by-products that are formed. Therefore, the separation process can be simplified, at least in principle. For example, data from Fig. 10-8 of Ref. (1) indicate that in the spallation yield-vs.-mass-number curve when Bi^{209} is used as a target the full-width-at-half-maximum (FWHM) is as shown in Table I.

Table I

Characteristics of Dependence of Production Cross Section on Product Mass for a Bismuth-209 Target

Proton Energy (MeV)	40	400	4000
Maximum Cross Section ($\sigma_{max.}$, mb)	950	108	18
Location of $\sigma_{max.}$ (mass number)	206	196	~180
FWHM (mass numbers)	3	11	68

It is interesting to contrast this dependence on energy with the invariable situation that obtains in the thermal neutron fission of U^{235}, in which the maximum yields occur at fixed masses and the FWHM is approximately 17 mass numbers for each of the two peaks in the fission yield curve. It must be acknowledged that this apparent advantage of spallation over fission is not as great as it might seem at first, for two reasons: (1) As long as any by-products at all are produced, which is the case in both processes, some separation scheme is necessary, and often the important consideration is not the number of impurities present but rather whether there are impurities present with chemical properties similar to those of the product. (2) If one has available an existing accelerator, the particle energy may not be variable, and if the energy is so high as to give an objectionably flat yield-vs.-mass curve, there may be little that one can do about it except to try to degrade the energy with absorbers placed ahead of the target -- a procedure that has the two-fold disadvantage of reducing the total intensity of the beam and of spreading it out over a larger area.

Cross Sections of Spallation Reactions (3)

The systematics of spallation have been well worked out by Rudstam[2]. Although Rudstam's original paper should be consulted for the derivation of his cross-section formulation and his discussion of the fit of the data, it will be useful at this point to examine his formulation in order to note the effect of certain variables on the cross section and to obtain a clearer picture regarding what can and can not be done to change product yields.

Rudstam gives the following expression for the cross section (in millibarns) for the production of a nuclide with atomic number Z and mass number A from a target of mass number A_t either protons or neutrons of energy E (MeV):

$$\sigma(Z,A) \approx [F(A_t)][f_2(E)][P]\{1 - [0.3/(P\,A_t)]\}^{-1} \exp\{-P(A_t - A) - 11.8\,A^{-0.45}\,|Z - 0.486\,A + 0.00038\,A^2|^{3/2}\} \quad . . . (1)$$

for $(P\,A_t) \geq 1$,

where $P = 20\,E^{-0.77}$ for E<2100 MeV, ... (2)

and $F(A_t)$ and $f_2(E)$ are given by graphs from which the following values were read:

A_t	0	40	80	120	160	200
$F(A_t)$, millibarns	200	600	1050	1650	2350	3200

(For interpolation, we assume a strictly linear relationship between pairs of values of $F(A_t)$; from the nearly linear relationship of the entire set of values, it can be seen that this assumption introduces no significant error.)

E MeV	$f_2(E)$	E MeV	$f_2(E)$	E MeV	$f_2(E)$	E MeV	$f_2(E)$
50	4.1	90	3.0	130	2.3	170	1.7
60	3.8	100	2.8	140	2.1	180	1.6
70	3.3	110	2.6	150	2.0	190	1.5
80	3.1	120	2.4	160	1.9	200	1.4

For E≥240 MeV, $f_2(E) = 1$.

(4)

Effect of Varying Energy. Rudstam[2] states that an inspection of the cross-section formula indicates that for a given combination of target and spallation product, the maximum yield is obtained for

$$P \approx 1/(A_t - A) \quad \ldots\ldots\ldots\ldots\ldots\ldots (3)$$

He also notes that the corresponding irradiation energy is obtained from Equation (2) above and that substituting these values in Equation (1) above gives the maximum independent yield of the nuclide with atomic and mass numbers Z and A. For example, if A_t and A are kept constant (e.g., at 100 and 97, respectively) and E is varied (e.g., from 298 to 235 to 121 MeV), the cross section indeed goes through a maximum -- in this case the relative values being 0.119, 0.124, and 0.112, respectively. Thus, if one considers only one particular target for producing a given product, there is an optimum energy given by the relationship

$$1/(A_t - A) \approx 20\ E^{-0.77} \quad \ldots\ldots\ldots\ldots\ldots (4)$$

for E<2100 MeV.

However, in practice, before an irradiation energy, three factors in addition to this apparent optimum energy must be considered:

1. Unless a variable-energy machine is available, reduction of beam energy requires the use of absorbers, which also results in attenuation of the beam intensity, in beam spreading, and in the production of secondary bombarding particles produce contamination in the target. This effect becomes more pronounced as initial beam energy increases.

2. Use of a higher energy of the bombarding particle requires a correspondingly thicker target to stop the entire beam or to slow the bombarding particles down to a particular energy. The effect of beam energy on target thickness and the effect of target thickness on beam attenuation via nuclear interaction are discussed more fully below. At this point it is sufficient to note that excessively high energies require awkwardly thick targets if the beam is not to be wasted and the process allowed to become inefficient.

3. One should also not overlook the fact, brought out in Table I above, that, as the bombarding energy goes up, the selectivity of product goes down and one produces considerably more contaminating by-products that have to be removed.

(4)

Effect of Varying Target. Inasmuch as it may be either impossible or undesirable to vary the bombarding energy and since the spallation process is not restricted to a particular target, a more practical question may be: "In general, what is the best target to use to produce a given nuclide with a fixed bombarding energy?" If Z, A, and E are kept constant and A_t is varied, one sees that the maximum yield of $(Z,A)_E$ is obtained when A_t is close to A. For example, if E is 800 MeV (corresponding to P = 0.116) and A_t is taken successively as 105, 107, 109, and 111, the relative cross sections of (Z,A) are 92.8, 75.1, 60.8, and 49.2.

[Note that there is no discrepancy between this statement and Equation (3), which predicts a maximum yield, since in Equation (3) P, rather than A_t, is being varied].

Calculation of Product Activity (3)

Before deriving an equation by which the spallation product activity can be calculated, it should be noted that the Rudstam formula is for a "thin" target, i.e., one in which the beam intensity and the particle energy are not significantly reduced as the beam traverses the target. The attenuation in beam intensity can be taken into account in a straightforward manner by multiplying the initial intensity, I_o, by $\exp(-n\sigma_s x)$, where n is the number of atoms per cubic centimeter of target, σ_s is the total nuclear cross section of the target (in square centimeters per atom), and x is the target thickness (in centimeters).

However, if the target is thick enough to degrade the energy of the unattenuated part of the beam, one has to be concerned about the effect of energy on the cross section. The targets of interest to the isotope producer are those that are thick enough to stop all or a large fraction of the beam. For example, the tabulations that comprise the bulk of this report are based on initial proton energies of 200 MeV, and the target thicknesses are taken to be whatever is necessary to slow the protons to 50 MeV. Clearly in this case the effect of the changing energy during traversal of the target must be considered. It turns out that in the region of $A_t - A = 3$, which, according to the discussion in the preceding section, is the region of high yield (for a given A) and hence the region of greatest practical importance and interest, the cross section for the production of a particular product from a given target is the same for a 200-MeV particle as for one of 50 MeV (the approximate energy below which reactions other than spallation predominate), and the corresponding yield from a 100-MeV particle is only 43% higher than these values. Thus, for values of A close to A_t the cross section is sufficiently constant as not to require a correction for variation with energy as the projectile is slowed down while traversing the target.

Unfortunately, as A moves away from A_t this is no longer true, and the decrease in cross section with decreasing energy during target traversal can no longer be ignored. Application of a rigorously true factor to correct for the variation of cross section with energy would be very difficult and not worth the effort, particularly inasmuch as Rudstam does not claim his formulation to be more exact than a factor of three anyway.

Therefore, we have compensated for the decrease in cross section during traversal in the following manner. We have calculated the energy, E_f, at which the cross section for producing each nuclide drops to less than one-third of the production cross section at 200 MeV. Then we calculate the distance traversed by the particle in going from 200 MeV down to E_f, and we use this distance as the effective target thickness, ignoring the remainder of the distance required to reduce the energy to 50 MeV. (By ignoring this region, we fail to take into account some activity produced in the region where the cross section is less than one-third of that at 200 MeV; on the other hand, this tends to compensate for the fact that in the region in which the cross section is still greater than one-third of that at 200 MeV, we use the 200-MeV cross section rather than an average cross section. In any case, it must be emphasized, the error thus introduced becomes greater, the farther we move away from A_t, but the farther we move from A_t, the less important and less interesting is the case for isotope production.)

On this basis, we derive the following expression for $Y_{Z,A}$, the activity (in millicuries) of ${}_ZL^A$ at the end of a bombardment with particles whose incident energy is 200 MeV:

$$Y_{Z,A} = K\ I\ (1 - e^{-\lambda T})(N_t/\text{at.wt.})(\Delta R)\Big\{0.473\ A_t\ F(A_t)\ (A_t - 0.0887)^{-1} \exp\Big[-0.338(A_t - A) - 11.8\ A^{-0.45}\ |Z - 0.486\ A + 0.00038\ A^2|^{3/2}\Big]\Big\} \quad \ldots\ldots\ldots\ldots (5)$$

where K = 102.5,
I = beam current (in microamperes),
λ = decay constant of ${}_ZL^A$ (in reciprocal units of T),
T = length of bombardment (in reciprocal units of λ),
N_t = fractional abundance of target isotope (or 1.0 for the natural element),
at.wt. = atomic weight of target element,
ΔR = target thickness (in grams/cm²), and
A_t = mass number of target isotope.

It is worth noting that Equation (5) is independent of type of bombarding particle and applies to protons, neutrons, deuterons, or alpha particles (although an insufficiency of data prevented Rudstam from verifying his formulation for heavy ions). However, in applying this equation, one must not overlook the fact that different particles of the same energy have different ranges in a given target, and, as noted below, care must be taken not to apply the equation to a target of thickness greater than that which will slow the particle down to 50 MeV or to E_f (see above), the thinner of the two targets where there is a choice. If thicker targets are actually used in practice, Equation (5) applies only to the region just described. Obviously, radioactivity will be produced beyond this region, but at energies lower than 50 MeV nuclear reactions other than spallation will predominate, and Equation (5) can not be expected to give either the correct distribution of products or the proper value of the quantity of a given product in these near-end regions.

The specific formulations for ΔR were derived from Ref.

(1) and are as follows:

For $Z_t > 10$:

$$\Delta R = 30.332 + 0.225\, Z_t - \left\{ (R_{air})_{E_f} \left[0.90 + 0.0275\, Z_t + (0.06 - 0.0086\, Z_t)(\log E_f) \right] \right\} \quad (6)$$

For $2 < Z_t < 11$:

$$\Delta R = 33.254 - 0.578\, Z_t - \left\{ (R_{air})_{E_f} \left[1.00 + (0.06 - 0.0086\, Z_t)(\log E_f) \right] \right\} \quad (7)$$

Z_t is the atomic number of the target. The units of ΔR are grams/cm^2, and the logarithm is to the base 10. Table II will facilitate the use of Equations (6) and (7) in calculating the proper target thickness to use. E_f was obtained by the following procedure: An energy, E, was picked, and the ratio σ_E/σ_{200} was calculated as a function of $(A_t - A)$, where σ_{200} is the cross section for production of mass A by a 200-MeV particle; by trial and error, pairs of values of $(A_t - A)$ were found such that the ratio σ_E/σ_{200} just bracketed the value 1/3; then graphical interpolation was used to locate the value of E_f that would make σ_E/σ_{200} exactly 1/3 at given values of $(A_t - A)$. Values of $(R_{air})_{E_f}$, the proton range in air at the energy E_f, were read from graphs in Ref. (3).

Table II

Values of E_f and Corresponding Proton Ranges in Air as a Function of $(A_t - A)$

$A_t - A$	E_f	$(R_{air})_{E_f}$	$A_t - A$	E_f	$(R_{air})_{E_f}$
2	50	2.517	14	128	13.5
3	50	2.517	15	133	14.4
4	50	2.517	16	137	15.1
5	50	2.517	17	141	15.9
6	63	3.81	18	144	16.5
7	75	5.22	19	147	17.0
8	86	6.65	20	150	17.8
9	95	7.96	21	152	18.2
10	103	9.0	22	154	18.5
11	111	10.4	23	157	19.2
12	117	11.5	24	159	19.6
13	123	12.5	25	161	20.1

The values shown in Table II are for $A_t = 100$. They depend very slightly on A_t, the dependence being so small as not to be worth considering. Values beyond $(A_t - A) = 25$ are not shown, because such a region so far removed from the target mass is of no practical interest and because 200-MeV protons possess insufficient energy to evaporate more than about 25 nucleons anyway.

Equation (5) assumes explicitly that the target volume is 1 cm^3 of the target element in question. It also assumes implicitly that the entire charged-particle beam passes through this volume for a distance ΔR equal to the thickness of the target. This implies that the area of the target being considered is $(D/\Delta R)$ cm^2, where D is the density of the element in grams/cm^3. Substitution of typical real values into this expression will show at once that such a target is too long and narrow to be practical. For example, in the case of an aluminum target, D would be 2.7 g/cm^3 and ΔR would be 30.3 g/cm^2 (= 11.2 cm), giving an area of 0.089 cm^2, which corresponds to a diameter of 3.4 mm. Even if a beam of high-energy charged particles could be focused or collimated down to a diameter of 3.4 mm, the problem of lining up so long and narrow a target with the beam and, worse yet, the problem of dissipating the heat generated in such a concentrated target would be formidable. On the other hand, production of the activity predicted by Equation (5) requires only that the thickness be ΔR and the area be at least as great as $D/\Delta R$ or greater. Increasing the area that the target presents to the beam will not increase the total amount of radioactivity producible inasmuch as the latter is determined by the beam current (for a given target, provided that the area is $\geq D/\Delta R$); what it will do is to diminish the activity producible per cubic centimeter.

It is probably worth mentioning that, although Equation (5) assumes elemental targets, it may be used with targets that are alloys, compounds, or mixtures of elements provided that the following modifications are taken into account. First, ΔR should be computed for the actual target to be used. This is done by calculating the range of the incident particle in the composite target by means of the procedure, outlined in Ref. (1), which involves summing up the weighted stopping powers of the individual elemental components; in a similar fashion the range of a particle of 50 MeV or of E_f MeV is calculated, and the difference between the two ranges is ΔR. By use of this value for ΔR and the appropriate values for A_t, Equation (5) can be solved for each individual elemental component of the target. Multiplying each such solution by the volume fraction of the element in the composite target and summing these results will give the total $Y_{Z,A}$. However, this is a time-consuming procedure, and its tediousness increases in direct proportion to the number of components in the target. On the other hand, Rudstam states[2] that Equation (1) is expected to be valid only to within a factor of three on the average, with possibly an even greater error for very light or very heavy targets (due to the lack of experimental data with which to establish the correctness of the formula for such targets) and for targets that are far from stability (because the formula is based on distribution data from targets near stability, not for extreme cases). Moreover, the tabulations below already include ΔR for elemental targets, and the extreme values of ΔR are 25.1 and 45.3, a variation of only $\pm$29% about the median. Therefore, in view of these factors, it seems pointless to go through the procedure of correcting from the elemental ΔR values used in the tabulation to the exact ΔR for a particular composite target under consideration, and for composite targets we suggest that one merely look up $Y_{Z,A}$ values for each elemental component, multiply them by the volume fraction of the element in the target, and sum these weighted $Y_{Z,A}$ values. It seems particularly appropriate to make no more effort than this inasmuch as it is quite probable that in practice the target thickness actually used will not be exactly ΔR anyway. In spite of this, the tabulation below will be very helpful if used on a relative basis in that it will give at a glance the best target element with which to make a given product and the by-products likely to be formed in such a target, in addition to the magnitude of the quantities that can be produced.

Some Additional Practical Considerations (3)

Before the computer solution of Equation (5) is discussed, it will be of interest to consider some additional general problems of practical interest. For example, if one wishes to produce a given isotope by spallation (assuming a completely free choice of target, i.e., the optimum target for that isotope), is there an optimum energy that will produce a maximum total amount of activity of that isotope? If so, what is that energy? If not, what effect does energy have?

Peak cross sections (i.e., maximum chain yields) decrease with increasing energy, but the peak (in the mass-yield curve) becomes broader and shifts away from the target mass. On the other hand, ΔR increases with increasing energy, so that perhaps there is an optimum energy at which, even though the cross section of interest is decreasing, the ΔR has increased enough to produce a maximum activity. Alternatively, if there is no maximum, perhaps the ΔR increases faster than the cross section decreases, so that the net effect is an increase in activity of a given nuclide with increasing bombarding energy.

To answer these questions, we calculated the cross sections for $A_t = 100$ and $A_t - A = 3$, 6, and 9 at eleven bombarding energies ranging from 800 MeV down to 100 MeV. The range-energy relationships noted above were used to convert these energies to linear distances of penetration into the target. Graphical plotting indicated that within a given distance interval the cross-section variation could be regarded as being linear with distance without introducing a significant error. The average cross section for a given interval was then taken to be $(\sigma_i + \sigma_f)/2$, where σ_i is the cross section for the production of a given nuclide at the beginning of the distance increment and σ_f is the corresponding cross section at the end of the distance increment.

The effect of beam attenuation was accounted for by calculating the average beam intensity, $\bar{I}$, for each interval from the following:

$$\bar{I} = I_o \left[\exp(-n\sigma_s x_2) - \exp(-n\sigma_s x_1) \right] \left[n\sigma_s (x_1 - x_2) \right]^{-1} . \quad (8)$$

where I_o is the beam intensity initially,
n is the number of target atoms per cm^3,
σ_s is the total (geometric) nuclear cross section (in cm^2/atom), and
x is the linear distance in the target.

The following product was calculated for each distance interval:

$$(x_2 - x_1)(\bar{I})(\sigma_i + \sigma_f)/2.$$

These products were then summed over target thicknesses corresponding to those required to slow the protons down to 50 MeV from their respective initial energies (which ranged from 100 MeV to 800 MeV).

Results are shown in Table III for the case in which $Z_t = 44$ (i.e., for a metallic ruthenium* target).

Table III

Effect of Energy on the Relative Activity Produced in a Ruthenium Target for Three Isotopes of a Given Product Element

(normalized to the 200-MeV induced activity of mass 97)

Initial Energy (MeV)	I_f	$A_t - A = 3$	$A_t - A = 6$	$A_t - A = 9$
100	0.949	0.280	0.035	0.005
200	0.809	1.000	0.236	0.064
225	0.778	1.097		
300	0.654	1.392		
400	0.512	1.646		
500	0.391	1.819		
600	0.293	1.914		
700	0.220	1.952		
800	0.160	1.942	1.127	0.695

[I_f is the fraction of original beam intensity remaining (after nuclear interactions) when the energy has been reduced to 50 MeV.]

From the results shown in Table III, it might appear that there is an optimum energy (at least for the "typical" case calculated) around 700 MeV or slightly higher. However, several practical considerations show this to be illusory. To increase the activity by the maximum possible amount (which is not even a factor of two) relative to what is produced at 200 MeV, one would have to use a target that is over eight times as thick. For example, to produce with an 800-MeV beam 1.94 times as much activity as one could produce with a 200-MeV beam, one would have to use 25.5 cm of ruthenium metal instead of 2.95 cm; similarly, an aluminum target to slow 800-MeV protons down to 50 MeV would have to be 89.2 cm thick, whereas only 11.1 cm would suffice for 200-MeV protons. Clearly, the higher energies require targets that are so thick that they are either very difficult to handle and process or very expensive or both.

Table III also clearly shows another disadvantage of the use of too high a bombarding energy, viz., the enhanced production of unwanted by-products. For example, at 200 MeV only 23.6% as much mass 94 is produced as mass 97 of the same element and only 6.4% as much mass 91, whereas with 800-MeV protons, the mass-94 isotope activity is 58% of the mass-97 activity and the mass-91 activity is 36% of that of the mass-97 activity.

If one uses a higher-energy beam without using a correspondingly thicker target, the activity of a particular isotope of interest is actually less than what would have been produced by a lower-energy beam. For example, as noted above, it requires 2.95 cm of ruthenium to slow a 200-MeV proton down to 50 MeV. If a 2.95-cm target is used at the higher energies, the ratio of yields from the 700-MeV beam to those from the 200-MeV beam is only 39% (for mass 97 and constant product Z). This decrease occurs because at 700 MeV only 20% of the total activity produced is found in the first 2.95 cm of ruthenium, so that, even though the total activity produced in 25.5 cm is 95% greater than that produced in 2.95 cm by 200-MeV protons, the amount of mass 97 produced at 700 MeV in the first 2.95 cm is 20% x 1.95 = 39% of that 200 MeV would produce. The situation is illustrated graphically for the 800- and 200-MeV cases in Figure 1, where the relative activities and distributions of mass 97 (for a given product element) in a ruthenium target are shown as a function of axial penetration of the beam.

Aside from the question of product yields, increasing the energies of the bombarding particles causes a considerable increase in the production of high-energy neutrons, which, in turn, greatly complicate the shielding problem.

Computer Calculation of Activities (3)

Equations (5), (6), and (7) have been programmed for computer solution, and the results are shown in Tables V and VI. The remainder of the text of this report is devoted to an explanation of the computer solution (in contrast to the foregoing discussion, which applied to the equations, themselves).

*All of these calculations were carried out for a Ru^{100} target.

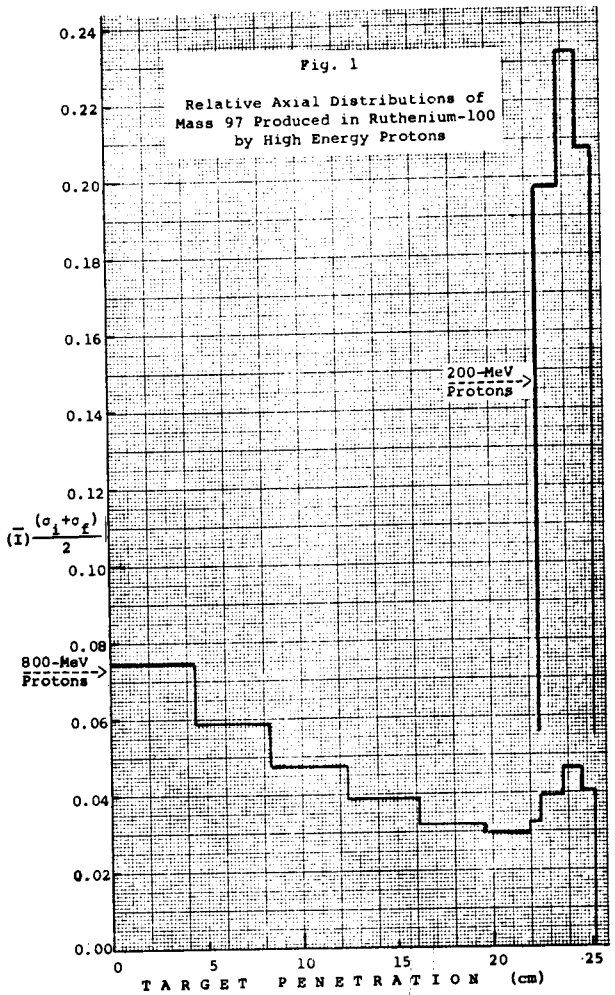

Fig. 1

Relative Axial Distributions of Mass 97 Produced in Ruthenium-100 by High Energy Protons

First, it must be emphasized that the yields shown are independent yields for the particular nuclide in question. In many cases there exist precursors that have half-lives short enough to contribute to the activity of the nuclide in question. Where this occurs, the independent yields of these precursors should be found (see Table VI) and added to that of the product of interest (making appropriate correction for the effect of half-life on activity).

Results for radioactive products with half-lives of less than one minute are not printed, because they are not likely to be of direct primary interest. Where they occur as precursors of a desired nuclide, their cross sections can be crudely estimated by extrapolation from appropriate values in Table VI and a correction thus made for their effect.

The integrated beam current (i.e., the time-averaged current rather than the instantaneous current per pulse) that strikes the target is assumed to be 200 μA. For some other current, I, multiply the results by I/200.

The irradiation time assumed is 24 hr, and the results are as of the end of the bombardment (no radioactive decay included). For products with half-lives of less than 443 min, the activity values will be within 10% of the saturation activity (i.e., the activity at infinite bombardment time). For products with half-lives longer than 231 days, multiplication of the results by 365 will give the annual production rate to within 10%. For products with half-lives between 433 minutes and 231 days, if an accurate correction is desired for an irradiation time other than 24 hr, multiply the results by $(1 - e^{-0.693\,T/\tau})/(1 - e^{-0.693/\tau})$, where T is the length of irradiation time

in days and τ is the product half-life in days. However, in view of the above discussion concerning the accuracy of the cross-section formula and the errors involved in the use of an inexact δR value, this half-life correction could undoubtedly be made mentally with sufficient accuracy for most purposes.

The input data were taken from Ref. (4).

Table V is arranged by product. Products are identified by atomic number, Z, and mass number, A. The half-life is shown for ready reference, the units being S = second, M = minute, H = hour, D = day, Y = year, and T = megayear.

In Table V are listed the acitivities (in millicuries) of $_ZL^A$ producible from various targets. The first column gives the atomic number of the target, and the final column the activity produced when the natural element is used as a target. Intervening even columns give the activity produced when the target is the pure separated isotope whose mass number appears in the preceding odd column.

In all cases, the number following the letter E is the exponent of the power to which the factor 10 must be raised before multiplying it by the coefficient preceding the E. For example, 2.3E-05 = 2.3×10^{-5}, and 4.9E+04 = 4.9×10^{4}.

To keep Table V from being too bulky, results are omitted for natural-element targets that produce less than 0.1% of the activity that can be produced from the most prolific natural-element source of that product.

Table VI is arranged by target (i.e., by atomic number, Z, of the target) and shows, in the next to the last column on the right, the activity (in millicuries) of the product whose atomic number and mass number are shown in the first two columns, respectively, that is produced when the natural element is used as the target. Column 3, labeled "half-life" is a reference column that shows mainly the half-lives of the respective radioactive products. However, since Table VI also includes stable products, Column 3 also shows the percent isotopic abundance in which a particular product nuclide is found in the natural element. This is indicated by the suffix letter A, which should not be confused with the mass number heading for Column 2; like the half-lives, these data are input, rather than output, and have nothing to do with amounts of these individual nuclides produced in spallation. Intervening columns show the activities of the same product produced when pure separated isotopes of the target are irradiated, the mass number of the target isotope being shown at the top of the column. The cross section (averaged over all of the isotopes of the natural element for which activity results are printed in columns to the left) is printed in the final right-hand column; the unit is millibarns.

Due to an artifact inherent in the manner in which the computer program was designed, no results are shown for metastable isomers. In cases where the ground-state isomer has a half-life of <1 minute, e.g., chlorine-34, no results at all appear for the isotope. In cases where the ground-state isomer has a half-life of >1 minute, e.g., rhodium-102 (209-day ground state) or cadmium-113 (stable ground state), only the results for the ground state appear. One can readily interpolate a crude estimate of the cross section in question and, using it, calculate the activity of an unlisted metastable isomer by hand quite simply.

From the cross-section column, one can see at a glance how the relative locations (on the nuclide chart) of the target, product, and line of greatest stability affect the spallation yield. Moreover, there may be special cases in which one wishes to calculate the weight of a particular stable isotope produced, especially in cases of very long irradiation. (As an illustration of the order of magnitude of the effect involved, it may be useful to point out that a 200-μA beam of 200-MeV protons continuously bombarding a 2-cm-diameter target would transmute the surface of the target at the rate of ~1% per year; viewed in another light, this rate is equivalent to generating solid impurities at the rate of ~25 ppm per day.)

In an effort to prevent Table VI from being too bulky while at the same time presenting enough information to be useful for most purposes, no results are printed for those products in which either the activity produced from the natural-elemental target (if the product is radioactive) or the production cross section from the natural element is less than 10^{-3} of the respective values for the nuclide produced in greatest yield. If special cases require results for by-products produced in lesser amounts, the authors can supply a more complete table on request.

The value of zero as a result in either table does not necessarily mean that no activity is produced. It may mean that the Rudstam formula does not apply in that case and that the computer was ordered to skip the calculation. This is true, for example, when $A_{target} - A_{product} < 2$, for which no results will be found*. Thus, the tables appear to show that potassium-38 can not be produced by proton bombardment of potassium-39 but that similar treatment of potassium-40 and potassium-41 will yield potassium-38 in the amounts indicated (160 and 110 curies, respectively). Obviously, proton bombardment of potassium-39 will produce potassium-38, but not in the yield that blind use of the Rudstam formula would have given. This artifact should also be remembered when the average cross section or the activity produced from the natural element is considered, because the results printed are simply the sums of the products of the respective results for each isotope in the target multiplied by the abundance of that isotope. It is for this reason that the tables appear to show only 8 Ci of potassium-38 producible from natural potassium, even though it correctly indicates that irradiation of potassium-40 and potassium-41 individually would produce ten to twenty times that amount; for the same reason, the 590-μb cross section shown for elemental potassium is unrealistically low. This kind of misinterpretation can be avoided by remembering to look to see whether a zero appears in a location for which there is a corresponding target mass number.

Finally, attention is called to the fact that a particular nuclide that appears in one table will not necessarily appear in the other. The reason for this is that a nuclide might be produced from a given target in a yield that is $>10^{-3}$ times its yield from the target that is the most prolific in forming it; such a nuclide would be included in Table V. However, the yield of that same nuclide from the same target might be $<10^{-3}$ times the yield of the nuclide that is produced in maximum yield in that same target; in this case, the $<10^{-3}$-yield nuclide would be omitted from Table VI. For example, germanium-77 is shown in Table V as being produced from natural molybdenum at a daily rate of 0.3 mCi but it is omitted from Table VI because molybdenum will produce niobium-90 at a daily rate of 360 Ci which is clearly $\gg 10^3$ greater than that for the production of germanium-77. An even more interesting case is that of strontium-90, which is shown in Table V as being producible from zirconium-92, -94, and -96 at (independent) daily rates of 0.16, 0.081, and 0.039 mCi respectively; however, strontium-90 does not appear at all in Table VI because its relatively long half-life and low formation cross section make its activity well below 10^{-3} times the yield of the peak product, regardless of what target is used.

(HPR)

References (3)

1. G. Friedlander, J. W. Kennedy, and J. M. Miller, Nuclear and Radiochemistry, 2nd ed., Wiley, New York, 1964.

2. G. Rudstam, Systematics of Spallation Yields, Naturforschung. 21a (7): 1027-41 (1966).

3. M. Rich and R. Madey, Range-Energy Tables. UCRL-2301 (March 1954).

4. D. T. Goldman and J. R. Roesser, The Chart of the Nuclides, 9th ed., revised to July 1966; distributed by Educational Relations, General Electric Company, Schenectady, N. Y. 12305.

5. A. A. Caretto, Jr., Literature Survey of Nucleon, 2-Nucleon Reaction Cross Sections at Energies Above 100 MeV, NYO-10693 (July 1964).

*Such results will be found in Ref. (5).

FIRST ENTRIES FROM Table V

Spallation Products Produced by 200-MeV Protons

(arranged by product)

...one-day irradiation

...200 microampere beam

...no calculations shown for products with half-lives less than one minute

...no yields included if cross section is <0.001 times the maximum cross section for producing that product

...expected accuracy: within a factor of 3

...Zero values in activity columns mean Rudstam formula does not apply in those cases; zero does not necessarily mean that no activity is produced. See text (page 5, column 2, paragraph 1) for precautions to observe in interpreting results when product mass is within two units of target mass

...other pertinent notes discussed in text of report

...Key:

D = day

H = hour

M = minute

S = second

T = megayear

Y = year

	TARGET Z	MONOISOTOPIC TARGET A/MILLICURIES														NATURAL MILLI CURIES
PRODUCT Z= 4	4	9	4.9E+03	0	0.	0	0.	0	0.	0	0.	0	0.	0	0.	4.9E+03
PRODUCT A= 7	5	10	3.2E+03	11	2.1E+03	0	0.	0	0.	0	0.	0	0.	0	0.	2.3E+03
HALF LIFE= 53.000 D	6	12	1.4E+03	13	9.1E+02	0	0.	0	0.	0	0.	0	0.	0	0.	1.4E+03
	7	14	5.8E+02	15	3.8E+02	0	0.	0	0.	0	0.	0	0.	0	0.	5.8E+02
	8	16	2.4E+02	17	1.6E+02	18	1.0E+02	0	0.	0	0.	0	0.	0	0.	2.4E+02
	9	19	6.7E+01	0	0.	0	0.	0	0.	0	0.	0	0.	0	0.	6.7E+01
	10	20	4.3E+01	21	2.8E+01	22	1.9E+01	0	0.	0	0.	0	0.	0	0.	4.1E+01
	11	23	1.5E+01	0	0.	0	0.	0	0.	0	0.	0	0.	0	0.	1.5E+01
	12	24	9.8E+00	25	6.5E+00	26	4.4E+00	0	0.	0	0.	0	0.	0	0.	8.8E+00
PRODUCT Z= 4	6	12	1.0E-04	13	6.7E-05	0	0.	0	0.	0	0.	0	0.	0	0.	9.9E-05
PRODUCT A= 10	7	14	4.5E-05	15	3.1E-05	0	0.	0	0.	0	0.	0	0.	0	0.	4.5E-05
HALF LIFE= 2.700 T	8	16	2.0E-05	17	1.3E-05	18	8.6E-06	0	0.	0	0.	0	0.	0	0.	2.0E-05
	9	19	5.6E-06	0	0.	0	0.	0	0.	0	0.	0	0.	0	0.	5.6E-06
	10	20	3.6E-06	21	2.4E-06	22	1.6E-06	0	0.	0	0.	0	0.	0	0.	3.4E-06
	11	23	1.2E-06	0	0.	0	0.	0	0.	0	0.	0	0.	0	0.	1.2E-06
	12	24	8.1E-07	25	5.4E-07	26	3.6E-07	0	0.	0	0.	0	0.	0	0.	7.3E-07
	13	27	2.4E-07	0	0.	0	0.	0	0.	0	0.	0	0.	0	0.	2.4E-07
	14	28	1.6E-07	29	1.1E-07	30	7.3E-08	0	0.	0	0.	0	0.	0	0.	1.6E-07
PRODUCT Z= 6	6	12	0.	13	2.9E+05	0	0.	0	0.	0	0.	0	0.	0	0.	3.5E+03
PRODUCT A= 11	7	14	2.0E+05	15	1.3E+05	0	0.	0	0.	0	0.	0	0.	0	0.	2.0E+05
HALF LIFE= 20.500 M	8	16	9.1E+04	17	6.0E+04	18	3.9E+04	0	0.	0	0.	0	0.	0	0.	9.0E+04
	9	19	2.5E+04	0	0.	0	0.	0	0.	0	0.	0	0.	0	0.	2.5E+04
	10	20	1.6E+04	21	1.1E+04	22	7.1E+03	0	0.	0	0.	0	0.	0	0.	1.6E+04
	11	23	5.5E+03	0	0.	0	0.	0	0.	0	0.	0	0.	0	0.	5.5E+03
	12	24	3.7E+03	25	2.4E+03	26	1.6E+03	0	0.	0	0.	0	0.	0	0.	3.3E+03
	13	27	1.1E+03	0	0.	0	0.	0	0.	0	0.	0	0.	0	0.	1.1E+03
	14	28	7.3E+02	29	4.9E+02	30	3.3E+02	0	0.	0	0.	0	0.	0	0.	7.1E+02
	15	31	2.2E+02	0	0.	0	0.	0	0.	0	0.	0	0.	0	0.	2.2E+02
PRODUCT Z= 6	8	16	9.2E-02	17	6.3E-02	18	4.4E-02	0	0.	0	0.	0	0.	0	0.	9.2E-02
PRODUCT A= 14	9	19	3.0E-02	0	0.	0	0.	0	0.	0	0.	0	0.	0	0.	3.0E-02
HALF LIFE= 5730.000 Y	10	20	2.0E-02	21	1.3E-02	22	8.5E-03	0	0.	0	0.	0	0.	0	0.	1.8E-02
	11	23	6.6E-03	0	0.	0	0.	0	0.	0	0.	0	0.	0	0.	6.6E-03
	12	24	4.4E-03	25	2.9E-03	26	1.9E-03	0	0.	0	0.	0	0.	0	0.	4.0E-03
	13	27	1.3E-03	0	0.	0	0.	0	0.	0	0.	0	0.	0	0.	1.3E-03
	14	28	8.7E-04	29	5.8E-04	30	3.9E-04	0	0.	0	0.	0	0.	0	0.	8.4E-04
	15	31	2.6E-04	0	0.	0	0.	0	0.	0	0.	0	0.	0	0.	2.6E-04
	16	32	1.8E-04	33	1.2E-04	34	7.9E-05	36	3.7E-05	0	0.	0	0.	0	0.	1.7E-04
PRODUCT Z= 7	7	14	0.	15	2.5E+05	0	0.	0	0.	0	0.	0	0.	0	0.	9.9E+02
PRODUCT A= 13	8	16	1.7E+05	17	1.2E+05	18	8.0E+04	0	0.	0	0.	0	0.	0	0.	1.7E+05
HALF LIFE= 9.960 M	9	19	5.3E+04	0	0.	0	0.	0	0.	0	0.	0	0.	0	0.	5.3E+04
	10	20	3.4E+04	21	2.3E+04	22	1.5E+04	0	0.	0	0.	0	0.	0	0.	3.2E+04
	11	23	1.2E+04	0	0.	0	0.	0	0.	0	0.	0	0.	0	0.	1.2E+04
	12	24	7.7E+03	25	5.1E+03	26	3.4E+03	0	0.	0	0.	0	0.	0	0.	6.9E+03
	13	27	2.3E+03	0	0.	0	0.	0	0.	0	0.	0	0.	0	0.	2.3E+03
	14	28	1.5E+03	29	1.0E+03	30	6.8E+02	0	0.	0	0.	0	0.	0	0.	1.5E+03
	15	31	4.6E+02	0	0.	0	0.	0	0.	0	0.	0	0.	0	0.	4.6E+02
	16	32	3.1E+02	33	2.1E+02	34	1.4E+02	36	6.4E+01	0	0.	0	0.	0	0.	3.0E+02
PRODUCT Z= 8	8	16	1.5E+04	17	1.0E+04	18	7.2E+03	0	0.	0	0.	0	0.	0	0.	1.5E+04
PRODUCT A= 14	9	19	4.9E+03	0	0.	0	0.	0	0.	0	0.	0	0.	0	0.	4.9E+03
HALF LIFE= 71.000 S	10	20	3.2E+03	21	2.1E+03	22	1.4E+03	0	0.	0	0.	0	0.	0	0.	3.0E+03
	11	23	1.1E+03	0	0.	0	0.	0	0.	0	0.	0	0.	0	0.	1.1E+03
	12	24	7.3E+02	25	4.8E+02	26	3.2E+02	0	0.	0	0.	0	0.	0	0.	6.6E+02
	13	27	2.1E+02	0	0.	0	0.	0	0.	0	0.	0	0.	0	0.	2.1E+02
	14	28	1.4E+02	29	9.5E+01	30	6.4E+01	0	0.	0	0.	0	0.	0	0.	1.4E+02
	15	31	4.3E+01	0	0.	0	0.	0	0.	0	0.	0	0.	0	0.	4.3E+01
	16	32	2.9E+01	33	2.0E+01	34	1.3E+01	36	6.1E+00	0	0.	0	0.	0	0.	2.8E+01

FIRST ENTRIES FROM Table VI

Spallation Products Produced by 200-MeV Protons

(arranged by target)

...one-day irradiation

...200 microampere beam

...no calculations shown for products with half-lives less than one minute

...no yields included if either the yield or the cross section is <0.001 times the maximum yield or the maximum cross section, respectively, produced in the target

...expected accuracy: within a factor of 3

...Zero values in activity columns mean Rudstam formula does not apply in those cases; zero does not mean that no activity is produced

...see text (page 5, column 2, paragraph 1) for precautions to observe in interpreting activity values and "AVG SIGMA" values when product mass is within two units of target mass.

...other pertinent notes discussed in text of report

...Key:

A = % abundance of (stable) isotope in natural element

D = day

H = hour

M = minute

S = second

T = megayear

Y = year

TARGET Z= 3

PRODUCTS Z	A	HALF LIFE	MONOISOTOPIC TARGET A/MILLICURIES 6	7	0	0	0	0	0	0	0	0	0	NATURAL MILLI CURIES	AVG SIGMA
2	3	.000 A													2.1E+00
2	4	100.000 A													4.9E+01
1	1	99.990 A													2.5E-01
1	2	.015 A													2.6E+01
1	3	12.300 Y	7.0E+01	4.3E+01	0.	0.	0.	0.	0.	0.	0.	0.		4.5E+01	4.3E+00

TARGET Z= 4

PRODUCTS Z	A	HALF LIFE	MONOISOTOPIC TARGET A/MILLICURIES 9	0	0	0	0	0	0	0	0	0	0	NATURAL MILLI CURIES	AVG SIGMA
4	7	53.000 D	4.9E+03	0.	0.	0.	0.	0.	0.	0.	0.	0.	0.	4.9E+03	7.2E+00
3	6	7.420 A													4.7E+01
3	7	92.580 A													2.4E+01
2	3	.000 A													1.1E+00
2	4	100.000 A													2.5E+01
1	1	99.990 A													1.3E-01
1	2	.015 A													1.4E+01
1	3	12.300 Y	1.7E+01	0.	0.	0.	0.	0.	0.	0.	0.	0.		1.7E+01	2.2E+00

TARGET Z= 5

PRODUCTS Z	A	HALF LIFE	MONOISOTOPIC TARGET A/MILLICURIES 10	11	0	0	0	0	0	0	0	0	0	NATURAL MILLI CURIES	AVG SIGMA
4	7	53.000 D	3.2E+03	2.1E+03	0.	0.	0.	0.	0.	0.	0.	0.		2.3E+03	4.1E+00
4	9	100.000 A													2.7E+01
3	6	7.420 A													2.7E+01
3	7	92.580 A													1.4E+01
2	3	.000 A													6.3E-01
2	4	100.000 A													1.4E+01
1	1	99.990 A													7.5E-02
1	2	.015 A													7.8E+00
1	3	12.300 Y	1.1E+01	6.7E+00	0.	0.	0.	0.	0.	0.	0.	0.		7.5E+00	1.3E+00

TARGET Z= 6

PRODUCTS Z	A	HALF LIFE	MONOISOTOPIC TARGET A/MILLICURIES 12	13	0	0	0	0	0	0	0	0	0	NATURAL MILLI CURIES	AVG SIGMA
6	11	20.500 M	0.	2.9E+05	0.	0.	0.	0.	0.	0.	0.	0.		3.5E+03	9.8E-02
5	10	19.780 A													6.1E+01
5	11	80.220 A													5.3E-01
4	7	53.000 D	1.4E+03	9.1E+02	0.	0.	0.	0.	0.	0.	0.	0.		1.4E+03	2.8E+00
4	9	100.000 A													2.4E+01
3	6	7.420 A													1.8E+01
3	7	92.580 A													9.4E+00
2	3	.000 A													4.3E-01
2	4	100.000 A													9.9E+00
1	2	.015 A													5.3E+00
1	3	12.300 Y	4.2E+00	2.7E+00	0.	0.	0.	0.	0.	0.	0.	0.		4.2E+00	8.6E-01

II. ISOTOPE TECHNOLOGY DEVELOPMENT

RADIOISOTOPE METHODS OF ANALYSIS AND CHARACTERIZATION OF ELASTOMERS* (2)

D. R. Campbell and W. C. Warner**

Supplementary Keywords: (INDUSTRY / INDUSTRY, RUBBER / TRACER / LABELED REAGENT / ACTIVATION ANALYSIS / MOESSBAUER EFFECT / AUTORADIOGRAPHY / ACTIVATION, PHOTON / POLYMERIZATION / CROSS-LINKING / SORPTION / REVIEW, TECHNICAL / BIBLIOGRAPHY / DIFFUSION / ISOTOPE EXCHANGE / CHEMISTRY, ANALYTICAL / RADIOCHEMISTRY / ACTIVATION, NEUTRON / DATING / HYDROGEN-3/ CARBON-14/ SULFUR-35/ CHLORINE-36 / ZINC-65 / MANGANESE-56 / OXYGEN-15 / TIN-119 / KRYPTON-85 / PHOSPHORUS-32 / CALCIUM-45/ CHROMATOGRAPHY / REACTION MECHANISM / PHYSICAL PROPERTY / RADIOMETRIC ANALYSIS / RADIORELEASE / SODIUM-24 / COPPER-64 / ARSENIC-77 / STRONTIUM-90 / THALLIUM-204)

Abstract.

The following aspects of the use of radioisotopes in rubber technology are reviewed (with 146 references): application of isotopes in studies on vulcanization and the interaction of compounding ingredients (estimation of state of cure, radiochromatography in separation and exchange studies, determination of polysulfide bonds by sulfur exchange, detection of nonexchange interactions, sulfur-accelerator exchange reactions); diffusion and dispersion (role of diffusion and dispersion in elastomer technology, radioisotope diffusion studies and polymer structure, methods of study of sulfur diffusion and dispersion, diffusion and dispersion of components other than sulfur, significance of radiochemical purity of labeled penetrants); adsorption and coagulation (solids adsorption on dipped tire cord and coagulation, ionic deposition, and gelation of latexes); radioreagent methods; and applications of special radioisotope techniques (activation methods of elemental analysis, dating and identification of products, detection of physical transformations of elastomers, application of the Moessbauer effect, use of the clathrate form of inclusion complexes).

(Introduction)

Radioactivity applied to rubber technology encompasses such diverse areas as the effect of radiation on elastomers, use of strong gamma and beta sources for process control, and isotope methods to measure tire tread wear. These applications of radioisotopes have received considerable attention in recent years and the principles and techniques have been discussed extensively in both reviews and original papers. Significant contributions, however, have also been made in advancing elastomer technology through analytical use of radioisotopes of carbon, hydrogen, sulfur, and other beta emitters, as well as by special radioisotope techniques.

---

*This paper was published in Rubber Chem. Technol. 42: 1-29 (Feb. 1969) and is reprinted here by permission.

**The General Tire and Rubber Company, Akron, Ohio.

This survey discusses recent advances achieved with beta emitters in vulcanization, diffusion, dispersion, adsorption, coagulation, and determination of functional groups in polymers. In addition, the value of activation analysis and other radioisotope investigative methods for characterization of elastomers is shown.

(4) *Scope: radioisotopes as analytical tools.* In the decade since the review by Blokh[1] of the role of sulfur-35 in vulcanization, increased use of radioisotopes in elastomer technology has paralleled development of new elastomeric materials and has reflected the growing need for more specific and sensitive analytical techniques in this field. In addition to development of new methods employing radioisotopes as indicators in analysis and characterization of raw and vulcanized elastomers, this period has witnessed refinements in tracer methodology and application of established principles to studies of vulcanization in the form of procedures suitable for routine application. Use, for example, of tagged reagents for determining functional groups in unvulcanized polymers and of elemental sulfur-35 for radiometrically estimating state of cure represent recent advances in the analytical chemistry of elastomers. Evolution of isotope exchange as an analytical technique *per se* also illustrates maturation of isotope technology in rubber chemistry. Although this principle for characterizing mobility of sulfur atoms in accelerators and in elucidating mechanisms of exchange had been well established, more recent work has demonstrated the applicability of elemental labeled sulfur as a chemical probe for semiquantitative determination of polysulfide linkages in absence of other exchangeable forms of sulfur. Comparable advances may be observed in studies of diffusion in elastomers. Rates of diffusion of sulfur, antioxidants, and plasticizers in rubber compounds and ultimate uniformity of distribution of these ingredients are important factors in reproducible compounding. The specific and sensitive nature of radioisotope techniques recommends this approach for studying diffusivity and numerous applications of these methods have appeared in this period. In addition, there have been notable developments in use of radioisotopes for determination of trace elements in elastomers; for study of latex coagulation and adsorption; for product identification; and for study of microstructure of certain polymers. Other novel applications involve the recently discovered Mössbauer effect and the clathrate form of inclusion complexes.

In the context of applications of radioisotopes in rubber technology outlined above, this survey is concerned with uses of labeled elements and compounds as indicators and chemical probes in analytical characterization of raw and cured elastomers. The role of tagged atoms for study of diffusion in these materials is interesting because of the importance of diffusion in rubber chemistry and the relationship of this facet of polymer characterization to other radioisotope methods of elastomer analysis. Additional uses of radioisotopes in the elastomer field are considered when these represent analytical means for quantitative determination of constituents of elastomeric compositions or are of value in characterizing elastomers qualitatively.

(4) *Previous surveys of radioisotope applications.* Earlier reviews by Kaplunov and Tarasova[2], Jones[3], and Stadelmann[4] describing uses of radioactive materials and radiation sources in several areas of elastomer technology were supplemented by reports of Gehman[5] and of Shimorda and co-workers[6] dealing with beta emitters in rubber research. An extensive survey of applications of radioisotopes in the rubber industry was also furnished by Jahn[7]. More recently, Oubridge[8] detailed radiotracer techniques for study of some important aspects of polymer technology and Lewis[9] emphasized the potential role of radioisotope methods. Other surveys have dealt with applications of stable as well as radioactive isotopes in polymer chemistry, wherein this approach is used essentially for elucidation of specific

mechanisms of polymer formation. Bevington[10] discussed selected references which illustrate principles involved in the use of these substances in studies of polymers and polymerization. Ayrey[11] subsequently presented a comprehensive review emphasizing the role of radiotracers in elucidation of mechanisms of initiation, propagation, and termination in addition polymerization. Krumbiegel[12] discussed several salient applications of stable and radioactive isotopes in the chemistry of elastomers. Combined use of infrared spectra and radioisotope methods for studying vulcanization was also reviewed by Blokh[13].

(4) *Technique and methodology*. Efficient use of radioactivity as an analytical tool requires knowledge of the several facets of radiation characterization, including nuclear instrumentation, modes of interaction of radiation with matter, counting statistics, and self-absorption and scattering of beta particles, as well as tracer methods. There are several excellent sources where these basic aspects of the radioisotope approach are discussed extensively. Overman and Clark[14] furnished a text which provides significant practical guidance together with a sound introduction to instrumentation, radiation physics, and counting statistics. The versatile technique of liquid scintillation counting was described in a compilation edited by Beil and Hayes[15]. In addition, Reference 16 provides specific examples of the investigative role of radiosiotope techniques in the physical sciences. These works help provide the background desirable for successful application of radioisotope methods to diverse areas of elastomer technology.

VULCANIZATION AND THE INTERACTION OF COMPOUNDING INGREDIENTS (3)

(4) *Estimation of state of cure*. The complex transformations occurring in the preparation of vulcanizates make characterization of these products a challenging aspect of polymer chemistry. Sulfur-35 has played a dominant role in radioisotope investigations of elastomer crosslinking. However, exchange reactions of sulfur, which have been investigated by extra-polymeric radioisotope techniques, limit application of quantitative isotope methods under circumstances of intensive interaction which may occur in vulcanization. Several workers have, nevertheless, successfully used elemental sulfur-35 for estimating state of cure and for determining bound sulfur under specific conditions. The techniques, involving end-window counting of elastomeric specimens, are radiometric, *i.e.*, the methods are based on direct measurement of initial and residual activities.

The radiometric approach to estimation of state of cure was employed by Hofmann-Bang and Pedersen[17] in studying the accelerating capacity of *bis-p*-tolylsulfonyl mono-, di-, and tri-sulfides and of dibenzoyl tri- and tetrasulfides in natural rubber. The method is illustrative of that used in subsequent work. Compounds were prepared with elemental sulfur-35 and, after vulcanization for different times, were extracted with acetone to remove sulfur which had not been insolubilized. Assays of thin, extracted, discs were then made using an end-window G-M tube and scaler. Residual activity was a measure of gross bound sulfur. Although decay corrections were used in this instance, concurrent counting of an unextracted specimen is desirable to obviate decay corrections and reduce the effect of variations in counting system efficiency. Mixtures of rubber and accelerator showed no tendency to vulcanize in absence of sulfur; however, significance of possible isotope exchange in presence of curing agent was not considered. In subsequent work, Pedersen[18] used the radiometric method for bound sulfur in conjunction with a chemical probe and isotope exchange to differentiate several forms of combined sulfur in natural rubber vulcanizates compounded with sulfur-35 and

(parts per hundred rubber)

tetramethyl thiuram disulfide. Extracted samples representing different states of cure were assayed to determine bound sulfur, subjected to exchange in solution with ordinary sulfur, and reassayed to obtain a quantitative measure of exchangeable sulfur. Following this operation, the specimens were contacted with methyl iodide, which reacts preferentially with allylic sulfur, and a sulfur donor; subsequent radioassays demonstrated the coexistence of at least two different bound sulfur types in the vulcanizates. Results of this investigation were correlated with aging stability of the cured rubber

Rohde[19] studied the radiometric method for determining bound sulfur in natural rubber vulcanizates accelerated with diphenylguanidine in the presence of approximately 12 phr zinc oxide. Free sulfur in benzene-methanol azeotrope extracts was determined concurrently using potassium cyanide for formation of thiocyanate; the latter was determined argentimetrically by conductance titration after removal of excess cyanide. Excellent agreement was observed between values for bound sulfur determined chemically by difference and those obtained from radioassay of specimens before and after extraction. The data were used to calculate reaction order of sulfur combination and initial rate of sulfur consumption; kinetics of vulcanization were in good agreement with previous studies. Usefulness of the radiometric approach for rapid, quantitative characterization of accelerator-free systems became apparent in this work.

Although use of tagged sulfur thus represents an accurate and sensitive means for determining combined sulfur in vulcanizates which do not contain sulfur-bearing curatives, effect of the exchange of elemental sulfur with that present in the majority of accelerators must be considered in more common systems. Rhode[20] subsequently investigated exchange under different conditions of cure using representative accelerators in natural rubber in the presence of varying quantities of zinc oxide. The simple radiometric technique of direct vulcanizate examination was supplemented here by radioassay of extracts using liquid scintillation counting in conjunction with column chromatography for separation of elemental sulfur removed. By means of this counting method, radioactivity in extracts could be determined rapidly and accurately. Free sulfur was differentiated from that in accelerators by cyanide-thiocyanate titration. Comparison of results for free sulfur in extracts by the chemical method with those obtained from measurement of total activity gave an indication of extent of isotope exchange during vulcanization. When free sulfur content as calculated from total activity of the chromatographically separated elemental sulfur fraction was lower than free sulfur content obtained from total activity of the extracts, the formation of soluble intermediates was indicated. Accelerators used were mercaptobenzothiazole, 2,2′-dithiobisbenzothiazole, zinc diethyldithiocarbamate, tetraethyl thiuram disulfide, and *N*-dicyclohexyl-2-benzothiazolesulfenamide. Rate of exchange of sulfur with these compounds was negligible in comparison with rate of combination with rubber under the experimental conditions. End window counting was also shown to be accurate in presence of side reactions occurring in the tetraethyl thiuram disulfide-sulfur system and with the sulfenamide-sulfur combination when the latter was used in absence of zinc oxide. Radioassay of extracted specimens at very early stages of cure was less satisfactory than was radioassay of extracts for determining free sulfur; the latter approach, moreover, was suitable for characterizing vulcanization throughout the range of curing times studied. Most of the formulations contained zinc oxide at the level of 10–14 phr. At approximately 5 phr the reduced content of inorganic compound resulted in higher transmission, during extraction, of the compounds for the relatively weak beta radiation of sulfur and thus led to negative

results for free sulfur in completely vulcanized specimens assayed by direct counting. Application of liquid scintillation counting to lightly-filled formulations is thus a significant development in the use of sulfur-35 in quantitative estimation of state of cure.

The method combining liquid scintillation counting with column chromatography was also used by Pedersen[21] in studies of the sulfur-diphenylguanidine system. Total free sulfur was determined by radioassay of acetone extracts and elemental free sulfur was determined after removal of sulfur-containing compounds in the extracts on alumina. Vulcanizates could normally be characterized by the expression

$$\log S_f = -kt + \text{constant} \tag{1}$$

where S_f is free sulfur, phr, t is vulcanization time, sec, and principally by the rate constant k. The technique may be useful for studying displacement of k caused by introduction of a new component into a curing system. A principal feature of the method is rapidity with which determinations of total free sulfur may be made. Since both combined and elemental sulfur is present in extracts, completion of the chromatographic step is necessary for further characterization of the systems.

Formation of zinc sulfide during vulcanization requires an analytical method for sulfur present in this compound in order that the portion insolubilized in this manner may be determined and differentiated from that combined with polymer. Although this distinction was not made in the studies previously discussed, quantitative estimation of zinc sulfide may also be made using elemental sulfur-35. Vas'kovskaya and Dogadkin[22] did this in establishing kinetics of zinc sulfide formation in natural rubber vulcanized with mercaptobenzothiazole and diphenylguanidine. The vulcanizates, after extraction with acetone and determination of total combined sulfur, were swollen in ether under nitrogen. Hydrogen sulfide-^{35}S, generated by addition of hydrochloric acid, was absorbed in cadmium chloride solution. The vulcanizates were dried and bound sulfur was determined radiometrically. Below the optimum point of vulcanization both zinc sulfide and polymer-linked sulfur were present, while after this point only zinc sulfide was formed. Amount of zinc sulfide produced during vulcanization, however, could not be taken as a measure of disulfide crosslink formation.

4 *Radiochromatography in separation and exchange studies.* Usefulness of radiochromatographic techniques in establishing conditions for quantitative separations necessary in analytical and exchange procedures has been demonstrated by several workers. Pedersen[23] employed column chromatography in conjunction with liquid scintillation counting for isolation and radioassay of elemental sulfur-35 in admixtures with several accelerators. This method was shown to be useful for locating the position of components in the eluate in conventional analysis; for studying exchange reactions of accelerators and sulfur using either labeled component; and for determining elemental sulfur and some accelerators accurately when these are present in only very small amounts. Examples include determination of the conditions required for separation of sulfur from tetramethyl thiuram disulfide and 2,2′-dithiobisbenzothiazole, and study of rate of decomposition of tetramethyl thiuram disulfide in sulfur-free vulcanizates. Khodzhaeva and Kissin[24] used paper radiochromatography for investigating exchange reactions involving sulfur, tetramethyl and tetraethyl thiuram disulfide, and certain metal salts of diethyldithiocarbamic acid. After effecting exchange in sealed ampoules at elevated temperatures, these workers separated the components on paper chromatograms which were then divided into small segments; the latter were assayed in-

dividually by end window counting. Exchange was calculated from the expression

$$\% \text{ exchange} = \frac{2\sum(I_1)}{\sum(I_1) + \sum(I_2)} \times 100 \qquad (2)$$

where I_1 and I_2 are net activities of the separated substance and sulfur, respectively, under the activity maxima. Conditions were established for quantitative separation of elemental sulfur from tetramethyl thiuram disulfide and from the lead, copper, cobalt, iron, zinc, cadmium, and nickel salts of diethyldithiocarbamic acid, as well as for separation of these salts from tetraethyl thiuram disulfide. The technique had a relative error of 1 to 2 per cent. Moravek[25] and co-workers described a similar approach for characterizing exchange reactions of elemental sulfur-35 with compounds containing mobile sulfur atoms. The method proposed is suitable for following rate of exchange in a homogeneous system without interrupting the reaction. Aliquots of solution are removed at intervals and spotted on paper, after which the chromatograms are developed and assayed. From activity ratios of exchange reaction components at equilibrium, exchange equilibrium constant, exchange coefficient, and per cent exchange may be calculated. That portion of sulfur-35 which is unreacted at equilibrium may be obtained from a scan of the chromatogram as quotient of the radioactivity of the area for the element by the sum of this area and that of the compound. The technique is useful for studying kinetics of preparative methods for accelerators which employ exchange with elemental sulfur, such as the recent procedure of Cifka and Vins[26] for preparation of labeled xanthates.

4 *Determination of polysulfide bonds by sulfur exchange.* Formation of sulfur-containing crosslinks among polymer molecules is the desired reaction in vulcanization of elastomers with elemental sulfur and accelerators. Nature of these crosslinks, rate and manner of their formation, and nature and extent of reactions leading to other structures within the vulcanizate are significant aspects of the process. Importance of these factors in ultimate network formation and utility of various chemical and physical methods for their study have been the subject of several reviews. Dogadkin and co-workers[27–29] discussed the several types of sulfur crosslinks in vulcanizates and mechanisms leading to their formation with certain accelerators. Dogadkin and Shershnev[30] also surveyed the specific role of accelerators in vulcanization. Scheele[31] pointed out the good agreement between mathematical, kinetic, and experimental data pertaining to determination of polysulfide sulfur in vulcanizates. Saville and Watson[32] presented an extensive review of the status of structural characterization of sulfur-vulcanized natural rubber networks and discussed use of chemical probes for determining the various chemical structures. Gaczynski[33] considered different techniques proposed for estimating crosslinking in cured elastomers.

An important aspect of network characterization is the relationship of type and concentration of intermolecular bonds to physical properties. The ability of sulfur atoms which are not attached to carbon in polysulfide linkages to exchange with elemental sulfur permits semiquantitative estimation of polysulfide sulfur and such data may be used to characterize changes brought about by environmental influences. In compounds accelerated with diphenyguanidine, for example, capacity of bound sulfur to exchange with elemental sulfur passes through a maximum during vulcanization. At the same time, relative ability of sulfur to exchange, calculated per unit bound sulfur, decreases monotonically[28]. Dogadkin[34] described analytical use of this exchange reaction in investigations of kinetics of crosslink

formation and discussed the significance of changes in polysulfide bond concentration induced by heat and stress relaxation at elevated temperatures and during fatigue of vulcanizates. Type of sulfur crosslink affects fatigue relations significantly and isotope exchange with radioactive sulfur revealed that fatigue produces an increase in polysulfide concentration at room temperature and a decrease at higher temperatures; a similar effect was observed on swelling maxima in the system studied. Beniska[35] made use of this isotope exchange technique in conjunction with swelling measurements and chemical determinations of bound sulfur in studying cleavage of polysulfide crosslinks. Average number of sulfur atoms in a crosslink was determined by exchange, as well as by conventional procedures, and showed a maximum in dependence on time of vulcanization for the systems examined. Value of this technique for determining polysulfide sulfur in linkages introduced by gamma radiation has also been demonstrated. Tarasova and co-workers[36] and Dogadkin and co-workers[37,38] irradiated several elastomer-sulfur mixtures and used elemental sulfur-35 for estimating the proportion present in exchangeable form. In addition, Blokh and co-workers[39] applied this method to determine polysulfide bonds in a study of the mechanism of action of zinc compounds as accelerators. Dogadkin and Tutorskii[40] also used this reaction, together with conventional analyses, for characterizing benzothiazolylhydropolysulfide formed in the exchange reaction involving mercaptobenzothiazole and sulfur.

(4) *Detection of non-exchange interactions.* Incorporation of a radioactive isotope into the structure of an organic accelerator permits quantitative determination of accelerator fragments bound to elastomer molecules during physical and chemical treatment and represents an extremely useful approach for studying interactions involving these components. Principal advantage of the technique is the excellent sensitivity with which residual activity may be detected. From the concentration of irreversibly bound, pendent residues, and from comparison of specific activity of combined fragments with that of extractable moieties, inferences can be made concerning the nature of the reactions.

Accelerators tagged with sulfur-35 or carbon-14 were used by several investigators for determining molecular groups derived from compounding ingredients and attached to elastomer molecules during vulcanization and mastication. Combined benzothiazyl thiyl groups in sodium butadiene and styrene-butadiene rubber introduced during vulcanization in absence of sulfur were determined by treating vulcanizates with a solution of 2,2′-dithiobisbenzothiazole labeled in the disulfide bridge[30]. Tutorskii and co-workers[41] investigated the mechanism of unsymmetrical dissociation of this accelerator to yield a benzothiazyldisulfur radical which is assumed to be more active in relation to crosslinking than the monosulfide radical. Extent to which unsymmetrical cleavage of the compound occurred was estimated by comparing the specific activity of sulfur in the vulcanizate with that in the acetone extract. Dogadkin and co-workers[42] determined combined mercaptobenzothiazyl groups introduced into natural rubber during both vulcanization and cold milling. Concentration of accelerator fragments combined in vulcanizates was estimated quantitatively by end window counting. The labeled modification of the accelerator contained radioactive sulfur only in the thiazyl ring and exchange reactions with elemental sulfur during vulcanization were thus without effect on accuracy of the method for combined mercaptobenzothiazyl groups. Results demonstrated the interdependent character of the interaction of this accelerator with sulfur and rubber. Prashchikina and co-workers[43] used sulfur-35 to label certain derivatives of thiobenzoic acid and studied the mechanism of their activity as accelerators of mastication. The systems examined form free radicals which initiate

degradation of macromolecules by adding to double bonds. Residual radioactivity served as a quantitative indicator of concentration of fragments attached to molecular chains.

In studying the mechanism of disulfide bond fission in polysulfide polymers, Novoselok and co-workers[44] used sodium hydrosulfide-^{35}S in the presence and absence of sodium sulfite; the results show that in rupture of such bonds in polydisulfides only the sulfur-sulfur bond is subject to fission.

Interaction of carbon black with sulfur-35 at vulcanization temperatures was investigated by Blokh and Yaroshevich[45], as well as by Dogadkin and co-workers[46]. In addition, Blokh and Melamed[47] examined the effect of heat on adsorption of radioactive sulfur by carbon black in the presence of mercaptobenzothiazole and tetramethyl thiuram disulfide.

Extensive application of tagged sulfur to quantitative study of the more common vulcanization systems has been augmented recently by use of curatives labeled with radiocarbon for characterizing sulfur-free crosslinking reactions. Ballini and co-workers[48] demonstrated the significance of cumyl-^{14}C peroxide in vulcanization of ethylene-propylene copolymers. Ginzburg and co-workers[49] investigated the nature of the interaction of 2,6-*bis*-(hydroxymethyl)-4-*tert*-butylphenol with unsaturated elastomers using the labeled compound. The data indicated that addition proceeds rapidly and crosslinking more slowly, suggesting a two-step reaction; hydroxymethyl groups were found to participate in addition and crosslinking. Use of accelerators labeled with carbon-14 may prove advantageous for accurate determination of accelerator-derived pendent groups, which are of particular significance in networks formed with the tetramethyl thiuram disulfide-zinc oxide system[32]. Accelerators labeled in this manner may also be useful in conjunction with radioactive sulfur, either elemental or combined in accelerators, for further characterization of networks. Although similar radiation characteristics of the radioisotopes require their preliminary separation, availability of the rapid and versatile radioassay technique of liquid scintillation counting offsets this disadvantage.

(4) *Sulfur-accelerator exchange reactions: recent investigations.* Rate and extent of isotope exchange with elemental sulfur as a criterion for predicting reactivity of accelerators during vulcanization has been reviewed in detail[1,50]. Subsequent investigations using this technique for quantitative characterization of reaction of sulfur and accelerators are cited here only to indicate the course of more recent work.

Intensification of isotope exchange between sulfur and mercaptobenzothiazole in presence of free amines was demonstrated by Blokh and Zdanovich[51]; this observation parallels that of the accelerative effect of amines in vulcanization. Otto[52] examined the exchange of sulfur in amine salts of N-disubstituted dithiocarbamic acids with elemental sulfur-35 as a function of temperature, concentration of reaction components, and nature of the solvent. Several investigators studied exchange reactions of sulfenamides in detail. Dogadkin and co-workers[53,54] compared the vulcanization characteristics of S-(diethylaminomethyl)-2-mercaptobenzothiazole and S-(morpholinomethyl)-2-mercaptobenzothiazole with the corresponding sulfenamides in regard to their ability to exchange with 2,2′-dithiobisbenzothiazole containing radiosulfur. The substituted methyl derivatives were more active accelerators and exhibited a higher rate of exchange than the common sulfenamide compounds. Fel'dshtein and co-workers[54–58] studied further the mechanism of action of mercaptobenzothiazole sulfenamides as accelerators in conjunction with the same exchange reaction. These investigators[59,60] also used exchange reactions with elemental sulfur-35 to characterize the lability of sulfur in several derivatives of mercaptobenzothiazole sulfenamides. Kuzina and Gur'yanova[61] employed the

technique in studying mobility of sulfur in thiurams, isothiocyanates, and dithiocarbamates. Blokh and co-workers[62] investigated the effect of benzoic acid and the anhydrides of phthalic and maleic acids on rate of exchange of thiol sulfur of mercaptobenzothiazole with elemental sulfur in presence of diphenylguanidine. The acidic substances retarded exchange at 125° C but did not exhibit this action at 145° C, confirming empirical information about these compounds. Azami and Shizuka[63] described kinetic studies of exchange of elemental sulfur with tetramethyl thiuram mono- and disulfide and 2,2′-dithiobisbenzothiazole; reaction of the *bis*-type accelerators with sulfur is characterized by an induction period and appears to occur in two consecutive steps. They[64] also examined rate of exchange of sulfur with mercaptobenzothiazole and its cyclohexylamine salt and with piperidinium pentamethylene dithiocarbamate. Reactions of these compounds did not involve an induction period and were zero order in the early stages.

Reported investigations of exchange reactions of sulfur-accelerator systems have until recently been made almost exclusively in homogeneous solutions or melts. Possible effect of zinc compounds, such as the oxide, stearate, dialkyldithiocarbamates, and mercaptobenzothiazole salt, on the reaction, although recognized, has received less attention. Isotope exchange reactions involving elemental sulfur and that present in organic or zinc-containing accelerators and effect of zinc oxide on these reactions in heterogeneous systems were the subject of recent work by Shizuka and Azami[65], who examined the sulfur-zinc dimethyldithiocarbamate interaction; the results support a reaction mechanism in which free radicals formed in thermal dissociation of sulfur-zinc bonds activate elemental sulfur by disrupting the ring structure. These workers also studied the reaction between zinc oxide and tetramethyl thiuram disulfide in xylene, rubber, and the solid phase[66], as well as that between zinc oxide and mercaptobenzothiazole in xylene and in rubber[67].

DIFFUSION AND DISPERSION (3)

(4) *Role of diffusion and dispersion in elastomer technology.* The transport phenomenon of diffusion is extremely important in elastomer technology and determination of diffusion coefficients or simple qualitative estimation of rate of diffusion has been the subject of research having both theoretical and practical interest. Quantitative methods for following diffusion of low molecular weight organic compounds in elastomers are useful in characterizing the relationship between structure of the polymer and that of the penetrant. The data may assist in development of theoretical principles, such as those relating polymer structure to internal frictional losses. Similarly, techniques for determining the diffusion coefficient of free sulfur in elastomers at different temperatures permit calculation of the energy of activation for diffusion and estimation of effects of compounding ingredients on diffusion. The value of techniques by which movement of minor ingredients in compounded elastomers can be followed is apparent from consideration of the effect of distribution of these constituents on properties of the finished articles. Moreover, low solubilities of many of these substances in rubber may, through diffusion, lead to migration to the surface of the products; subsequent crystallization on the surface produces objectionable blooming. Synergistic antioxidant effects may also have their origin in diffusion phenomena. An excellent comprehensive review of diffusion in elastomers has been presented recently by van Amerongen[68]. The principal facets of this phenomenon considered here are those which concern application of radioisotope techniques to quantitative and qualitative characterization of diffusion of compounding ingredients in elastomers.

(4) *Radioisotope diffusion studies and polymer structure* Auerbach and co-

workers[69] used organic compounds, *e.g.* octadecane, labeled with carbon-14 to study diffusion in elastomers of molecules comparable in size and structure to segments of chain molecules. This technique was proposed as a possible means for obtaining information on structure and molecular friction forces in polymers. The experimental procedure was a modification of that used earlier[70] in studies of diffusion of sulfur in rubber. With the organic substances, however, two layers of polymer of equal and uniform thickness were brought into intimate contact. Initially, the lower layer contained a known, uniform concentration of radioactive compound and the upper layer contained none. As a result of diffusion the concentration of tagged compound was ultimately the same in both layers. The concentration gradient at the top is zero and this fact together with the low penetration of the beta radiation of carbon-14 assured that a radioassay at the top surface by an end window counter was an accurate measure of concentration at the surface. The diffusion coefficient was calculated from the expression

$$\frac{C_e - C}{C} = \frac{4}{\pi}\left[\exp\frac{-D\pi^2 t}{d^2} - \frac{1}{3}\exp\frac{-9D\pi^2 t}{d^2} + \frac{1}{5}\exp\frac{-25D\pi^2 t}{d^2}\cdots\right] \quad (3)$$

where C_e = equilibrium count rate at top surface, counts/minute,

C = count rate at top surface at time t, sec,

d = thickness of composite test specimen (both layers), cm,

D = diffusion coefficient, cm^2/sec.

The diffusion coefficient, or diffusivity, D, relates the rate of transfer of diffusing substance through unit area of a section to the concentration gradient measured normal to the section. This assumed proportionality, known as Fick's first law, is expressed as $R = -D\partial c/\partial x$, where R and c are the rate of transfer per unit area and concentration, respectively, of the diffusing substance and x is the space coordinate measured normal to the section. A more general equation, which is valid for one-dimensional diffusion, is Fick's second law,

$$\partial c/\partial t = D\,(\partial^2 c/\partial x^2) \quad (4)$$

This equation expresses change in concentration of diffusing substance as a function of place and time when diffusion is independent of concentration, which is the condition usually assumed at very low concentrations. The above equation may be solved in several ways to permit handling experimental data and calculation of D. A further example is the integrated form frequently used in studies involving diffusion of sulfur-35,

$$c = [m/(\pi Dt)^{1/2}]\exp\,(-x^2/4Dt) \quad (5)$$

where m is the total amount of substance diffusing. The appropriate boundary conditions are defined experimentally. Several mathematical approaches useful in investigating diffusion in elastomers are included in the review by van Amerongen[68].

Data were obtained by Auerbach and co-workers[69] to show effects on diffusion of parameters of the polymer system such as unsaturation, solution viscosity, and crosslink density. In addition, they suggested that the method may be useful for studying possible prevulcanization structural changes in elastomers. Also, frictional forces deduced from diffusivity measurements had some correspondence to high frequency viscoelastic phenomena which involve small units of structure comparable in size to segments of the polymer molecules.

(4) *Methods of study of sulfur diffusion and dispersion.* Baldi and Zannetti[71] used the method[70] based on measurement of activity at the upper surface of a specimen whose lower surface was in contact with elemental sulfur-35 to determine diffusion coefficients and solubility of sulfur in copolymers of ethylene with propylene and 1-butene. Since energy characteristics of the beta particle emitted by sulfur-35 are very similar to those of carbon-14 considered previously, count rate at the surface was an accurate measure of concentration. These investigators also studied mobility of sulfur in the copolymers at elevated temperatures using cylindrical specimens which were sectioned after a suitable diffusion time. Laminae were cut from the cylinders in the direction perpendicular to that of sulfur migration and activity in each of these sections was measured. Assuming diffusion into a semi-infinite medium of an instantaneous source in the form of an extremely thin radioactive layer, the authors calculated diffusion coefficients using the integrated form of Fick's second law. Results obtained by this approach were of the same order of magnitude as those observed with the method of Auerbach and Gehman.

Inability of bound sulfur, presumed to be present entirely as non-polysulfide linkages in natural rubber, to undergo exchange with similarly bound sulfur or to migrate was shown by Ludwig[72], using separate test specimens and sulfur-35. Two compounds, consisting of 100 parts rubber and 15 parts labeled and unlabeled sulfur, respectively, were prepared and vulcanized to be 2 mm thick. After extraction with acetone, the specimen containing radioactive sulfur was held in contact with that which contained ordinary sulfur for five hours at 135° C. The specimen initially free of radioactivity was microtomed and radioactivity in each layer was determined following oxidation of sulfur to sulfate and precipitation as the benzidine salt. Very small amounts of activity present in the specimen which initially contained no radioactivity were attributed to migration of low molecular weight sulfur compounds which were incompletely removed during extraction.

Effect of carbon black content on rate of diffusion of sulfur in rubber at elevated temperatures was also investigated by Auler and Boström[73]. Discs of mixes free of sulfur and accelerators, but containing different amounts of carbon black, were brought into contact under pressure with a mix containing sulfur-35 at temperatures between 110° and 120° C for five hours. Layers were microtomed from cylinders cut from the composite specimens and activity of each was determined as barium sulfate-^{35}S after oxidation. The logarithm of per cent sulfur c in each layer, as determined from specific activity, was plotted against the square of diffusion distance x. Since $\ln [c_0/(\pi Dt)^{1/2}]$ is a constant in this experimental approach, diffusion coefficient D is defined by $\ln c = \text{Constant} - (x^2/4Dt)$.

Diffusion rate was dependent on temperature and carbon black content; effect of black concentration increased with increasing temperature and above 80° C exceeded that of temperature. Diffusion of sulfur in rubber compounds may thus be kept within desired limits by variation of black content.

Chernykh and co-workers[74] examined the effect of carbon black pH on rate of diffusion of sulfur-35 in copolymers containing either methylvinylpyridine or carboxylic monomer units. Use of a basic active furnace black caused marked increase in diffusion coefficient for the elastomer made with the pyridine derivative and decrease in the carboxylic polymer. Results were interpreted in light of possible formation of chemical bonds between rubber and filler. Other investigators also studied diffusion of sulfur in elastomers quantitatively using the radioactive element. Blokh and co-workers[75] characterized sulfur migration through several barrier materials in studying cable insulation. Mozisek[76] measured diffusion coefficient through a tread rubber containing carbon black by a modification of the original

end-window counting method[70]. A thin rubber disc was placed over a uniformly thin layer of sulfur on mica and count rate was followed at the surface. From the equation

$$I = [I_0/(\pi Dt)^{1/2}] \exp\ (-x^2/4Dt) \tag{6}$$

where I_0 = original count rate, I = count rate after t sec, x = specimen thickness, cm, the expression

$$\ln [I(t)^{1/2}] = \ln [I_0/(\pi D)^{1/2}] - (x^2/4Dt) \tag{7}$$

may be derived. For a single specimen at constant temperature, $\ln [I_0/(\pi D)^{1/2}]$ is a constant and the value of D may be obtained graphically from a plot of $\ln [I(t)^{1/2}]$ against $1/t$. Accuracy of the method is good at low temperatures with small values of t and for $x^2/4Dt > 1.5$. End window counting was also used for determination of diffusion coefficients of solvents labeled with carbon-14, as well as of elemental sulfur, in synthetic elastomers[77].

Uniformity of sulfur distribution in compounded rubber has practical significance since it is one of the main prerequisites in production of rubber with reproducible physical properties. Similarly, migration or diffusion of sulfur under the diverse conditions used in compounding and curing many types of multi-ply articles is an important factor in control of such processes Auler and Boström[73] studied these factors for giant tires. Blokh and co-workers[78,79] used end-window counting to study sulfur distribution on a mill; to estimate sulfur migration through fabric in multi-ply products; and to study local variations in concentration of crosslinks in automobile tires caused by differences in vulcanization kinetics in the body of the compounds and in the boundary layers. Blaunshtein and Berman[80] compared several methods for effecting distribution of sulfur during compounding. Sulfur added in dispersion in liquid petrolatum gave compounds having better homogeneity than those with sulfur added as a masterbatch or mixed with a softener. In addition, sulfur was more uniformly distributed when added on a mill than when added in a Banbury mixer. Blokh and Kormil'tseva[81] investigated diffusion of sulfur in boot compound and interpreted the results in terms of mono and polysulfide bonds. Epshtein and co-workers[82] also used radioactive sulfur in a study of migration during vulcanization of tires.

Autoradiography, or recording of the distribution of radioactivity in a specimen by means of photographic emulsions, has been useful for quantitative and qualitative characterization of sulfur dispersion. Theory and general practice of this technique have been considered in detail by Yagoda[83] and more recently by Boyd[84], who included an extensive discussion of possible sources of error in the method. Since sulfur-35 emits a relatively weak beta particle only, a nuclear emulsion sensitive to this radiation is selected. Grain concentration in the emulsion determines the probability of a particle striking a grain and is thus an important factor in sensitivity. Good resolution, or differentiation between adjacent active areas, requires a fine grain emulsion. Sensitivity, however, is reduced as grain diameter is decreased and choice of grain size is thus a compromise. Resolution also increases with decreasing emulsion thickness and thin emulsions are therefore desirable. Mozisek and Klimanek[85] considered these and other pertinent variables, such as exposure time, in contact autoradiography with sulfur-35 while using the technique to study dispersion of sulfur in milled rubber. The method may be made quantitative by preparing mixes with different concentrations of radioactivity and measuring darkening of the film with a photometer. Similarly, homogeneity of sulfur distribution may be determined using a recording microphotometer. In contrast to poor resolution characteristics of end-window counting, autoradiography offers a

resolution of at least 50 microns for sulfur-35. In a corresponding investigation Yokose and co-workers[86] used this technique to study dispersion of sulfur in butyl rubber and to follow its rate of combination with the elastomer during vulcanization.

(4) *Diffusion and dispersion of components other than sulfur.* Migration of plasticizers and antioxidants is also an important aspect of elastomer technology which is amenable to investigation with tagged compounds. Hartmann and co-workers[87–89] studied diffusion of several carboxyl-labeled esters of phthalic acid and aliphatic alcohols in rubber compounds using a quantitative microautoradiographic method. Plasticizer was placed in a thin layer between two vulcanized specimens of rubber and pressure was applied. After definite time intervals, the specimens were sectioned in the direction of plasticizer migration and autoradiographs were made of the plane surfaces. Distance from the surface of the rubber to the point where concentration of plasticizer was one-half the surface concentration was determined from the autoradiographs by means of a microphotometer. Using the integrated form of Fick's second law valid for the condition wherein $x_{1/2}$ is the half-width of the concentration distribution, characterized here as the point where radiation intensity is one-half that at the surface, the diffusion coefficient could be calculated from the expression $D = (0.25/\ln 2)(x^2_{1/2}/t)$. A second experimental approach, in which diffusion of plasticizer from one elastomer specimen into a second was effected, was less satisfactory. Diffusion decreased with increasing carbon chain length and degree of branching of the alkyl moiety.

In autoradiographic diffusion studies, the labeled penetrant must possess a specific activity sufficiently high to permit exposure periods which are very short in comparison with diffusion times; low exposure temperatures are also desirable to reduce further diffusion. The autoradiographic method may be used to follow diffusion and dispersion of other compounding ingredients, *e.g.*, accelerators and antioxidants, tagged with either carbon-14, sulfur-35, or tritium.

Maloshuk and co-workers[90] studied the effect of migration of labeled butyl phthalate in polyisobutylene on self-adhesion; radiation intensity at the surface was followed by end-window counting and increased to a maximum corresponding to amount of ester migrating to the surface.

A novel approach to measurement of diffusivity of extender oils in elastomers was employed by Lewis and Deviney[91]. They tagged the aromatic and polar fractions of oils by means of a Friedel-Crafts reaction with propyl-^{14}C bromide and labeled the separated paraffinic fraction using methylene diradicals generated by photolysis of diazomethane-^{14}C. A thin disc of rubber compounded with the labeled oil was then vulcanized to a disc of oil-free compound having the same dimensions. After vulcanization, migration of the oil at elevated temperatures was followed by end-window proportional counting. Diffusivity was calculated using the initial count rate at the surface of the tagged disc and the count rate at the surface of the originally oil-free disc, measured at different times. The effect of simulated working conditions on oil migration between compounds cured separately was studied using combustion and liquid scintillation counting techniques to supplement end-window assay. Diffusion coefficients, expressed as an average, decreased with time for a specific oil fraction in a rubber at constant temperature. The decrease reflected the molecular weight heterogeneity of the labeled oil.

For determination of diffusion coefficients of 2,6-di-*tert*-butyl-4-methylphenol-^{14}C and phenothiazine-^{35}S in polypropylene, Gromov and co-workers[92] used the "thick-layer" method discussed by Zhoukovitsky[93]. A very thin coating of the substance of high specific activity was applied to a relatively thick specimen of polymer and decrease of surface activity with time was followed. The equation describing varia-

tion of concentration, c, as a function of time and depth of penetration, is

$$c = [m/(\pi Dt)^{1/2}] \exp(-x^2/4Dt) \tag{8}$$

where m, grams of substance deposited, is used in conjunction with an integral characteristic of radiation absorption and scattering to relate the fraction of the initial activity at time t to the diffusion coefficient; the latter is obtained from a plot of the fraction of initial activity as a function of $1/t^{1/2}$. Radiation characteristics of sulfur-35 and carbon-14 are advantageous in this technique since the low-energy beta particles are readily absorbed in the polymer. Evaporation of the small amounts of labeled substances is a possible source of error; this effect, however, may be reduced by incorporating the compound between two layers of polymer.

thousand

thousand

Diffusion from a thin layer of tritiated polyisoprene, molecular weight 8 / to 28 \ into natural rubber at elevated temperatures was studied in a similar manner by Bresler and co-workers[94] by determining rate of decrease of surface activity. Coefficient of diffusion was derived by comparing experimental curves, obtained by plotting the fraction of initial activity, I/I_0, at time t, as a function of the logarithm of t, with the theoretical $I/I_0 = f(\ln \mu^2 Dt)$, where μ is the experimentally determined linear absorption coefficient of tritium in rubber and f is a function of integral functions. The very low maximum energy of tritium beta particles is advantageous here, since sensitivity is high as a result of strong absorption by the polymer; diffusion coefficients of the order of 10^{-13} to 10^{-14} cm^2/sec may be determined in ten to twenty hours using this radioisotope. End-window counting cannot be used with tritium under these conditions, however, and an internal proportional counter was employed. The specimen was sealed within the counter, which was equipped with an internal heater to provide precise temperature control. Skewis[95] similarly investigated self-diffusion in styrene-butadiene, butyl, ethylene-propylene, and natural rubber. Tritiated polymers were obtained by irradiating mixtures of the respective polymers with lithium-6 carbonate in a neutron field. Diffusion coefficients, accurate to at least an order of magnitude, were obtained from theoretical plots of I/I_0 against Dt, which were prepared using various assumed values of film thickness and experimentally determined absorption coefficients. Good agreement was observed between values for the diffusion coefficient of a styrene butadiene copolymer measured with both carbon-14 and tritium at 25° C.

Migration of pentaerythritol and the barium and cadmium salts of stearic and myristic acids in styrene butadiene rubber was measured by McHenry[96] in a study of the synergistic antioxidant action of these ingredients. Compounds were prepared containing both additives, one of which was tagged with tritium, and were aged under different conditions. Small amounts were removed from the surface of each specimen with a buffer and the particles collected were separated according to size. Specific activity of the particles was determined by means of liquid scintillation counting, wherein the insoluble material was suspended in the scintillator solution with a thixotropic gel powder. The data revealed higher surface concentration and lower rate of loss of pentaerythritol in presence of the soaps; rate of loss of the soaps, on the other hand, was unaffected by presence of pentaerythritol. Increased surface concentration of pentaerythritol in presence of the soaps apparently enhanced the function of the substance as an antioxidant.

Other quantitative radioisotope studies of diffusion based on the techniques discussed here were made by Gilbert and co-workers[97], who pointed out their value for measuring plasticizer migration in elastomers.

Dispersion of silica in rubber was investigated by Hermann and co-workers[98],

using phosphorus-32 adsorbed on the filler as an indicator; distribution of the silica was followed with the aid of a microautoradiographic technique. A strong beta-emitter was selected in this instance to offset self-absorption occurring in the filler.

(4) *Significance of radiochemical purity of labeled penetrants.* When organic compounds labeled with radioisotopes are used in diffusion studies, accuracy may be affected significantly by radiochemical purity of the substance whose migration is to be followed. Radiochemical purity, or proportion of sample activity which is in the stated chemical form, is affected by diverse factors; most important among these are method of synthesis, specific activity, storage time and conditions, and chemical structure. These and other aspects of the stability of tagged organic compounds have been considered in detail by Bayly and Evans[99] and by Rochlin[100]. Importance of radiochemical purity determinations at the time of use is emphasized by recent work of Muhs, Bastin, and Gordon[101], who analyzed six commercially available hydrocarbons containing carbon-14. Although chemical purity was greater than 99 per cent in all cases, radiochemical purity was no greater than 50 per cent. Since radioactive impurities may consist of polymeric species of molar specific activity comparable to that of the expected compound, as well as of substances having comparable volatility but higher specific activity, accurate determination of diffusion coefficients or qualitative estimation of migration requires preliminary purification of the labeled substance. A description of the method used to assure radiochemical purity of tagged compounds in diffusion studies is thus desirable and may be considered as a necessary adjunct to such work. Preparative scale gas chromatography, where applicable, is a useful and convenient means of purification[101].

ADSORPTION AND COAGULATION (3)

(4) *Solids adsorption on dipped tire cord.* The extreme sensitivity with which radiation may be detected has made the radioisotope approach valuable for investigating the nature and extent of adsorption of both resin and latex solids by synthetic fabrics used in modern tire construction. Here significant variables are weight of solids deposited per unit length of cord and depth of penetration of adhesive in the dipped cord. Both of these factors are amenable to quantitative characterization with labeled substances.

Determinations of weight percent latex solids on cord may be made using resin or latex synthesized from a labeled organic precursor or by means of a water soluble inorganic compound. Although use of a tagged resin or elastomer represents a definitive method for studying adsorption of the respective components, this technique is unsuitable for rapid measurement of uniformity of distribution of solids over extensive lengths of cord; low energy of the beta particles from available isotopes leads to marked self-absorption and requires combustion of segments for accurate analyses. If, however, a strong beta emitter is added to the cord dip, absorption of radiation in the organic matrix is negligible and activity on the cord may be monitored continuously by a glass-walled Geiger tube mounted longitudinally. Relationship between count rate and concentration of dip components on cord may be established by calibration based on gravimetric or chemical analysis and, since activity is proportional to weight of adsorbed material, this radiometric technique may be used to monitor dipping under conditions of standard cord geometry. Suitability of phosphorus-32 for this application was demonstrated by Mozisek[102–104]. The isotope was added as disodium phosphate in an amount insignificant in comparison with dip solids concentration. The cord was dried and drawn

beneath a detector connected to a recording count rate meter to obtain a continuous record of cord impregnation. Although short half-life is desirable for production control in order that activity may quickly decay to an acceptable level, the rapid decrease in activity requires frequent standardization; this disadvantage is accentuated if sodium-24 and arsenic-77, also recommended by the author, are employed. Accuracy of the radiometric method is determined by accuracy of the calibration and precision of decay corrections. Inherent value of this technique lies in the speed with which a quantitative evaluation may be made of the effect of experimental conditions, such as tension and squeezing, on quantity of dip solids per unit length of cord. At a concentration of 0.5 millicurie of phosphorus-32 per liter, precision of representative measurements was $\pm 3\%$[102]. Oubridge[8] showed that accurate measurement of dip solids adsorbed on cord segments was possible by the radiometric method alone, thus obviating calibrations made by gravimetric or chemical analysis.

Characterization of depth of penetration of dip solids into the fiber structure of cord is also feasible using autoradiography and isotopes emitting only weak beta particles. As in quantitative measurement of dip adsorption, two approaches are possible and these involve either a labeled component or addition of a water-soluble inorganic compound. Here, however, labeling by means of the organic moiety has been preferred since availability of the very weak beta-emitter tritium offers potentially excellent resolution in autoradiographs. Since formaldehyde is in common cord dip formulations, it may be labeled with tritium and incorporated into the system. The method has been described by Park[105,107] and by Yokoyama and Onchi[106]. After dipping, squeezing, drying, curing, washing and redrying, the cord was mounted in a polymer block formed by polymerizing methyl methacrylate. Sections 1 mm thick were removed and lifted under suitable autoradiographic emulsion floated on water; photomicrographs were made from the autoradiographs obtained after exposures varying from a few days to several weeks. Effects of cord tension and variation between dips caused by differences in degree of coagulation of the latexes, as well as differences in behavior of nylon and viscose cord, could be demonstrated. Since only formaldehyde is labeled, the autoradiographs reflect concentration and distribution only of the phenol-formaldehyde component of the dip. As an alternative to use of tritium, Mozisek[102] employed trace amounts of sodium sulfate-^{35}S added to the formulation. Darkening on the photomicrographs was measured with a microphotometer and concentration maxima of adsorbed material were estimated from the data. Quantitative interpretation of the data required establishment of the experimental relationship between film darkening and specific activity of the radioactive indicator. Application of this technique involves the assumption that dip solids are adsorbed by the cord in the manner of sodium sulfate.

A corollary to radioisotope investigations of cord-dip adsorption phenomena is use of tagged substances to study nature and location of failure in rubber-cord adhesive systems. This was done by Boguslavskii and co-workers[108] in examining factors affecting bond strengths in systems of this type. Strontium-90 with calcium oxalate carrier was dispersed in ammonium caseinate and the dispersion was added both to dips and to rubber compounds on the mill. Cords passed through radioactive material were cured on slabs of nonradioactive polymer and, conversely, cords treated with inactive dip were cured on carcass compounds labeled with the inorganic substance, which does not diffuse in rubber. Cords and rubber were then separated by a standard ply-separation test and transferred activity was determined radiometrically by end-window counting. Effect of dips of different composition on proportion of initial activity transferred to rubber or to cord was investi-

gated extensively. It was concluded that bond strength can be increased by simultaneously increasing both cohesive and adhesive properties of the dipping composition.

(4) *Coagulation, ionic deposition, and gelation of latexes.* Methods for separation of polymers from latexes produced in emulsion polymerization are based on addition of electrolytes. Determination of the stability of latexes toward these additives is thus an important aspect of their characterization. Small amounts of cation irreversibly bound to the polymers, when coagulation occurs through formation of water-insoluble compounds by reaction of cations with stabilizer anions, may be determined accurately using a radioisotope of the cation. Studies of coagulations with calcium-45 chloride in this circumstance led Sandomirskii and Vdovchenkova[109] to propose the term "calcium number", defined as number of milliequivalents of calcium combined with one gram of coagulum, as a measure of stability of a latex to electrolytes. Relative stabilities of latexes may thus be determined quantitatively: the higher the calcium number, the greater is the amount of electrolyte required to coagulate the latex. Calcium number was independent of latex concentration and decreased on aging, dialysis, or centrifugation. Additional experiments with sodium tridecylate-^{14}C as stabilizer showed that total conversion of this substance to insoluble calcium salt is unnecessary for coagulation.

Calcium-45 also proved advantageous in a similar study by Sandomirskii and Vdovchenkova[110] of ionic deposition of rubber, a phenomenon of considerable importance in applied latex technology. In this instance, a mixture of a concentrated solution of calcium-45 chloride and kaolin was placed on a glass slide and immersed in latex for definite periods of time, after which deposited polymer gel was removed and assayed. Milliequivalents of calcium associated with one gram of deposited rubber was termed in this case "calcium equivalent," in order to distinguish it from the previously defined calcium number. This concept was shown to be useful for characterizing behavior of latexes in ionic deposition. Concentration of coagulant solution and duration of deposition were, for example, without effect on calcium equivalent, whereas amount of rubber deposited increased with coagulant concentration; the requirement of a definite quantity of cations for deposition of a definite quantity of rubber was thus proved. In general, calcium equivalent decreased with dilution of the latex as a result of desorption of stabilizer from latex particles. However, behavior of latexes with different protective substances could not be predicted in ionic deposition from a comparison of calcium equivalents; this comparison was applicable only to latexes having similar stabilizer systems. From an investigation using zinc-65 oxide and ammonium salts in latex gelation[111], a zinc equivalent analagous to the calcium equivalent was proposed for characterizing latexes in which gelation is induced with these substances. The relationship, however, between cation equivalent and latex concentration was not the same in gelation as in ionic deposition; zinc equivalent increased with dilution of the latex due to formation of less dense gels. The value was independent of amount of gelation agent. As in the case of calcium equivalent the concept was useful for quantitative study of effects of aging, dialysis, and type of stabilizer.

Sensitivity of the radioisotope method was made use of by Kolechkova and Poddubnyi[112] in studies of the concentration of salts of dibutylnaphthalene sulfonic acid and of calcium in coagulum, serum, and wash water as a function of the conditions of latex coagulation and washing. The anion was labeled with sulfur-35 and calcium-45 was used to determine calcium concentration. Inferior properties of polymers coagulated with calcium chloride, in comparison with sodium chloride, were attributed to presence of calcium dibutylnaphthalene sulfonate and stearate, as well as of calcium chloride, in the products.

RADIOREAGENT METHODS (3)

Adequate structural characterization of synthetic elastomers requires specific and sensitive methods for determining both terminal and internal functional groups introduced during polymerization. Internal recurring groups in the polymer chain are commonly introduced through a bifunctional monomer in polymerization and usually may be determined by chemical or physical methods. End groups, or those arising mechanistically in addition polymerization, are often present only in concentrations which are below sensitivities of conventional techniques. Principal value of estimations of end groups in addition polymers has been in elucidating mechanism of polymerization. Quantitative use of labeled compounds for this purpose has been reviewed by Ayrey[11]. The need exists, however, for accurate methods whereby terminal functional groups may be determined in addition polymers without incorporation of radioactive substances in the polymerization system.

Reaction of a functional group in a polymer with a substance containing a radioactive isotope and removal of excess labeled reactant offers in principle a means to determine small concentrations of organic structures in macromolecules. Use of a tagged reactant in this manner for formation of a radioactive derivative which may be separated and assayed for combined activity has been termed the "radioreagent" technique. A discussion of this facet of radiochemical analysis and its differentiation from other methods involving application of radioisotopes to analytical chemistry has been presented by Reynolds and Leddicotte[113]. Several conditions exist, however, for successful use of this technique. Conversion of functional groups to the desired derivatives must be quantitative or reproducible to a known degree. Moreover, a "clean-up" technique must be available whereby excess reagent may be seperated from radioactive polymer without loss of activity through degradation; mechanical losses are permissible provided these do not involve molecular weight fractionation. Finally, a suitable radioassay method, applicable to radioreagent as well as polymer, is required. Concentration, E, of tagged group in the polymer following reaction is given by the equation $E = S_p/S_r$ where E is expressed in equivalents per gram, S_p is specific activity of polymer isolated in radioactivity units per gram, and S_r is specific activity of reagent in the same radioactivity units per equivalent. Since the labeled macromolecule may differ significantly in molecular weight from the molecule before reaction, concentration, C, of functional group to be determined in the original sample in equivalents per gram may be related to E by the expression $C = E/1 - (E)(W_1 - W_2)$ where W_1 is weight of the molecular group introduced and W_2 is weight of the molecular group displaced; $W_1 - W_2$ thus represents increase in equivalent weight through derivative formation.

The radioreagent technique may be used to determine number average molecular weight when reaction stoichiometry is assumed to be known and a labeled group may be introduced into each polymer molecule. Howland and co-workers[114] used this principal to determine molecular weight of polybutadiene prepared in an emulsion system with *tert*-alkyl mercaptans tagged with sulfur-35 as chain transfer agents. Experimental conditions were selected to minimize effect of initiation and termination reactions. Presence of one modifier unit in each elastomer molecule was assumed. Average molecular weight of primary chains determined in this manner was used in conjunction with that obtained by osmometry to estimate crosslink density.

Absorption spectroscopy is valuable for routine determination of functional groups in elastomers if proximity of other bands does not obscure the band char-

acteristic of the group to be studied. When an interference of this type exists, the difficulty may be overcome provided that the structure can be converted quantitatively to a configuration having a resolvable absorption band. Reaction with a radioreagent then furnishes a means for standardizing the spectroscopic method. This principle was used by Kramm and co-workers[115] as basis of an infrared technique for determining hydroxyl groups in oxidized polyethylene. In this instance hydroxyl groups were converted to acetyl groups with acetic-2-^{14}C anhydride, after which excess reagent was hydrolyzed and the polymer isolated. The C–O stretching vibration band of the acetylated product was used for estimation of ester content, which was then equated to concentration of hydroxyl groups.

Determinations of carbonyl groups on the surfaces of very thin polyethylene sheets subjected to oxidative media were made by Nitzl[116] using 2,4-dinitrophenylhydrazine-^{14}C for formation of labeled derivatives. Treated specimens were placed in a dilute sulfuric acid solution of this reagent to effect reaction and residual labeled compound was removed by washing. Radioactivity on the surface was determined using a flow gas counter and, with a calibration made by counting the radioreagent, could be converted to concentration of carbonyl groups on the assumption that these were formed in the same amounts on both surfaces of the specimens. If the sheets are thicker than the range of carbon-14 beta particles, however, this assumption is not required and the two surfaces may be assayed independently.

Determination of small concentrations of double bonds in elastomers is an important aspect of polymer characterization since these unsaturated centers represent points at which vulcanization, degradation, or other modification of the macromolecule may occur. Chemical techniques are in general useful to a lower unsaturation limit of approximately 0.10 millimole of double bond per gram and accuracy at this level is usually dependent on rigorous purification of the polymer, particularly with regard to removal of antioxidants. McNeill[117] stressed the need for improved sensitivity in analytical methods for very small concentrations of double bonds in elastomers and approached the problem through use of elemental chlorine-36, a pure beta emitter with a very long half-life, as a radioreagent. This substance may be prepared from palladous chloride and manipulated quantitatively on a vacuum line. The method was applied initially to butyl rubber and reaction of chlorine with double bonds of the isoprene type proceeded without serious side reactions. In absence of light and air the reaction is anomalously one of substitution rather than addition and two atoms of chlorine are incorporated for each double bond present. Comparison of the radioreagent method for unsaturation in butyl rubber with the iodine monochloride procedure of Lee, Kolthoff, and Johnson[118] revealed the former technique to be affected less by amount of excess reagent; good agreement was observed, however, between the two methods with representative polymer samples. Chlorine-36 is thus a useful reagent for determining unsaturation in micro amounts of butyl rubber, as well as in specimens of this elastomer having very low concentrations of double bonds. McGuchan and McNeill[119,120] subsequently extended the technique to determination of unsaturation in polyisobutene, prepared at $-78°$ C with stannic chloride as catalyst. With the aid of model compounds and low molecular weight polymer, the reaction between chlorine and terminal unsaturation present in this elastomer was shown, as in butyl rubber, to be one of substitution rather than addition. Examination of the stoichiometry, however, revealed that a monochloro derivative was formed, rather than the dichloro product obtained with butyl rubber. These results indicate that application of radiochlorine to determination of unsaturation in macromolecules requires preliminary estimation of the number of atoms entering the polymer

molecule for each double bond present and that model compounds are desirable for these introductory studies.

The availability of anionic polymerization systems, whereby addition polymers may be prepared having terminally reactive carbon-metal bonds, has led to development of a new class of difunctional macromolecules which are capable of undergoing subsequent extension or crosslinking reactions. The functional groups in these polymers, for which the term "telechelic" has been proposed[121], are introduced by contacting the alkali metal-terminated precursors with low molecular weight compounds, such as carbon dioxide, carbon disulfide, or ethylene oxide. Concentration of the functional groups in the derivatives may be established accurately by appropriate analyses. The reactions of the carbon-metal bonds, however, are sensitive to experimental conditions and an analytical technique for determining active centers in the precursors is useful in assessing the efficiencies of these processes with regard to yield of desired product. Campbell and Warner[122] made use of the immediate and irreversible reaction of the carbon-lithium bond with aliphatic alcohols containing hydroxylic tritium to determine this structure in polybutadienyllithium:

$$—CH_2^{\ominus}Li^{\oplus} + RO^3H \rightarrow —CH_2{}^3H + ROLi$$

The method was employed to evaluate efficiency of the low temperature carboxylation of organolithium precursor. Hsieh[123] has also indicated utility of this reaction in characterizing anionic polymerization systems. A particular advantage of the technique is its applicability to studies of rate of change of carbon-lithium content during polymerization, since aliquots may be removed from the system and terminated in a hydrocarbon solution of excess alcohol without introducing a significant error attributable to isotope effects. Subsequent investigations have shown that, with the aid of liquid scintillation counting, the method may be used for determining carbon-lithium molarities of solutions of polymeric organolithium derivatives[124].

APPLICATIONS OF SPECIAL RADIOISOTOPE TECHNIQUES (3)

(4) *Activation methods of elemental analysis*. Need for extremely sensitive methods for determining trace amounts of certain catalytically active metals, such as copper and manganese, in natural rubber has long been recognized and advent of synthetic elastomers prepared with diverse organometallic catalysts has extended this need to other elements. Advantage may be taken of the high sensitivity of detection of radioisotopes in this application provided that a suitable technique is available whereby elements of interest may be converted to radioisotopes having useful half-lives and radiation characteristics. Artificial radioactivity thus induced in the specimen may then be detected and determined quantitatively by standard methods. Techniques for production of radioisotopes of the pertinent elements commonly involve introduction of the specimen into a flux of moderated neutrons or gamma photons.

In the usual method of neutron activation analysis, the specimen is placed in a nuclear reactor at a location characterized by a uniformly high flux of slow neutrons for a period sufficient to produce a measurable amount of the radioactive species of the element to be determined. Irradiation time is dependent on half-life of the isotope produced and little advantage is obtained by irradiating for more than three or four half-lives. A typical reaction is that of manganese, which yields

a radioactive isotope with half-life 2.6 hours:

$$^{55}\mathrm{Mn} + {}_0^1n \rightarrow {}^{56}\mathrm{Mn} + \gamma$$

Number of disintegrations per second, A_t, of a given isotope of an element at time t after start of irradiation is expressed by

$$A_t = N\phi\sigma[1 - \exp(-0.693t/T)] \tag{9}$$

where N = total number of nuclei of element present in the specimen

ϕ = slow neutron flux, neutrons/cm^2/sec

σ = activation cross section, in units of 10^{-24} cm^2 or barns

T = half-life of radioisotope.

Weight W of element, in grams, is given by

$$W = \frac{A_t M}{6.02 \times 10^{23}\phi\sigma(1 - \exp[-0.693t/T])} \tag{10}$$

where M = atomic weight of desired element.

Using cross section values of each isotope of a stable element and known half-life values, activity which would result from activation of one microgram of an element in a given neutron flux may be calculated. For manganese-56 and copper-64, which are the radioisotopes obtained with manganese-55 and copper-63, these saturation activities in a readily attainable reactor neutron flux of 10^{11} neutrons/cm^2/sec are 8.8×10^5 and 1.7×10^5 disintegrations per minute per microgram, respectively. With an assumed detection efficiency of twenty per cent, quantities of these elements, in micrograms, which will provide activities of 100 counts per minute above background are 5.7×10^{-4} for manganese and 2.9×10^{-3} for copper. Although measurement of absolute induced activities is feasible, use of a standard sample containing a known weight of element obviates determination of counting efficiency and of neutron flux at the point of irradiation. Depending upon presence of elements yielding isotopes having interfering radiation characteristics, chemical separations may be necessary following activation. Where these separations are not required and activities are thus determinable instrumentally by the comparative technique, the method may be considered nondestructive. Chief limitations of the procedure have their origin in nuclear properties of the atom. Advantages of the method are high sensitivity and accuracy for many elements which are not conveniently determinable by standard methods of trace analysis. In addition, if an element is present in an amount sufficient to permit identification of its half-life and radiation energy, the concentration may be determined in a straightforward manner. Lyons[125] has compiled an excellent presentation of the many facets of this versatile technique.

Several investigators have used neutron activation for trace elements in elastomers. Dalziel and Hsia[126] determined copper in the ash of natural rubber latex, employing homogeneous sulfide precipitation to resolve the gamma activity of copper-64. Isotopes with half-lives in the range of 10 seconds to 30 minutes were used to advantage by Chinaglia and co-workers[127] and by Guinn[128] to determine aluminum and titanium with sensitivities of one and five parts per billion, respectively, as well as vanadium and chlorine in elastomers. Takeuchi and Ishii[129] described the determination of sodium and Simkova and co-workers[130] accurately determined iodine in polymers. In addition, Walker and Eggebraaten[131] employed this technique to estimate quantitatively the nitrogen content of a rubberized

sealant in the range 3 to 5 per cent; the method was readily adaptable to routine use and four specimens could be analyzed in twenty minutes with a relative reproducibility of at least ±1 per cent. The fast neutron flux required for this application was derived from an accelerator.

Use of gamma quanta for activation analysis of oxygen in rubber has been described by Chepel' and co-workers[132,133]. The specimen is irradiated with photons produced in a betatron, synchrotron, or linear accelerator to transform oxygen-16 to oxygen-15, which has a half-life of two minutes:

$$^{16}O + \gamma \rightarrow {}^{15}O + n$$

Identification of oxygen-15 is made by means of emitted positrons or by the two gamma rays formed in annihilation of the positrons. Although carbon-12 undergoes a similar reaction with gamma quanta to yield carbon-11, the radioisotope of oxygen may be differentiated from that of carbon on the basis of the energy difference between the gamma rays produced in the respective positron annihilation reactions. Sensitivity of the method is 0.03 weight per cent oxygen and accuracy is 1 to 2 per cent in samples having an oxygen content in the range of 0.3 to 5 per cent. The method is advantageous for quantitative determinations of oxygen in rubber during processing and aging.

(4) *Dating and identification of products.* Accurate methods for identifying and dating rubber products, especially those of small size produced in large quantities, are a valuable aid in the interpretation of data obtained in end use applications involving aging and deterioration. Conventional dating methods, such as serialization, are inadequate for high volume items and often unreliable under conditions of severe wear and degradation. Gregson and co-workers[134,135] indicated a practicable and potentially versatile approach to the difficulty of elastomer product identification and dating. The method is based on incorporation of two radioisotopes into the compound which differ significantly in half-life. One of the isotopes must have a relatively long half-life and serves as a reference standard for the pair, whereas the other, of much shorter half-life, serves as timer species. Time elapsed since formulation of the mixture is measured by change in initial ratio of timer to standard species and may be calculated from the age equation for nuclide pairs:

$$t = 1.442[\tau_1\tau_2/(\tau_2 - \tau_1)] \ln (R/R_0) \qquad (11)$$

where t is age; τ_1, half-life of timer species; τ_2, half-life of standard species; R, ratio of activities of standard and timer species at time t; and R_0, initial ratio of standard and timer species.

Experimental transmission measurement data are used in place of the nuclide ratio in the above equation and modification of the reference method wherein the nuclide emitting the more penetrating radiation is used as the plot standard permits direct calculation of extrapolated transmission values required in timing applications. Small initial ratios of standard to timer in the range of 1.0 to 0.25 are desirable and minimal errors are observed in time intervals between one and five timer half-lives. Effect of self-absorption in use of the method with dated rubber compounds was overcome by employing plot standards which appear infinitely thick to the more energetic nuclide of the pair. A high degree of radiochemical purity in the isotopes is necessary, particularly when the contaminant radiation has an energy which makes its resolution from that of the pair difficult and when its half-life is greater than that of the timer species. Low-level beta and gamma detection systems are necessary for determining the ratio of nuclides since actual product applications require minimal amounts of radioactivity to meet the

exempt concentrations specified by federal regulations. Under these conditions, an accuracy of ±5 per cent in product age is attainable with the procedures.

An alternative to incorporation of a radioisotope into an elastomeric composition at the time of manufacture for product dating and identification is addition of an extremely small concentration of an indicator element and subsequent conversion of the substance to a radioactive form by neutron activation. A reported application of this approach is addition of one or more elements having capture cross sections for slow neutrons of 1 to 2100 barns and irradiation of the polymer in a nuclear reactor[136]. The indicator element is usually present at 10^{-3} to 10^{-8} per cent by weight of polymer and gives radioisotopes having half-lives in the range of twenty minutes to seven days. Elements used are manganese, indium, lanthanum, or iodine, or their compounds.

Miller, McNall, and Rehner[137] used zinc-65 soaps incorporated in elastomers as a tag or label to differentiate between products differing in unsaturation. Addition of the soaps to butyl rubber permitted this polymer to be distinguished quickly, by means of a Geiger counter or scintillation detector, from untagged natural rubber, SBR, and acrylonitrile-butadiene copolymers. Relative amounts of the tagged elastomer of lower unsaturation in a mixture with the other products could also be determined using this technique.

(4) *Detection of physical transformations of elastomers.* Although a variety of well-established techniques are available for investigating physical processes and changes in polymers, recent novel and simple experimental methods have been reported which make use of radiation characteristics of beta-emitting isotopes.

High resolution attainable in tritium autoradiography was used to advantage by Moyer and Ocho[138] in development of a radioisotope procedure for study of polymer microstructure. Effective range of tritium beta radiation in photographic emulsion is approximately one micron and radioactive regions may be readily distinguished in a specimen at separations of less than two microns. The method is based on the principle that impurities are excluded from the crystalline network during crystallization of an impure material. Impurities in the form of tritiated additives were incorporated into polymer melts and, after crystallization in thin films under controlled conditions, autoradiographs of the specimens were made using the stripping film technique of Pelc[139]. Tritiated additives were dilauryl thiodipropionate for polypropylene and reduced polymer of low molecular weight for polyethylene. Exposure times for autoradiographs were three to twenty days, depending on specific activity of additive and its concentration in the sample. Photomicrographs were taken of the autoradiographs, and of the corresponding areas in the polymer films, using polarized light. By this technique, inferences could be made concerning formation of different types of spherulites observed in the respective systems. Extension of the method to crystalline and noncrystalline polymers mixed with additives which were partially or entirely immiscible with the polymer revealed that shape, size, and distribution of labeled deposits were readily discernible, indicating that useful information was obtainable with such systems as well.

Perhaps the most important parameter characteristic of elastomers and other amorphous polymers is the glass transition temperature. This is the temperature at which large segments of the main chain become mobile and below which only vibrational motions of the polymer segments and atomic groups occur. Methods of determining this temperature have been based upon measurements of changes in specific heat and specific volume, or determinations of dynamic mechanical, dielectric, and other physical properties as a function of temperature. Many of these methods require substantial experimental time and are not applicable to highly

crystalline polymers. A potentially rapid, accurate, and reproducible technique based on beta-particle transmission measurements was developed by Zannetti and co-workers[140] and is applicable to crystalline as well as amorphous polymers; phase transition temperatures may be determined using the same technique. A thin specimen of polymer is mounted in a chamber controlled at various temperatures and above a source consisting of mercurous chloride containing the pure beta emitter chlorine-36. Maximum energy of the beta particle emitted by this isotope is well-suited to absorption studies in organic media. Radiation of intensity I_0 incident upon the lower surface of the polymer is attenuated. On an essentially empirical basis this may be expressed as a first order approximation by

$$I = I_0 \exp\ (-k\rho x) \tag{12}$$

where I is radiation intensity at the upper surface of the specimen; k, mass absorption coefficient; ρ, specimen density; and x, specimen thickness.

Mass absorption coefficient k is dependent on the nature of absorbing medium and is independent of temperature and physical state of the specimen. Value of I is thus dependent on density and thickness of the specimen and density plays the dominant role in this relationship. Temperature of the specimen is raised in increments of 2° to 5° C and change in radiation intensity above the polymer is followed with a Geiger tube. Observed activity is plotted as ordinate against temperature as abscissa and transition temperatures are characterized by intersection of straight lines of different slopes. Rapidity with which a determination may be made is dependent largely on both source activity and statistical accuracy desired; in the most favorable cases accuracy of the transition temperature was ±1° C. Good agreement was observed between results obtained by the beta-particle absorption method and those found by previous techniques.

Klason, Kubat, and de Ruvo[141] used a more active source of a stronger beta emitter, thallium-204, to attain greater statistical accuracy in comparable counting times. Increased precision in the assays permits resolution of secondary and first-order transitions in regions of comparatively small changes in thermal expansivity. Moreover, this modification, wherein transmission measurements are made on specimens which are not clamped in position, exhibits the expected discontinuous increase in transmission at the glass transition temperature as the temperature is raised. Klason and co-workers[141] attributed the decrease in the slope of the curves above the transition temperature, observed in some of the plots of Zannetti and co-workers[140], to distortion effects resulting from clamping the specimen. The method was also shown to be suitable for measurement of the coefficient of thermal expansion.

4 *Application of the Mössbauer effect.* Identification and quantitative evaluation of chemical forms in which an element may be present in a given matrix, under circumstances favorable to several possible combinations, is a requirement common to many investigations in chemistry and physics. A recent physical discovery potentially useful in such studies is the Mössbauer effect, which concerns the resonant energy of gamma rays emitted and absorbed by a radioisotope when the latter is present in a crystal lattice and the effect of recoil of the nucleus on this energy. Emitter and absorber are necessarily the same radioisotope and the significant observation made by Mössbauer was that presence of both in a crystal lattice eliminated the effect of nuclear recoil on resonant energy. The phenomena of resonance and absorption of gamma rays combine to produce a spectrum which is dependent in large measure on the chemical environment of absorbing nucleus; identification of compounds of the element is possible through matching of Möss-

bauer spectra, since these are extremely sensitive to changes in the chemical form of the element. Implementation of the method requires, in addition to a source of the element of interest and common gamma ray detection equipment, a device for moving the absorber relative to the emitter. A concise description of the technique and its potential application has been given by Goldanskii[142].

An interesting application of the Mössbauer effect is the work of Christov and co-workers[143], who studied changes in the chemical form of tin when this element was used as stannous chloride to accelerate vulcanization of natural rubber by a phenol-formaldehyde resin. The gamma-emitting isotope was ^{119}Sn. The emitter was tin dioxide and absorber was present initially as $^{119}SnCl_2$ in either hydrated or anhydrous form. During vulcanization the chloride was largely transformed to dioxide; stannous hydroxy chloride was identified as an intermediate. Carbon black exerted a profound effect on the reaction. The relationship between unchanged stannous chloride and physical properties of vulcanizates led these investigators to propose the Mössbauer effect as a new method for controlling resin vulcanization of rubber.

(4) *Use of the clathrate form of inclusion complexes*. The existence of clathrates, or inclusion complexes in which atoms or molecules of one substance are completely caged within the crystal lattice of another compound, has long been known. Recently, however, these crystalline mixtures, in which the components are present in constant but not stoichiometric proportions, have become valuable as analytical tools with the availability of the radioisotope krypton-85. Although this element may be stably incorporated in solids of all types by ion-bombardment or by heating at high temperature and pressure[144], the modification of concern here is that involving inclusion of the labeled gas within the crystal framework of a reactive compound such as hydroquinone. Basis for use of these clathrates in analysis is the fact that any chemical reaction involving host compound is accompanied by release of radioactive krypton. The isotope emits a beta particle of moderate energy, together with a minor gamma component, and may be determined by conventional radioassay techniques. Quantity of krypton liberated is proportional to amount of occluding compound participating in the chemical reaction; knowledge of reaction stoichiometry permits determination of the substance of interest. In principle the method represents a technique for estimating trace concentrations of substances which react in a known manner with the crystalline moiety. Of topical significance is the reaction of ozone with hydroquinone, which readily participates in clathrate formation with krypton. Chleck and Ziegler[145] first used this procedure in measuring atmospheric ozone concentrations. Aging studies of elastomers in presence of ozone require ozone determinations in the parts per hundred million range and sensitivity with which radioisotopes may be detected suggests the radioactive clathrate approach. An investigation of this type was made by Thelamon-Meynard and Picot[146]. Ozone could be determined in the concentration range of 0.5 to 22 parts per million, but the expected sensitivity and response time were not achieved.

(REG)

REFERENCES (3)

[1] G. A. Blokh, *Gummi Asbest* **10**, 610 (1957); RUBBER CHEM. TECHNOL. **31**, 1035 (1958).
[2] M. Ya. Kaplunov and Z. N. Tarasova, *Kauch. Rezina* **16**(3), 15 (1957).
[3] E. W. Jones, *Rubber J. Int. Plastics* **134**, 128 (1958).
[4] L. Stadelmann, *Gummi Asbest* **12**, 457 (1959).
[5] S. D. Gehman, *Mon. Summ. Automob. Engng. Lit.* **59**(5), *Abs.* No. 48 (1959); SAE Preprint, Annual Meeting, 1959.
[6] I. Shimorda, M. Mozisek, L. Klimanek, and I. Staroba, *Proc: Conf. on Use of Radioisotopes in the Phy. Sci. and Ind.*, Intern. At. En. Agency, Vienna, 1962, pp. 147–55.

[7] H. Jahn, *Kaut. Gummi* **11**, WT102 (1958).
[8] P. S. Oubridge, *J. Int. Rubber Ind.* **1**, 143 (1967).
[9] J. E. Lewis, *Rubber J.* **149**, 82 (1967).
[10] J. C. Bevington, *Advan. Polym. Sci.* **2**, 1 (1960).
[11] G. Ayrey, *Chem. Rev.* **63**, 645 (1963).
[12] P. Krumbiegel, *Isotopentechnik* **2**, 282 (1962).
[13] G. A. Blokh in "Vulcanizatsiya Rezin. Izdelii", Yaroslavl, 1960, pp. 114–31.
[14] R. T. Overman and H. M. Clark, "Radioisotope Techniques", McGraw-Hill, New York, 1960.
[15] C. G. Bell, Jr., and F. N. Hayes, eds., "Liquid Scintillation Counting", Pergamon Press, London, 1958.
[16] S. Rothchild, ed., "Advances in Tracer Methodology", Volumes I–IV, Plenum Press, New York, 1963, 1965, 1966, 1968.
[17] N. Hofman-Bang and H. Leth Pedersen, *Acta Chem. Scand.* **12**, 861 (1958).
[18] H. Leth Pedersen, *Proc. Intern. Rubber Conf., Washington, D. C.*, 1959, pp. 555–64; RUBBER CHEM. TECHNOL. **33**, 181 (1960).
[19] E. Rohde, *Kaut. Gummi Kunstst.* **17**, 105 (1964).
[20] E. Rohde, *Kaut. Gummi Kunstst.* **18**, 74 (1965).
[21] H. Leth Pedersen, *Acta Chem. Scand.* **17**, 2466 (1963).
[22] M. A. Vas'kovskaya and B. A. Dogadkin, *Nauchn. Tr. Dnepropetr. Khim.-Tekhnol. Inst.*, No. 12, Part 2, 241 (1961).
[23] H. Leth Pedersen, *Acta Chem. Scand.* **16**, 870 (1962).
[24] I. V. Khodzhaeva and Yu. V. Kissin, *Kolloidn. Zh.* **23**, 322 (1961); RUBBER CHEM. TECHNOL. **35**, 449 (1962); *Colloid J. USSR* **23**, 268 (1961).
[25] J. Moravek, Z. Nejedly, and J. Filip, *Science* **138**, 146 (1962).
[26] J. Cifka and V. Vins, *J. Labelled Compds.* **1**, 189 (1965).
[27] B. A. Dogadkin, "Vulcanizate Structures", Deutsche Kautschuk-Gesellschaft Meeting, Cologne, May, 1958.
[28] B. A. Dogadkin, *J. Polym. Sci.* **30**, 351 (1958).
[29] B. A. Dogadkin, Z. N. Tarasova, and I. I. Goi'berg, *Proc. Fourth Rubber Technol. Conf., London*, 1962, p. 65.
[30] B. A. Dogadkin and V. A. Shershnev, *Usp. Khim.* **30**, 1013 (1961); RUBBER CHEM. TECHNOL. **35**, 1 (1962).
[31] W. Scheele, *Kolloid-Z. Z. Polym.* **211**, 63 (1966).
[32] B. Saville and A. A. Watson, RUBBER CHEM. TECHNOL. **40**, 100 (1967).
[33] R. Gaczynski, *Polimery* **11**, 103 (1966).
[34] B. Dogadkin, *Khim. Nauka i Promy.* **4**, 55 (1959); *Kaut. Gummi* **12**, WT5 (1959)
[35] J. Beniska, *Plasticke Hmoty Kaucuk* **2**(4), 101 (1965); *CA.* **62**: 16483*g*.
[36] Z. N. Tarasova, M. Ya. Kaplunov, V. T. Koslov, N. A. Klauzen, and B. A. Dogadkin, *Vysokomol. Soedin.* **2**, 1201 (1960).
[37] B. A. Dogadkin, Z. N. Tarasova, M. S. Fogel'son, and A. I. Kashlinski, *Dokl. Akad. Nauk SSSR* **141**, 90 (1961).
[38] B. A. Dogadkin, Z. N. Tarasova, M. Ya. Kaplunov, V. T. Koslov, I. A. Klauzen, and V. S. Matveev, *Tr. 2-go, [Vtorogo] Vses. Soveshch po Radits. Khim., Akad. Nauk SSSR, Otd. Khim. Nauk*, Moscow, 1960, p. 554.
[39] G. A. Blokh, N. N. Podosinnikov, I. P. Cherenyk, *Izv. Vysshikh Uchebn. Zavedenii, Tekhnol. Legkoi Prom.* **1960**, No. 3, p. 50.
[40] B. A. Dogadkin and I. A. Tutorskii, *Kolloidn. Zh.* **20**, 279 (1958); *Colloid J. USSR* **20**, 266 (1958).
[41] A. Tutorskii, L. V. Ginzburg, and B. A. Dogadkin, *Zh. Fiz. Khim. SSSR* **33**, 1401 (1959).
[42] B. A. Dogadkin, I. A. Tutorskii, and D. M. Pevzner, *Dokl. Akad. Nauk SSSR* **112**, 449 (1957); RUBBER CHEM. TECHNOL. **31**, 348 (1958).
[43] A. S. Prashchikina, E. N. Gur'yanova, A. E. Grinberg, and G. K. Sadovskaya, *Kauch. Rezina* **25**(9), 35 (1966); *Soviet Rubber Technol.* **25**(9), 36 (1966).
[44] F. B. Novosclok, V. N. Sokolov, N. P. Apukhtina, and R. A. Schlyakhter, *Vysokomol. Soedin.* **7**, 1726 (1965); *Polymer Sci. USSR* **7**, 1901 (1965).
[45] G. A. Blokh and A. G. Yaroshevich, *Dokl. Akad. Nauk SSSR* **116**, 105 (1957); *Proc. Akad. Sci. USSR, Sect. Phys. Chem.* **116**, 583 (1957).
[46] B. A. Dogadkin, Z. V. Skorodumova, and N. V. Kovaleva, *Kolloidn. Zh.* **20**, 279 (1958); *Colloid J. USSR* **20**, 259 (1958).
[47] G. A. Blokh and Ch. L. Melamed, *Izv. Vysshikh Uchebn. Zavedenii, Tekhnol. Legkoi Prom.* **1959**, No. 2, p. 28.
[48] G. Ballini, L. Baldi, and E. diGiulio, *Chim. Ind.* (*Milan*) **46**, 1338 (1964); RUBBER CHEM. TECHNOL. **39**, 521 (1966).

[49] L. V. Ginzburg, V. A. Shershnev, and B. A. Dogadkin, *Dokl. Akad. Nauk SSSR* **152**, 335 (1963).
[50] G. A. Blokh, *Legkaya Prom.* **14**, 45 (1954); RUBBER CHEM. TECHNOL. **33**, 1010 (1960).
[51] G. A. Blokh and V. S. Zdanovich, *Zh. Obsch. Khim.* **28**, 2652 (1958).
[52] R. Otto, *Kernenergie* **3**, 321 (1960).
[53] B. A. Dogadkin, I. I. Eitington, M. S. Fel'dshtein, Z. N. Tarasova, E. N. Gur'yanova, Lin Yang Ch'in, N. A. Klauzen, and D. M. Pevzner, *Kolloidn. Zh.* **21**, 427 (1959); *Colloid J. USSR* **21**, 415 (1959).
[54] M. S. Fel'dshtein, I. I. Eitington, and B. A. Dogadkin, *Dokl. Akad. Nauk SSSR* **128**, 736 (1959); RUBBER CHEM. TECHNOL. **33**, 357 (1960).
[55] M. S. Fel'dshtein, I. G. Chernomorskaya, E. N. Gur'yanova, and I. I. Eitington, *Zh. Prikl. Khim.* **34**, 2073 (1961); RUBBER CHEM. TECHNOL. **35**, 652 (1962).
[56] M. S. Fel'dshtein, I. G. Beskina, and E. N. Gur'yanova, *Zh. Prikl. Khim.* **38**, 1118 (1965).
[57] M. S. Fel'dshtein, M. V. Gorelik, I. G. Beskina, and T. P. Kononova, *Zh. Prikl. Khim.* **37**, 2696 (1964).
[58] M. S. Fel'dshtein, I. I. Chernomorskaya, I. I. Eitington, E. N. Gur'yanova, and B. A. Dogadkin, *Kauch. Rezina* **20**(10), 15 (1961); *Soviet Rubber Tech.* **20**(10), 13 (1961).
[59] M. S. Fel'dshtein, B. A. Dogadkin, I. I. Eitington, G. P. Shcherbachev, and N. P. Strel'nikova, *Zh. Prikl. Khim.* **32**, 893 (1959).
[60] B. A. Dogadkin, M. S. Fel'dshtein, G. P. Shcherbachev, I. I. Eitington, N. P. Strel'nikova, D. M. Pevzner, and I. Smirnova in "Vulkanizatsiya Rezin. Izdelii", Yaroslavl, 1960, p. 69.
[61] L. S. Kuzina and E. N. Gur'yanova, *Zh. Fiz. Khim. SSSR* **33**, 2030 (1959); RUBBER CHEM. TECHNOL. **34**, 600 (1961).
[62] G. A. Blokh, R. Ya. Shilo, E. V. Tsiponyk, and E. A. Eroshkina, *Zh. Obsch. Khim.* **32**, 2800 (1962).
[63] T. Azami and H. Shizuka, *Nippon Gomu Kyokaishi* **38**, 1100 (1965); *CA.* **64**: 9925*a*.
[64] T. Azami and H. Shizuka, *Nippon Gomu Kyokaishi* **39**, 17 (1966); *CA.* **64**: 12927*h*.
[65] H. Shizuka and T. Azami, *Nippon Gomu Kyokaishi* **39**, 905 (1966); *CA.* **67**: 22666*g*.
[66] H. Shizuka and T. Azami, *Nippon Gomu Kyokaishi* **39**, 999 (1966); *CA.* **67**: 2536*m*.
[67] H. Shizuka and T. Azami, *Nippon Gomu Kyokaishi* **40**, 467 (1967); *CA.* **68**: 113733*p*.
[68] G. J. van Amerongen, RUBBER CHEM. TECHNOL. **37**, 1065 (1964).
[69] I. Auerbach, W. R. Miller, W. C. Kuryla, and S. D. Gehman, *J. Polym. Sci.* **28**, 129 (1958).
[70] I. Auerbach and S. D. Gehman, *Anal. Chem.* **26**, 685 (1954).
[71] L. Baldi and R. Zannetti, *Chim. Ind.* (*Milan*) **44**, 1350 (1962); RUBBER CHEM. TECHNOL. 36, 660 (1963).
[72] R. Ludwig, *Kaut. Gummi* **12**, WT59 (1959); RUBBER CHEM. TECHNOL. **33**, 1029 (1960).
[73] H. Auler and S. Boström, *Kaut. Gummi* **15**, WT37 (1962); RUBBER CHEM. TECHNOL. **35**, 621 (1962).
[74] Z. V. Chernykh, V. G. Epshtein, and B. P. Tikhomirov, *Kolloidn. Zh.* **28**, 900 (1966); *Colloid J. USSR* **28**, 726 (1966).
[75] G. A. Blokh, Z. P. Kormil'tseva, L. A. Olshanskaya, and V. N. Kolobenin, *Vestn. Electroprom.* **27**, 66 (1956); RUBBER CHEM. TECHNOL. **31**, 356 (1958).
[76] M. Mozisek, *Plaste Kaut.* **6**, 65 (1959).
[77] M. Mozisek, *Plasticke Hmoty Kaucuk* **3**, 332 (1966); *CA.* **66**: 76686*m*.
[78] G. A. Blokh, V. Ya. Demidionova, G. P. Miklukhin, I. I. Kukhtenko, A. F. Rekasheva, R. V. Nikulina, and M. I. Przhebylskii, *Legkaya Prom.* **15**, 28 (1955); RUBBER CHEM. TECHNOL. **33**, 1015 (1960).
[79] G. A. Blokh, Z. P. Kormil'tseva, D. B. Boguslavskii, V. I. Bakharev, and B. P. Tikhomirov, *Kauch. Rezina* **17**(7), 33 (1958).
[80] I. M. Blaunshtein and M. L. Berman, *Kauch. Rezina* **17**(7), 31 (1958).
[81] G. A. Blokh and Z. P. Kormil'tseva, *Izv. Vysshikh Uchebn. Zavedenii, Tekhnol. Legkoi Prom.*, 100 (1959).
[82] V. G. Epshtein, N. I. Semenov, and B. P. Tikhomirov, *Kauch. Rezina* **17**(7), 36 (1958).
[83] H. J. Yagoda, "Radioactive Measurements with Nuclear Emulsions", John Wiley and Sons, Inc., New York, 1949.
[84] G. A. Boyd, "Autoradiography in Biology and Medicine", Academic Press, New York, 1955.
[85] M. Mozisek and L. Klimanek, *Plaste Kaut.* **5**, 371 (1958).
[86] K. Yokose, H. Kakimoto, and T. Arai, *Nippon Gomu Kyokaishi* **32**, 460 (1959); *CA.* 54: 13707*h*.
[87] G. Hartmann and G. Schlesier, *Isotopentechnik* **1**, 229 (1960/61).
[88] G. Schlesier, G. Hartmann, and G. Hofmann, *Plaste Kaut.* **9**, 442 (1962).
[89] G. Hartmann, *Monatsber. Deut. Akad. Wiss. Berlin* **3**, 383 (1961).
[90] Yu. S. Maloshuk, A. T. Titarenko, V. G. Raevskii, and S. S. Voyutskii, *Mekh. Polim.* **1966**(6), 857.

[91] J. E. Lewis and M. L. Deviney, RUBBER CHEM. TECHNOL. **40**, 1570 (1967).
[92] B. A. Gromov, V. B. Miller, N. B. Neiman, and Yu. A. Shlyapnikov, *Intern. J. Appl. Radiation Isotope* **13**, 281 (1962).
[93] A. A. Zhoukovitsky, *Intern. J. Appl. Radiation Isotopes* **5**, 159 (1959).
[94] S. E. Bresler, G. M. Zakharov, and S. V. Kirillov, *Vysokomol. Soedin.* **3**, 1072 (1961); *Polymer Sci. USSR* **3**, 832 (1962).
[95] J. D. Skewis, RUBBER CHEM. TECHNOL. **39**, 217 (1966).
[96] W. D. McHenry, *U.S. Dep. Comm., Office Tech. Serv., PB Rept.* 150, 729 (1960); *Rubber Age* **90**, 627 (1962); RUBBER CHEM. TECHNOL. **35**(3), 692 (1962).
[97] B. L. Gilbert, J. L. Kalinsky, and W. F. Lauro (to U.S. Dept. of Defense), U.S. 2,915,639 (January 12, 1959).
[98] W. Herrmann, G. Hartmann, H. K. Bothe, and G. Hofmann, *Kernenergie* **3**, 663 (1960).
[99] R. J. Bayly and E. A. Evans, *J. Labelled Cmpds.* **2**, 1 (1966).
[100] P. Rochlin, *Chem. Rev.* **65**, 685 (1965).
[101] M. A. Muhs, E. L. Bastin, and B. E. Gordon, *Intern. J. Appl. Radiation Isotopes* **16**, 537 (1965).
[102] M. Mozisek, *Plaste Kaut.* **6**, 273 (1959).
[103] M. Mozisek, *Kaucuk Plasticke Hmoty* No. 4, 109 (1961).
[104] M. Mozisek, *Jaderna Energie* **8**, 242 (1962); *CA.* **57**: 15379*f*.
[105] G. S. Park, *J. Soc. Dyers Colourists* **76**, 624 (1960).
[106] S. Yokoyama, and Y. Onchi, *Sen-i Gakkaishi* **16**, 1050(1960); *CA.* 55: 4972*e*.
[107] G. S. Park, *Textile Inst. Ind.* **1**(8), 8 (1963).
[108] D. B. Boguslavskii, B. P. Tikhomirov, and V. G. Epshtein, *Kauch. Rezina* **19**(1), 51 (1960); *Soviet Rubber Tech.* **19**(1), 47 (1960).
[109] D. M. Sandomirskii and M. K. Vdovchenkova, *Kolloidn. Zh.* **20**, 80 (1958); *Colloid J. USSR* **20**, 75 (1958).
[110] D. M. Sandomirskii and M. K. Vdovchenkova, *Kolloidn. Zh.* **20**, 214 (1958); *Colloid J. USSR* **20**, 205 (1958).
[111] D. M. Sandomirskii and M. K. Vdovchenkova, *Kolloidn. Zh.* **22**, 69 (1958); *Colloid J. USSR* **22**, 73 (1958).
[112] M. F. Kolechkova and I. Ya. Poddubnyi, "Fiz-Khim. Metody Analiza i Issled. Produtov Proizv. Sintetikh Kauchuka", Vses. Nauchn.-Issled. Inst. Sintetikh Kauchuka, 1961, p. 118.
[113] S. A. Reynolds and G. W. Leddicotte, *Nucleonics* **21**(8), 128 (1963).
[114] L. H. Howland, A. Nisonoff, L. E. Dannals, and V. S. Chambers, *J. Polym. Sci.* **27**, 115 (1958); RUBBER CHEM. TECHNOL. **32**, 706 (1959).
[115] D. E. Kramm, J. N. Lomonte, and J. D. Moyer, *Anal. Chem.* **36**, 2170 (1964).
[116] K. Nitzl, *Papier* **21**, 393 (1967).
[117] I. C. McNeill, *Polymer* **4**, 15 (1963); RUBBER CHEM. TECHNOL. **36**, 1071 (1963).
[118] T. S. Lee, I. M. Kolthoff, and E. Johnson, *Anal. Chem.* **22**, 995 (1950).
[119] R. McGuchan and I. C. McNeill, *J. Polym. Sci.* **A4**, 2051 (1966).
[120] R. McGuchan and I. C. McNeill, *J. Polymer Sci.* **A5**, 1425 (1967).
[121] C. A. Uraneck, H. L. Hsieh, and O. G. Buck, *J. Polym. Sci.* **46**, 535 (1960).
[122] D. R. Campbell and W. C. Warner, *Anal. Chem.* **37**, 276 (1965).
[123] H. L. Hsieh, *Rubber Plastics Age* **46**, 394 (1965); RUBBER CHEM. TECHNOL. **39**, 491 (1966) (Reference 17 therein).
[124] D. R. Campbell and W. C. Warner, unpublished work.
[125] W. S. Lyon , ed., "Guide to Activation Analysis", D. van Nostrand Co., Inc., Princeton, New Jersey, 1964.
[126] J. A. W. Dalziel and R. C. H. Hsia, *Chem. Ind.* (*London*) **1960**, 1043; *J. Sci. Food Agr.* **12**, 127 (1961).
[127] B. Chinaglia, L. Ciuffolotti, G. B. Fasolo, and R. Malvano, *Energia Nucl.* (*Milan*) **9**, 503 (1962).
[128] V. P. Guinn, Proc. Seminar *Prod. Use Short-Lived Radioisotopes Reactors*, Vienna, 1962, *Part* 2, p. 3.
[129] T. Takeuchi and D. Ishii, *Kobunshi* **12**(135), 446 (1963).
[130] M. Simkova, F. Kukula, and J. Slunecko, *Chem. Zvesti* **19**, 115 (1965); *CA.* **62**: 15428*c*.
[131] L. J. Walker and V. L. Eggebraaten, *Proc. Intern. Conf. Modern Trends in Activation Analysis*, College Station, Texas, 1965, pp. 169–171.
[132] L. V. Chepel' and B. I. Viting, *Zh. Analit. Khim.* **18**, 865 (1963).
[133] L. V. Chepel', B. A. Chapyzhnikov, G. N. Mikhailova, E. V. Zhuravskaya, and A. S. Kuz'minski, *Kauch. Rezina* **25**(3), 49 (1966); *Soviet Rubber Tech.* **25**(3), 39 (1966).
[134] T. C. Gregson and W. R. Miller, "Isotopic Method for Age Determination of Industrial Products", U.S. Dep. Comm., Office Tech. Serv. Rept. TID-15034 (1961).
[135] T. C. Gregson, S. W. Waisbrot, and S. D. Gehman, *Nucleonics* **19**(6), 90 (1961).

[136] French 1,369,167 (to Farbwerke-Hoechst A.G.) (August 7, 1964); *CA.* **62**: 16456*g*.
[137] A. L. Miller, L. R. McNall, and J. Rehner, Jr. (to Esso Research and Eng. Co.), U.S. 2,904,693 (September 15, 1959).
[138] J. D. Moyer and R. J. Ocho, *Science* **142**, 1316 (1963).
[139] S. R. Pelc, *Intern. J. Appl. Radiation Isotopes* **1**, 172 (1956).
[140] R. Zannetti, P. Manaresi, and L. Baldi, *J. Polym. Sci.* **62**, S33 (1962); *Chim. Ind. (Milan)* **43**, 1310 (1961); *ibid.* **44**, 1114 (1962).
[141] C. Klason, J. Kubat, and A. deRuvo, *Rheol. Acta* **6**, 390 (1967).
[142] V. I. Goldanskii, "The Mössbauer Effect and its Application in Chemistry", Acad. Sci. USSR, Moscow, 1963 (Consultants Bureau, New York, 1964).
[143] D. Christov, Cv. Bontschev, B. Skortschev, D. Dimov, and S. Ormandziev, *Kaut. Gummi* **19**, 418 (1966).
[144] D. Chleck and O. Cucchiara, *Intern. J. Appl. Radiation Isotopes* **14**, 599 (1963).
[145] D. Chleck and C. Ziegler, *Proc. Conf. Use of Radioisotopes Phys. Sci. Ind.*, Copenhagen, Part 2, 351, 1961.
[146] C. Thelamon-Meynard and G. Picot, *Bull. Lab. Rech. Cont. Caout.* No. 75, 24 (1965).

FABRICATION OF SEMICONDUCTOR DEVICES AND SILICON MICROCIRCUITS BY NEUTRON-TRANSMUTATION DOPING (2)

Summarized by Helen P. Raaen

Supplementary Keywords: (REACTOR / INDUSTRY / INDUSTRY, ELECTRONICS / PRODUCTION IN SITU / ENRICHED STABLE ISOTOPE USE / ELECTROLYSIS / DOSIMETRY / DID OPEN LITERATURE / ES CADMIUM-113 / SILICON-31)

(Editor's Note: In an early issue of this review, an article on neutron-transmutation doping[1] included the prediction: "Further development of this process could lead to the fabrication of complex devices and entire microcircuits at low cost by reactor irradiation of semiconductor crystals enclosed in a suitable 'radiation die' of absorber material." The prediction has been very nearly realized through the continued work of Klahr and Cohen.[2,3] The progress of their work, which was supported by the Division of Isotopes Development (DID), is described in several publications.[4-7] The fabrication, by neutron-transmutation doping, of semiconductor devices and silicon microcircuits is summarized below. The summary was prepared from two reports by Klahr and Cohen,[2-3] which contain explicit descriptions of all phases of the work. Since the principles and basic equations of neutron-transmutation doping have already been discussed,[1] they are not given in detail here.)

(Introduction)

Neutron-transmutation doping produces electronically active impurities in germanium or silicon with a spatial pattern defined by a slit pattern in a material that is opaque to thermal neutrons—an irradiation die. The irradiation die permits neutrons to enter the selected regions; the neutrons then transmute, for example, silicon nuclei to the dopant phosphorus.

The basic technology of transmutation doping has now been mastered. From the fabrication of single electronic components, the work has progressed through the partial fabrication of simple microcircuits toward the fabrication of complex microcircuits in silicon. In addition to natural cadmium, the enriched stable isotope ^{113}Cd is used as an irradiation die for the microcircuits. The practical and reproducible techniques and procedures combine the methods of semiconductor fabrication with those of nuclear reactor irradiation technology. They are sufficiently different from other processes and sufficiently extensive in scope to constitute a new technology. The most important technological results of this work appear in the controllability and predictability of the doping.

For microcircuitry fabrication, transmutation doping has three areas of potential advantage:

1. Performance, that is, achievement of device characteristics not obtainable by other processes (diffusion or epitaxy);
2. Cost (either few-of-a-kind or many-of-a-kind production; and
3. Controllability of fabrication.

Semiconductor Devices (3)

The work on semiconductor devices resulted in

1. Demonstration of reproducibility and predictability in the doping of germanium and silicon;
2. Improvements in spatial resolution and control in the doping; and
3. Fabrication of individual prototype electronic devices and simple electronic circuits.

The variables studied included

Thermal-neutron fluence (nvt):	10^{18} to 3×10^{20} n/cm^2
Cadmium ratio:	7 to 30
Irradiation die material:	cadmium, 2 to 20 mils thick
Irradiation die backing:	aluminum, nickel, steel, copper
Slit width:	2 to 50 mils

Slit type:	single- and double-sided
Irradiation capsule material:	aluminum and stainless steel
Duration of irradiation:	5 days to 3 wk
Semiconductor material:	silicon and germanium
Initial semiconductor resistivity:	0.01 to 100 Ω cm
Capsule design:	cylinder and flat-plate

The specific results were

1. Fabrication of surface field-effect transistors (SFET's) of acceptable quality;
2. Fabrication in both silicon and germanium of resistors, diodes, and capacitors having a variety of characteristics;
3. Use of a surface oxide layer and its associated inversion region in transmutation-doped devices;
4. Practical use of thin irradiation dies—2 mils of cadmium or less (The thin dies permit spatial control to within 1 to 2 mils along the specimen surface; the use of oxide surface layers permits control to within 1000 Å normal to the surface); and
5. Partial fabrication of simple microcircuits.

Techniques were developed for the following operations necessary to the transmutation-doping process:

1. Fabricating irradiation-die materials which consisted of a thin layer of cadmium bonded to a thicker layer of metal that is transparent to thermal neutrons (e.g., copper or steel);
2. Photoetching the irradiation die;
3. Encapsulating the irradiation die and semiconductor specimens;
4. Specifying the neutron flux and the semiconductor resistivities to ensure the proper doping of the spatial regions, that is, to ensure that P-N junctions are formed; and

5. Adapting various standard semiconductor techniques to the transmuted specimens to fabricate electronic devices.

Methods and Device Characteristics (4)

Transmutation-produced devices will differ radically in geometry and configuration from devices of similar function produced by diffusion or epitaxy, both of which tend to produce planar structures that consist of layers of constant doping parallel to the large-area surface of the devices. The junctions are therefore parallel to the large-area surface. On the contrary, transmutation doping tends to produce regions of constant doping perpendicular to the surface (a clear-through doping configuration). Thus, transmutation-produced P-N junctions tend to be perpendicular to the surface. This overstates the difference, since neutron transmutation can also easily produce structures parallel to the surface, and the transmuted regions need not extend clear through the semiconductor specimen. In a neutron-transmutation-doped device, a straightforward copy of a conventional device will be neither feasible nor useful in most cases. Rather, the neutron-transmutation device will use a configuration that exploits its own characteristics and advantages. Both the device and the microcircuit produced by neutron-transmutation doping will be designed to reproduce or to improve upon the function or the purpose of the comparable conventional device—not its geometry or doping profile.

Rectifying Diodes. (5) Most of the diodes were made by use of the doping configuration that yields adjacent P and N regions extending clear through the specimen; the P-N junction is therefore normal to the surface. Such diodes have been formed in silicon with induced-dopant concentrations on either side ranging from 3×10^{14} to 3×10^{16} atoms/cm^3. The ratio of resistivities on the two sides has ranged from 50:1 in some diodes to 1:1 in others. Reverse breakdown voltages have ranged from 25 to 50 V, relatively high values characteristic of the rather shallow concentration gradients produced in the junctions. Eventual breakdown voltages are probably considerably higher than these values,

because breakdown appears to be due to surface shorts. The diodes fabricated to date have relatively large areas (~2000 mils^2). The absence of a short over the relatively large area attests to the uniformity of the doping. The reverse leakage for such a diode is in the range 0.1 to 1 μA, which is very small for a diode of such large area.

Transistors. (5) With the use of natural-cadmium irradiation dies, it is not feasible to obtain spatial resolution better than 1 mil in doping of adjacent regions. This restriction seems to imply that conventional bipolar transistors would be marginal at best, since a base region 1-mil thick would give a low amplification factor. Therefore, in the area of active components, the most promising device appears to be the surface field-effect transistor (SFET), also called the metal oxide semiconductor (MOS) or insulated-gate field-effect transistor (IGFET).

Ihantola and Moll[8] and others have suggested that SFET's, because of their favorable electronic characteristics, would constitute useful amplifier devices for very general applications in microcircuitry. This type of transistor can be readily made by transmutation doping. It consists of two N-type regions with a P-type region between them. When an insulating layer is placed on the surface with a metallic contact on the layer, a reverse bias voltage on this contact produces an N-type channel in the P-type region that connects the two N regions. The basis of this effect is simple capacitance across the oxide layer, with a positive charge on the adjacent P-type layer; thus, an N-type bridge is made across the surface between the two N-type regions. Therefore, the SFET works by modulating the surface conductivity and thus controlling the current flow from the first N-type region (source) to the second N-type region (drain).

The SFET is fabricated in neutron-transmutation geometry as follows. The operating transistor structure is made by irradiating a uniformly doped P-type silicon specimen through an irradiation die to obtain an N-P-N structure normal to the surface. The specimen is then annealed and stained to reveal the exact

location of the P and N regions. (The staining is not necessary if precision-aligned masks are subsequently used.) An oxide film of predetermined thickness is grown on the surface of the silicon by heating it in a wet-oxygen atmosphere for a specified time. The oxide film is then removed above the N-type regions by etching. Electrical measurements between the two N-type regions show that an N-type "inversion layer" is formed on the surface of the P-type region under the oxide. This thin ($\lesssim 1\ \mu$) inversion layer forms the conducting channel between the source and the drain. Aluminum is then evaporated over the oxide on the channel to form the gate electrode, and the oxide is chemically removed from the rest of the specimen. The N-type regions are electrically isolated before the inversion layer channel is formed by the oxide deposition. An appropriate bias voltage on the gate electrode nullifies the inversion layer, thus removing the conducting channel. This nullification occurs at ~12 V. At gate voltages between 0 and 12 V, the effective thickness of the channel is varied; the source-to-drain current is thus varied for a given source-drain voltage.

Several SFET's were made by neutron-transmutation doping and were tested. Figure 1 gives a schematic diagram of the transistor structure and of the circuit for obtaining its DC characteristics and also the electronic characteristic curves, which are similar to those of a pentode, a typical field-effect transistor. Adequate performance of the SFET's was demonstrated.

The type of SFET described here is termed a "depletion type," because the channel width is decreased with increasing gate voltage. It is expected that "enhancement type" SFET's in which the channel width increases with increasing gate voltage can also be fabricated with equal ease.

Voltage-Variable Capacitors. (5) The diodes made by neutron-transmutation doping can function as voltage-variable capacitors, because their capacity decreases with reverse voltage. Such a neutron-transmutation-doped diode, used

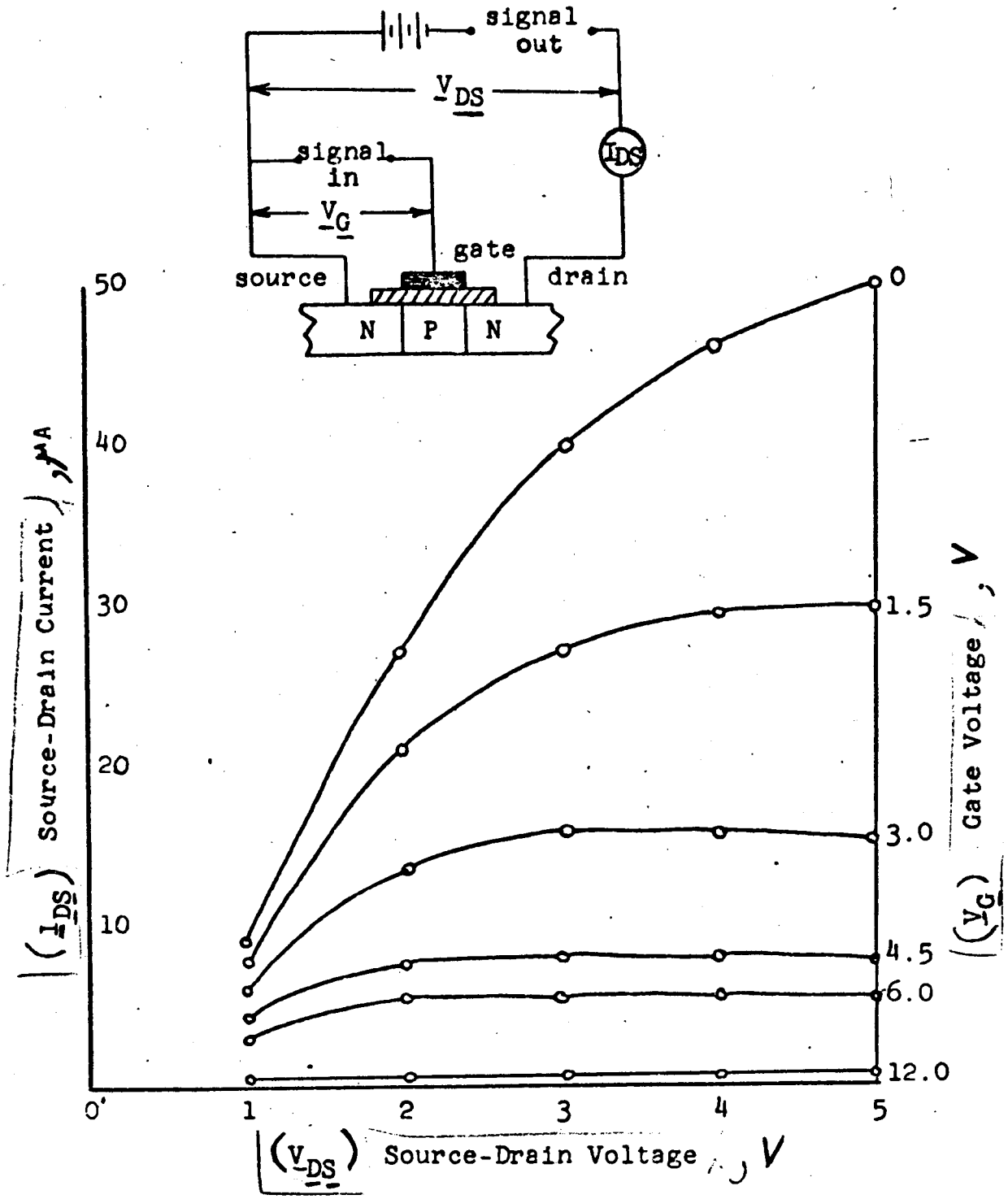

Fig. 1. Schematic diagram and characteristic curves of an SFET made by neutron-transmutation doping.

as a voltage-variable capacitor typically has the properties:

Capacitance at zero reverse voltage, C_o	$\approx$ 60 pF
Reverse breakdown voltage	$\approx$ 50 V
Capacitance swing	$\approx$ 400% (maximum to minimum)

The relatively large value of C_o is due to the large area of the junction in the clear-through configuration ($\sim 10^3$ mils^2) despite the relatively wide space-charge region of the junction, which can be attributed to the shallow concentration gradient. In silicon, for example, capacitances of the order of 10^4 pF per square centimeters are obtained, corresponding to space-charge-region widths of 1 μ, for concentration gradients in the range 10^{19} atoms/cm^4. This relatively shallow gradient is useful for producing a large reverse breakdown voltage. The homogeneity of the doping permits one to produce such relatively large-area junctions with a small fraction of short circuits in the junction.

Resistors. (5) A resistor compatible with neutron-transmutation doping can be produced in three ways so as to provide

1. the inversion region under an oxide layer in a P-type region between two N-type regions, or vice versa,
2. a clear-through (or partial-depth) doped region isolated by an adjacent doped region of type opposite from that of the other devices on the monolith, or
3. a thin-film type resistor evaporated onto an oxide layer over the semiconductor.

Resistors of the first two kinds have been made and tested. The inversion-region resistor (type 1) can be used for high resistance values of the order of 10^3 to 10^5 Ω or more. Furthermore, the resistance can be adjusted by use of a trimming bias on an evaporated-metal electrode over the oxide layer. The second type of resistor can be used to produce resistance values in the tens or hundreds of ohms.

Microcircuits. (5) The feasibility of producing microcircuits by neutron-transmutation doping was demonstrated by fabricating two relatively simple microcircuits in silicon—a full-wave rectifier bridge equivalent to a four-diode bridge (Fig. 2) and a computer-logic matrix for readout of a set of flip-flop register states (Fig. 3). The P and N regions were distinguished by etching and staining. The configurations are clearly nonconventional. In Fig. 3B, diodes are to the left. Interconnections were made by use of a wire border; they can also be made by thin-film evaporation. Line widths in the final doped specimens ranged from 15 to 30 mils. The irradiation dies were 2- to 10-mil thicknesses of cadmium, which gave an ultimate doped-line width of ~1 mil. The resistors are type 2, with values $\sim 10^3\ \Omega$. Capacitances of the diodes are ~50 pF. The switching time constant is therefore ~0.1 μsec.

In the fabrication of microcircuits, the entire doping configuration is inserted in a single irradiation, followed by oxide deposition, oxide etching, evaporation of metal contacts, and attachment of wire leads using a wire bonder. It should be possible to fabricate almost any microcircuit from the individual components discussed above. The work to fabricate complex microcircuits is described in the latter part of this summary.

Appraisal of Transmutation Doping for Microcircuit Fabrication (4)

Performance. (5) The performance advantages for transmutation-doped devices stem from the various unique geometric configurations that can be produced; for example,

1. The doped regions can be of very uniform concentration.
2. Clear-through doping can be achieved. This type of doping can permit interconnections to be made on the bottom of the slice. It can also be used to increase the number of devices on each slice.
3. P-N junctions can be formed either perpendicular to the semiconductor surface by clear-through doping or parallel to the surface at a desired depth.
4. Junctions with desired concentration gradients can be formed in either high- or low-resistivity material.

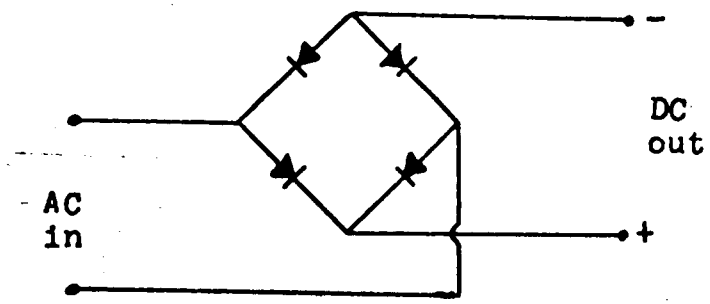

A. Equivalent conventional circuit

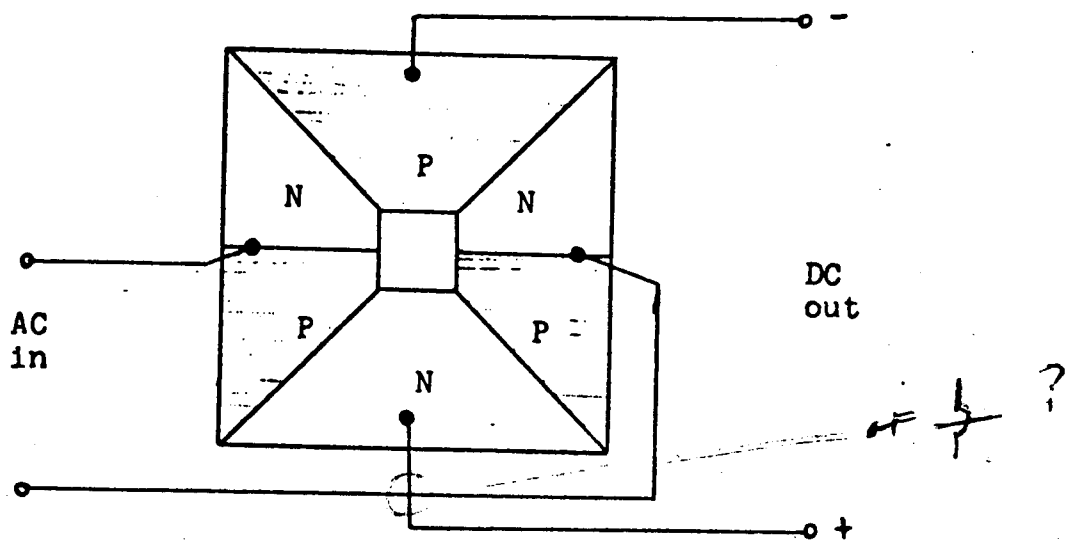

B. Schematic diagram of doping configuration

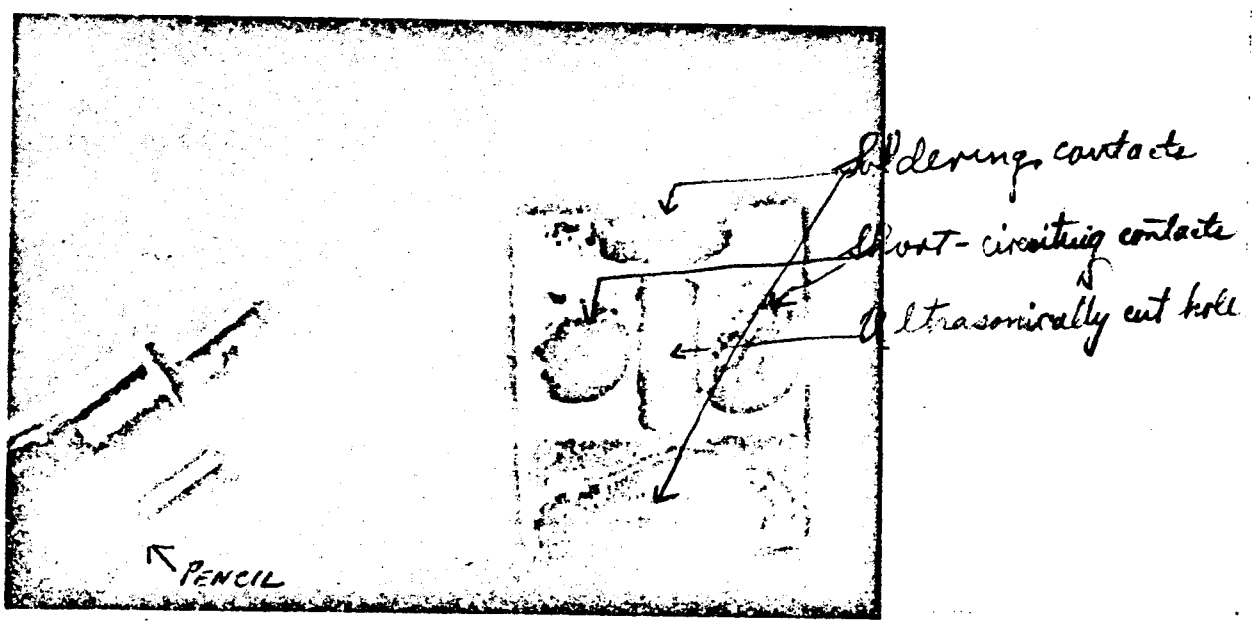

C. Under-the-microscope view

Fig. 2. Full-wave rectifier bridge fabricated by neutron-transmutation doping.

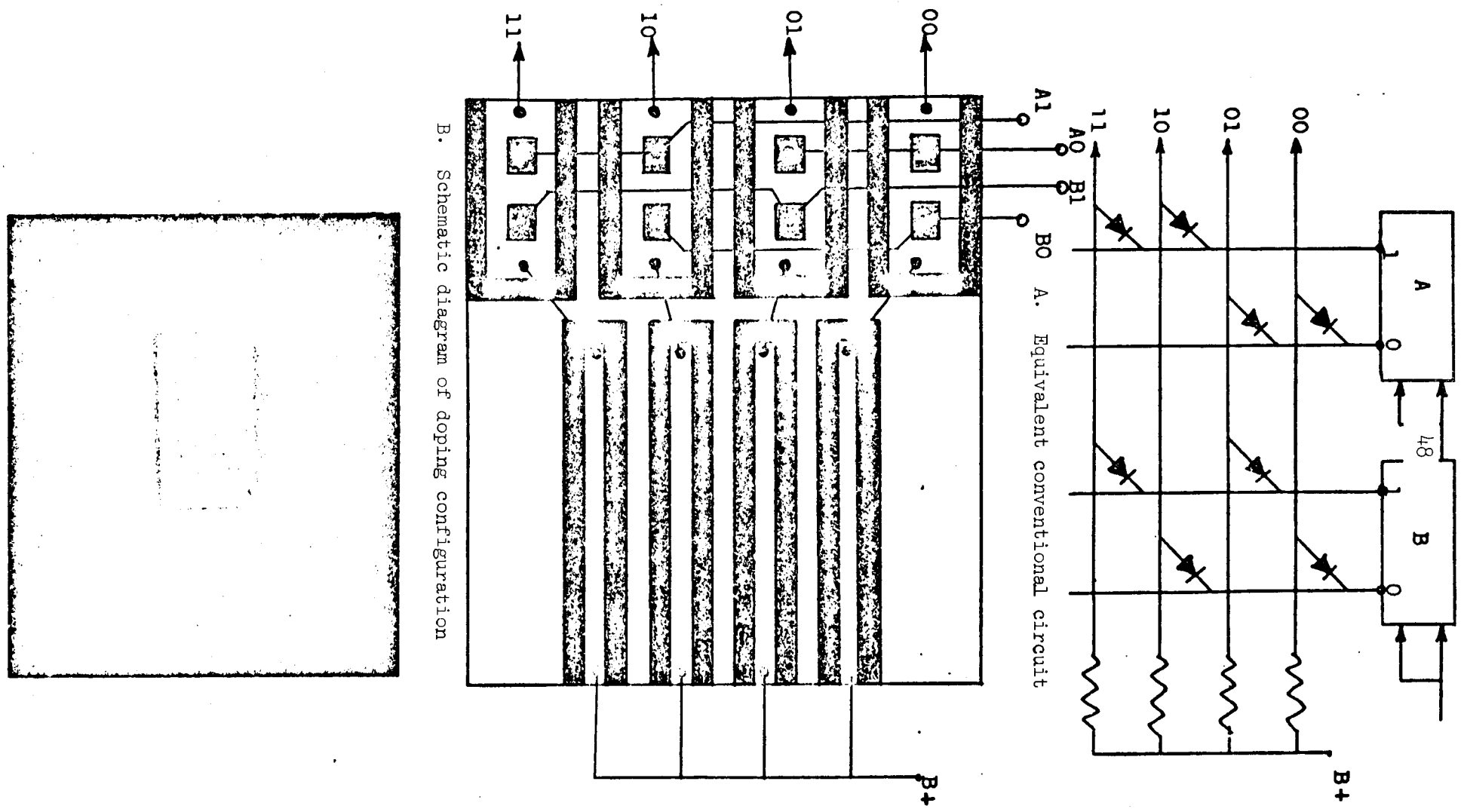

A. Equivalent conventional circuit

B. Schematic diagram of doping configuration

C. Under-the-microscope view

Fig. 3. Computer logic matrix fabricated by neutron-transmutation doping.

5. Junctions with large reverse breakdown voltages and large capacitance changes can be formed by appropriate choice of concentration gradients.

6. Intricate three-dimensional doping patterns can be produced with appropriate radiation-die designs.

7. Isolation regions can be readily formed.

8. The magnitude of the doping concentration can be precisely predicted and controlled.

9. Combinations of transmutation doping and diffusion can lead to configurations that combine the advantages of both processes.

10. Transmutation doping has a number of processing advantages. It is a one-step process. It can be performed at relatively low temperature, thus eliminating impurity sources. The semiconductor can be protected by an oxide layer throughout the irradiation process.

11. Some evidence exists that pre-irradiated and annealed semiconductor devices, such as those produced by neutron transmutation, have greater resistance to deterioration caused by subsequent irradiation.

Cost. (5) The irradiation cost constitutes a small part of the overall cost of the final electronic device produced by neutron-transmutation doping. The cost can range from 3 to 30 cents per device, depending on the reactor, the irradiation charge schedule, and the scale of irradiation. Irradiation costs are small compared with subsequent labor costs for processing the microcircuit devices. Present point-of-sale prices range from ~$100 to $500 for a 30-component microcircuit in large-scale production. There are prospects that transmutation doping can materially lower costs of comparable devices.

For many-of-a-kind production, the following facts point to low-cost processing: (1) Irradiation costs (including capsule opening) are low. (2) Neutron-transmutation doping is significantly simpler than diffusion or epitaxy; processing of devices, which constitutes most of their cost, may therefore be less. (3) Predictability and controllability of the transmutation should result in a lower fraction of rejects than other processes can yield.

In few-of-a-kind production, the controllability and predictability of transmutation doping should lead to significant cost advantages. If the neutron

flux is known, there are no elaborate setup costs, the only one being that of fabricating the irradiation die. The predictability of the irradiation procedure avoids an expensive cut-and-try period.

Controllability. (5) Important advantages of transmutation doping are the predictability and controllability of the process in silicon and germanium. Only the following preliminary data are needed: (1) initial resistivity of the specimen, (2) irradiation-die slit geometry, and (3) neutron fluence/exposure. For about two-thirds of the specimens one can then predict directly by calculation alone: (1) spatial location of P-N junctions and of each of the resulting regions and (2) concentrations and final resistivities after irradiation and annealing.

Important characteristics of the transmutation doping process are

1. Spatial resolution obtainable between doped and undoped regions,
2. Degree of spatial control attainable in the doping (i.e., concentration gradients and doping configurations), and
3. Precision with which a dopant can be inserted in a desired concentration.

The spatial resolution will depend primarily on the thickness of the die, since the minimum width of a slit that can be etched into the die will be of the same order as the die thickness. The die thickness is a function of the shielding provided by the die material. Thus, the spatial resolution of adjacent regions doped by neutron transmutation will depend on the irradiation-die technology as follows:

Cd (natural)	1 to 2 mil
^{10}B	6 to 12 μ
^{113}Cd	3 to 6 μ

It is apparent that with the ^{10}B or ^{113}Cd irradiation-die technology, the spatial resolution attainable is comparable with that achieved in other processes. Cadmium-113 is expensive (~$1/mg), and a technology for fabricating ^{10}B dies has been studied but is not yet developed.

Concentration gradients have been controllably produced in the range 10^{18} to 10^{21} atoms/cm^4 in silicon and in a range wider by a factor of 100 in germanium. Furthermore, the gradient can be designed by adjusting the slit pattern of the irradiation die and the doping level.

The precision with which a dopant can be inserted in a desired concentration is at least 5% per irradiation. This means that if two irradiations are performed on the same specimen, a precision of 0.5% is attainable. In general, very high precision is obtainable for multiple irradiations. Even the 5% figure per irradiation is remarkably good.

Predictability of Doping Configuration (4)

The predictability of doping configuration was evaluated experimentally. Qualitatively, it was desired to determine whether the expected configurations can actually be produced; quantitatively, whether predicted resistivities were achieved. The experimental results were obtained from three radiation capsules exposed in either location A-7 of the core of the Oak Ridge Reactor (ORR) or the Pool Hanger Facility outside the core. The core facility gives an integrated thermal-neutron fluence of ~3 x 10^{20} n/cm^2 during a 3-wk irradiation. Once the reactor goes critical, access to the core is cut off; hence, the duration of irradiation cannot be controlled precisely. On the other hand, the pool capsules receive an integrated thermal-neutron fluence of the order of 1.5 x 10^{19} n/cm^2 in ~1 wk. However, the duration of irradiation and hence the fluence can be specified to within 5%. In each capsule, several doping configurations were produced in specimens of silicon, germanium, or both. The maximum information obtainable from each specimen includes

1. resistivity in each uniformly doped region,
2. concentration of majority carriers in each uniformly doped region,
3. P-N junction characteristics across each junction in both forward and reverse bias, and
4. dimensions and geometric configuration of each uniformly doped region.

The individual regions of concern are often very small——a minimum dimension of

10 mils (0.25 mm) down to one-tenth this value. Some selected results follow.

Table 1 gives data on the spatial variation of transmutation concentration in multiple-junction (striped) regions. Note the consistency of the induced concentration in similar regions.

Table 1. SPATIAL VARIATION OF TRANSMUTATION CONCENTRATION IN MULTIPLE-JUNCTION (STRIPED) REGIONS IN SILICON

Region type	Width, mils		Transmutation-induced concentration, atoms/cm^3
	Nominal	Actual	
			x 10^{15}
N	40	39.7	10.2
P	25	23.4	7.45
N	40	40	10.2
P	30	28.5	7.48
N	40	43.4	11.0
P	25	23	7.49
N	40	39.5	10.1
P	40	39.6	7.28

Figure 4 is a diagram of the concentration changes in the large-area regions of germanium specimens within nine irradiation / dies. When the solid line crosses the zero axis and the dotted line does not, a P-N junction is obtained.

The overall conclusion is that the predictability of doping configurations is very good. Some less-general conclusions can be drawn about the predictability of transmutation doping in silicon and in germanium:

1. Measurements and analysis of both the transmutation concentration and its spatial variation agree well with predicted values based on neutron-flux measurements, or on neutron-flux estimates when detailed flux measurements are not available.

2. Transmutation-induced concentrations agree well with the flux values when the values are known. However, in a new experiment, the local

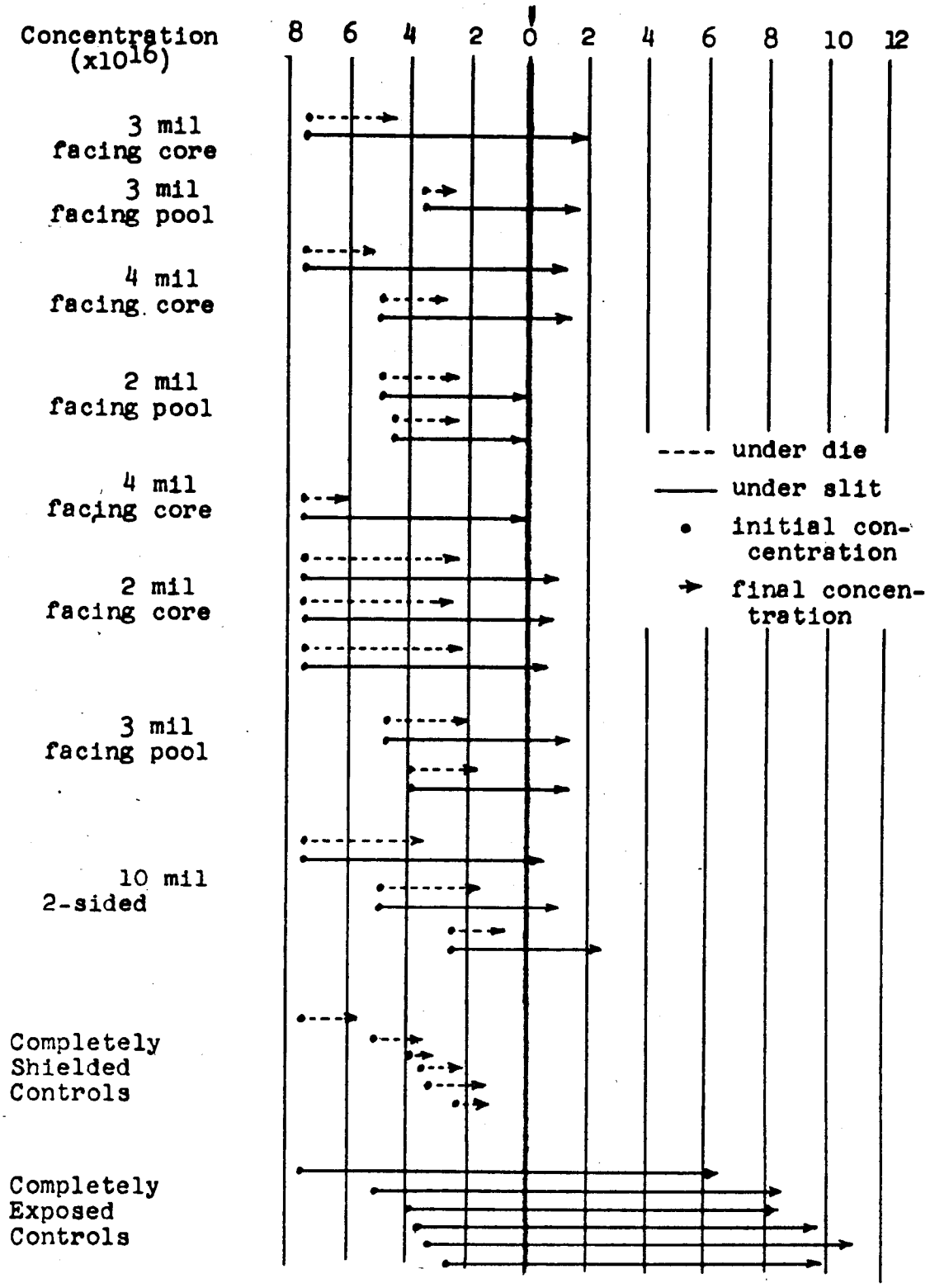

Fig. 4. Diagram of concentration changes in neutron-irradiation-doped germanium specimens.

variation of the flux within a capsule cannot be predicted in detail. Mappings of the thermal-flux variation within a radiation capsule have shown very large flux variations (as much as a factor of 4 across the capsule) depending on the arrangement and configurations of the cadmium irradiation dies. These large flux variations occur across a length of 6 in. or less in the pool facility of the ORR. Such large variations have not been found in the core irradiations.

3. In view of the strong dependence of the local thermal-flux variation within the capsule on configuration and layout of the irradiation die within the capsule, a "two capsule philosophy" must be adopted. Before the actual production capsule is irradiated, a preliminary test capsule, identical with the production capsule, must be irradiated. The purpose of this preliminary capsule is to measure with monitor foils the detailed flux variation within the test capsule. Then, material that has suitable initial resistivity can be chosen to ensure complete success with the production capsule.

4. When the flux is suitably monitored, the transmutation-induced concentration can be specified to arbitrary accuracy. When two flux monitors are attached to the capsule and read during the irradiation period, the neutron fluence can easily be specified to within 5%. When a number of flux monitors are attached to the capsule and removed according to an appropriate time schedule, it is apparent that the fluence can be specified to arbitrary accuracy.

5. The ratio of transmutations under the die to transmutations under the slit depends, in practice, on

   a. cadmium ratio at the irradiation location,

   b. irradiation die thickness,

   c. local variations in thermal flux through the capsule, and

   d. geometry of the slit pattern.

When these factors are taken into proper account, the ratio of transmutations in the unshielded region to those in the shielded region can be predicted sufficiently well to ensure the conversion of regions under the slit with high reliability.

Development of Transmutation Technology (4)

Transmutation technology includes

1. design and fabrication of the irradiation capsule;
2. irradiation of the capsule and monitoring of the neutron fluence exposure;
3. design and fabrication of irradiation dies;
4. photoetching of the irradiation die pattern;
5. packaging of the irradiation die within the irradiation capsule;
6. postirradiation processing of the semiconductor specimens and post-irradiation measurements;
7. preirradiation measurements and selection of semiconductor specimens and irradiation conditions; and
8. semiconductor-device processing, including surface metallization, oxide deposition, and attachment of contacts.

Brief discussions of these areas of work follow.

The irradiation capsule must provide radiation and thermal protection, be designed for easy opening in a hot cell and expendability, and be watertight and compatible with the reactor water. The most convenient solution to these requirements is a flat-plate design (Fig. 5). The capsule consists simply of two aluminum or stainless-steel plates, each 1/2 x 3 x 7 in. A rectangular recess is milled to a depth of ~100 mils in the inner surfaces of the plates. The irradiation-die packets are placed in this recess, and a compressible lead gasket is laid on the recess rim, the two plates are then bolted together. The pressure flattens the gasket, which provides a watertight seal.

The capsule must be irradiated in a reactor location which has adequate thermal flux that is fairly uniform before the capsule is inserted, low cadmium ratio, ease of access at all times, and provision for monitoring any flux

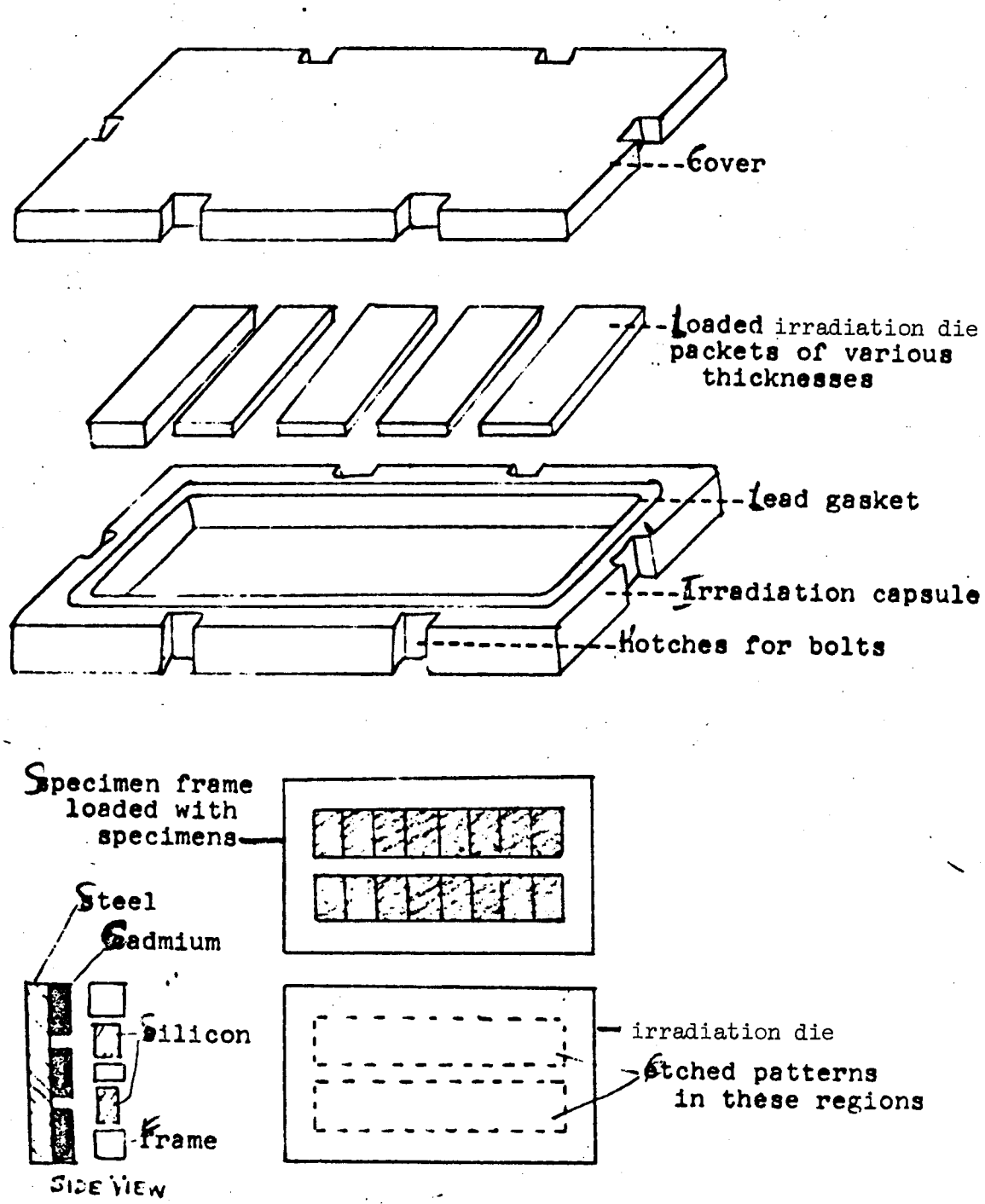

Fig. 5. Schematic views of typical flat-plate irradiation capsule and packet assembly.

asymmetry. The pool location P-4 in the ORR meets these requirements, with a thermal flux of ~2 x 10^{13} n/cm^2·sec and a cadmium ratio in the range 20 to 40. Access to the capsule can be had at all times by simply lifting the hanger to which the capsule is attached. A 3:2 front-to-back asymmetry in the flux is present.

Photoetching is the most practical and satisfactory method for making irradiation dies. Photoetching requires thin sheets of cadmium (2- to 10-mils thick, depending on the purpose) bonded to a strong substrate material that is substantially transparent to thermal neutrons. Both steel and copper have been used successfully in thicknesses of 20 to 50 mils; the cadmium is bonded to the substrate metal by cold-rolling. The only photoetching problem is etching the photoresist pattern to engrave the cadmium. Techniques were developed that give high etch factors.

The irradiation-die package is a three- or five-layered sandwich in which the semiconductor specimens are immobilized to within 1 mil. A number of the packages are fitted within the irradiation capsule. The package holds the specimens tightly against the irradiation dies and provides a convenient means of loading the capsule and of unloading the specimens in a hot call. A typical and convenient semiconductor-specimen size is ~100 x 200 x 10 mils.

Postirradiation processing of the semiconductor specimens includes annealing to remove radiation-produced defects, etching and staining to reveal doped region configurations, testing for semiconductor type (P or N), and measuring of resistivity and concentration.

A key element in the design of transmutation-doped devices is the selection of the specimen resistivity together with the irradiation conditions. The irradiation conditions can be summarized in two variables: the total thermal neutron fluence, which can be specified to within 3%, and the B/A ratio (transmutations under the die to transmutations under the slits), which can be specified to within 10 to 20% based on previous experience.

The techniques required in the manufacture of SFET's and integrated circuits were applied to some transmutation-doped specimens. They include the production of uniform insulating oxide layers of predictable thickness, the evaporation of contacting metallic films onto specific regions, and the attachment of conduction leads to small selected areas. Ways were developed to form and use high-precision masks in the final processing of the neutron-transmutation-doped semiconductors.

Complex Microcircuits (3)

The extension of neutron-transmutation doping to the fabrication of complex microcircuits in silicon required new methods for

1. predicting the spatial pattern of the neutron flux when irradiation dies are used;
2. applying silicon dioxide technology to transmutation-doped configurations;
3. fabricating irradiation dies by use of ^{113}Cd integrally plated onto silicon wafers and of irradiation capsules for silicon wafers;
4. designing microcircuits compatible with transmutation-doped configurations;
5. etching irradiation dies, oxides, and metallization layers to high resolution; and
6. making good electrical contacts to transmutation-doped silicon.

Two applications of microcircuit fabrication were studied for which transmutation appears to have unique capabilities:

1. failure-free microcircuit doping over large areas (an entire wafer) taking advantage of the uniformity of the neutron flux and
2. bi-type high-resistivity silicon substrates that can be processed subsequently by diffusion into complementary MOS circuits.

Fabrication of bi-type high-resistivity silicon substrate material was demonstrated. Furthermore, although large-area microcircuits have not yet been produced in this work, the principal difficulties seem well understood. The primary obstacle was that no single specific irradiation location has been available in the one reactor (ORR) where known and

reliable neutron-flux parameters could be applied in the capsule designs. A successful irradiation requires a neutron fluence that is controlled within a precision of 10 to 20%. Thus, because the necessary information for their various irradiation locations was lacking, one capsule was overirradiated and two were underirradiated. Nevertheless, the entire processing method and procedures for microcircuit production were developed, and it was shown that all the required operations can be performed.

The advantages of transmutation doping were enumerated above. Compared with diffusion and epitaxial deposition, the technique also has certain disadvantages:

1. The maximum dopant concentration attainable in silicon is relatively low, usually in the 10^{15} atoms/cm^3 range. It does not seem economically reasonable to exceed 5×10^{16} atoms/cm^3.
2. The spatial resolution of doped regions obtainable by transmutation doping is considerably inferior to that obtainable by diffusion or epitaxy. Transmutation doping requires an irradiation die at least 5 mils thick for natural cadmium, or at least 0.6 mil thick for ^{113}Cd. Since these dies must be etched and the etch resolution corresponds to the cadmium thickness, a minimal spatial resolution of 5 mils for natural cadmium or 0.6 mil for ^{113}Cd is obtained. Although the 0.6-mil resolution is not too much coarser than that obtainable for surface resolution by diffusion, the natural-cadmium resolution is much coarser.
3. Whereas the diffusion process permits diffused-region widths parallel to the surface to be controlled to within 1 μ, this control is not possible by transmutation. To obtain a thin doped region parallel to the surface by transmutation techniques, it is necessary to use the inversion region under an oxide layer grown on the silicon surface.

In view of these disadvantages, silicon microcircuits that use bipolar transistors do not seem to be practical because of the difficulty in controlling

base-region thickness to within a few microns. However, those that use MOS transistors of the SFET type would seem to be practical, because these transistors use the thin inversion region under an oxide. In an MOS microcircuit, the role of transmutation doping is to produce electrically isolated regions that can serve as the source and drain of an SFET whose inversion region extends between them under the oxide surface. The unique possibility for transmutation in this application is to produce small doped regions free of defects over a large-area silicon wafer. To do this, it is necessary to obtain maximum resolution for adjacent doped regions. This required the use of ^{113}Cd as the irradiation-die material.

Another economically useful application exists for transmutation techniques in silicon microcircuitry that would not require ^{113}Cd. This is the preparation of bi-type doped regions of high resistivity in a silicon wafer, for subsequent processing into complementary MOS microcircuits by diffusion doping. Complementary MOS circuits have the advantage of lower power requirements and lower power dissipation by a factor of $\sim 10^3$ over conventional microcircuits. The term "complementary" implies that both P- and N-channel SFET's are needed in the same circuit, which in turn requires that P- and N-type substrates be adjacent to each other on the same silicon crystal. Furthermore, these substrates should be of high resistivity (10^{14} to 10^{15} atoms/cm^3 concentration) for best performance. It is not possible to fabricate such substrates by diffusion, since these low concentrations cannot be obtained. However, these specifications can be readily met by transmutation. The sizes of the individual P- and N-type regions that are to be substrates for further diffusion processing are of the order of 10 to 30 mils, thus permitting the use of the relatively inexpensive natural-cadmium irradiation dies.

The irradiation capsules used in the work on complex microcircuits were simple aluminum plates with niches to hold circular silicon wafers. These plates were placed between aluminum covers, and reactor water was circulated through them. Cadmium-113 was electroplated onto the silicon wafers over an oxide layer,

and the irradiation-die pattern was photoetched into the cadmium. Thus, the irradiation die is an integral part of the silicon wafer. After irradiation, the irradiation-die pattern is acid-etched off the silicon in a hot cell. The radioactivity is then low enough to permit the silicon wafer to be shipped through the mail.

Spatial Doping Patterns in Silicon (4)

As was the case with germanium, irradiations that successfully produces neutron-transmutation doping require precise knowledge of the neutron flux within the irradiation die and of the proper duration of irradiation. This information is gained by use of cobalt flux-monitors to determine the neutron flux outside the irradiation capsule and by irradiating a mock-up capsule to measure flux values within the capsule. Because the ORR schedule did not permit two-capsule experiments, the control of irradiations in this work was less exact than desired. Therefore, actual dopant concentrations were likewise significantly different from those desired. In most cases, the doped pattern can be predicted quantitatively from the initial irradiation-die configuration, the neutron fluence, and the initial dopant concentration. It is possible to calculate the flux at a point within the semiconductor under a given die pattern. This flux is proportional to the total solid angle of view that is unobstructed by cadmium. Calculations based on such a simple "optical model" can account for the distinctness or for the coalescence of separate doped regions.

The predictability of the doped pattern is very significant; it is potentially one of the most important advantages of the transmutation-doping process. The mathematical predictability of the doping pattern in the silicon by use of an optical model of the irradiation die makes it apparent that a digital computer code could be used to design and analyze irradiation-die patterns. The mathematical prediction of a detailed doping pattern must take into account three sets of factors:

1. The total solid angle seen at any point within the silicon, assuming that the cadmium is opaque. If the neutron flux were constant all

around the specimen and if the flux had an isotropic angular distribution (over 2 π steradians), one could calculate the pattern directly from this simple optical model.

2. The variation of the flux over the surface of the irradiation die, due to absorption by the cadmium, and the variation of the neutron angular distribution. This effect may be called the flux depression by the irradiation die.

3. Gross variations in the flux across the capsule due to the reactor.

It was not deemed desirable to write a computer code in the present work. Nevertheless, analytical calculations based on this model were performed for a number of simple geometries. The calculations produce sets of isoflux (isoconcentration) surfaces that are very useful and illustrative. These surfaces have guided the design of irradiation dies to produce desired doping configurations by transmutation.

The analytical calculations of transmutation-doped configurations based on the simple optical model will indicate the degree of doping-geometry control achievable by transmutation techniques in silicon. In practice, doping geometry is controlled by (1) fabricating irradiation dies with the desired slit pattern, and (2) selecting the proper combination of initial P-type concentration and neutron fluence / exposure for the silicon. The calculations therefore permit one to predict the final junction location and the resulting concentration gradient for a given initial P-type concentration and fluence / exposure for various irradiation-die patterns. Since concentration gradients as well as isoflux lines are obtained, the error limits of a particular irradiation-die design can also be estimated. Calculations were made for five slit configurations:

1. a single long slit in an otherwise opaque irradiation die,
2. a single long absorbing stripe on an otherwise open surface,
3. two adjacent long slits and other long multiple slit configurations,
4. circular hole in an otherwise opaque irradiation die, and
5. circular absorbing disk in an otherwise open surface.

The single-long-slit flux pattern can be used to approximate a finite single slit, except near its ends. The single-long-absorbing-stripe flux pattern can be used to approximate a finite absorbing stripe, except near its ends. The two-adjacent-slits flux pattern can be constructed from the superposition of patterns from two single slits. Since neutron flux is a scalar quantity, superposition calculations can be used to determine any complex irradiation-die configuration that consists of individual elements whose flux patterns are known. The calculation consists in summing the contributions to the flux at each point from each of the individual source elements that make up the irradiation-die pattern. Thus, the flux pattern for multiple-slit configurations, for example, can be calculated as the superposition of single-slit contributions.

The circular-hole pattern can be used in a gross sense to represent the flux pattern for a square hole or for any small finite slit. The pattern of an irradiation die that contains a number of holes, or of holes and slits, can be calculated by superposition. The circular-disk flux pattern can also be used in a gross sense to represent any small finite absorbing area.

In this discussion, for simplicity, the effects of nonthermal neutrons (epithermal-energy neutrons) are ignored; they account for ~20% of the transmutations in the unshielded silicon. Thus, the discussion will be concerned with the 80% of the transmutations in silicon that are produced by thermal neutrons.

First, consider completely exposed specimens of silicon. For an irradiation thermal-neutron fluence of 2.25×10^{19} n/cm^2 (as measured by a cobalt monitor adjacent to the specimen), one produces 40×10^{14} N-type impurity atoms per cubic centimeter in the silicon. If one subjects specimens of various initial P-type concentrations to this irradiation, those whose initial concentration is $>40 \times 10^{14}$ atoms/cm^3 will remain P-type, whereas those whose initial concentrations are $<40 \times 10^{14}$ atoms/cm^3 will become N-type.

Let the silicon specimens be placed against a sheet of irradiation die material (cadmium). For simplicity, the irradiation die will be considered to be completely opaque to thermal neutrons and very thin. For the same irradiation, the specimens will now obtain an N-type dopant concentration of only 20 x 10^{14} atoms/cm^3, since half the unperturbed incident flux has been obstructed by the irradiation die. Thus, only those specimens whose initial concentration was <20 x 10^{14} atoms/cm^3 P-type will be converted to N-type, whereas all the others will remain P-type.

Long Slit in an Irradiation Die. (5)

Now consider an irradiation die in which the silicon is completely enclosed by the neutron absorber except for a single long slit on one side (Fig. 6). (The one-sidedness of the slit pattern leads to the term "one-sided irradiation die," since the other side is completely opaque to thermal neutrons.)

The neutron flux entering through a long slit (hence the induced dopant concentration) forms a two-dimensional pattern in the plane perpendicular to the slit. The magnitude of the flux at any point under the plane of the upper die is proportional to the angle formed by the lines that connect the edges of the slit to the point in question. Figure 7 shows a point O beneath the center of the slit, which intercepts all neutrons with directions within the angular arc AOB. If a circle is constructed that passes through points A, B, and O, the angle θ is measured by one-half the intercepted arc AB. This same angle is also formed by connecting points A and B to any point on the circle. Thus, the circle drawn in two dimensions represents a three-dimensional cylindrical surface that is an isoflux surface. Every point on that surface sees the same neutron flux and thus receives the same concentration of induced impurities per cubic centimeter along that surface.

When a specimen of silicon is irradiated through an irradiation die, the P-N junction is formed along that surface where the induced impurity level exactly matches the initial concentration. On one side of the junction, the induced impurity level exceeds the initial concentration, and the material is

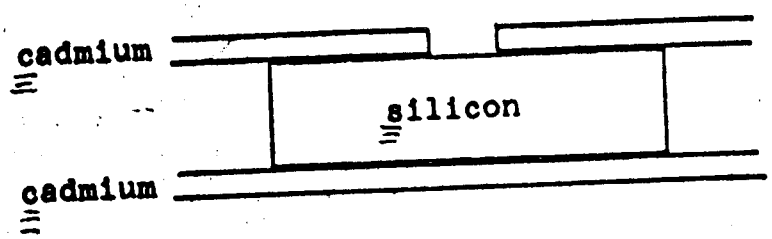

Fig. 6. Cross section of a one-sided irradiation die.

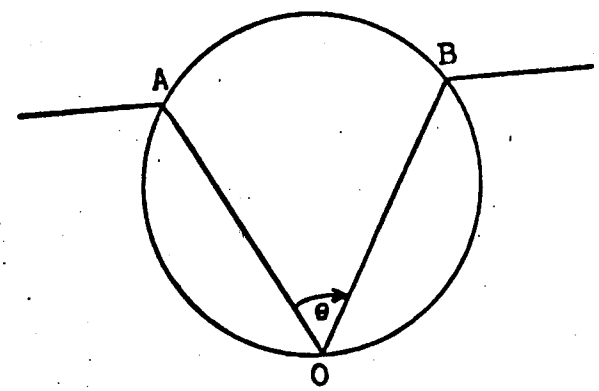

Fig. 7. Isoflux lines along a circular locus.

converted to N type, whereas the induced impurity level on the other side is insufficient to convert the P-type material.

The radius r of the isoflux circle and the distance h of the circle from the plane of the irradiation die are given as functions of the incident-flux angle θ and the half-slit width w (Fig. 8) by the relations

$$h = w \cot \theta$$

$$r = w \csc \theta$$

since $\phi/2 = \tan \theta = w/h$.

The angle ϕ is indicated in the diagram.

Now denote by 100% the maximum flux level possible between the two irradiation dies. Then draw a series of arcs that connect the edges of the die and indicate the percentages of the maximum flux along each arc. Figure 9 shows the result.

It is plain from the geometry that the "100%" arc is the line that connects the edges of the slit. For the points on the surface of the semiconductor specimen between the edges of the slit, the upper die has no shielding effect; they receive the full 100% of the flux coming from the top. Of course they do not receive any flux from the bottom, since the lower die is unbroken. Thus, 100% flux is only one-half the unperturbed flux at best. Any point below that surface sees even less than the 100% on the surface because of the shielding of the die.

Now consider a set of specimens between the irradiation dies described, subjected to this irradiation, and note that those specimens whose starting dopant concentration was $>20 \times 10^{14}$ atoms/cm^3 do not convert at all. Those with $<20 \times 10^{14}$ atoms/cm^3 have a cylindrical-shaped junction produced in them.

The 75% curve corresponds to the junction shape and location in the specimen whose starting concentration was 75% of 20×10^{14} (15×10^{14}) atoms/cm^3, whereas the 30% curve corresponds to the junction shape and location in the specimen whose initial concentration was 30% of 20×10^{14} (6×10^{14}) atoms/cm^3.

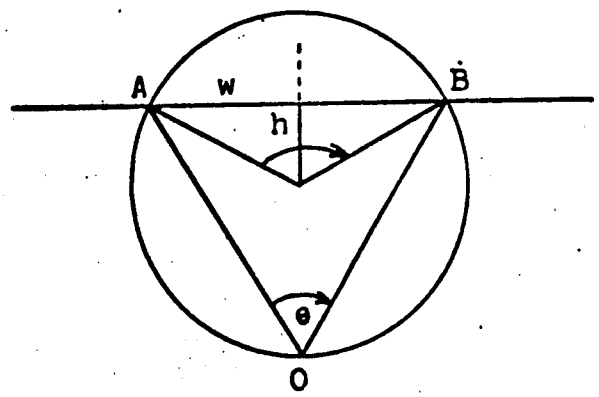

Fig. 8. Isoflux circle geometry.

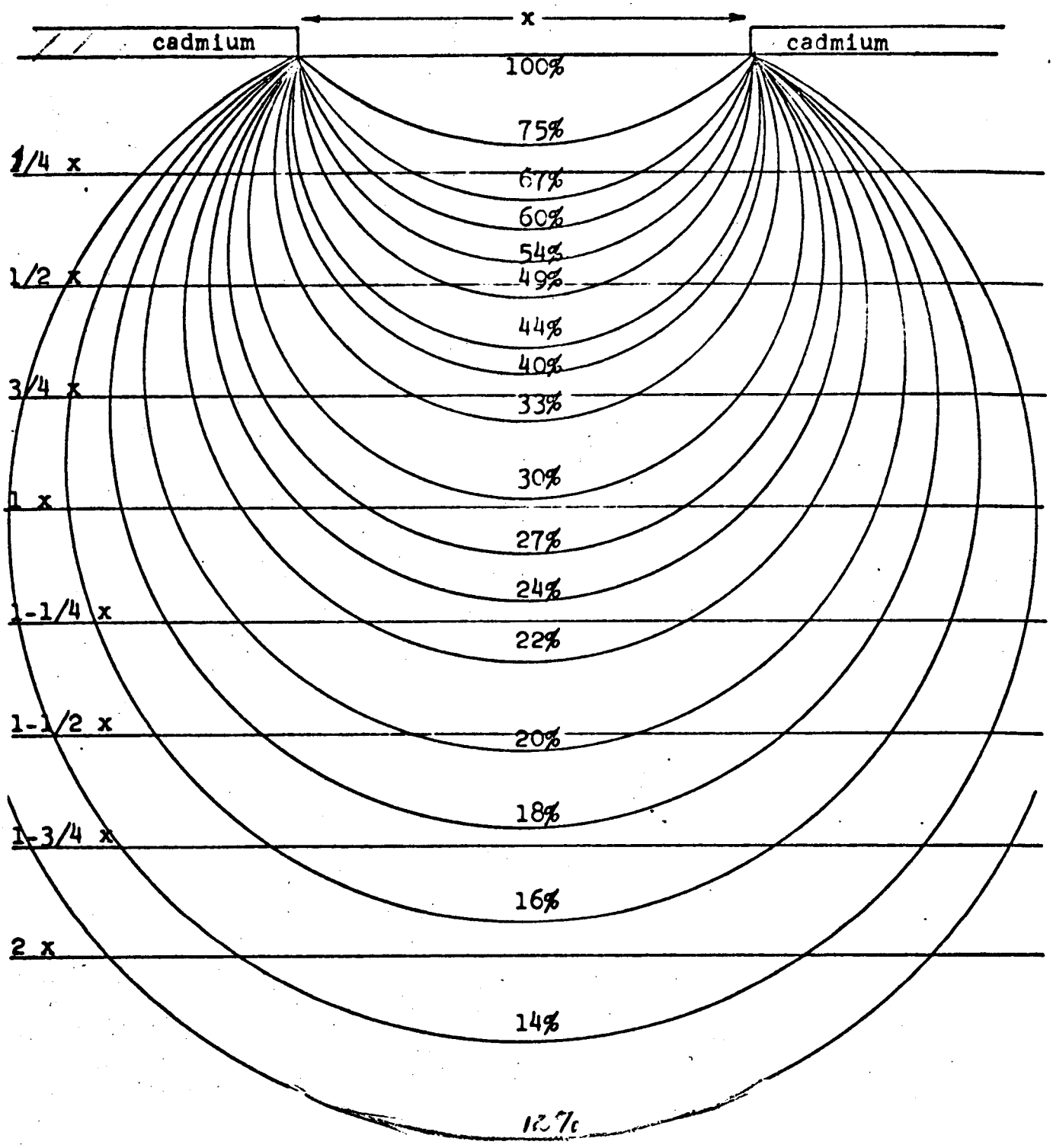

Fig. 9. Isoflux lines for an infinite slit (specimen completely shielded on bottom surface).

Figure 9 is given as a universal curve, that is, in terms of the slit width as the unit dimension. It can therefore be used to design any configuration that involves long slits in a one-sided die.

Other Configurations. (5) The long absorbing stripe on an otherwise open surface is the geometrical complement of the long open slit. Just as the slit produces an N-type cylindrical region, the long absorber stripe produces a P-type cylindrical region. Here the entire specimen is exposed (to one-half the total flux, since a completely opaque die is used on one side) except for the region under and near the neutron-absorbing stripe. The isoflux lines for this die pattern are identical in shape and location with those of Fig. 9 except that the percentage figures are 100% minus the percentages indicated on Fig. 9.

Configurations of multiple slits can be calculated at each point simply by adding the flux contributions from the individual slits. For two adjacent slits, the double-slit pattern degrades into the single-stripe pattern at lower flux surfaces.

Consider a completely opaque irradiation die with a circular hole in it. To determine the isoflux lines under a circular hole, one notes the following facts.

The area of the spherical surface formed by the intersection of a sphere of radius r and a cone whose apex is at the center of the sphere and whose half-central angle is ϕ is given by the relation $2\pi r^2 (1 - \cos \phi)$.

The fraction f of the maximum flux receivable from one side, received at the apex of the cone is given by

$$f = \frac{2\pi r^2(1 - \cos \phi)}{2\pi r^2} = (1 - \cos \phi) \qquad 0^\circ \leq \phi \leq 90^\circ$$

Isoflux surfaces, to first-order approximation, are spheres whose centers are a distance h beneath the center of the hole and whose radii shall be called r.

$\theta = 2$ where $h = w \cot \theta$, $r = w \csc \theta$.

As in the case of the infinite slit and stripe, the shielding disk is the complement of the exposed hole. There is a real advantage, however, in using shielding dots instead of exposed holes when small shallow regions are desired. When the finite thickness of the irradiation die is taken into account, it was easier to design with dots than with holes.

Adjustments for Fast Flux and Leakage of Thermal Neutrons. (5) Two significant sources of transmutation-induced impurities are the absorptions of fast neutrons and thermal neutrons that leak through the necessarily thin cadmium irradiation die. The simplest way to correct for these effects is to determine their magnitudes as accurately as possible and then to increase the initial concentration by this amount, thus nullifying the background effects. The degree to which the background values can be evaluated determines the accuracy of the final junction shape and location.

Selection of Irradiation Conditions: Design Procedure. (5) The analytic calculation procedure described above was applied to the selection of irradiation conditions for a capsule. The example consisted of irradiation / die patterns in the form of two cadmium strips with an unshielded strip between them. Detailed calculations were worked out for selecting the conditions.[3]

Semiconductor Processing Techniques (4)

Special techniques required in processing semiconductors for use in microcircuit fabrication include

1. making small-area ohmic contacts to relatively lightly doped N-type silicon;
2. growing silicon dioxide layers with good insulating properties and with modulatable inversion regions;
3. annealing silicon dioxide layers to reduce surface charge so that the degree of inversion-region modulation can be increased;
4. indexing the doped regions on silicon wafers, corresponding to specified regions on photoresist masks (the indexing is used to align the masks);

and

5. designing, fabricating, and using photoresist masks in the oxide- and metal-etching steps that are required after the doping.

Making ohmic contacts is required especially for transmutation doping in silicon because of the low N-type concentrations produced by economical transmutation. The conventional method for making ohmic contact to doped silicon (either P- or N-type) is to evaporate aluminum onto the semiconductor and bake it in. This process is satisfactory for P-type silicon, whether lightly or heavily doped. It is also satisfactory for the highly doped N-type surfaces that are used in a diffusion processing. However for the low N-type concentrations produced by transmutation, an aluminum contact is not ohmic. Modifications of conventional contact methods are therefore required that give ohmic contacts for highly doped N-type silicon.

The second and third techniques are of special importance. The MOS transistor appears to be the most useful for fabrication by transmutation techniques. The bipolar transistor, to be most efficient, requires fabrication of individual doped regions whose dimensions are measured in microns. This requirement is of marginal practicality in transmutation, where the minimum thickness of the ^{113}Cd irradiation die is ~10 μ leading to minimal doped-region widths also of ~10 μ. The straightforward way to obtain spatial region thicknesses of the order of 1 μ or less by transmutation doping is to use the inversion region under silicon dioxide, whose thickness is of this order. Hence, the MOS transistor becomes the basic active device to be used for transmutation doping in silicon. It is for this reason that the growth of oxide layers in silicon becomes the single most important processing technique for transmutation microcircuitry. This process is identical with the conventional processing steps in MOS circuit fabrication,[9,10] which consists in growing an electrically insulating oxide and annealing the oxide to ensure that the inversion region beneath the oxide can be modulated at convenient voltages. However, at present the required processing techniques are almost an art, each practitioner being required to develop his own methods.[11-13]

The indexing and masking processes are very similar to those used in diffusion processing. Because the individual transmutation-doped regions are not easily visible under the microscope by their color, some modifications of the conventional indexing and mask-alignment procedures are necessary.

For making ohmic contacts, three methods were evaluated:

1. Electroless nickel plating;
2. electroplating with a gold solution containing a P-type dopant for P-type silicon and an N-type dopant for N-type silicon; and
3. vacuum evaporation of a gold alloy with N-type dopant for N-type silicon and of aluminum for P-type silicon.

The most practical method for making good electrical contacts to low-doped N-type silicon was found to be the vacuum evaporation of gold-antimony alloys.

Three methods of thermal oxidation of silicon have been used: oxidation in dry oxygen, oxidation in wet oxygen bubbled through 95°C water, and oxidation in steam at various pressures. At first this work centered principally about the wet-oxygen method, because it is several times as fast as the dry-oxygen process, and oxides without pinholes can be obtained by avoiding condensation of water on the specimens. However, these oxides when used in SFET gates had so many surface states associated with them that one could not modulate inversion-layer conductivity at electric field strengths below breakdown. When the dry-oxygen method was used, it was much easier to obtain SFET action. A typical procedure that gives SFET action includes 15 min in dry oxygen, 80 min in wet oxygen, and 15 min in dry oxygen to give an oxide thickness of 4000 Å. Bulk conductivity modulation was observed at 16-V bias, which corresponds to $\sim 7 \times 10^{11}$ charges/cm^2. The improvement was almost certainly due to the absence of water in the initial oxidation. The use of exclusively dry oxidation with certain precautions provided a considerable further reduction in surface-state density. Eventually the dry-oxygen method was used almost exclusively. Its disadvantage is the long time (several hours) required to obtain a film thickness of several thousand angstroms. Its advantage is that cleanliness of the oxide is much more

easily obtained, which leads to a higher fraction of oxides with good inversion-region modulation.

Annealing of the oxide to remove surface charge is required. The action of an SFET depends on the ability to vary the width of the inversion region under the oxide, which in turn depends on the fixed charge density at the silicon—silicon oxide interface. To modulate the inversion-region width, it is usually necessary to anneal the oxide after it is grown. A two-step annealing procedure is fairly common in the semiconductor industry for removal of surface charge, Q_{ss}, in MOS devices.[12] This annealing is to be distinguished from that used to remove radiation damage in irradiated silicon. The first annealing step, however, will be efficacious for simultaneously removing surface charge and radiation damage. There are two sources of Q_{ss} on silicon oxide. One (called "slow surface states") is the mobile impurity ions, principally Na^+, which can be avoided by eliminating "dirt," principally salts and organic compounds, in the course of surface preparation. A Q_{ss} $<2 \times 10^{11}$ electrons/cm^2 can certainly be obtained, with regard to this source. The other (called "fast surface states") is thought to be due to silicon ions diffusing a hundred angstroms or so into the SiO_2. Such sources can be reproducibly controlled over a range of 10^{10} to 10^{12} electrons/cm^2 by appropriate annealing and ambient conditions. If SiO_2 is grown from dry oxygen and is quickly quenched, the Q_{ss} is $\sim 2 \times 10^{11}$ electrons/cm^2; this process gives an easy-to-modulate oxide. If, however, it is permitted to cool slowly in oxygen, air, or water vapor (or even in nitrogen or argon gas that contains trace impurities), the Q_{ss} will be high ($\sim 10 \times 10^{11}$ electrons/cm^2). Therefore, one would suggest a 1-hr anneal at 900°C in dry high-purity nitrogen or argon after the samples get back from the reactor. The purpose of this high-temperature anneal is to eliminate the defect structure at the silicon—silicon dioxide interface; however, it cannot be eliminated completely. There still exist unattached silicon bonds, which act as charge centers unless they are compensated—for example, by introducing hydrogen

ions into the layer.

The conventional photolithographic technique in semiconductor processing is as follows:

1. A thin layer of an organic-monomer photoresist material is deposited uniformly on the surface to be etched. When this material is exposed to ultraviolet radiation, it polymerizes and becomes resistant to acids.
2. The photoresist is exposed to ultraviolet radiation through a precise photographic masking transparency. The surface is then immersed in an acid, and the nonpolymerized material is washed off. The polymerized material remains to protect the surface from etching solutions.
3. An etching solution is applied, and the unprotected surfaces are etched away. If the surface is an oxide, for example, diffusion can then be performed through the slits in the oxide.
4. A new surface is then formed, either by further oxide growth, by evaporation of a metallic contact layer, or by exposure of the semiconductor surface by etching and cleaning. The photolithographic process is then applied to the new surface in the same way as described above.

At least three photographic mask transparencies are used for processing a transmutation-doped slice:

1. for etching slit pattern in the cadmium irradiation die before irradiation.
2. for etching slit pattern in the oxide for metallic contacts to the silicon (this is done after irradiation).
3. for etching the required electrical interconnection pattern on a metallic film evaporated onto the oxide.

Since the transmutation pattern is not visible on the wafer, special markings are required for the highly precise mask alignment. Several methods can be used. One is to scribe a set of reference marks on the wafer. An etching procedure can also be used in which tiny cross marks are etched into the oxide in a precise

pattern, which can be produced by conventional photoresist techniques. The oxide-modulation properties are not affected by this treatment. The use of high-precision registry masks requires that wafers be polished to a maximum surface irregularity of 1 mil.

Design of Microcircuits (4)

Except for simple diodes, circuit components cannot be fabricated by transmutation techniques without additional processing. The function of transmutation is simply to insert a pattern of isolated doped regions in a silicon base. It is then necessary to grow modulatable oxides and to deposit metallization patterns. The microcircuits that can be considered will therefore consist of

1. SFET's,
2. resistors in the kilohm and megohm ranges,
3. capacitors, and
4. diodes.

It is unlikely that bipolar transistors can be produced by transmutation, because the required degree of spatial control is not sufficiently precise, even when ^{113}Cd irradiation dies are used. Therefore, the SFET must be the principal active element in the microcircuit.

These components, which are discussed above, can be made by first doping a desired spatial pattern in the silicon; the function of the transmutation is to produce nearby doped regions that are electrically isolated from one another. A modulatable oxide is grown over the doped pattern, and a pattern of electrical contact holes is then etched into the oxide. Finally, a pattern of metallic contacts and metallic interconnection strips is evaporated over the insulating oxide layer.

One important potential area of use for transmutation doping in silicon is the production of bi-type silicon wafers for subsequent processing into complementary MOS circuitry. Transmutation doping in microcircuitry is potentially capable of doping reproducibly over a large area without any failed elements.

Reproducible doping demands relatively small spatial variation in the flux over the dimensions of a silicon wafer (~1 in.). Therefore, wafers must be separated from one another during irradiation by ~3/4 in. Device imperfections caused by the diffusion process, by crystalline defects in the silicon, or by small dust particles would be avoided by transmutation doping. In the present state of the semiconductor art, for silicon specimens with doping patterns greater than 80 by 100 mils the fraction of rejects becomes excessive. If transmutation doping can produce silicon wafers in which closely spaced doping patterns with dimensions of 500 by 500 mils (0.5 by 0.5 in.) are present without imperfections at least 25% of the time, this doping could be economically attractive for some applications.

As an example, consider large-scale read—write memories of large capacity on a single chip. Such a chip could replace a magnetic-core memory for high-speed digital-computer applications, or a magnetic-drum memory for lower-speed applications. A prototype circuit for such a device might be a 2- or 4-phase shift register. The single stage of a 2-phase register might consist of six SFET's and two capacitors and store a single bit. By setting 200 such stages in series in a closed loop, one can circulate 200 bits in each loop in 5 μsec (25-nsec delay time per stage). A chip with 1×10^4 circuits could contain 50 such loops, corresponding to a 50-bit word. Thus, a single chip could store 200 words of memory, each comprising 50 bits; a 16-K memory would consist of 80 such chips plus two pulse-generator clocks. The economics of fabricating such a read—write memory may be appraised roughly. If a silicon chip 500 by 500 mils can be doped by transmutation without defects and if subsequent oxide etching and metallization are defect-free, there will be $\sim 1 \times 10^4$ circuits on the chip, each capable of storing one bit, at a circuit density of 25 square mils per circuit. Present large memories cost ~3 cents per bit storage capacity; the cost can be expected to be reduced to between 1 and 2 cents per bit in a number of years. Thus, a large chip would cost at least $100. The extrapolated fabrication cost of such a chip by transmutation is considerably less than this if such chips are produced in significant volume.

The fabrication of large defect-free circuits requires large-scale uniformity in the semiconductor processing as well as in the doping in order to produce large regions in which defect-free doping patterns can be inserted. In particular, one requires uniformity of the ^{113}Cd plating and of the silicon surfaces prior to oxidation. Streak- and scratch-free ^{113}Cd plating of uniform thickness can be achieved, and silicon surfaces can be smoothed to a tolerance of 1 mil by appropriate lapping and polishing.

Four microcircuits, embodying three to ten MOS transistors each and more complex than the two discussed above, were studied for fabrication by transmutation processing; they were

1. AND-OR-NOT gate for computer applications,
2. two-phase shift register,
3. two- or three-stage amplifiers, and
4. multivibrator oscillators.

Of these, the multivibrator oscillator is selected for illustration here. Figure 10 shows the circuit diagram and the cadmium and metallization patterns required. The resistances R are obtained by using inversion regions; MOS transistors, denoted by Q, use inversion regions with separately connected gates. Metallized layers over an oxide are used for capacitors. The etch pattern through the oxide is shown as the dark regions.

Fabrication of Irradiation Dies and Capsules (4)

It was necessary to prepare adjacent doped regions with spacings of about 2 to 4 mils, for fabricating SFET's having appreciable amplification. This resolution can be accomplished only by use of irradiation dies made of ^{113}Cd. Thus, techniques were developed for depositing thin layers of cadmium and for photoetching detailed slit patterns into them.

Cadmium layers of 0.6- to 1.2-mil thickness were used. Cadmium in these thicknesses can be etched with relative ease. Although, for etching, a 1-mil layer of cadmium is considered to be thick and a nonvertical etch wall is obtained, etch factors higher than 1 (corresponding to a 45° etch wall) are usually obtained.

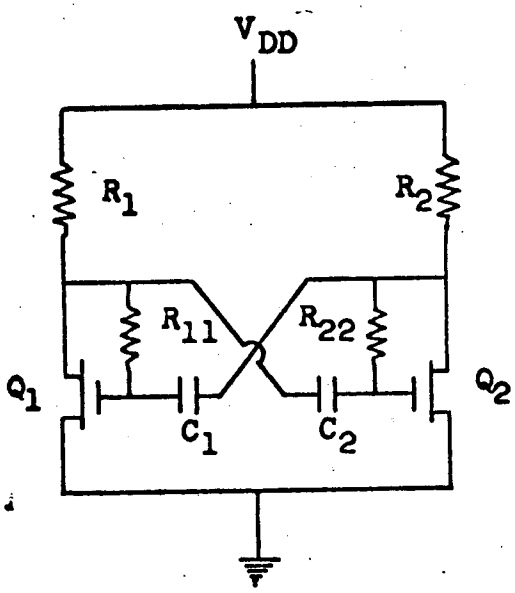

A. Circuit Diagram

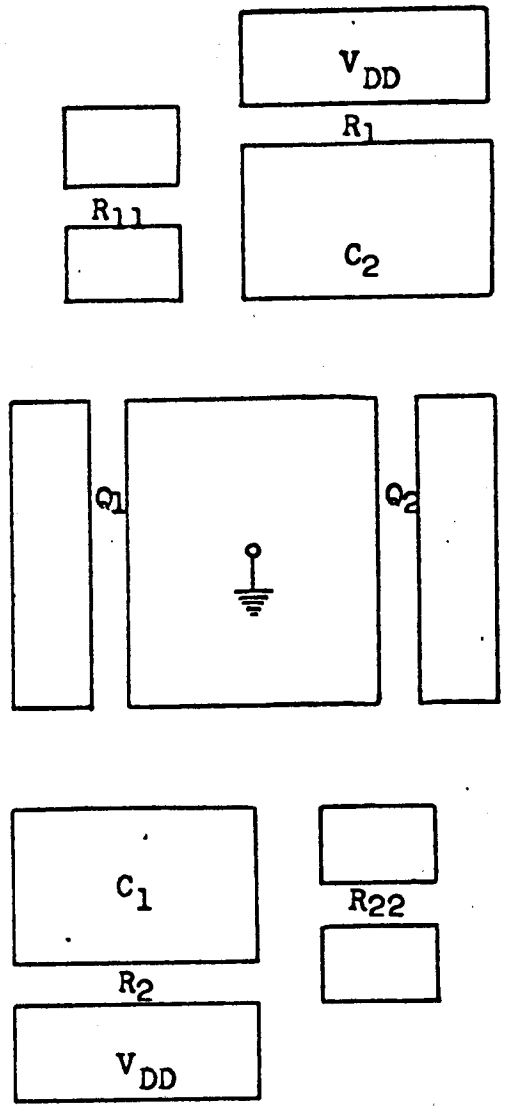

B. Cadmium Pattern

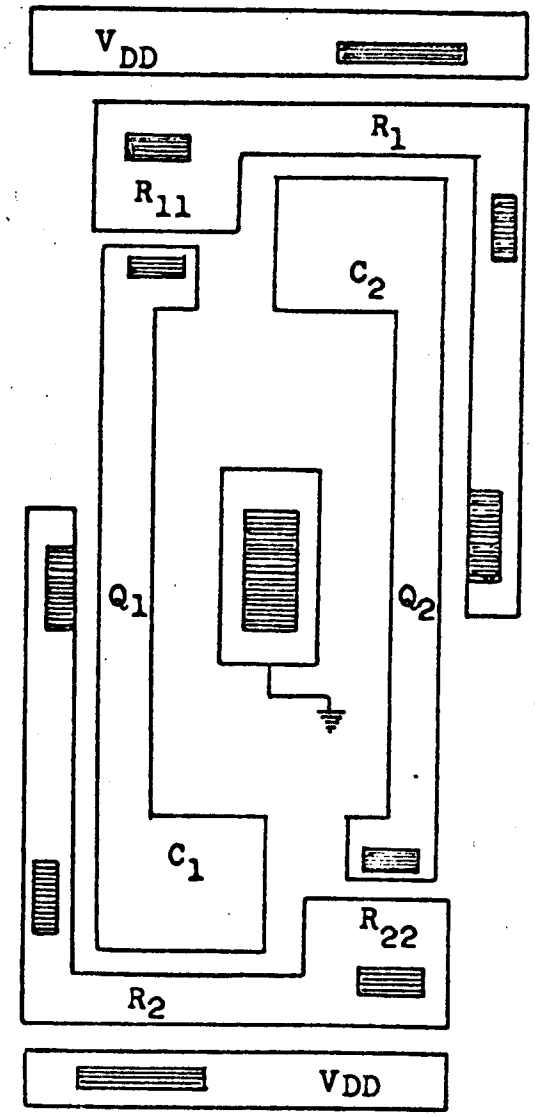

C. Metallization Pattern

Fig. 10. Multivibrator oscillator.

when necessary. Ammonium nitrate solution (60 g/liter) is an effective etchant, and conventional photoresist protects the cadmium. Such a solution will etch through a 1.2-mil cadmium layer in ~30 min.

A more difficult problem was to deposit the ^{113}Cd on the silicon. An electrolytic method was developed for depositing the ^{113}Cd directly on an oxide layer grown on the silicon wafer. Use of an electroplated irradiation die, integral with the specimen surface, avoids the problem of motion of the irradiation die and specimen relative to each other. When close spacings are the objective, the irradiation die will be one-sided, with an opaque cadmium sheet on the opposite side of the wafer.

Some work was done on natural cadmium irradiation dies for use in fabricating large-area SFET configurations and bi-type silicon patterns consisting of alternate layers of high-resistivity P- and N-type material. These dies were fabricated mechanically, the simplest method for the relatively large patterns (minimum spatial resolution of 10 to 15 mils) possible for natural cadmium.

The irradiation capsules were much simpler and more easily fabricated than those used to fabricate single components. The reactor pool water was permitted to circulate freely in each capsule, and the distance between specimens was greater. Also, the silicon specimens and wafers were simply seated in recesses of the aluminum capsule.

<u>^{113}Cd Dies</u>. (5) A thin layer (0.5- to 1-mil thick) of ^{113}Cd is an effective irradiation die, since the thermal absorption cross section of ^{113}Cd is about eight times that of natural cadmium. The use of such a thin layer will permit line resolution of 0.5 to 1 mil in the doping, which is about the resolution attained in commercial doping. Cadmium-113 was plated both directly onto silicon and onto an oxide layer grown on silicon. The latter was more convenient and was perfected; it is described briefly here.

A silicon wafer of suitable resistivity receives, by photographic reduction and masking, a pattern of areas to be plated with ^{113}Cd. The wafer is then oxidized to an oxide thickness of ~4000 Å. A corner of the wafer is tested to

determine that the oxide will withstand an electric field and have a low surface-state density. A thin layer of Nichrome (a few hundred angstroms thick) is vacuum-evaporated onto the oxide. Then a layer of nickel or copper is electrolytically deposited on the Nichrome. The ^{113}Cd is then plated onto the nickel. Whereas the Nichrome and nickel layers are $<1\ \mu$ thick, the ^{113}Cd thickness must be at least 10 μ. A 30-μ layer (~1.25 mils) will be electrolytically deposited on a 1-in.-diam wafer in ~40 min at a current of 50 to 100 mA. A conventional cadmium-plating solution is used in which ^{113}CdO is present.

The effect of cadmium removal on the properties of the oxide layer must also be considered. After the irradiation, the cadmium layer, as well as the thin films underneath it, must be chemically removed in the hot cell, but the oxide layer must remain. The cadmium layer and films are removed with a solution of nitric acid or aqua regia. However, a fast etch on the oxide layer is also performed to remove any diffusants in the oxide. In this process the oxide film thickness will be decreased from 4000 to ~3000 Å. It is necessary to verify that electrical characteristics of the oxide, that is, the ability to modulate the inversion-region thickness under the oxide, are preserved after the fast etch following irradiation. This fast etch is comprised of buffered hydrofluoric acid, which removes ~1000 Å of oxide per minute. Hence, a 1-min etch will be required.

For high-resolution circuits, refinements in the plating technique were needed to eliminate streaks in and adhesions to the plating and to increase the adherence of the heavy plate (up to 1.5 mils) to the evaporated layer on the oxide.

Natural-Cadmium Dies. (5) Natural-cadmium irradiation dies were made of nominally 10-mil-thick cadmium to give clear-through doping configurations. They were fabricated mechanically rather than by etching. The procedure consists in drilling out holes and punching out inserts by clamping the material between steel pieces ~5/32-in. thick.

Irradiation Capsule. (5) The irradiation capsule used in this work differed from the previous capsules (Fig. 5) in several important ways:

1. The capsule was completely open to the water of the reactor pool. This arrangement tends to prevent any flux depression by the capsule.
2. The silicon specimens, encased in their irradiation dies, were separated from each other by ~3/4 in., which is more than the mean free path of a thermal neutron in water. This spacing should prevent "crosstalk" between specimens——that is, depression of the neutron flux at one specimen by the irradiation die at an adjoining specimen.

It was an objective to minimize flux depression and to make the flux uniform over the dimensions of each specimen. The uniformity of the flux over a specimen is the characteristic that makes transmutation doping attractive for large-scale integrated circuits, since the doping will then be the same in identical slit patterns throughout the specimen, regardless of their number. Figure 11 is a diagram of an irradiation-die packet assembly; Fig. 12 is a capsule section.

Irradiation Capsule Experiments (4)

Four irradiation capsules were prepared and irradiated. Each contained a number of silicon specimens that comprised several irradiation experiments, which are described below.

Capsule A. (5) The purpose of Capsule A was threefold:

1. to produce doped configurations that might be processed into SFET's,
2. to test the geometric predictability of the doped patterns, and
3. to irradiate the silicon specimens without "crosstalk" (mutual interference) and in a water-filled capsule.

The irradiation dies were fabricated mechanically of natural cadmium in geometric patterns by the methods previously described. They were irradiated in location P-3 of the ORR pool hanger; the design value of neutron fluence was 43×10^{18} n/cm^2.

The results were as follows. The capsule was overirradiated. The desired doped configurations were transferred onto a number of specimens. However, the

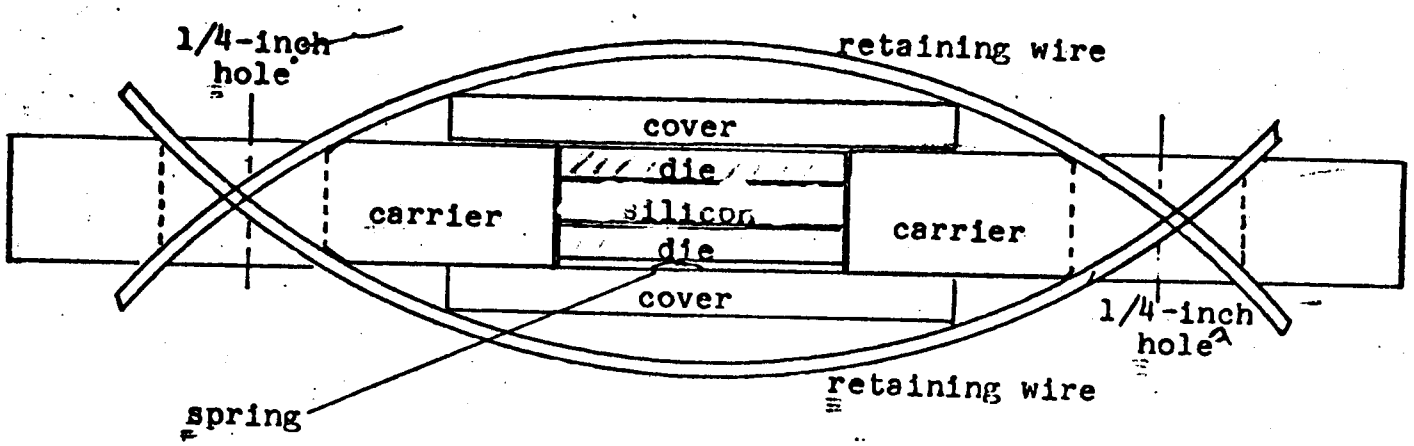

Fig. 11. Irradiation die packet assembly.

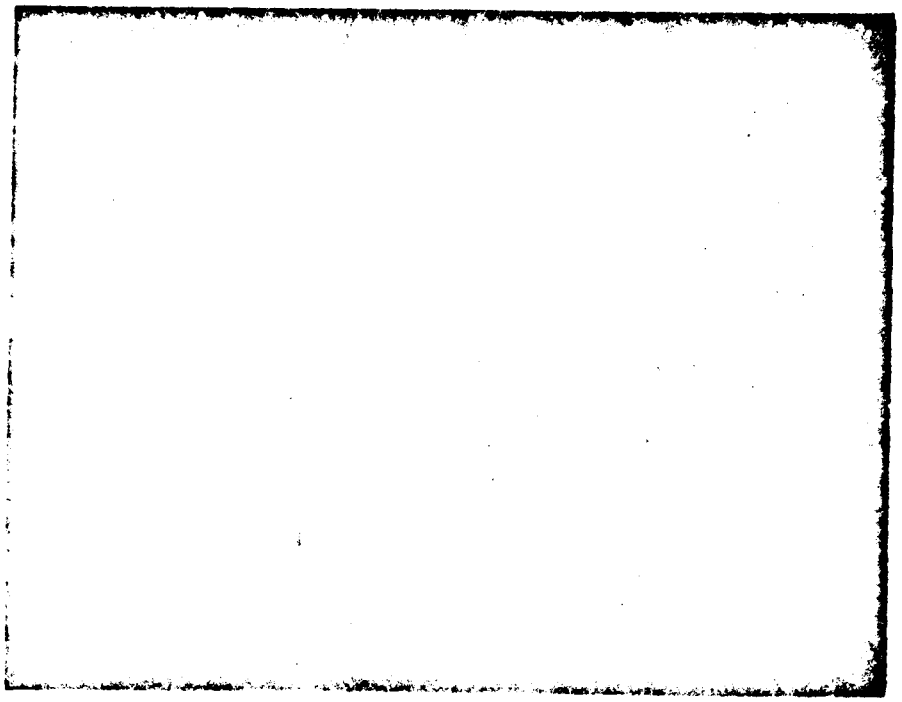

Fig. 12. Capsule B section for bi-type material showing a natural cadmium irradiation die.

configurations were not clear-through, and the isolated regions that were to be source and drain were present only near the surface. Consequently, in the course of lapping and oxide-growing, the doped regions were obliterated from the silicon specimens. Nevertheless, the desired pattern was produced. This confirmed the geometric predictability of the complex circular pattern. The irradiation of specimens without mutual flux interference was also demonstrated.

Capsule B. (5) There were three objectives in the design of Capsule B:

1. By use of natural-cadmium irradiation dies, to produce bi-type high-resistivity silicon chips suitable for complementary MOS circuits;
2. by use of ^{113}Cd irradiation dies, to produce doped configurations suitable for fabrication into SFET's; and
3. to gain experience in the fabrication and in the use of ^{113}Cd irradiation dies.

Both the natural-cadmium irradiation dies and the ^{113}Cd dies were of relatively simple geometry; they consisted of adjacent strips of cadmium-shielded and unshielded regions. In the natural-cadmium dies, the strip spacing was 15 mils; in the ^{113}Cd dies, the minimum spacing was 3 mils. The natural-cadmium dies were fabricated mechanically; the ^{113}Cd dies, by electroplating and photoetching.

The Capsule B was fabricated in two sections spaced ~3 in. apart, one section for the natural-cadmium dies and the other for ^{113}Cd dies. The design value of the neutron fluence specified was 43×10^{18} n/cm^2. Irradiation of Capsule B was begun in the P-3 location. However, the flux in this location was too low because of neighboring experiments that contained neutron absorbers. It was necessary to re-irradiate Capsule B after the absorbers were removed. Consequently, the section of Capsule B that contained the ^{113}Cd experiments was overirradiated.

Capsules C and D. (5) The objectives of experiments with Capsules C and D were:

1. to fabricate doped configurations over large areas of the silicon wafers;

2. to determine whether irradiated oxide layers can be modulated—that is, whether gate electrodes can modulate the polarity of the inversion region under an irradiated oxide;
3. to demonstrate the processing of silicon wafers with electroplated and photoetched irradiation dies;
4. to fabricate SFET's; and
5. to fabricate several types of microcircuits.

Capsule C contained irradiation dies for two types of microcircuits; Capsule D, for two other microcircuits.

Initial plans called for irradiation of Capsule C first and Capsule D later. However, the usual irradiation site P-3 was not available when needed. Therefore, the simultaneous irradiation of both capsules was initiated in the only accessible location; the irradiation conditions of the location were not known.

The new irradiation site proved to have a low flux, and it became apparent that the irradiation could not be completed there. Personnel of the ORR then fabricated a capsule-hanger facility at location P-4 in the reactor pool, directly adjacent to the core face. An advantage was that no foreign experiments would intervene between the capsules and the core. The neutron flux was found to be 4.5 times greater than in the previous location. On this basis, the irradiation time for a nominal transmutation-induced dopant concentration of 80×10^{14} atoms/cm^3 was estimated to be 3-1/2 days. Actually, only about half this concentration resulted.

The consequences of the underirradiation of Capsules C and D were that no microcircuits of acceptable quality were obtained. Nevertheless, on those wafers whose initial resistivity was compatible with the irradiation, large areas of properly doped configurations were produced. Detailed data were obtained on the electronic properties of the specimens.[3]

The selected Figs. 13 and 14 for Capsule D illustrate the sequence of patterns and configurations associated with the transmutation doping of a silicon wafer.

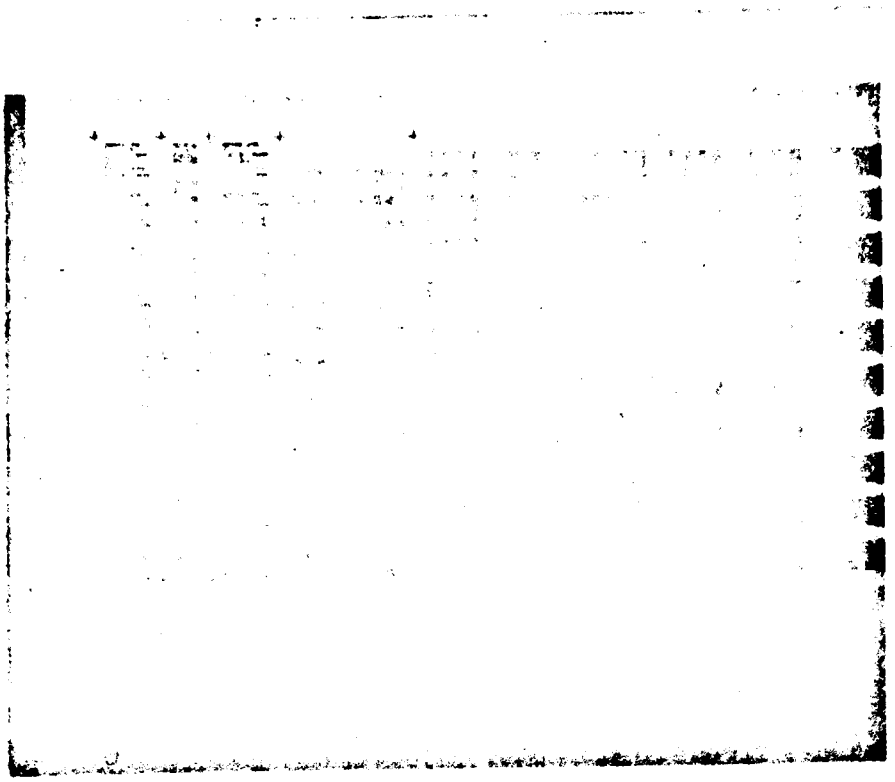

Fig. 13. Patterns used in etching cadmium irradiation dies for capsules C and D.

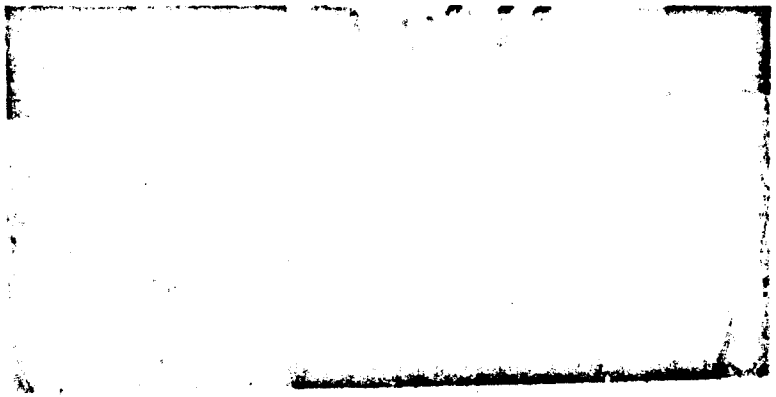

A. ^{113}Cd irradiation-die pattern (electroplated and etched)

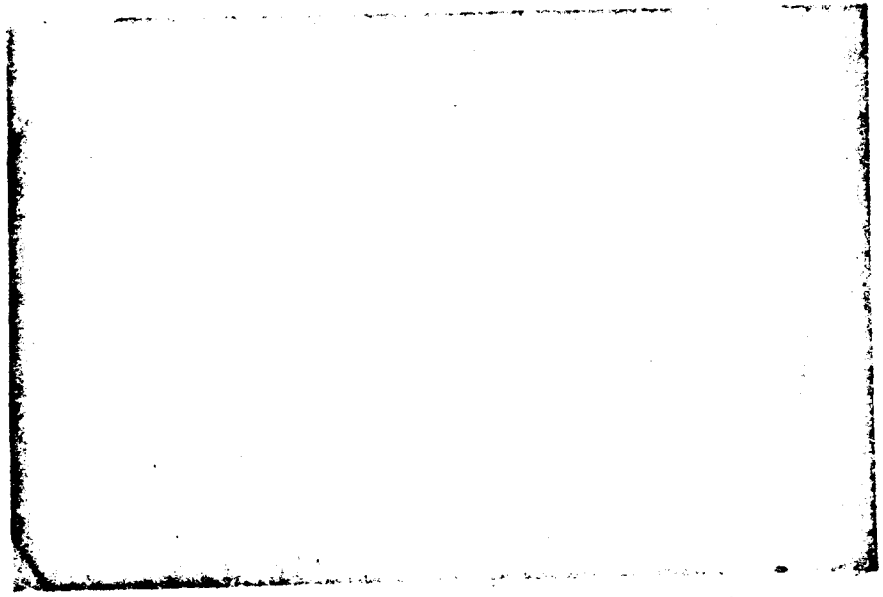

B. Doped configuration (etched and stained)

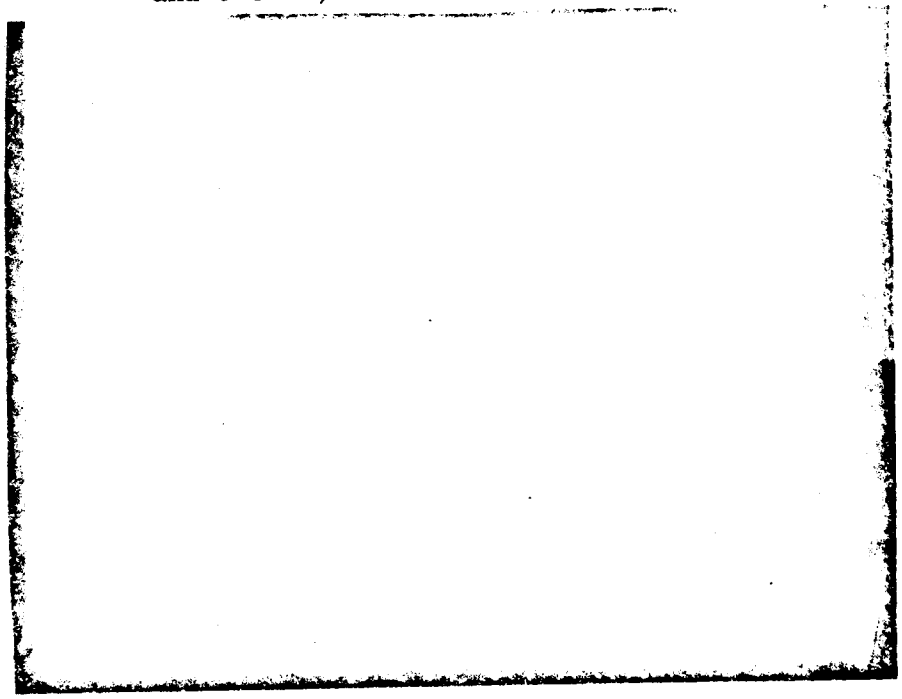

C. Contact holes for etching through the oxide layer

D. Pattern of metallization over the oxide

Fig. 14. Patterns on the silicon wafer of Capsule D.

General Results. (5) The general results of the irradiation experiments were:

1. Although SFET action was observed in a number of doped configurations produced in the irradiation experiments, the SFET characteristics were of poor quality. This result seems to be directly attributable to failure to obtain the desired neutron fluence within the irradiation capsule.
2. Although sections of some wafers gave large-area doped configurations as predicted, the actual doping concentrations were significantly different from the desired values. This difference resulted in poor device characteristics.
3. Only in the case of the bi-type doped configurations was a large percentage of the specimens properly doped. In most of the other wafers, inhomogeneities in the neutron flux prevented the large-area control of the doping that was desired.
4. Despite the observed poor device characteristics, the qualitative ability of the transmutation-doping process to produce the desired devices was verified.
5. All the semiconductor processing steps that were required have been successfully practiced.

Conclusions (3)

Concerning the practical applicability of transmutation doping for fabricating silicon microcircuits, it is concluded that:

1. There appear to be no insurmountable technical problems in the processing of large-area silicon microcircuits by transmutation doping. However, practical difficulties in irradiation-die design and reactor processing have prevented successful demonstration of this method.
2. It is impractical to attempt irradiation processing for silicon microcircuits without regular access to a specific location within a reactor, where characteristic properties of the irradiation may be tested and relied upon. The difficulties of long waiting times for an irradiation

location, long turn-around times (~3 mo instead of 2 or 3 wk) and the necessity to switch from one location to another have made it impractical to monitor the neutron fluence within an irradiation capsule and difficult to obtain the desired fluence.

3. The use of transmutation doping in silicon to produce bi-type material for complementary MOS circuits was successfully demonstrated. In this area, transmutation has a unique capability that is of potential importance for logical circuits with low power consumption. A detailed description of the advantages of transmutation doping for making bi-type silicon substrates for complementary MOS circuits is presented.[1]

4. This program has led to the development of a complete step-by-step processing method for fabricating large-area microcircuits in silicon. However, economic practicability of this procedure remains to be demonstrated.

Because of present difficulties in securing an appropriate irradiation facility with well-controlled flux levels and short experiment turn-around time, one would conclude that in future work on silicon microcircuits emphasis should be placed on transmutation processing of bi-type silicon substrates for complementary MOS circuits, where this process offers a uniquely advantageous capability.

References (3)

1. Neutron Transmutation Doping, Isotop. Radiat. Technol. 2(2): 149-57 (Winter 1964); see also ibid., 3(4): 263-4 (Spring 1967).
2. C. N. Klahr and M. S. Cohen, Fabrication of Semiconductor Devices by Neutron Transmutation Doping, USAEC Report NYO-3124-2, Fundamental Methods Associates, Inc., June 1966.
3. C. N. Klahr and M. S. Cohen, Fabrication of Silicon Microcircuits by Neutron Transmutation Doping, USAEC Report NYO-3124-3, Fundamental Methods Associates, Inc., Dec. 31, 1968.
4. C. N. Klahr, Fabrication of Semiconductor Devices by Neutron Transmutation Doping, USAEC Report NYO-10088, Fundamental Methods Associates, Inc., Dec. 31, 1962.
5. C. N. Klahr and M. S. Cohen, Fabrication of Semiconductor Devices by Neutron Transmutation Doping, USAEC Report NYO-3124-1, Fundamental Methods Associates, Inc., Dec. 31, 1963.
6. Ibid., Trans. Am. Nucl. Soc., 6(2): 414 (1963).
7. C. N. Klahr and M. S. Cohen, Neutron Transmutations Dope Semiconductors, Nucleonics 22(4): 62-5 (1964).
8. H.K.J. Ihantola and J. L. Moll, Design Theory of a Surface Field Effect Transistor, Solid State Electron. 7(6): 423-30 (1964).
9. A. S. Grove, B. E. Deal, E. H. Snow, and C. T. Sah, Investigation of Thermally Oxidized Silicon Surfaces Using Metal-Oxide-Semiconductor Structures, Solid State Electron. 8(2):145-63 (1965).
10. A. S. Grove, P. Lamond, et al., Stable MOS Transistors, Electro-Technology 76(6): 40-3 (1965).
11. S. R. Hofstein, Stabilization of MOS Devices, Solid State Electron. 10(7): 657-70 (1967).
12. P. Balk, P. J. Burkhardt, and L. V. Gregor, Orientation Dependence of Built-In Surface Charge on Thermally Oxidized Silicon, I.E.E.E. Proc. 53: 2133-4 (1965).
13. B. E. Deal, M. Sklar, A. S. Grove, and E. H. Snow, Characteristics of the Surface-State Charge Q_{ss} of Thermally Oxidized Silicon, J. Electrochem. Soc. 114(3): 266-74 (1967).

DETECTION OF ART FORGERIES BY X-RAY-FLUORESCENCE SPECTROSCOPY (2)

Richard Frankel*

Supplementary Key Words: (ARCHEOLOGY / X-RAY FLUORESCENCE / CADMIUM-109 / MEASUREMENT, COMPOSITION / MEASUREMENT AND CONTROL SYSTEM/ FORENSIC INVESTIGATION)

(DTIE: Insert abstract here from following page.)

X-ray-fluorescence spectroscopy is a technique in which radiation is allowed to impinge on a material so as to induce in the material x radiation whose energy is characteristic of one or more components of the material. The reflected, or "fluoresced," x radiation is identified with a spectroscope. A convenient instrument for carrying out this technique is the Kevex Ray, marketed by Kevex Corp. ($20,000 - 25,000) which contains a gamma-emitting radionuclide—^{109}Cd—as the source of primary radiation.**

Description of Instrument (3)

The Kevex x-ray fluorescence spectrometer uses a multichannel analyzer and can analyze many elements at once (Fig. 1). A radioisotopic source irradiates a sample. The individual atoms in the sample reemit x rays that are characteristic of each element in the sample, and the detector absorbs them. Electrical charge pulses, proportional in amplitude to the energy of the individual photons from the detector, are amplified and converted to voltage signals for the input to a pulse height analyzer. The pulse height analyzer sorts and displays the resulting spectrum, which can be read out with a X-Y plotter or with printed or punched tape. Two-stage excitation greatly improves the quantitative assay performance of the instrument over that of other systems.

A typical detector is a lithium-drifted silicon semiconductor 30 mm^2 and mm in sensitive depth. Other high-performance detectors are obtainable, ranging from 10 mm^2 to 750 mm^2 and up to 5 mm in sensitive depth. While the detector should be stored at liquid nitrogen temperatures, it can withstand 25 temperature cycles (room temperature to 78°K) and 100 hr storage at room temperature without degradation in resolution.

*Analytical Instrument Division, Kevex Corporation, 898 Mahler Road, Burlimgame, Calif. 94010.

Abstract. An x-ray-fluorescence spectrometer that contains a multichannel analyzer, and thus can determine several elements simultaneously, is described, together with applications of the instrument to the detection of art forgeries.

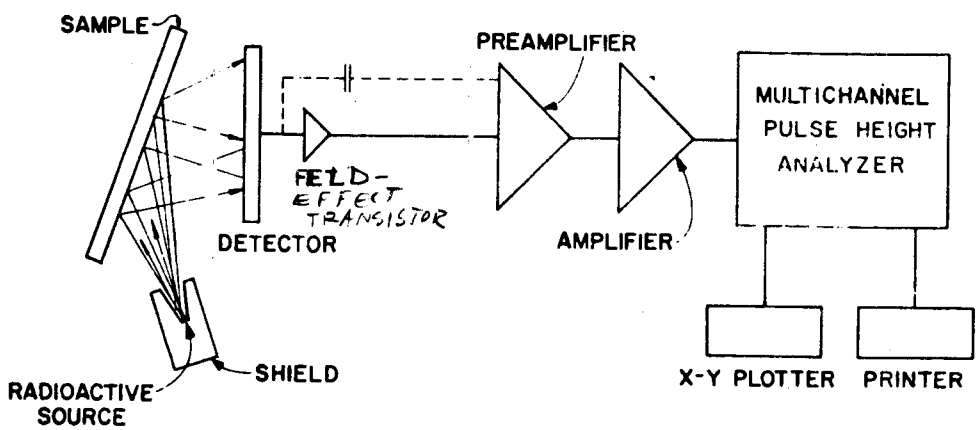

Fig. 1. Kevex Ray system for x-ray-fluorescence analysis.

The system contains two pulsers. By setting these at the extremes of the energy range to be analyzed, appropriate adjustments are made to the linear amplifier controls and pulse-height analyzer controls, so that the energy range of interest is spread over the desired number of channels. (The same adjustments apply to the operation of a single-channel analyzer.) The Kevex pulser is mixed in the first stage of the linear amplifier whereas the signal input is grounded, so that the pulse width registers in only one channel of the analyzer.

The limits of detection are a function of the resolution of the system, the matrix of the sample specimen, and the amount of time devoted to the assay. The assay is an integrating method in which the signal/noise ratio increases as a function of time.

Use in Detecting Art Forgeries (3)

The x-ray-fluorescence spectroscopy technique can be used to determine the elementary composition of the paint used in an art treasure without destroying or harming the painting in any way. Many fake masterpieces have baffled the experts, but the composition of the pigments, along with the artist's unconscious penchant for using certain ratios of pigments in certain common situations, makes it possible to approach the forgery-detection problem both qualitatively and quantitatively.

Pigment compositions vary with locale and date. White, for example, may be produced with lead, zinc, or titanium oxides, but zinc oxide was not produced before 1870, and titanium oxide was not used before 1900. Therefore if either zinc or titanium is found in white areas of a supposed early Renaissance painting, that painting is either a forgery or has been recently restored. A more subtle study—analysis of the paint on several works of a particular artist to determine the pigments characteristically used by him—would reveal paints that were particularly attractive to an artist and possibly the times in his career when he changed to a new paint. Differences between countries and centuries would most certainly be revealed, and differences between works of artists

painting in the same locality at the same time might show up. A particularly subtle relation is the use of similar mixtures of paints for the same situations, e.g., in painting the ear in portraits. Analysis of the paint on the ear of a possible forgery and comparison with a known-to-be-authentic portrait would certainly indicate a deviation from the particular artist's usual practice.

The Kevex x-ray-fluorescence spectrometer was used to study two paintings —one by Diego Velasquez, painted in 1658, and one by Paul Gauguin, painted in the latter part of the nineteenth century. Figure 2 shows the instrument standing in front of the Velasquez portrait of Queen Mariana of Austria, a painting currently valued at $1 million. The detector window is directed at the medallion in the portrait. After a -min irradiation, the painting was moved to a spot in front of a multichannel analyzer and the spectrums of the fluoresced x radiation from the medallion on the portrait subject's chest (Fig. 3a) and from the subject's forehead (Fig. 3b) were recorded.

The preponderance of lead in the pigments is clearly shown. In addition, strontium, calcium, and iron are shown in the medallion, but only strontium in the lighter tones of the forehead. Velasquez is known to have impregnated his canvas with a primer consisting of white lead paint and gesso (gypsum). He then applied a deep red layer over the priming except under the flesh areas, thus achieving considerable luminosity of the flesh tones as contrasted with the darker background.

Figure 4 shows the instrument in position to induce x rays in the small Gauguin portrait. In this x-ray spectrum (Fig. 3c) zinc is strongly in evidence, along with barium and sulfur, all three of which were absent in the earlier Velasquez portrait.

(MG)

This instrument used a single-channel analyzer, determining one element at a time.

Editor's note: A portable x-ray-fluorescence spectrometer and the theory on which it is based were described in Isotopes and Radiation Technology 5:280-4 (1968). Other nondestructive techniques are discussed in "Isotopic Methods of Examination and Authentication in Art and Archaeology," by F. J. Miller, E. V. Sayre, and B. Keisch, ORNL-IIC-21 (in press).

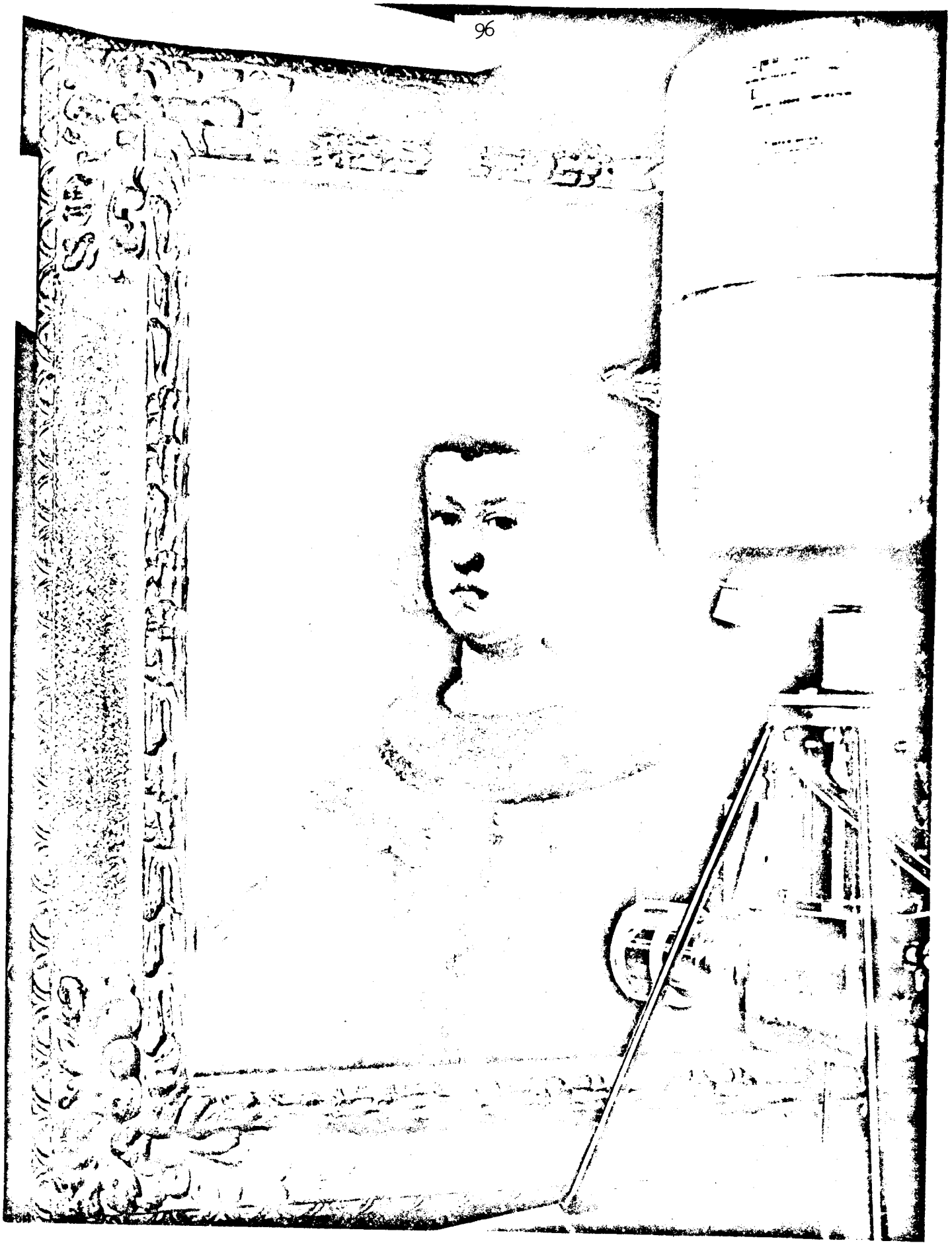

Fig. 2. X-ray-fluorescence instrument in front of portrait of Queen Mariana of Austria painted circa 1658 by Diego Velasquez (1599-1660).

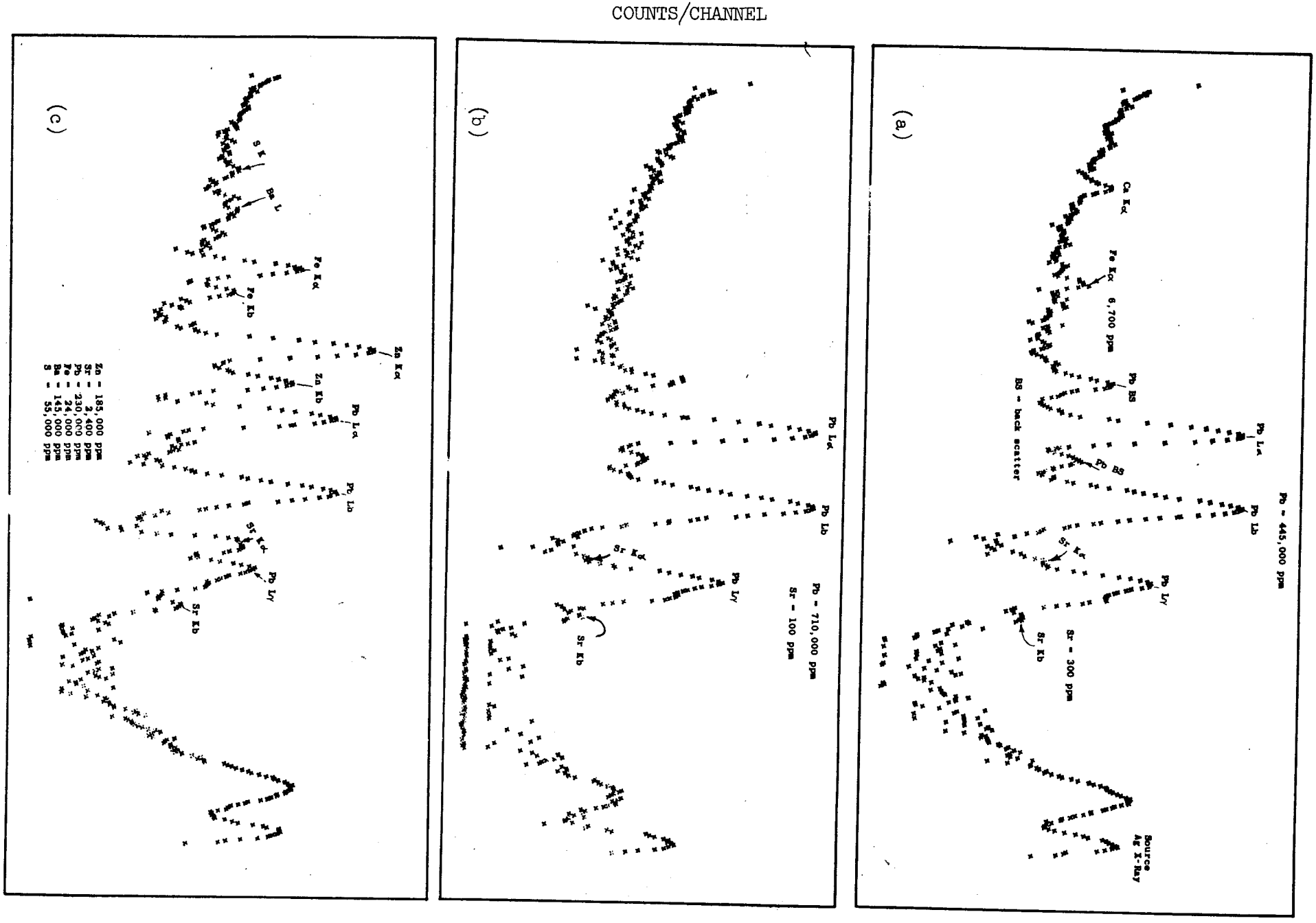

Fig. 3. X-ray-fluorescence spectrums induced by ^{109}Cd gamma radiation in (a) medallion on the chest of Velasquez's 1658 portrait of Queen Mariana of Austria, (b) forehead of same subject, and (c) a small portion of a 19th century portrait by Gauguin.

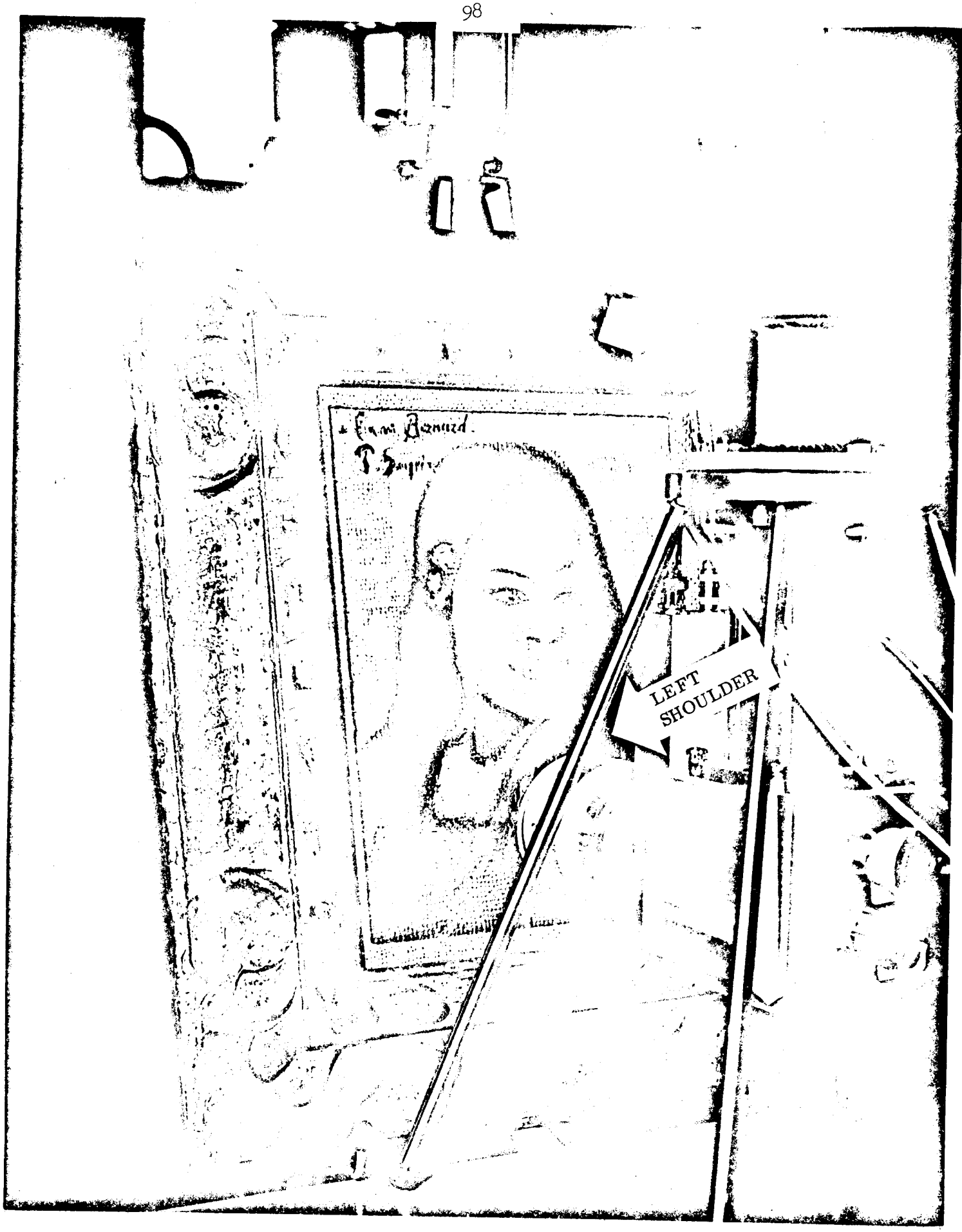

Fig. 4. Kevex-ray analyzing a small portion of a painting by Paul Gauguin (1848-1903).

PORTABLE RADIOISOTOPE X-RAY ANALYZERS — TECHNIQUES AND APPLICATIONS (2)

J. R. Rhodes*

Supplementary Key Words: (X-RAY FLUORESCENCE / COATING / CHEMISTRY, ANALYTICAL / MEASUREMENT, THICKNESS / INDUSTRY, MINING / INDUSTRY / EVALUATION / SOURCE, GAMMA / INSTRUMENT / MEASUREMENT AND CONTROL SYSTEM / INDUSTRY, PRIMARY METAL)

Abstract. Recent developments of sealed radioisotope sources emitting x rays and low-energy gamma rays, and of simple methods for exciting and measuring characteristic x rays of elements, have enabled the relatively sophisticated technique of elemental analysis by x-ray fluorescence to be applied in field conditions using portable battery-operated equipment.

A number of "portable x-ray analyzers" are now commercially available. These instruments, whose characteristics are reviewed in this paper, weigh 12 lb upwards, including batteries that have lives of 10 to 100 hr. They can perform quantitative elemental analysis of any preselected element from calcium to uranium at concentration levels from 0.1 to 100%.

Many potential and actual applications for this type of instrument have been evaluated. These include measurement of the thickness of a wide variety of coatings and analysis of ores, pigments, powders, solutions, alloys, and slags. Some of these uses are summarized in this paper.

(Introduction)

X-ray-fluorescence analysis is a sensitive and widely applied technique that until recently was thought of as a purely laboratory tool. However, in the last few years small, sealed radioisotope sources have been developed that can replace the x-ray tube and its high-voltage power supply. Also, greatly simplified methods of x-ray energy selection, based on x-ray filters, have been found adequate to isolate the characteristic x rays of the element to be determined. As a result, portable, lightweight, inexpensive x-ray-fluorescence analyzers have been developed for use in field and industrial situations.

*Columbia Scientific Research Institute, P. O. Box 6190, Austin, Texas 78702.

Such instruments have been available since 1965 and manufactured in the U.S.A. since about 1968. Their main uses have been in rapid assay of ore samples in the field, in field laboratories, and even on board ships. They have also found use in industry for alloy analysis in scrap sorting and identification of alloy types and for checking the concentrations of electroplating bath solutions. In these applications the advantages of rapid, in-situ measurements are significant. Decisions that would otherwise have awaited a laboratory report can be made on the spot; the number of samples that have to be sent back to the laboratory can be reduced by an order of magnitude; shipments of large quantities of the wrong alloy can be avoided; and so on.

The portable analyzers on the market at present are general-purpose instruments priced in the range $3000 to $5000. This is only a small fraction of the price of conventional laboratory equipment. X-ray analysis is thus available to people who have never before considered using it. As these people become more and more aware of the existence of such instruments, a wide range of new applications should be discovered. (Some of these ought to be large enough to justify development of special-purpose portable analyzers in an even lower price range.)

This paper points out the basic features common to these commercially available portable x-ray analyzers and summarizes some of their uses in elemental analysis.

Description of the Instrument (3)

The basic arrangement of probe and electronic unit has been previously described.[1] The probe is a thin sodium iodide crystal and includes a source and shield, filters, and sample holder. The arrangement of source, sample, and detector is compact, giving a very high efficiency of x-ray collection. An important characteristic of this geometry is the existence of a count-rate—distance plateau, such that if the sample is at a certain distance, small changes in that distance hardly affect the count rate. So surfaces with a roughness of

up to about 1/16 in. can be measured without significant geometrical errors.

Table 1 shows the main features of most of the commercially available portable x-ray analyzers. It is seen that four of the instruments use 2-in.-dia sodium iodide detectors, and three of these use a scaler output in preference to the rate meter. The usual sample diameter measured is 1.5 to 2 in. The one exception to this is the new Columbia Scientific Industries probe which can measure significantly smaller samples (Fig. 1).

Applications (3)

In 1967 and 1968, under a contract with the Division of Isotopes Development of USAEC, Texas Nuclear Division of Nuclear-Chicago Corporation built ten prototype instruments which were evaluated by potential users and also by Texas Nuclear. Table 2 summarizes the results of these evaluations.

These ten prototype instruments were leased (with purchase options) to potential users. Table 3 lists the fate of these instruments. This program was very successful; much was learned by both the instrument manufacturers and the potential users; some 14 evaluations were made and seven of the ten instruments were sold to either the first or second lessee. Over 20 different elemental determinations have been evaluated. The full details of these evaluations are presented in the final report[3] of this contract. Samples of one of the data sheets and a calibration graph are shown in Figs. 2 and 3.

(RHL)

References (3)

1. Portable Radioisotope X-Ray Fluorescence Analyzer, Isotop. Radiat. Technol. 5(4): 280-4 (Summer 1968).
2. J. R. Rhodes and T. Furuta, A Multielement Portable Radioisotope X-Ray Analyzer for Determination of Copper, Nickel, Iron, and Manganese, Trans. Inst. Min. Metall. , Sect. B, Appl. Earth Sci., Nov. 1968 (To be published).
3. J. R. Rhodes, X-Ray Analysis Using Radioisotope Sources, USAEC Report ORO-3224-14, Texas Nuclear Corporation, 1968.

Table 1. **RELEVANT PROPERTIES OF SOME COMMERCIALLY AVAILABLE PORTABLE X-RAY ANALYZERS**

MAKER	PROBE	FILTER PAIRS	S C A	OUTPUT	BATTERY LIFE, HR	WEIGHT, lb		SAMPLE DIA, in.
						PROBE	READ-OUT	
HILGER & WATTS	NaI (Tl) 2"	1	NO	Rate meter	100	3 1/2	15	1 1/2 TO 2
EKCO ELECTRONICS	NaI (Tl) 2"	1	YES	SCALER (10^6)	10	3 1/2	14	1 1/2 TO 2
NUCLEAR ENTERPRISES	NaI (Tl) 2"	1	YES	SCALER OR rate meter	10	3 1/2	10	1 1/2 TO 2
NUCLEAR CHICAGO	NaI (Tl) 2"	1	YES	SCALER (6.4×10^5)	50	3	12	1 1/2 TO 2
COLUMBIA SCIENTIFIC INDUSTRIES	NaI (Tl) 1 1/2"	1	YES	SCALER (10^6)	50	2	10	3/4 TO 1 1/2
PANAMETRICS	PROP. OR SCINT.	1	YES	SCALER (6.4×10^5)	50	4	14	1 1/2 TO 2
TELSEC	TWIN PROP COUNTER	6	NO	Rate meter DIFFERENTIAL	20	20	13	1 1/2 TO 2

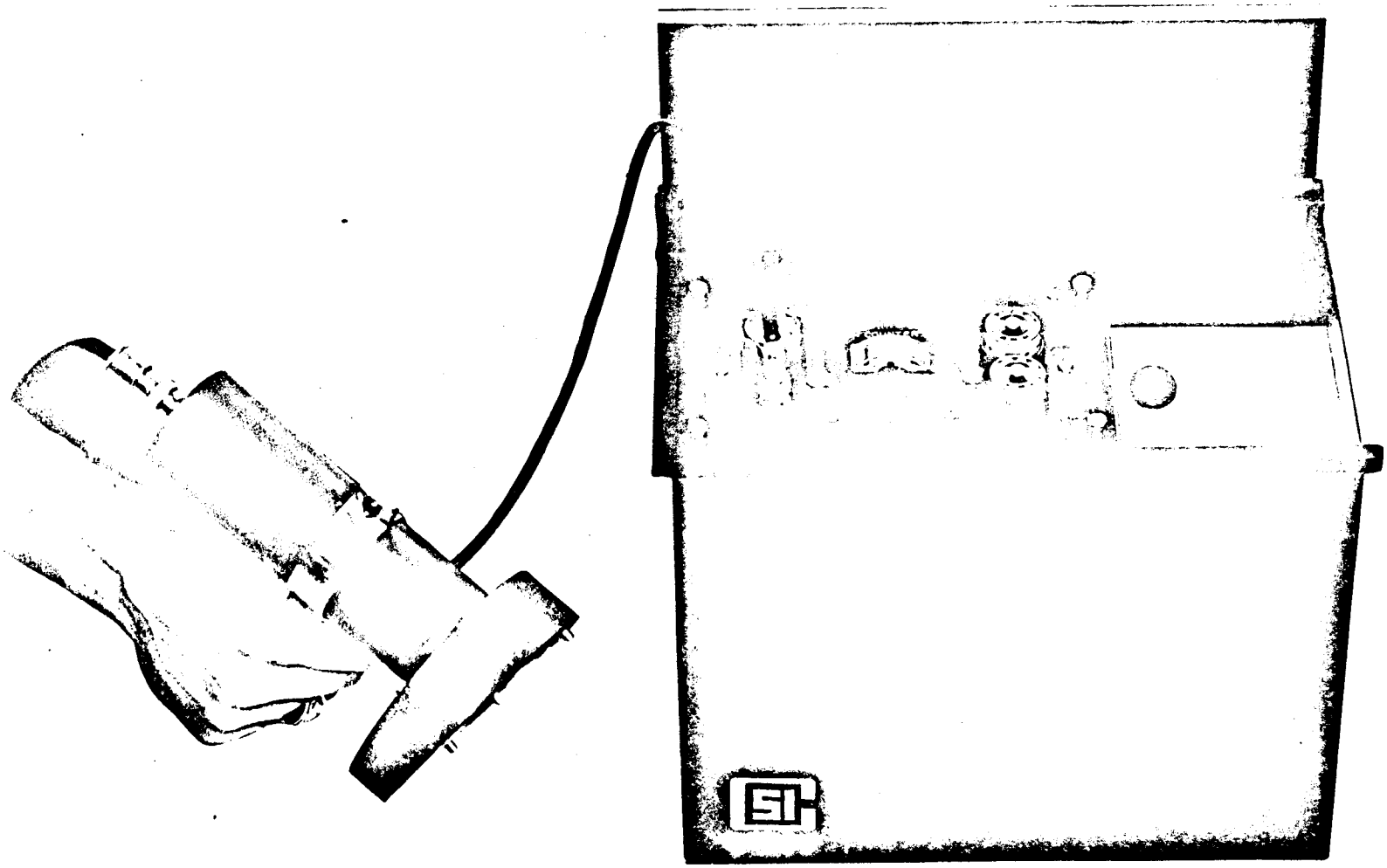

Fig. 1. Columbia Scientific Industries portable x-ray-fluorescence analyzer.

Table 2. EVALUATION OF PORTABLE ANALYZER. LIST OF STUDIES MADE.

	Determination	No. of Inquiries	Experimental Feasibility Study[2]	Technical Data Sheet[1]
1.	S in ores	1	Yes	No
2.	S in coal	Several	"	Yes
3.	Ash in coal[3]	1	"	"
4.	Cl in ores	1	No	No
5.	K in ores[4]	2	Yes	"
6.	Ca in cement raw mix	1	"	Yes
7.	Ti in ores	0	No	No
8.	V in ores	Several	Yes	Yes
9.	V in ores with Ti	"	"	"
10.	V in steels	"	"	"
11.	Cr in steels	"	"	"
12.	Cr in acid soln.	1	"	"
13.	Mn in ores	1	"	No[5]
14.	Mn in steels	Several	"	"
15.	Mn in acid soln.	1	"	Yes
16.	Mn in organic soln.	1	No	No
17.	Fe in organic soln.	1	"	"
18.	Fe in cement raw mix	1	Yes	Yes
19.	Fe in ores	1	"	No[5]
20.	Co in organic soln.	2	No	No
21.	Ni in organic soln.	2	"	"
22.	Ni in acid soln.	1	Yes	"
23.	Ni in ores	1	"	No[5]
24.	Cu in ores	Many	"	Yes[5]
25.	Cu in organic soln.	2	No	No
26.	Cu in acid soln.	1	Yes	"
27.	Zn in ores	0	"	"
28.	Zn in organic soln.	1	No	"
29.	Y in ores	1	"	"
30.	Nb in ores	1	"	"
31.	Mo in ores	Several	Yes	Yes
32.	Mo in steel	"	"	"
33.	Mo in soln.	1	No	No
34.	Mo in organic soln.	1	"	"
35.	Rh in acid soln.	1	Yes	"
36.	Ag in acid soln.	1	"	"
37.	Ag in ores	1	"	Yes
38.	Sn in ores	0	No	No
39.	Ta in ores	1	"	"
40.	W in ores	1	No	No
41.	W in steel	0	Yes	Yes
42.	Au in ores	1	"	"
43.	Au in acid soln.	1	"	No
44.	Pb in steels	1	No	"
45.	Pb in organic solution	1	"	"
46.	Pb in ores	0	Yes	"
47.	Th in ores[4]	2	"	"
48.	U in ores	Many	"	Yes
49.	U in ores[4]	2	"	No
50.	Cement in concrete	1	"	"

Notes:

1. Technical data sheets produced only when full set of calibration samples (artificial or natural) were available.

2. The inclusion of an analysis when an experimental feasibility study has not been made indicates that we have other evidence to show that the analysis is feasible.

3. X-ray backscattering.

4. Using radiometric gamma-ray probe.

5. Subject of paper on Mn nodule analysis.

Table 3. PROTOTYPE PORTABLE ANALYZER EVALUATION PROGRAM

Company	Analyses	Sources	Filters	Period	Remarks
U. S. Bureau of Mines Washington, D.C.	Cu	1 mCi ^{109}Cd	Co/Ni	Nov. '67 (Sold)	"A" Probe. Zn/Ga filters also sent for Au L.
	Au (K)	1 mCi ^{57}Co	Hf/W	(Sold)	"B" Probe.
	Ag in ores	14 mCi ^{241}Am + Ag and Sb targets		(Sold)	"C" Probe non-standard (annular).
Union Carbide	Mn	4 Ci $^{3}H/Zr$, 20 mCi ^{238}Pu	Cr/V	Oct.-Dec. '67	On-stream intermittent analysis of plating bath solutions.
Union Carbide Grand Junction, Colorado	V, U (L), Mo, Nb in ores	^{55}Fe, 1 mCi ^{109}Cd	Sc/Ti Ti/I Sr, Y, Zr	Nov. '67 (Sold)	
Panametrics Waltham, Mass.	Pb (L)	-	Empty Filter Tray	Nov.-Feb. '68	AEC contract work.
"	-	-	-	April '68 (Sold)	Purchased two electronic units, one with proportional counter HV and one without.
Kennecott Expl. Salt Lake City, Utah	Cu, Mo in ores	1 mCi ^{109}Cd	Co/Ni Zr/Y	Nov.-Jan. '68	
Kennecott Expl. Salt Lake City, Utah	Cu, Ni, Co, Mn, Fe	3 mCi ^{109}Cd	Ni, Co, Fe, Mn, Cr, V	Apr-July (then sold)	
Geological Survey of Canada Ottawa	Nb, Mo, U (L), Pb (L), Cu, Ni, Co, Zn, Fe, Sn in ores	1 mCi ^{109}Cd 500 mCi ^{147}Pm/Al	Zr/Y/Sr Ge/Ga Ni/Co Co/Fe Fe/Mn Cu/Ni Cr/Mn Pd/Ag	Jan-Feb. '68	
Union Carbide Hot Springs, Ark.	V in ores	20 mCi ^{55}Fe	Ti/I	Nov.-Feb. '67-'68 (then sold)	Two now in use for vanadium mine control
Continental Oil Company, Ponca City, Oklahoma	U (L) in ores	1 mCi ^{109}Cd	Zr/Y Zr/Ge	Feb.-Mar. '68	
Kerr-McGee Corp. Oklahoma City, Oklahoma	U (L), Mo, Cu ores U, Th, K (Nat. radioactivity)	3 mCi ^{109}Cd, ^{88}Y, ^{60}Co (10 μCi each)	Zr/Y/Sr Ni/Co	Jan-July '68	
Bethlehem Steel Bethlehem, Pa.	Fe, Mo	1 mCi ^{109}Cd	Mn/Cr	Apr-Sept. '68	Sorting steels.
	Cr V	20 mCi ^{55}Fe, 4 Ci $^{3}H/Zr$			
Newmont Expl. Danbury, Conn.	Cu in ores	3 mCi ^{109}Cd	Co/Ni	Aug-Oct. '68	Field analysis of copper.

TEXAS NUCLEAR PORTABLE ANALYZER

DATA SHEET NO. 17

ANALYSIS: Uranium in uranium ores

SAMPLES USED: U_3O_8 in sandstone samples
U_3O_8 range 0.01 to 0.17%

INSTRUMENTAL CONDITIONS:

Source:	1 mCi ^{109}Cd
Filters:	Zr/Y or Zr/Ge balanced
Crystal:	Be-windowed NaI(Tl)
Photomultiplier:	EMI Type 9656 KS
Preset Time Interval:	100 sec.
Preset Amplifier Gain:	~2/3
*Threshold Setting:	9.00
*Upper Level Setting:	1.00

SAMPLE CONDITIONS: Powdered samples in a 2 inch dia. sample holder. Measuring aperture dia.: 1-3/4 inch.

RESULTS: One standard deviation due to counting statistics = 0.006% U_3O_8 in 100 second count with each filter, using Zr/Y filters; 0.004% U_3O_8 using Zr/Ge filters.

REMARKS: The source activity can readily be increased by a factor of 5 so reducing the count time necessary to obtain a given sensitivity.

*Peculiar to particular amplifier setting and photomultiplier used.

Fig. 2. Typical data sheet for portable x-ray-fluorescence analyzer.

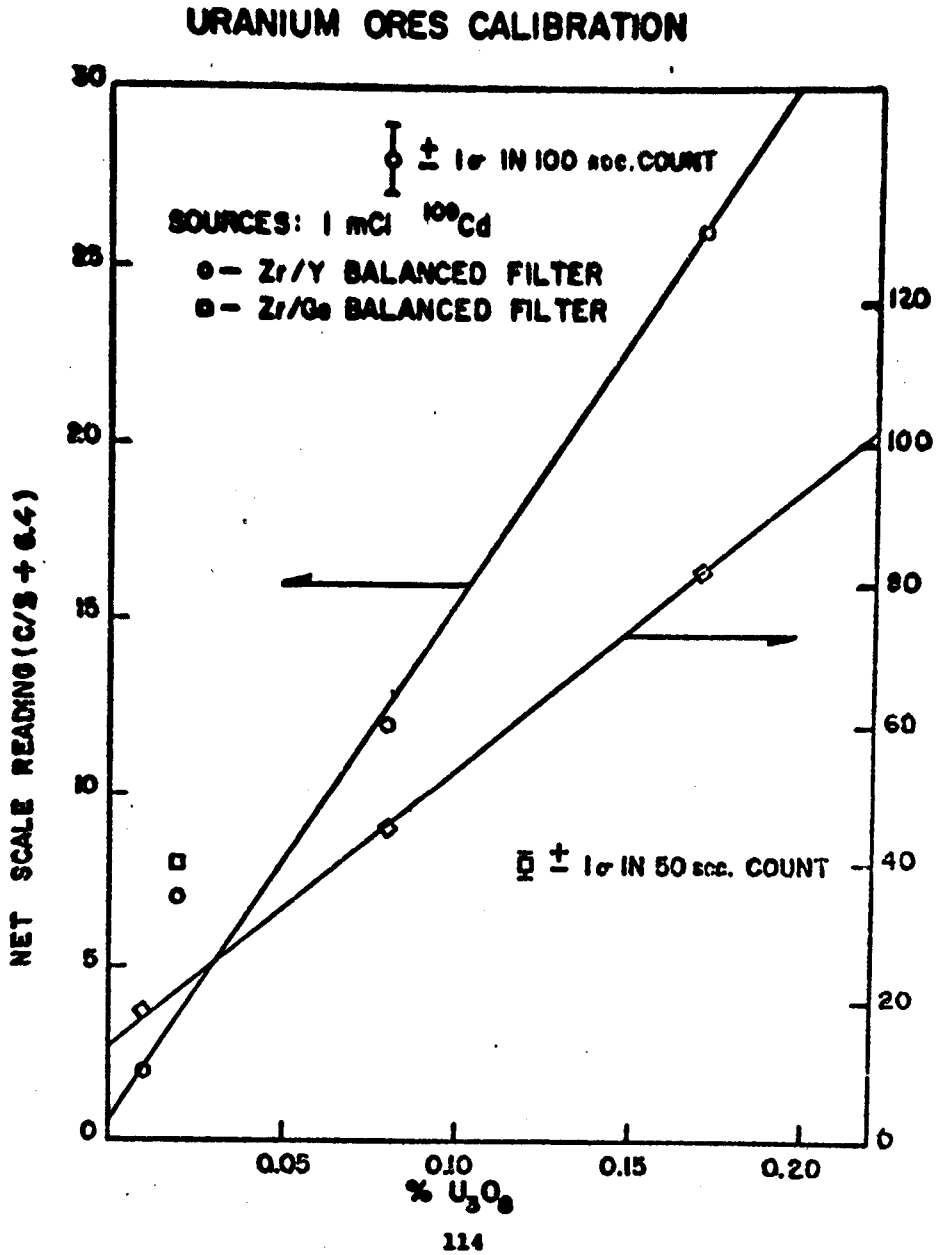

Fig. 3. Typical calibration curve for x-ray-fluorescence analyzer.

A RADIOCHEMICAL STUDY OF THE DIFFUSION OF IONS THROUGH PROTECTIVE FILMS (2)

by Alfred L. Glass and Jack Smith*+

Supplementary Key Words: (CHEMISTRY, PHYSICAL / INDUSTRY / INDUSTRY, PLASTICS / INDUSTRY, RUBBER / COATING / CORROSION / TRACER / MATERIAL TRACING / MULTIPLE TRACING / INSTRUMENT / COUNTING / PHYSICAL PROPERTY / MILITARY / THEORY, APPLIED / HYDROGEN-3 / SODIUM-22 / CHLORINE-36)

Abstract. The radioactive tracers ^{3}H, ^{22}Na, ^{36}Cl were used to measure the rates of diffusion of sodium and chloride ions and of water through various organic protective coatings and barriers. To provide information useful in improving protection against corrosion, the results were correlated with the electrochemical properties of the materials tested. The data acquired indicate that hydrolysis and ionization of polymer films in contact with water cause electrostatic charges on the film, which affect both the permselectivity of the film to ions and the rate of diffusion of the ions through the film.

(Introduction)

In previous studies[1-9] of the migration of ions through a membrane, the electrochemical properties of the membrane have been of chief interest. Before the advent of radioactive tracer techniques, accurate measurement of the small amounts of migrating ions was not possible. In the work described here, the radioisotopes ^{3}H, ^{22}Na, and ^{36}Cl were used to study the

*Aero Materials Department, Naval Air Development Center, Johnsville, Warminster, Pa. 18974.

+The authors thank Dr. G. K. Holmes, Superintendent of the Chemical Engineering Division of the Aero Materials Department for his interest, encouragement, and technical advice, which has contributed to the prosecution of this and other investigations.

migration of microquantities of Na^+ and Cl^- ions and of water (measured as H^+ ion) through eight selected organic protective coatings and barriers. The materials were studied in the form of films. The mechanism of permeation of the ions through the films was of particular interest. The work was reported originally in the Journal of Paint Technology,[10] which should be consulted for more detailed information than that given here. The procedures described were also used subsequently to investigate the effect of pigment on the diffusion of ions through protective films.[11]

Experimental Conditions (3)

Eight organic materials (Table 1) representative of those used by the Navy as protective coatings and barriers were selected for study. Those not already in film form were cast as films by a special procedure.[10] The film thicknesses were measured with a micrometer.

(Table 1)

Three solutions of radioisotopes were used. A solution that contained $^3H^+$ was prepared in dilute sodium chloride solution from carrier-free ^3H_2O. From carrier-free $^{22}NaCl$ in hydrochloric acid solution, a solution of $^{22}Na^+$ was prepared in dilute sodium chloride solution. From carrier-free $Na^{36}Cl$, a solution of $^{36}Cl^-$ was prepared in distilled water.

The apparatus was designed especially for the experiments. Figure 1 shows the diffusion cell. With the instrumentation shown in Figure 2, the quantities of $^{22}Na^+$ and $^{36}Cl^-$ that diffused through the films were measured continuously, except that for $^{22}Na^+$ measurement the Geiger tube was replaced by a

(Fig. 1)

(Fig. 2)

Table 1. RATES OF DIFFUSION OF H^+, Na^+, AND Cl^- THROUGH FILMS[a]

Film	Average Diffusion Rate, g/hr[b]					
	H^+	Cl^-		Na^+		
		Theoretical		Theoretical		
	Measured	From H^+ Values	Measured	From H^+ Values	From Cl^- Values	Measured
Aclar 191	7.87×10^{-6}	1.85×10^{-8}	None	1.20×10^{-8}	None	None
Cellulose acetate	1.95×10^{-2}	4.58×10^{-5}	4.66×10^{-7}	2.96×10^{-5}	3.02×10^{-7}	1.20×10^{-6}
Epoxy MIL-C-22750	1.23×10^{-4}	2.89×10^{-7}	1.51×10^{-9}	1.87×10^{-7}	9.77×10^{-10}	1.39×10^{-9}
Mylar	7.78×10^{-5}	1.83×10^{-7}	None	1.18×10^{-7}	None	None
Neoprene organic protective coating 1672A	4.90×10^{-4}	1.15×10^{-6}	2.57×10^{-7}	7.45×10^{-7}	1.66×10^{-9}	7.46×10^{-9}
Nitrocellulose acrylic lacquer MIL-L-19537	3.50×10^{-4}	8.23×10^{-7}	7.29×10^{-9}	5.32×10^{-7}	4.72×10^{-9}	None
Nylon 8200	9.24×10^{-3}	2.17×10^{-5}	1.31×10^{-7}	1.40×10^{-5}	8.47×10^{-8}	5.78×10^{-8}
Polyethylene	1.57×10^{-5}	3.69×10^{-8}	8.48×10^{-9}	2.39×10^{-8}	5.49×10^{-9}	None

[a] Migration from 0.053M NaCl through the film into distilled water.

[b] Per square centimeter of 1-mil-thick film.

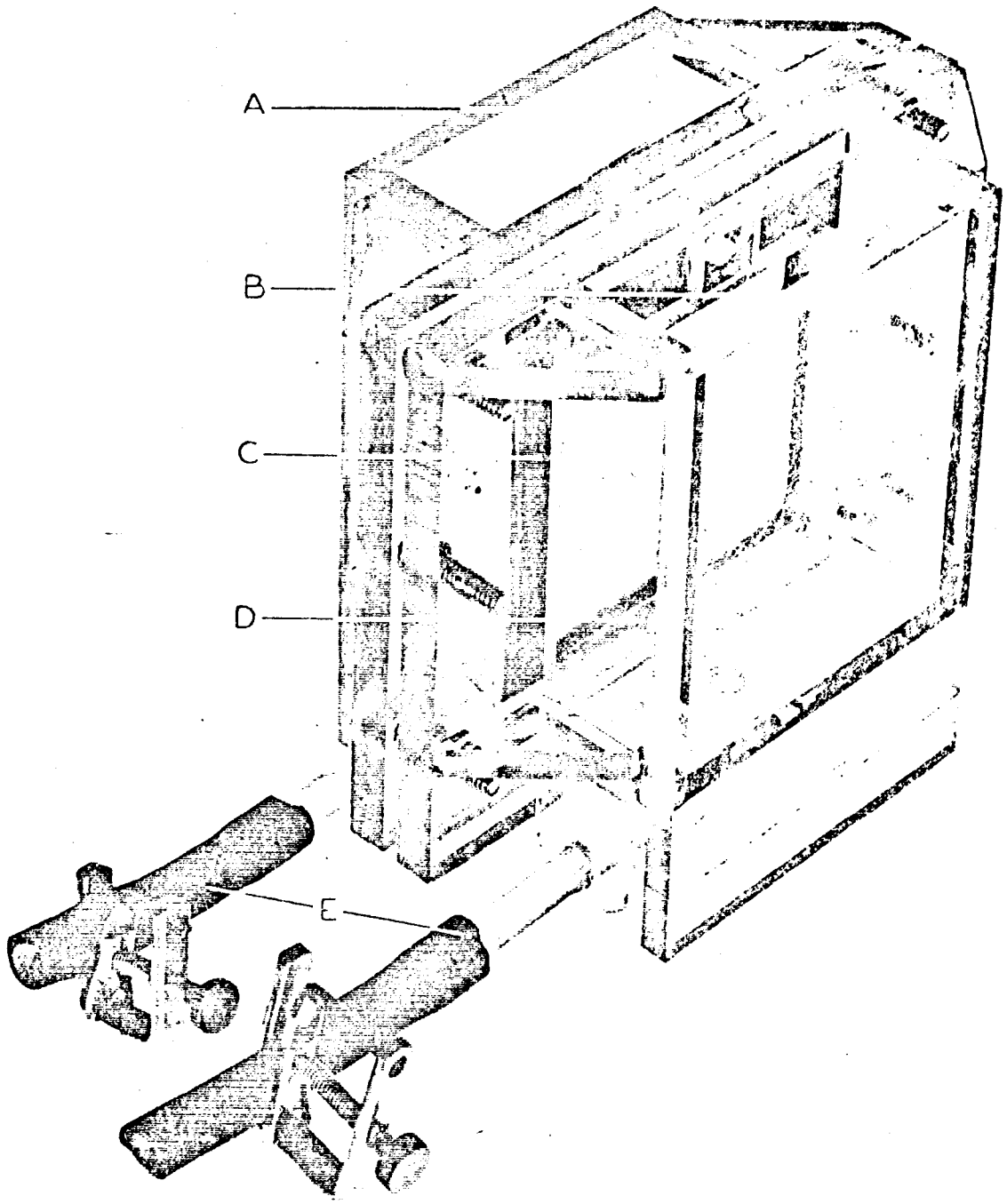

Fig. 1. Diffusion cell. (A, compartment for distilled water; B, compartment for radioisotope solution; C, gasket; D, test film of 2-3/4 x 2-3/4 in. exposed area; E, drains)

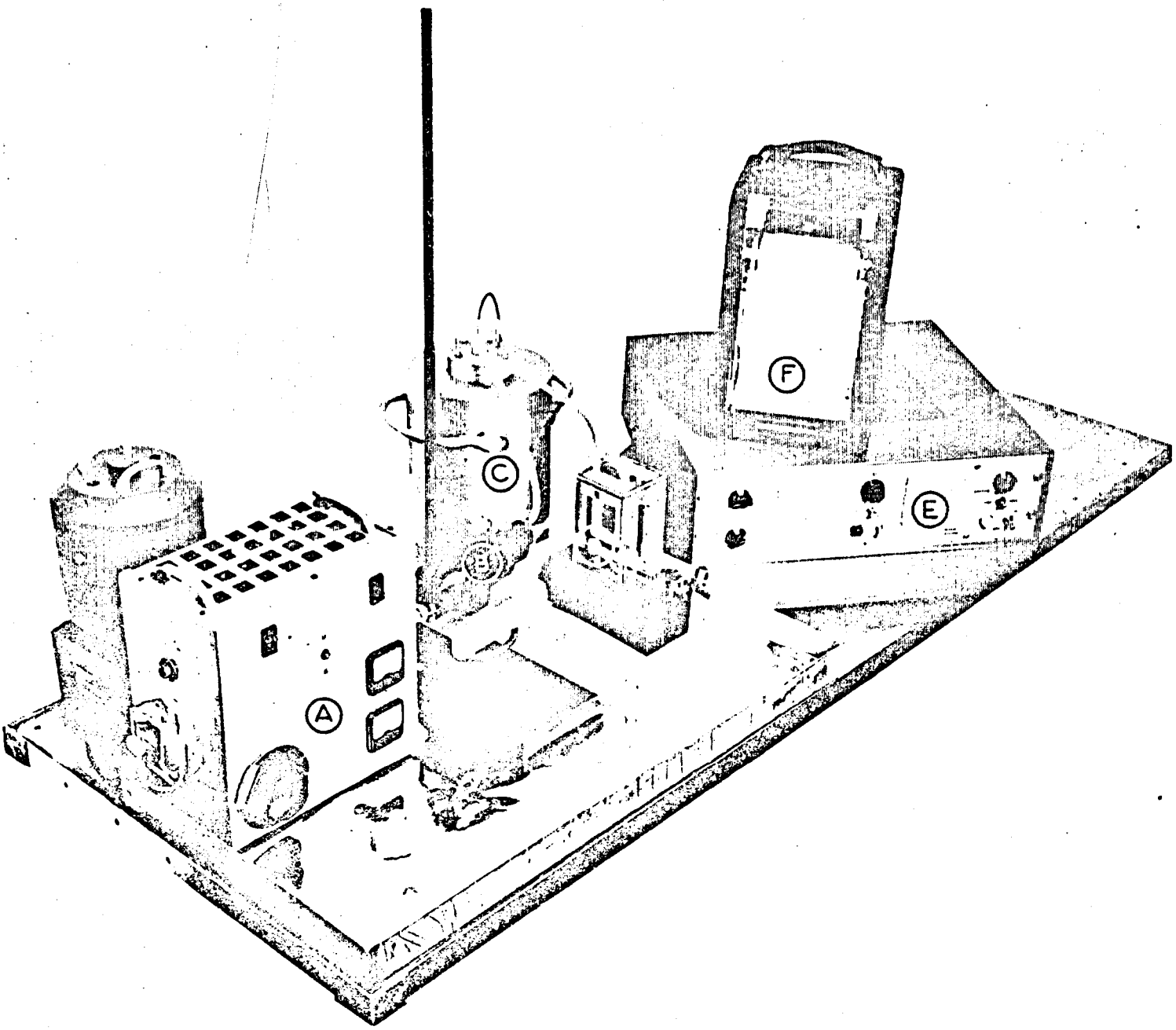

Fig. 2. Assembly of equipment for measuring $^{22}Na^{+}$ and $^{36}Cl^{-}$ that diffused through films. (A, rectifier; B, pump; C, shielded Geiger flow tube; D, diffusion cell; E, ratemeter; F, recorder)

well-type scintillation counter. It was necessary to measure $^{3}H^{+}$ discontinuously by liquid-scintillation counting.[10]

In the measurement of ion diffusion, the levels of liquid were the same in both compartments of the diffusion cell. During the permeation by $^{22}Na^{+}$ and $^{36}Cl^{-}$, water was pumped continuously through compartment A to the instrumentation. During permeation by $^{3}H^{+}$, the contents of the diffusion cell were undisturbed, and aliquots were removed intermittently from compartment A for measurement.

Results and Discussion (3)

The experimental work included a study of the rate of diffusion of H^{+}, Na^{+}, and Cl^{-} and the effects of film thickness, and of the concentration of ion in the solution from which it migrated, on the diffusion rate. From the results, information was gained about the relative degree of protection to be expected from the films and the mechanism of ion migration through them.

Table I gives the average rates of diffusion of H^{+}, Na^{+}, and Cl^{-} through the eight selected films. The data show that: (1) the average rates of diffusion differ with the type of film, (2) Na^{+} and Cl^{-} ions diffuse in amounts that are not proportional to their concentrations in the solutions from which they migrated and not in stoichiometric ratio to each other, and (3) the ratio of diffusing Na^{+} to Cl^{-} ions varies with film type.

From experimental measurement of the migration of H^{+} and Cl^{-} through nylon 8200 and 8205, the diffusion rate of the ion is indicated to be inversely proportional to the total thickness of the film but to vary with type of nylon and of ion. Nylon 8205 is more permeable than

nylon 8200; Cl^- diffuses faster through each than does Na^+.

Nonproportional decrease occurs in ion diffusion rate with decrease in the sodium chloride concentration of the solution from which the ion migrates. This effect was observed in a study of the diffusion of Na^+ and Cl^- through films of nylon, neoprene, and cellulose acetate. Nylon is permselective to Cl^-; neoprene and cellulose acetate are permselective to Na^+.

The postdiffusion ratio of NaCl to water deviates from the prediffusion ratio. Also, the diffused Na^+ ions are not in stoichiometric ratio to diffused Cl^- ions.

These deviations are interpreted to mean that permeation of ions through membranes involves factors other than the relative diameters of the ions (or their hydrated forms[12-14]) and of the film pores. According to the electrochemical concept of the diffusion process,[1-9] walls of film pores become electrostatically charged by ionization of certain groups in the chemical structure of the film. The sign (+ or -) of this charge, together with the charge and size of the ion and the size of the pores, determine whether an ion will diffuse through a film. The data from this study indicate that : (1) nylon has a positive pore charge (Cl^- diffuses faster than Na^+), (2) polyethylene has a positive pore charge and relatively small pore diameter (Cl^- diffuses; Na^+ does not), (3) nitrocellulose behaves similarly to polyethylene, (4) neoprene has a negative pore charge (Na^+ diffuses in stoichiometric excess of Cl^-), (5) epoxy behaves similarly to neoprene, and (6) cellulose acetate also behaves similarly to neoprene.

The establishment of a uniform ion-migration rate following an initial nonuniform rate is interpreted to indicate a Fickian-type[15-17]

diffusion process. This effect is shown in Figs. 3-6, which give

(Fig. 3)

(Fig. 4)

(Fig. 5)

(Fig. 6)

data on the diffusion rate of Na^+ and Cl^- through five types of film. The initial non-uniformity is believed to result from hydrolysis of the film, which proceeds to an equilibrium hydrolysis and produces sufficient electrical charge on the pores of the film to cause repulsion of certain migrating ions. This deduction is corroborated from diffusion studies on nylon and neoprene films presoaked in water, that is, at hydrolysis equilibrium. For these films, the initial nonuniform migration rate did not exist (m) — the rates were uniform from the start of the migration.

Conclusions (3)

This study, made possible through radioisotopes, provides information of value in the practical use, as films, of the typical corrosion-protective materials tested. It was shown experimentally that (1) the films are permeable to water and to certain anions and cations, (2) diffusion of ions through the films is inversely proportional to film thickness and directly proportional to time, and (3) on contact with water, the films hydrolyze and thus acquire electrostatic charges that cause them to become permselective.

(HPR)

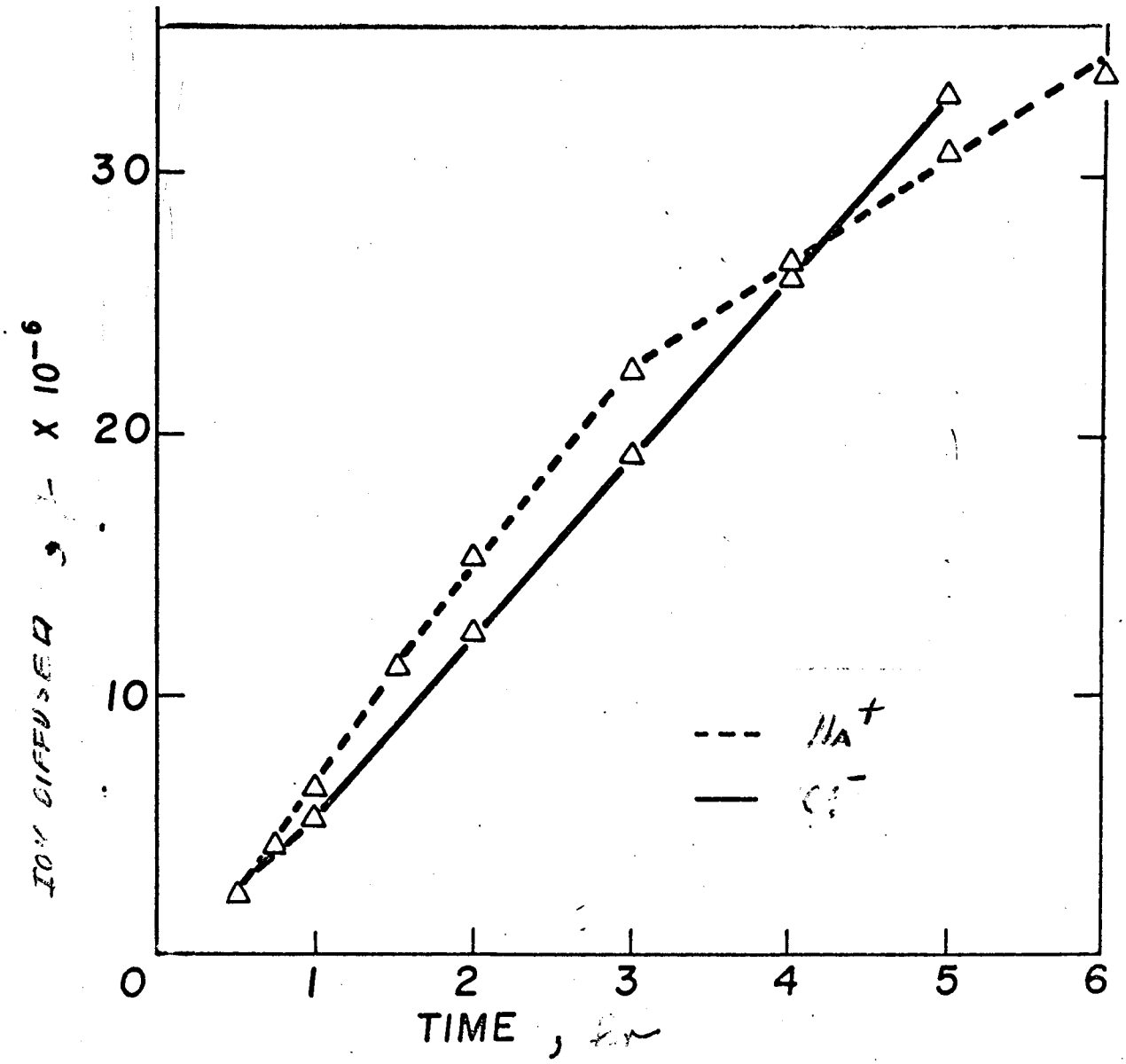

Fig. 3. Diffusion of Na^+ and Cl^- through nylon film.

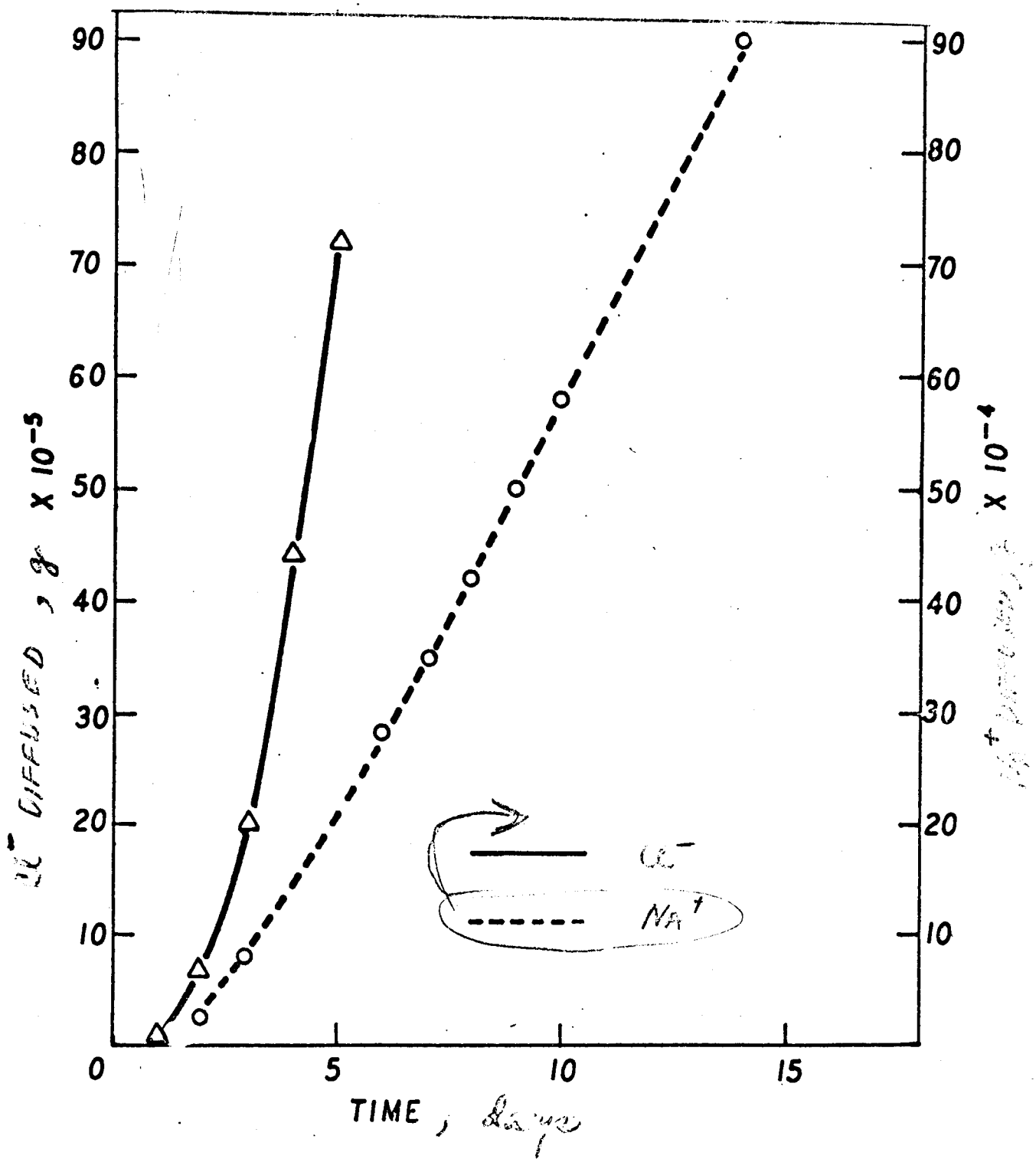

Fig. 4. Diffusion of Na^+ and Cl^- through cellulose acetate film.

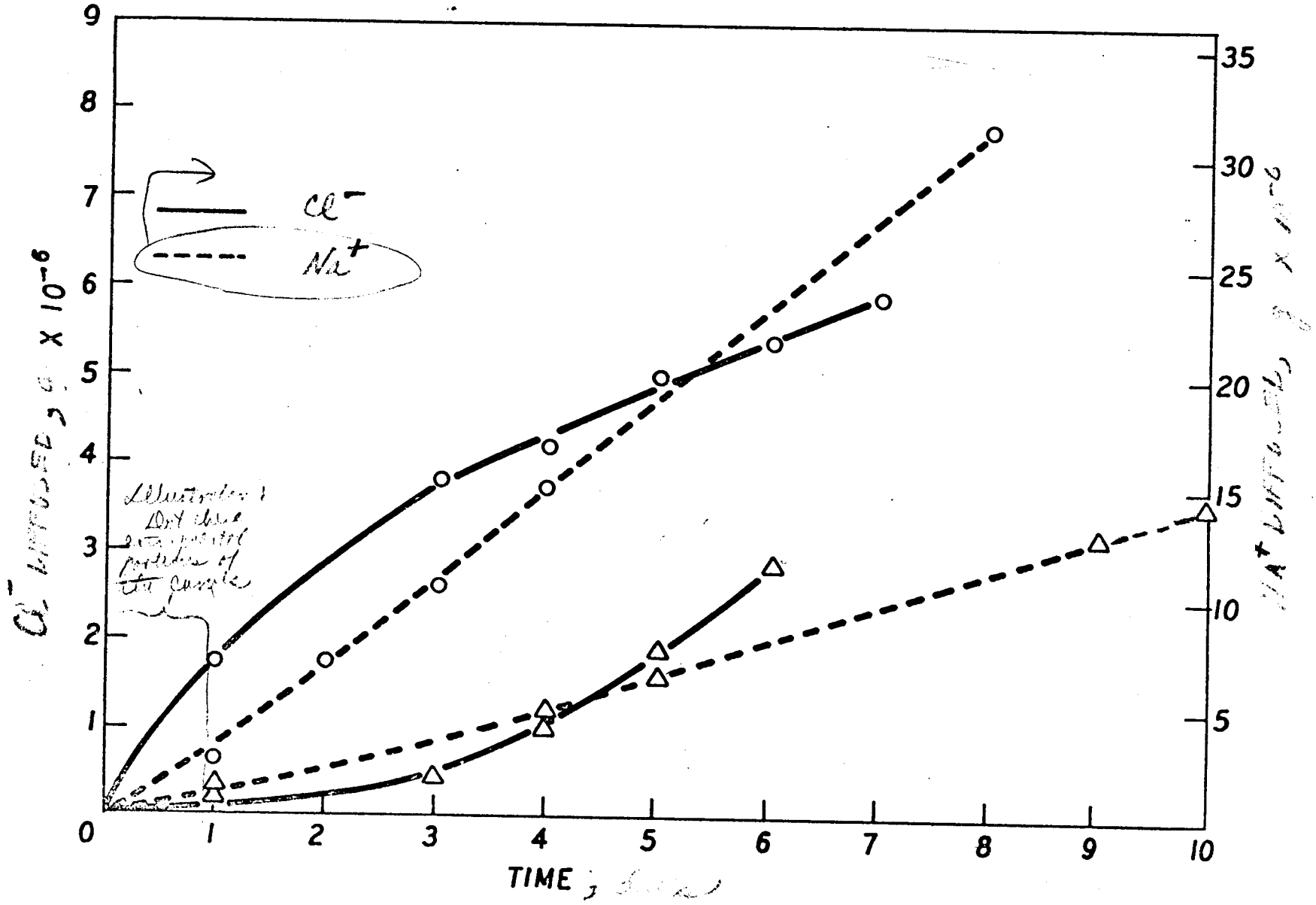

Fig. 5. Diffusion of Na^+ and Cl^- through neoprene (o) and epoxy (Δ) films.

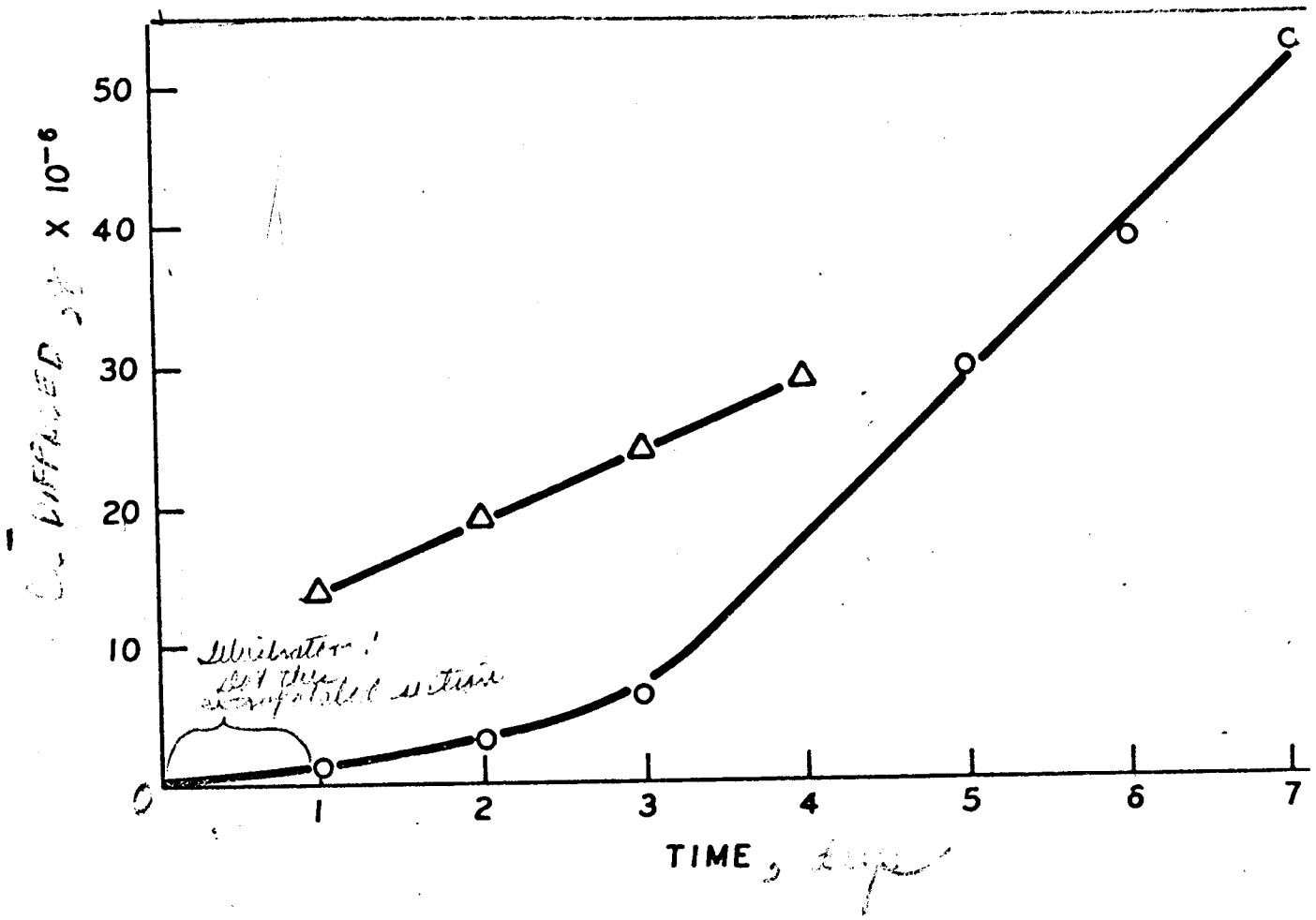

Fig. 6. Diffusion of Cl^- through nitrocellulose acrylic lacquer (o) and polyethylene (△) films.

References (3)

1. K. Sollner, Ion Transport Across Membranes, Academic Press, New York, 1954.
2. H. P. Gregor and K. Sollner, Improved Methods of Preparation of "Permselective" Collodion Membranes Combining Extreme Ionic Selectivity with High Permeability, J. Phys. Chem. 50: 53-70 (1946).
3. K. Sollner, The Electrochemistry of Porous Membranes, Chap. 4 in Electrochemistry in Biology and Medicine, T. Shedlovsky, Ed., Wiley, New York, 1955.
4. W. W. Kittelberger and A. C. Elm, Water Immersion Testing of Metal Protective Paints — Role of Osmosis in Water Absorption and Blistering, Ind. Eng. Chem. 38: 695-9 (1946).
5. W. W. Kittelberger and A. C. Elm, Water Immersion Testing of Metal Protective Paints — Role of Electroendosmosis in Water Absorption and Blistering, Ind. Eng. Chem. 39: 876-81 (1947).
6. W. W. Kittelberger and A. C. Elm, Diffusion of Sodium Chloride Through Various Paint Systems, Ind. Eng. Chem. 44: 326-9 (1952).
7. C. C. Maitland and J. E. O. Mayne, Factors Affecting the Electrolytic Resistance of Polymer Films, Offic. Dig., Federation Soc. Paint Technol. 34(452): 972-91 (1962); Chem. Abstr. 58: 669h (1963).
8. C. A. Kumins, Electrochemical Properties of Protective Coatings, Offic. Dig., Federation Soc. Paint Technol. 34: 843-61 (1962); Chem. Abstr. 59: 839d (1963).
9. N. W. Rosenberg, J. H. B. George, and W. D. Potter, Electrochemical Properties of a Cation-Transfer Membrane, J. Electrochem. Soc. 104: 111-5 (1957).
10. A. L. Glass and J. Smith, A Radiochemical Investigation into Diffusion of Ions Through Protective Films, J. Paint Technol. 38(495): 203-09 (1966); Chem. Abstr. 65: 201b (1966).
11. A. L. Glass and J. Smith, Radiochemical Investigation of the Effect of Pigments on the Diffusion of Ions Through Protective Films, J. Paint Technol. 39(511): 490-3 (1967); Chem. Abstr. 67: 74529j (1967).
12. H. J. Creighton and W. A. Koehler, Principles and Applications of Electrochemistry, 4th ed., Vol. I, Wiley, New York, 1943, p. 139.
13. R. J. Podolsky, The Structure of Water and Electrolyte Solutions, NM Lecture and Review Series 60-5, Naval Medical Research Institute, Bethesda, Md., Mar. 21, 1960.
14. G. Kortüm and J. O'M. Bockris, Textbook of Electrochemistry, Vol. I, Elsevier, New York, 1951, pp. 131-7.
15. A. Weissberger, Ed., Technique of Organic Chemistry, 3rd ed., Vol. I, Physical Methods of Organic Chemistry, Part II, Interscience, New York, 1960, p. 975.

16. J. Crank, The Mathematics of Diffusion, Clarendon Press, Oxford, 1956, p. 47.
17. R. M. Barrer, Diffusion In and Through Solids, University Press, Cambridge, 1941.

RADIOISOTOPIC GAGE FOR WIDTH CONTROL*

Supplementary Keywords: (MEASUREMENT, OTHER/MEASUREMENT AND CONTROL SYSTEM/CARBON-14 / INDUSTRY / INDUSTRY, PLASTICS / INSTRUMENT / PLANT SCALE / ENGLANG)

Mechanical control of width of layflat plastic tubing used for packaging is not very accurate because of the deformability of the film edges, and optical methods are not satisfactory for transparent or translucent materials. A radioisotopic-gage method has been developed in which there is no contact of the gage with the material monitored, and the results are independent of film color and surface properties and of ambient conditions.

The radioisotopic-monitoring system uses two ^{14}C beta sources and two detectors, one source-detector combination on either side of the moving tape (Fig. 1). The sources are mounted so that the tape screens half of each detector. The total area of free detector surfaces---and thus the sum of the two detector signals---remains constant for a constant width regardless of any lateral displacement of the tape. A change in the detector signal thus indicates a change in width. Relay set points are provided to produce a warning signal when width-deviation tolerance limits are exceeded.

In tests with the system on 30-μm-thick, 245-mm-wide polyethylene film, produced at a rate of 12.4 m/min, width variations of 0.5 mm were detected. Performance was also satisfactory with 80- to 300-mm-wide tubing produced at a rate of 33 m/min. Further, periodical width variations of 1 mm occurring over a 6- to 8-mm pass time---previously unrecognized---were detected. (MG)

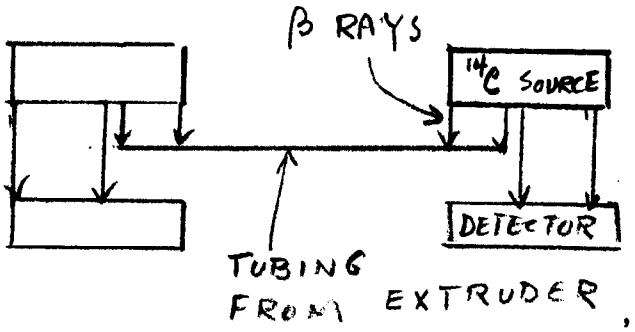

*Based on A. Kemper and P. Platzek, Nuclear Methods of Width Control in Layflat Tube Production, Brit. Plastics 41: 115-20 (June 1968).

PORTABLE NEUTRON RADIOGRAPHIC CAMERA USING ^{252}Cf (2)

by C. B. Shaw* and J. L. Cason*

Supplementary Key Words: (RADIOGRAPHY / PORTABLE / SOURCE, NEUTRON / INSTRUMENT)

Abstract. A first-generation portable neutron camera using ^{252}Cf as the source of neutrons was developed and constructed and is being used in studies on applications. Work to date indicates that a satisfactory neutron dose can be delivered at the object position with satisfactory resolution capability. The entire device - including containment, moderation, collimation, and control systems - is portable.

(Introduction)

Neutron radiography can be used in areas considered out of bounds (or at least of dubious value) by x- or gamma-ray radiographers, for example, in examination of light elements, many composites, rocket propellants, many aircraft components, electronic hardware, and biological specimens.[1] Neutron radiography offers an evaluation method for nuclear reactor fuels in the measurement of poison and hydride contents and enrichment levels. It also provides a usable radiographic tool for both pre- and post-irradiated materials to provide information as to component placement, swelling, rupture, and internal measurements.[2,3]

The rapid growth of neutron radiography applications has been hindered to some extent by the requirement that materials to be tested must be taken to a reactor or neutron generator for evaluation (Fig. 1). The advent of

---

*Battelle Memorial Institute, Pacific Northwest Laboratories (BNWL), Richland, Wash. 99352. BNL-SA-3090, prepared for presentation at a SNT Conf. at Los Angeles, March 1970 (shortened version).

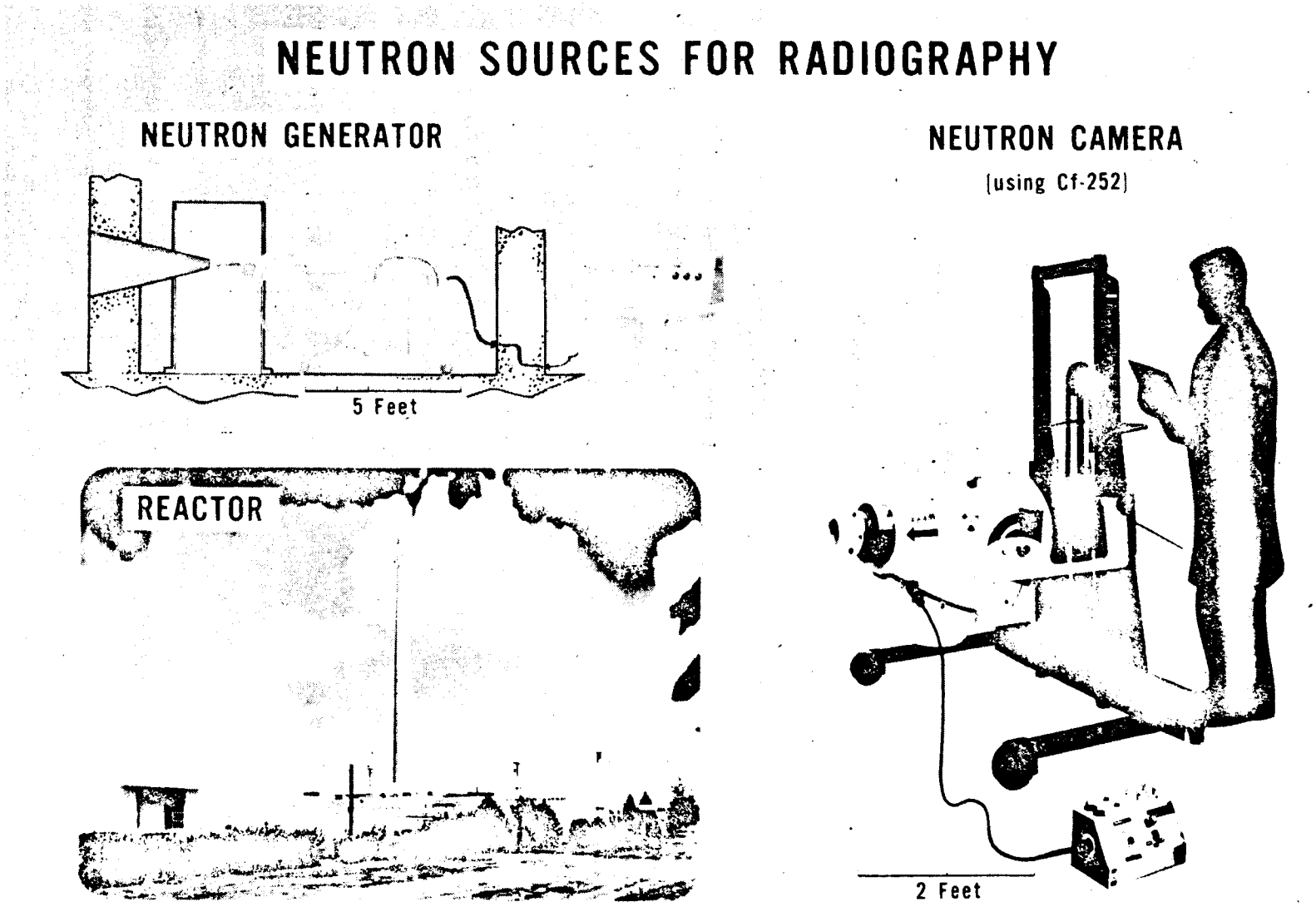

FIG. 1. Comparative Neutron Sources.

^{252}Cf, which has a neutron yield of about 1×10^{12} n/sec·g and a half-life of 2.63 yr, may change this picture. Californium-252 is considered a very attractive candidate for providing a high-neutron-flux portable source of compact size, and BNWL, under contract to the U.S. Atomic Energy Commission Division of Isotopes Development is conducting research on the development of portable neutron radiographic devices using ^{252}Cf.

Initially a computer-assisted analysis was used to determine optimum moderator and imaging materials as well as source-moderator-image material configuration for the use of ^{252}Cf. The fast neutrons from ^{252}Cf had to be moderated since the emphasis was on thermal-neutron radiography. The analytical study was followed by an experimental verification of the analytical predictions. The composite results of the studies provided the design requirements for the fabrication of a portable neutron camera (NC-1). The fabrication of the device was followed by initial flux measurements and neutron radiographs, which correlated with the analytical and experimental evaluation.

The development program is summarized here and the camera developed as a result of these studies is described.

Analysis (3)

A computer assisted analysis utilized an ANISN code with a UNIVAC 1108 computer to provide interpretative data regarding bare source spectrums, moderated spectrums for a given moderator material and thickness, the resultant flux, and the relative image-foil response. The moderators evaluated were paraffin, carbon (graphite), beryllium, titanium hydride, zirconium hydride, beryllium hydride, and water. Foil activities for imaging considerations were also calculated for gadolinium, dysprosium, gold, cadmium, and indium.[4]

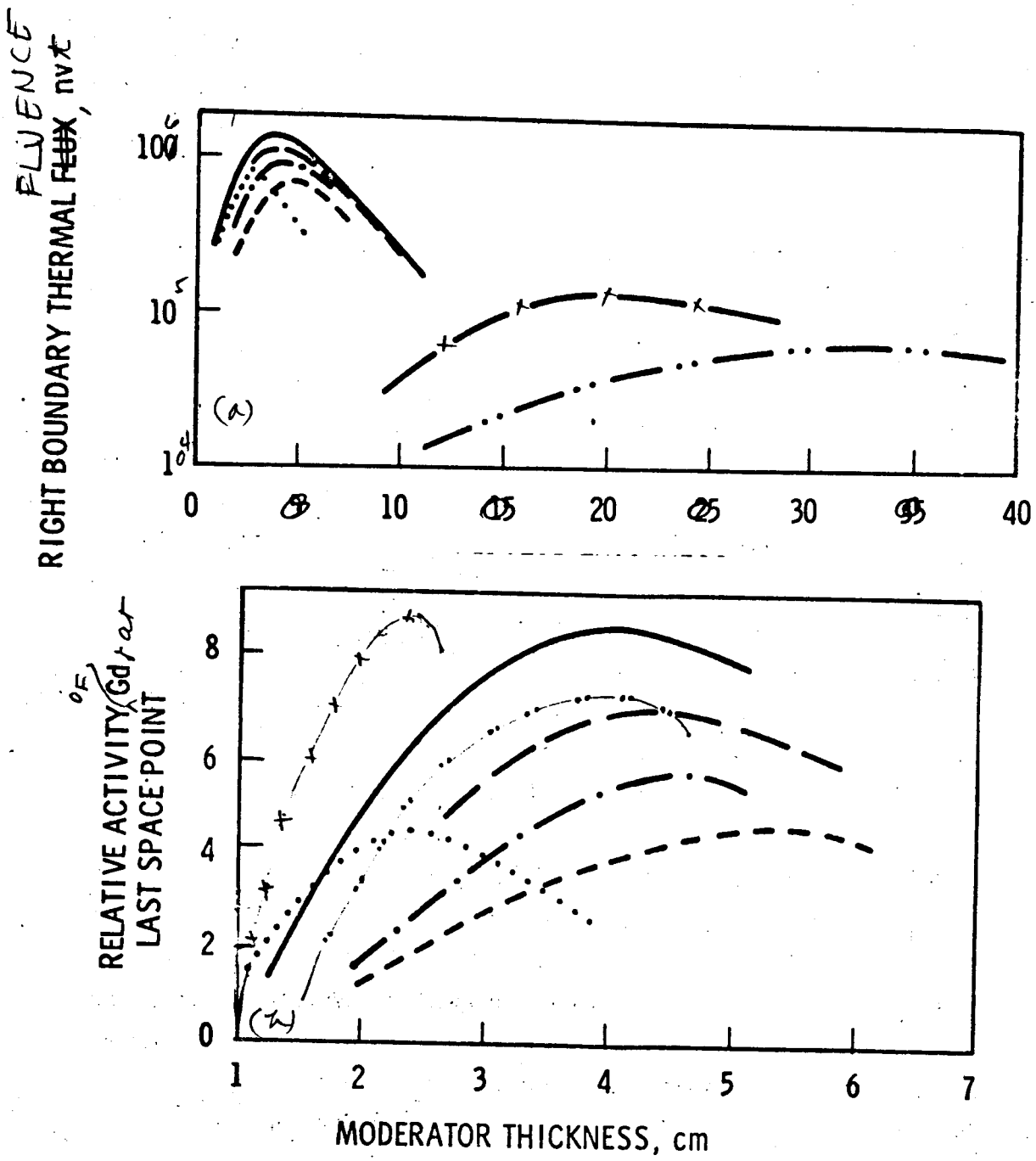

Fig. 2. (a) Calculated right boundary thermal fluence and (b) variation in gadolinium activity at last space point using ^{252}Cf source with various moderators. —— BeH_2; _ _ ZrH_2; = · = H_2O; ··· TiH_2; --- paraffin; -x- Be; -·-· C.

Numerical solution, by the ANISN code, of the multigroup form of the neutron-transport equation for the spherical-geometry case indicated solutions for distinct boundary conditions, thus supporting the requirements for developing a transportable neutron source. The boundary conditions imposed on the analysis were small source volume, steady-state intensity, and optimum moderation and image-foil activity response.

Optimum moderator conditions depended on simultaneously maximizing the thermal fluence at the outer radius of a sphere of moderator surrounding the source and the image-foil activity response at this outer position. Metal hydrides[5] were selected in part because of their high hydrogen content per cubic centimeter as compared to an equal volume of water and paraffin. Metal hydrides - ZrH_2 and TiH_2 in particular - also have the advantage of being able to be heated to 1273°K and cooled to below 10°K without adverse effects on their hydrogen content. Efforts were made to provide the data needed to permit an evaluation of the feasibility of neutron spectrum tailoring by providing various differential neutron plots for given moderator conditions.

Analysis of the results indicated that the feasibility of using ^{252}Cf for thermal neutron radiography was possible with a thermal fluence of about 10^6 nvt (based on a 268- μg source), although 10^4 is acceptable. As expected, the metal hydrides offered the greatest efficiency for moderating the neutrons, requiring an average of about 3.2 cm of material with a calculated thermal fluence of 1.2×10^6 nvt as well as providing an effective gamma filter. Water and paraffin were the second best moderators, needing about 5 cm with a thermal fluence of 7.0×10^5 nvt, and Be and C were the least efficient, requiring an average of about 25 cm of material with a fluence of about 1×10^5 nvt. Results also indicated the practicality of shifting the neutron spectrums by

varying the moderator material and/or thickness. A shift in the neutron spectrum leads to a corresponding shift in the image-foil response. This selective moderation would allow selection of the most appropriate neutrons for a given material thickness, material neutron cross-section, and image technique.

A summary of moderation data for various materials is plotted in Fig. 2a. All fluences should be corrected by multiplying the value from the figure by the actual source strength, calculated to be 6.48×10^8 n/sec. Optimum conditions can be determined by selecting the peak thermal fluence (right boundary fluence for a given thickness of moderator.

Image-foil responses are plotted in Fig. 2 b for the gadolinium activity that gives the optimum thickness of a given moderator to obtain peak response for a given image foil.

The data plotted in Fig. 2 will aid in the selection of moderator-image-foil combinations, thus obtaining conditions for the optimization of the radiographic results.

The thermal flux value predicted from the data plotted in Fig. 2 a aids in the calculation of the required exposure time for a given object material. Another factor influencing the selection of moderator material and thickness is the total fluence (thermal and fast) for a given moderator thickness. Neutron spectrum plots have been obtained by computer techniques for each moderator case.

Using the data thus generated, we are able to bypass the conventional methods of exposing subjects for radiography to a neutron beam obtained by inserting a collimator into a rather large, unwieldy isotope containment tank. An experimental device was constructed for use in verifying the computer analysis. The excellent agreement between analytical predictions and

experiments led to design and fabrication of a first-generation portable neutron camera, designated "NC-1" (Fig. 3).

Camera Design (3)

Studies were made on the use of metal hydrides as moderators, flux measurements, and initial radiographic resolution and imaging. A 268-μg ^{252}Cf source, obtained from ORNL, for experimental testing, had a neutron yield of 6.2×10^8 n/sec and was used in an experimental container designed for neutron radiography.

Experiments were performed to determine the optimum geometry and material for shielding ^{252}Cf. The materials evaluated were zirconium hydride, titanium hydride, paraffin, gadolinium oxide, cadmium, water, and a boron carbide--epoxy resin compound. This resin compound was the most effective shield for fast neutrons, with the resin providing enough hydrogen to moderate the fast neutrons and the boron carbide capturing the thermal neutrons. The half-value layer of this material for fast neutrons from ^{252}Cf was about 1 in.

Shielding data for the gamma radiation associated with ^{252}Cf decay were determined by optimizing the interrelated parameters. The inverse-square principle was used in determining the camera dimensions. The maximum gamma shielding obtainable with neutron shielding and moderator materials was considered, with use of a minimum of depleted uranium rather than a larger volume of lead to cut the remaining dose not accounted for by distance and neutron shielding. The result is the minimum size and weight of the final device. The final design also allowed for variable moderation and collimation.

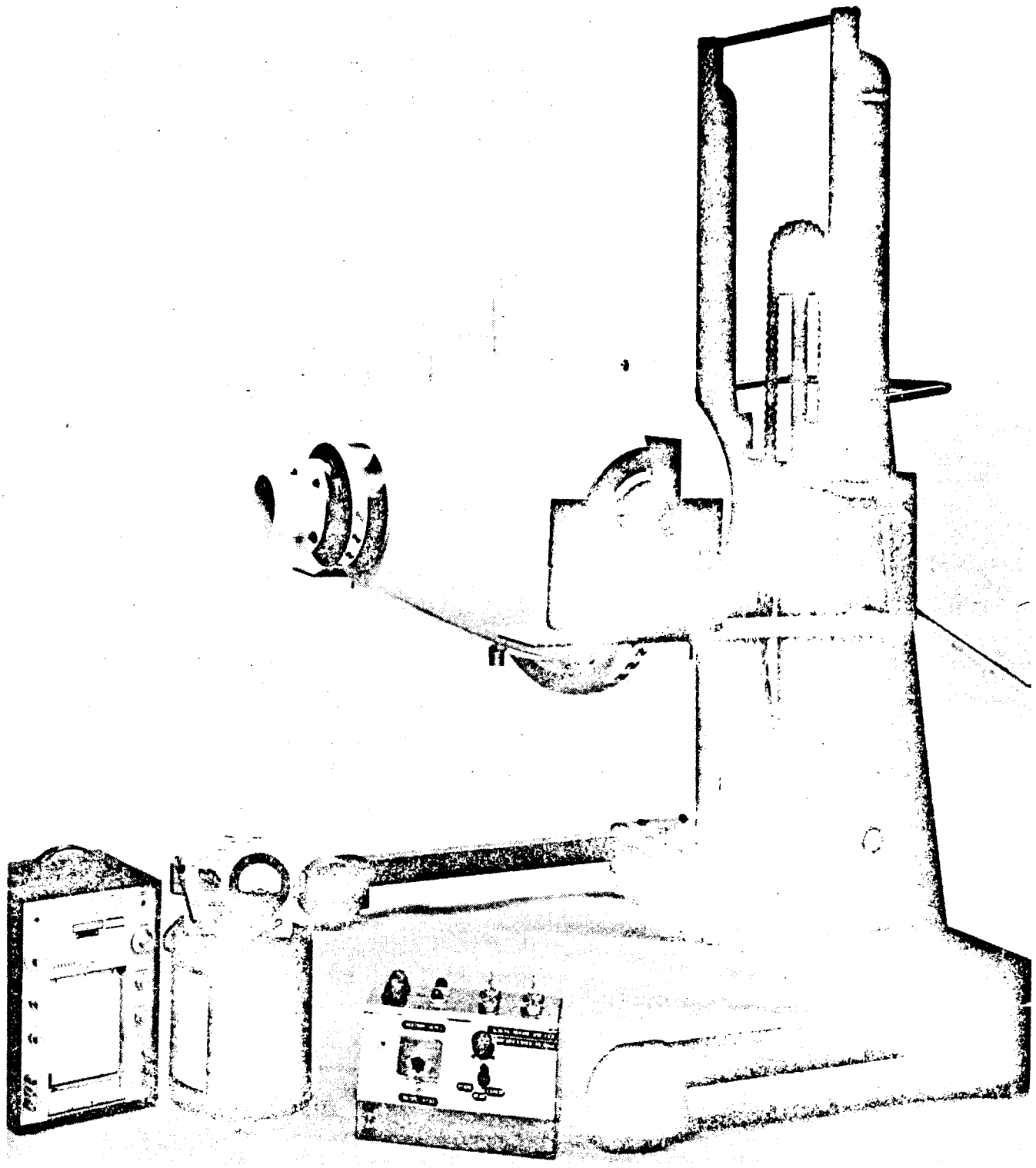

FIG. 3. Neutron Camera NC-1.

In the experimental evaluation of the moderators, ZrH_2 and paraffin were selected because these typify the two classes of potential moderators—metal hydrides and carbon-hydrogen compounds—considered in a portable device. Water was considered experimentally in the same class as paraffin because of the similar hydrogen densities. The average hydrogen density of the zirconium hydride used in these experiments is 7.5×10^{22} hydrogen atoms per cubic centimeter and of water, 6.7×10^{22} hydrogen atoms per cubic centimeter.[5,6] As expected, zirconium hydride was the more efficient moderator.

The analytical computer studies together with the experimental camera configuration provided the requirements for the design and fabrication of a prototype portable neutron camera (NC-1). Primary considerations were safety, size, weight, structural rigidity, simplicity, and operability.

The camera was constructed in a modular manner so that modification can be made for shielding, moderation, and collimation. It consists of an egg-shaped, laminated, glass-fiber outershell, two internal metal drums, shielding and moderator materials, adjustable metal holder for collimators and moderators, and an electric-motor-drive controller unit for rotating one of the internal metal drums.

The camera is designed so that a ^{252}Cf source positioned in the inner drum may be rotated by remote control or manually to two lockable positions. One position allows a neutron beam to be selectively moderated and radiographs to be produced; the other position is for storage of the source in a shielded location.

Evaluation (3)

The initial phases of the evaluation of NC-1 included flux measurements and operational and physical characterization of the construction materials used in the camera.

Flux measurements for the optimum case were made using the indium-foil activation technique for both bare and cadmium-covered foils. The results given correlate well with calculated values:

	Thermal Flux, MW	
	Calculated	Measured
Paraffin	6.7×10^5	6.6×10^5
ZrH_2	1.2×10^6	1.3×10^6

Neutron radiographs have been made which demonstrate the feasibility of using ^{252}Cf in a portable device for thermal neutron radiography. One of these radiographis with an image quality indicator and an x radiograph of the same object are shown in Fig. 4. One object consisted of small squares of various materials, which were, beginning on the left, from top to bottom,

0.010 in. of copper	0.010 in. of gold
0.060 in. of paraffin	0.010 in. of indium
0.040 in. of paraffin	0.020 in. of indium
0.020 in. of paraffin	0.030 in. of indium
0.020 in. of cadmium	0.015 in. of lead
0.040 in. of cadmium	0.030 in. of lead
0.060 in. of cadmium	0.045 in. of lead

The second object was a cadmium shim containing holes of various sizes from 0.013 to 0.125 in. diameter; the minimum separation between the holes was 0.010 in. and the greatest, 0.125 in. The third object consisted of three M-16 bullets, with a booby-trapped round on the extreme left, a tracer-loaded round in the middle, and a standard-load M-16 round on the right. It is obvious that the x radiography and the neutron radiograph provide different information concerning the objects. Figure 5 is a photograph, an x radiography, and a neutron radiograph of the same four bullets. Bullet A was an empty shell, B contained LSD, C contained marijuana, and D had a standard load.

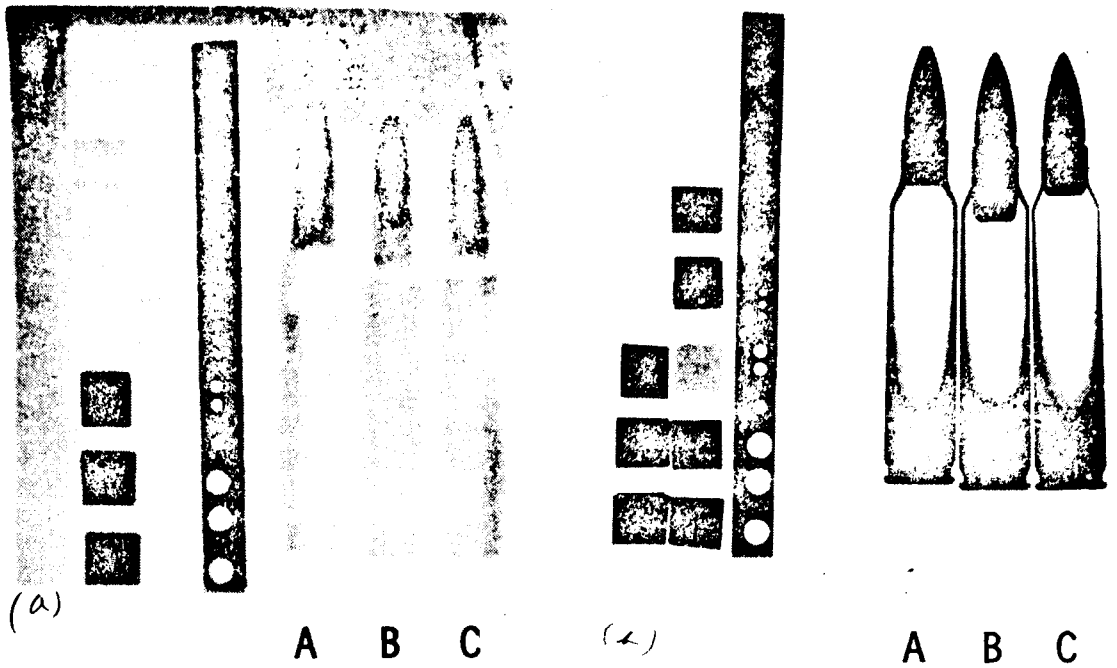

Fig. 4. (a) Neutron radiograph and (b) x radiograph of, left to right, small squares of copper, paraffin, gold, indium, and lead of various thicknesses (see text); cadmium containing different size holes; and M-16 bullets, where A is booby-trapped, B is tracer-loaded, and C has a standard load.

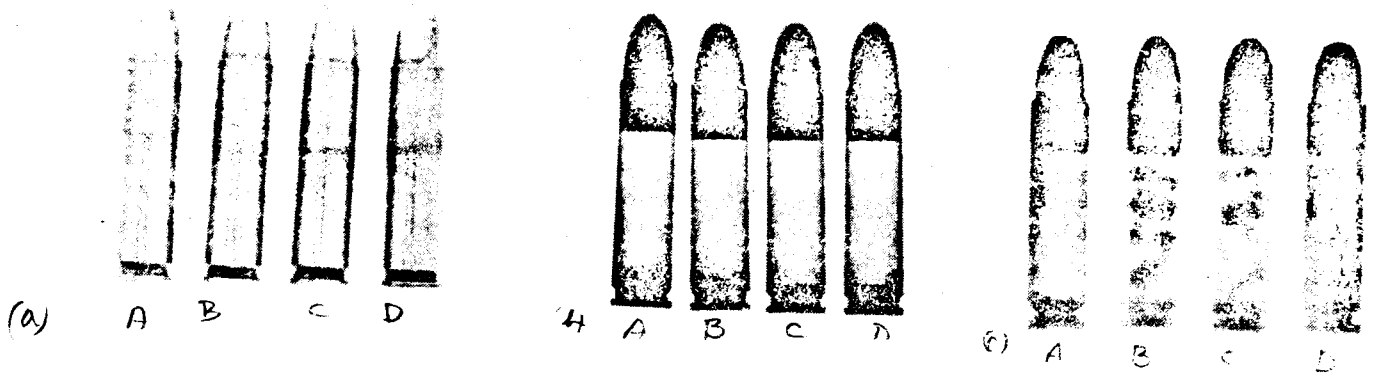

Fig. 5. (a) Photograph, (b) x radiograph, and (c) neutron radiograph of 30-caliber bullets. A, an empty shell; B, LSD load; C, marijuana load; C, standard load.

Using a direct technique with a neutron scintillation screen, a typical radiograph can be produced in less than 15 min. Neutron radiographs using an activation-transfer technique with a dysprosium or indium foil required several hours with the source strengths available at the time of the tests. With the larger sources now available, shorter exposure times can be expected.

The camera shell is made from 0.5-in.-thick Fiberglas-epoxy laminate, chosen because of the ease with which it can be molded into spherical and odd-angle shells; its high tensile strength (50 thousand psi); high compressibility (70 thousand psi); light weight; excellent neutron shielding characteristics; fire-resistance characteristics (self-extinguishing epoxy resin); resistance to acids and bases; high impact resistance (70 thousand psi); relatively low cost; and thermal and electrical conductance properties (insulator in both bases). The gamma and neutron dose rates at the surface of the device when the source is in the stored position are 50 and 200 mR/hr, respectively. The source position can be controlled and monitored remotely.

The camera appears to be suitable for use in reactor-fuel radiography, and for determination of polymer content and distribution in concrete. It can be operated manually, using batteries or house current (110 V ac). The measure of success of the project can perhaps be judged by comparing the 4400-lb container in which the ^{252}Cf arrived at Battelle Northwest with the 100-lb camera now in use or by comparing the experimental device, which was restricted to use in a shielded facility, with present use in a conventional x-ray laboratory.

Work is proceeding to fully evaluate the physical properties of the Fiberglas construction material for tensile strength, compressibility, thermal conductivity, etc. Efforts will be made to decrease the size and weight of the camera and to design neutron cameras for specific uses,

taking into consideration transport, environmental conditions, need for certain portions of the neutron spectrum and size of source material.

(MG)

REFERENCES

1. J. L. Cason. Neutron Radiography with ^{252}Cf in Forensic Science, BNWL-SA-2865, Battelle-Northwest, Richland, Washington, Oct. 1969.
2. H. Berger. Neutron Radiography - Methods, Capabilities and Application, Elsevier Publishing Co., New York, 1965.
3. J. L. Cason and C. B. Shaw. "Neutron Radiography with Cf^{252}", Transaction, American Nuclear Society, Vol. 12, No. 2, Nov. 1969.
4. W. Mueller, J. Blackledge, G. Libowitz. Metal Hydrides, Chapters 2, 7, 8, Academic Press, New York, 1968.
5. Unpublished Data. Battelle-Northwest, Richland, Washington, 1969. (Private communication with R. Van Houten and W. G. Baxter, General Electric Corporation NSD, Cincinnati, Ohio).

THE TOUR OF THE PORTABLE CESIUM IRRADIATOR—PART II

Supplementary Key Words: (FOOD PRESERVATION / INDUSTRY / INDUSTRY, FOOD / FOOD EVALUATION, SUBJECTIVE / SEAFOOD / VEGETABLE / GRAIN / FLOWER / INSECT CONTROL / FRUIT / POTATO AND ONION / REVIEW, POPULAR / DID REPORT / MOBILE / CESIUM-137 / INDUSTRY, TEXTILE / INDUSTRY, LEATHER)

Abstract. During 1968, the Portable Cesium Irradiator toured the western United States. The unit irradiated fresh and dried fruit, fresh vegetables, rice, potatoes, and other products in California, Arizona, and the Pacific Northwest states. The irradiator returned to Brookhaven National Laboratory in 1969 for modifications. The program was suspended because of budget restrictions.

(Introduction)

The first article[1] in this series described the start of the tour of the Portable Cesium Irradiator (PCI). Over 30,000 lb of products was irradiated in the period covered---August 11 to November 30, 1967. During 1968, the PCI toured the western states, was exhibited to the public, and demonstrated the effects of radiation to commercial food companies (Fig. 1). The unit returned to Brookhaven National Laboratory in 1969 for overhaul and modifications to bring it into compliance with new federal safety regulations. The modifications were completed in May 1969, but the demonstration program was suspended because of the severe budget restriction on the USAEC food irradiation program for FY1970. The PCI is now stored at Brookhaven National Laboratory. This article summarizes the last two reports[2,3] on the program and covers the last 6 months of the program through contractor reports.[4]

Results From 1967 Demonstrations (3)

One purpose in demonstrating the PCI to food industry members was to allow them to evaluate for themselves the effects of radiation on the specific foods in which they are interested. As part of their agreement with the AEC for use of the PCI, the commercial users were to report their observations.

Complete Evaluations (4)

Only one of the companies that used the PCI in 1967 has completed its evaluation. Caruso-Cerisi, Inc., Cincinnati, Ohio, tested irradiation of oranges, potatoes, strawberries, and tomatoes. This company is a fruit and vegetable wholesaler and normally does not hold produce long.

They reported very satisfactory results with straw-

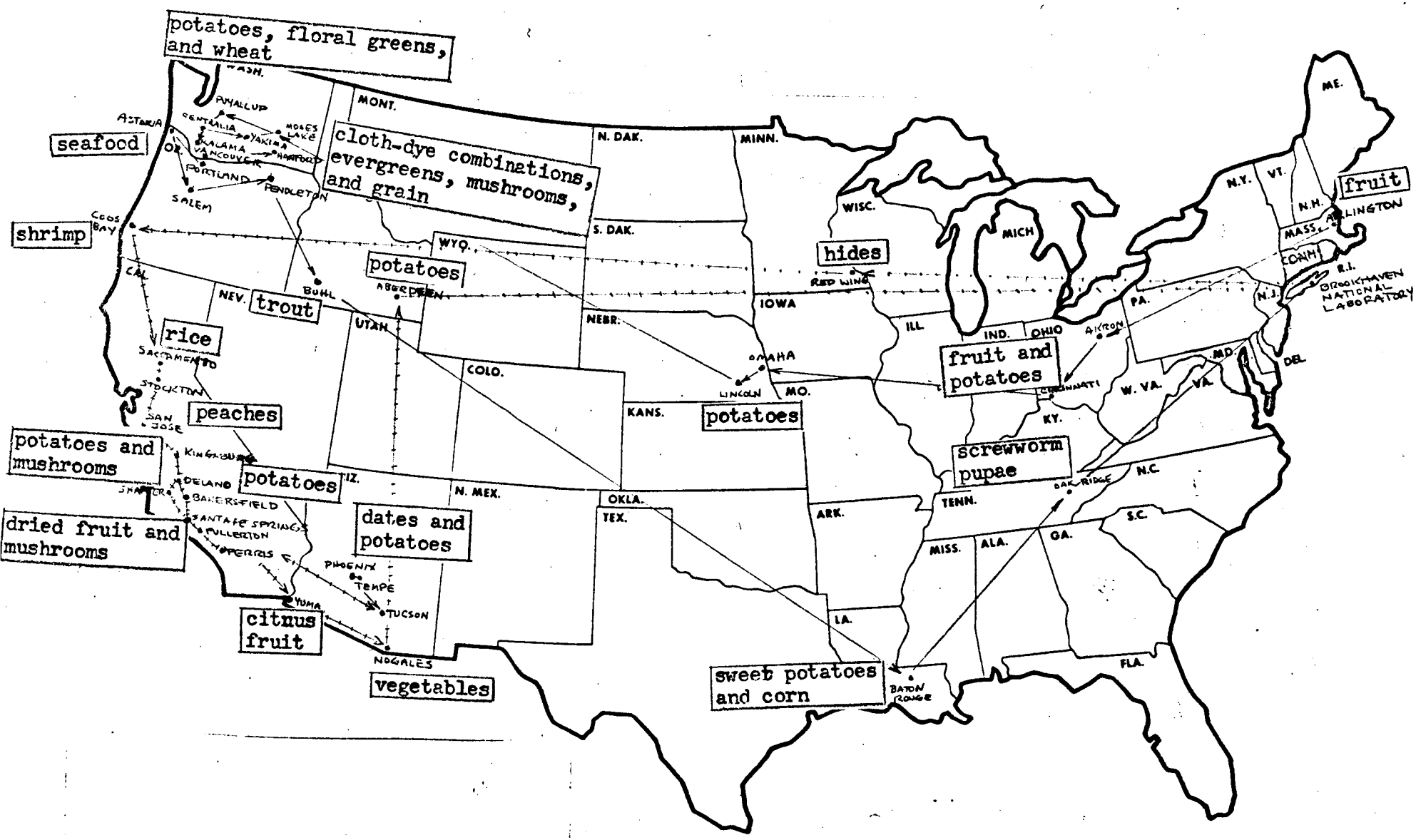

Fig. 1. A summary of the PCI tour.

——— First tour, Aug. 11, 1967 to May 16, 1968.

+—+—+ Second tour, June 4, 1968 to Jan. 4, 1969.

berries. Irradiated samples showed 60% less rot than controls after 20 days at 56 to 70°F (13 to 21°C). Decay of irradiated tomatoes was considerably less than that of controls under the same conditions. Irradiated oranges and potatoes showed little difference from controls over such a short period. Caruso-Cerisi believes that irradiation can be a great help in keeping strawberries but offers no great advantage to the wholesaler. The benefit would accrue mainly to the shipper, especially during shipping delays.

Incomplete Evaluations (4)

Potatoes were irradiated for three companies during 1967: K. T. Salem Co., Akron, Ohio; Kitty Clover, Omaha, Nebraska; and Weaver Potato Chip Co., Lincoln, Nebraska. The potatoes were placed in large well-labeled containers and were stored by each company. They were to be evaluated at a later date for sprout inhibition and other effects; no results from these demonstrations have been received.

Demonstrations During January 2--March 23, 1968 (3)

During January, holly, salal, huckleberry, fern, kamador, and seedlings were irradiated for G. R. Kirk Co., Puyallup, Washington. The unit was demonstrated to about 2,350 students at Centralia Junior College, Centralia, Washington. The PCI spent most of February being demonstrated to the public. Stops included the Yakima Chamber of Commerce, the Washington State Potato Conference and Trade Fair in Moses Lake, and Clark Junior College in Vancouver, Washington. At Kalama, 45 lb of wheat was irradiated for the Pacific Grain Grower's Association. In March, holly was irradiated for Brownell Holly Farms, Inc., Milwaukie, Oregon.

The irradiator broke down twice during this first period of operation. On January 9, a shuttle jammed during dosimetry runs. The PCI was taken to Hanford for repair. In a shielded facility at Hanford, the outer door of the irradiator was forced open, and a box was found that had fallen off the shuttle

tray and was obstructing passage of the shuttle. This situation was corrected, and the PCI was returned to service.

On March 6, another malfunction occurred. Again, the unit was driven to Hanford and placed in a shielded facility. A cam roller used to support the shuttle had become lodged in the inner door of the irradiator. Evidently, the bearings in the roller had seized because the radiation had polymerized the lubricant. The rollers were replaced with sliding tracks supported in the outer chamber, and the PCI resumed its demonstrations.

Results of Demonstrations (3)

Complete Evaluations (4)

No evaluations of the demonstrations that occurred in this first period of 1968 have been completed.

Incomplete Evaluations (4)

Brownell Holly Farms had holly irradiated to evaluate its retention of color, berries, and foliage. Three types of packages were used, and three doses of radiation were given (Table 1). This company was satisfied with the result and is interested in further testing of cut holly, holly wreaths, and other made-up holly items.

No other incomplete evaluations have been reported for this period.

Demonstrations During March 24--June 18, 1968 (3)

At the Oregon State University Seafoods Laboratory, the PCI processed red snapper, salmon, Dungeness crab, fish pellets, and fish extract. In April the unit irradiated 22 samples for Jantzen, Inc. to determine whether or not the dye-fast period of certain cloth--dye combinations could be extended by irradiation. Cut boughs of Sitka spruce, Douglas fir, hemlock,

Table 1 Response of Holly to Gamma Radiation

Package	Holly content, lb	Days after irradiation	Effect of dose: 50 krad	150 krad	300 krad	Control
Transparent ventilated cellophane bags	0.5 (undipped)	7	Lost	No change	No change	No change
		14	Lost	Good condition and color	Beginning to darken	Moist, good color, no discoloration or berry drop
		21	Lost	Some moisture, better than 300-krad treated	Some moisture, leaf darkening, and berry drop	Moist, saleable, good color leaves, no berry drop
Printed cardboard boxes	1 (undipped)	7	Lost	No change	No change	No change
		14	Lost	Dehydration, but no defoliation or berry drop	Discoloration and spoil	Unsaleable, but no berry or leaf drop
		21	Lost	Same	Same	Same
Standard fiberboard boxes, lined with laminated polyethylene refrigerator wrap	0.5 (dipped)*	7	No change	No change	No change	No change
		14	Very good	Some leaf darkening and berry drop	Marked defoliation, darkened leaves	No change
		21	Saleable, no defoliation or berry drop	Leaf discoloration and berry drop, but distinctly better than 300-krad treated	Total defoliation, black leaves, and moldy berries	Good quality, but some berry drop

*Standard α-naphthalene acid solution, used to protect against defoliation.

and grand fir were irradiated for the State Forestry Service of Oregon. West Foods, Inc., a producer of fresh mushrooms, participated in a shelf-life extension and transportation test of mushrooms. The irradiated product was shipped from Salem to Seattle under normal commercial conditions, and then was returned to Salem for evaluation. In a disinfestation demonstration, Pendleton Grain Grower's, Inc. had 50 lb of weevil-infested whole wheat irradiated. The unit moved to Buhl, Idaho, where rainbow trout were irradiated. Snake River Trout Co. kept 20 lb for in-house evaluation; 40-lb lots were sent to the Oregon State University Seafoods Laboratory and to the Bureau of Commercial Fisheries Laboratories in Seattle and in Gloucester, Massachusetts. An additional 20 lb was kept by Blue Lakes Trout Farms, Inc. for in-house evaluation. Three other demonstrations in Buhl involved irradiating potatoes for Campbell Soup Company, wheat for Colorado Mills, and a sludge of potato wastes for the Idaho Health Department.

In May, 1968, the PCI traveled to Baton Rouge, Louisiana, where weevil-infested sweet potatoes were irradiated. The unit also processed weevil-infested corn. The next stop on the tour was Oak Ridge, Tennessee; 30 South American industrialists were shown the unit. Screwworm pupae were irradiated for the U. S. Department of Agriculture.

The PCI moved to Red Wing, Minnesota, in June, 1968 and irradiated raw cattle hides and some finished leather.

During this period, one major and one minor malfunction occurred. At Oak Ridge, the shuttle again failed to retract clear of the inner door. The PCI was driven to Brookhaven National Laboratory for repairs. A pin in the shuttle drive-shaft pinion had sheared. The minor malfunction, which occurred at Red Wing, was repaired in the field.

Results of Demonstrations (3)

Complete Evaluations (4)

Jantzen, Inc., swimsuit and sportswear manufacturer, wanted to know if irradiation could increase the lightfastness of nylon cloth dyed with Kiton pure black dye, which is the combination that both fades most rapidly and is most popular. The tests consisted in irradiating predyed nylon cloth, cloth immersed in dye solution, powdered dye, nylon cloth padded with dye prior to irradiation, and nylon greige goods before being dyed and wet with dye. Doses applied were 0.1, 0.3, 0.5, 1.0, 3.0, 5.0, and 10.0 Mrads. All samples were tested for lightfastness and fabric elongation. The irradiated and control fabrics differed in neither color fastness nor fabric elongation. The Jantzen company thinks that a series of tests designed statistically to limit the number of variables might show some radiation effect.

The evergreen boughs tested by the State Forestry Service of Oregon were cut from Douglas fir, grand fir, Sitka spruce, and western hemlock. The purpose of the demonstration was to determine if radiation might allow the use as Christmas trees of species that are unsuitable because of their short needle-retention time. Samples were placed in plastic bags and inserted in cardboard boxes for irradiation to doses of 100, 300, or 500 krads. The samples were removed from the package and were hung tip down in a room at 65 to 70°F. Each morning, the butt end of each sample was thumped. Percent needles remaining on sample was plotted versus date thumped. Although some increase in needle-retention time was observed for Sitka spruce and grand fir, overall test results were inconclusive. Further tests with a wider range of doses on boughs cut during the normal dormant period would increase the significance of the results.

West Foods, Inc., Salem, Oregon, irradiated fresh mushrooms, stored them 1 day at 35°F, packaged them, and shipped them to Seattle. They were placed in a storecase at 45°F for 2 days and then were returned to West Foods for evaluation. The mushrooms did not grow or start to open until the fifth day after irradiation. Normal shelf life is about 3 days; with irradiation, an additional 3 days of shelf life was gained. West Foods, Inc. was very satisfied with the process, but because the company handles only a small amount of this product, it could not justify the cost of a commercial irradiator.

Snake River Trout Co. completed its evaluation of irradiated rainbow trout, and reports were submitted through this company by evaluators at the two Bureau of Commercial Fisheries Laboratories and at the Oregon State University Seafoods Laboratory. Freshly killed and eviscerated trout were washed, sealed in polyethylene pouches, and irradiated at 50, 100, or 200 krads. Trout irradiated at 50 and 200 krads were in very good condition 12 days later and were still edible 16 days later, even though storage conditions were not ideal. Irradiated trout were no better than the control trout when storage conditions were excellent. The Snake River Trout Co. thinks that irradiation could offer advantages in its operation, although these tests in themselves were inconclusive.

Incomplete Evaluations (4)

Ocean Foods of Astoria, Inc., Astoria, Oregon, evaluated red snapper fillets. Doses were 100, 200, or 300 krads. At 9 days after irradiation, irradiated fish were judged poorer in appearance than controls. There was no change in irradiated fish 5 days later, but the controls were spoiled. A third inspection a week later showed more discoloration and odor in the irradiated fillets; inspection at 31 days after irradiation showed that the irradiated fillets were spoiled. However, three cartons of fillets that had been irradiated but not inspected up to this time were opened, and the fish were found to be edible. Although longer holding time might increase sales, the company feels that the high cost of irradiation units, the unsteady supply

of raw product, and the low margin on sales of seafood would put the irradiation process beyond their means.

Bumble Bee Seafoods, Inc., Astoria, Oregon, received salmon that had been irradiated to 150 and 250 krads. They evaluated cut salmon steaks "several weeks later," at which time the irradiated samples were inferior to controls in appearance and flavor. The company is not in the cut-portion control phase of the fish business and is not interested in further work on fish irradiation.

Pendleton Grain Growers Association, Pendleton, Oregon, reported that irradiation is obviously very effective as an insect control. They feel that the method would be commercially attractive if grain could be treated at a rate of 10,000 to 15,000 bushels/hr and at a cost not greater than 1 cent/bushel.

No other test results are available from this series of demonstrations.

Demonstrations During June 18---August 10, 1968 (3)

At Coos Bay, Oregon, shrimp were irradiated for the University of Oregon. A small catch caused by bad weather conditions resulted in only a small amount of product being irradiated. In July, the PCI moved to Stockton, California. Potatoes were processed for General Potato and Onion Distributors, Inc., with doses used for both sprout inhibition and growth stimulation. In Delano, Calfornia, more potatoes were irradiated, again at dose levels of sprout inhibition and of growth stimulation. Participants were D. M. Steele and Sons, Inc. and Delano-Earlimart Potato Growers, Inc. The unit moved on to the California Potato Grower's Association in Shafter, California, where E. H. Meltler and Sons had potatoes irradiated at sprout-inhibition doses and The Kroger Potato Company had potatoes irradiated at growth-stimulation doses. In Perris, California, 2500 lb of potatoes was given growth-stimulation doses for the MSW Produce Company. California Mushroom Farms, Inc., Santa Fe Springs, provided 120 lb of mushrooms and 30 lb of cover soil for irradiation processing.

In August, raisins were irradiated for Sunmaid Raisins, Inc., Kingsburg, California. The raisins were spiked with confused flour beetles, dried fruit beetles, raisin moths, drimestid, and merchant beetles. In addition to the insect disinfestation study, bulk raisins and raisin paste were irradiated to study the effect on shelf life. The Dried Fruit Association of California had figs irradiated to study bacteria control and insect disinfestation. At San Jose, California, the PCI irradiated 750 lb of peaches for California Canners and Growers.

During this period, one small malfunction of the unit occurred at Perris, California. It was repaired with little difficulty.

Results of Demonstrations (3)

Complete Evaluations (4)

In tests for California Canners and Growers, whole peaches were irradiated and then stored under commercial conditions at either 32 to 35°F or 55 to 65°F. Peach slices were irradiated in sealed clear plastic pouches; half of the pouches contained the preservatives sodium benzoate (0.02%) and sodium metabisulfite (11 ppm). All were stored at 32 to 35°F. Peach halves were irradiated and then stored in 1-gal jars under a 0.05% solution of sodium benzoate at pH 2.5. The whole-peach controls stored at the higher temperature were entirely rotted in 4 days, but the irradiated peaches were only 50% rotted. The results were similar for peaches stored at 32 to 35°F; after 28 days, the controls were totally rotted but the irradiated peaches were only 50% rotted. The company's representative believes that the softening of the irradiated fruit is an advantage. The irradiated sliced peaches kept well but did not differ from the controls. Refrigeration failed after 46 days, and this experiment was terminated. Irradiation was ineffective as an aid in the preprocessing of peach halves. California Canners and Growers found

irradiation effective as a rot control method for fresh peaches. The company suggested that the process might most likely be used on chill-packed items.

Incomplete Evaluations (4)

The only reply from the participants at the Coos Bay, Oregon stop came from Eureka Fisheries. They received 18 lb of shrimp in 1-lb cans, irradiated at doses of 50, 100, or 200 krads. The company reported that the product was excellent. No storage data were given. They believe that, because of the limited available supply of the product, a change to the radiation method is not warranted at this time.

No other evaluations have been reported from the demonstrations condutted during this period.

Demonstrations During August 11---October 12, 1968 (3)

Dried fruits---apricots, peaches, and prunes---were irradiated for the Mayfair Packing Company, San Jose, California. Three other companies provided products to be irradiated in San Jose. The Sunsweet Packing Company irradiated fresh and dried prunes; the dried prunes were inoculated with bacteria. Mushrooms were irradiated for Stoller Research, as were some spawn substrates. Mixed dried fruits were irradiated for California Packing Corporation. The PCI moved to Fullerton, California, where orange juice in pints and quarts was treated for the Vim Corporation. In September, the unit was set up at the California Rice Growers Association, Sacramento, where rice and associated products were irradiated for growth stimulation, pasteurization, or sterilization. The first part of October was spent exhibiting the PCI to the public at various locations in Arizona.

Results of Demonstrations (3)

Complete Evaluations (4)

No complete evaluations resulted from this series of demonstrations.

Incomplete Evaluations (4)

All the dried fruits irradiated for Mayfair Packing Company were placed in accelerated storage. At the end of 1 week, both irradiated and control samples had an abundant growth of microorganisms. These results indicate that irradiation did not prevent microbial spoilage.

The primary objective in irradiating rice and rice bran was to evaluate radiation for extending the keeping quality of the products. Both grains were stored at 90°F or 120°F for 4 weeks after irradiation. Green rice gave good results under adverse storage conditions---low moisture content and high storage temperature. Irradiation of bran did not affect the properties tested. Rice hulls, parboiled rice, and seed rice were also processed. The Rice Growers Association of California has made no comment on the preliminary results, but radiation does not seem to have provided an advantage.

No other evaluations have been received, and of course none were expected from the public demonstrations.

Demonstrations During October 13---December 19, 1968 (3)

Dates were irradiated for Palmer Date and Citrus Garden, Mesa, Arizona, and cucumbers were irradiated for S. Klein Pickle Company, Inc., Phoenix, Arizona. In Tucson, chopped beef and precut potatoes were irradiated for a researcher at the University of Arizona. The rest of October was spent at public exhibitions.

In November, the PCI was displayed at the Arizona State Fair and at the National Potato Conference in Bakersfield, California. At Yuma, Arizona, Rancho del Sol and Arizona Growers both irradiated fruits to reduce decay and spoilage. The fruits included waxed and unwaxed grapefruit, lemons, navel oranges, and Hamlin oranges. At Arizona Western College, researchers irradiated Hamlin oranges, lemon seeds, citrus leaves, and picker's clothing infested with thrips

and spider mites. Dates were irradiated for Berryman Farms, Bard, California, for shelf-life extension studies.

In December, the PCI was set up at Nogales, Arizona, where eggplant was irradiated for Floriza Vegetable Distributors, bell peppers were irradiated for Kitty's Produce Company, and tomatoes were irradiated for Tricar Sales, Inc. The unit was also demonstrated to the public at Nogales. The PCI then moved to Aberdeen, Idaho, where 35,000 lb of potatoes was irradiated at sprout inhibition doses for the U. S. Army.

The second major malfunction of the year occurred at Aberdeen. As the shuttle moved in and out, it could be heard scraping the source guard; the shuttle was sagging because of the extreme wear on the bearings of the shuttle slide. Further irradiations were deemed unwise. Since the unit was scheduled for a major overhaul after a successful 1.5-yr operation, it was driven to Brookhaven National Laboratory.

Results of Demonstrations (3)

No results---incomplete or otherwise---of the demonstrations held during the last part of 1968 have been submitted.

Operations in 1969 (3)

On January 4, after a long trip delayed by weather conditions and holiday restrictions, the PCI arrived at Brookhaven National Laboratory. The scheduled modifications included replacement of the dual-axle 35-ft trailer with a triple-axle 40-ft trailer weighing three times as much as the original trailer, installation of a steelplate puncture shield and a crash frame, and improvements in the shuttle, door-drive systems, actuators, and controls. These changes were required to bring the irradiator into compliance with Title 10, Part 71 of the Code of Federal Regulations.

By April, the irradiator itself was reassembled and working. The new trailer was delivered; all modifications were completed and work was finished by May. The PCI was ready for another tour demonstration. Unfortunately, this program had to be suspended as part of the budget cut in the USAEC's food irradiation program. The Portable Cesium Irradiator is now stored at Brookhaven National Laboratory.

(FEM)

References (3)

1. The Tour of the Portable Cesium Irradiator, Isotop. Radiat. Technol., 5(4): 289-292 (Summer 1968).
2. W. B. Grant, W. E. Erlebach, and L. M. Sine, Jr., Demonstrations Conducted by the Portable Cesium Irradiator During the Period September 30, 1967---December 19, 1968, USAEC Report NYO-3740-4, July 1969. (Published with USAEC Report NYO-3740-5 in one volume.)
3. W. B. Grant, L. M. Sine, Jr., and W. E. Erlebach, Operation of the Portable Cesium Irradiator, Report for Period 11 August 1967---30 June 1969, USAEC Report NYO-3740-5, July 1969. (Published with USAEC Report NYO-3740-4 in one volume.)
4. E. B. O'Brien, Isotopes, A Teledyne Company, Contract AT(30-1)-3740, unpublished monthly reports.

IV. PROCESS RADIATION DEVELOPMENT

RADIATION GRAFTING ON COTTON TEXTILES AND FIBERS (2)

Allan S. Hoffman*

Supplementary Key Words: (GRAFTING / POLYMERIZATION / INDUSTRY / INDUSTRY, TEXTILE / SOURCE, GAMMA / COBALT-60 / ACCELERATOR/ BIBLIOGRAPHY / REVIEW, TECHNICAL / ECONOMICS / PLANT SCALE / PATENT)

Abstract. The literature (53 references) on radiation grafting of cellulose fibers is reviewed.

(Introduction)

Most textiles go through one or more finishing processes that modify their bulk or surface properties — e.g., crease recovery, shrink resistance, flammability, dyeability, stain and soil release, and static dissipation.[1,2] Such property modifications may also be effected by high-energy ionizing radiation, either through crosslinking or degradation of the polymer chains that make up the textile fiber or through graft copolymerization of various monomers to these chains. Graft copolymerization is by far the most important and versatile of the radiation techniques used with textiles and is the main consideration of this review.

Two very comprehensive reviews have appeared recently on radiation modification of textiles.[3,4] This paper, therefore, considers mainly two areas that have had the greatest recent impact on commercial application of radiation in textiles: crease recovery (or permanent press) and surface modification of wetting properties such as soil and stain release, with particular regard to celulosic materials.

Radiation Sources (3)

Radiation doses needed for grafting reactions are usually in the range 0.5 to 5 Mrads. Typical line speeds in a textile finishing plant are about

---

*Associate Professor of Chemical Engineering, Massachusetts Institute of Technology, Cambridge, Mass. This paper is a modification of one presented at the International Atomic Energy Agency Symposium on Utilization of Large Radiation Sources and Accelerators in Industrial Processing, Munich, Aug. 18-22, 1969.

300 ft/min, and thus, for a fabric to be continuously treated, the dose must be 50 to 500 Mrads/min since the total length along the moving fabric that is exposed to the radiation field is equivalent to 3 ft (achieved by festooning the fabric). Such dose rates are clearly many orders of magnitude above the range of radioactive sources—e.g., ^{60}Co which provides 10^{-6} to 10^{-2} Mrad/min—and are within and just above the 10^{-1} to 10^{2} Mrads/min provided by currently available electron accelerators, although machines that provide higher dose rates are under development.[5] Since a textile fabric is thin, it lends itself readily to processing by an electron beam. However, a batch process in which whole bolts of cloth are irradiated by a ^{60}Co source either before, during, or after exposure to monomer is conceivable. Various possible radiation-induced processes are shown in Fig. 1.

The only publicly announced commercial application of radiation processing in the textile industry uses electron accelerators.[6] The final decision as to whether or not to use radiation in a production process clearly rests on economic considerations. Cost estimates[7] for continuous electron processing of textiles range between 0.01 and 1 cent per running yard, depending on line speeds, dose, operating schedules, depreciation rates, etc.

Kinetic Considerations (3)

In an organic fiber, the polymer matrix is usually highly crystalline, and the crystallites may be highly distorted due to orientation of the fiber. This leads to small, narrow amorphous regions. Free radicals formed within the crystals must somehow diffuse to the edges or surfaces of the crystal lattice where they can react. Grafting reactions are restricted to amorphous regions or to defects in the crystalline structure, and therefore the mobility

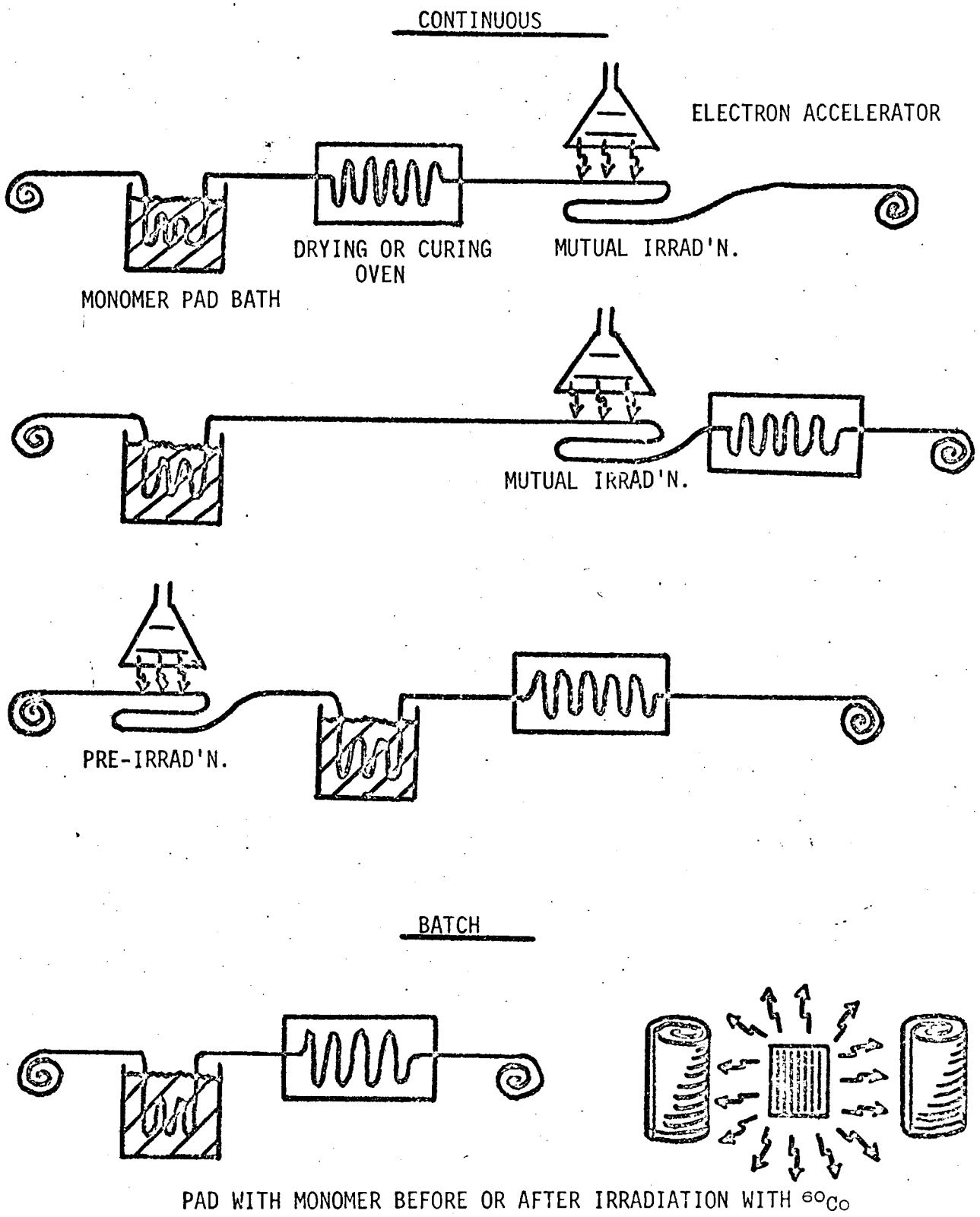

Fig. 1. Processes for radiation modification of textiles.

of a growing grafted chain will be especially low, leading to significant decrease in the mutual termination rate constant, k_t ("gel" effect).[8] Some chains may never terminate, being occluded or buried within the polymer structure, which may cause continued reaction after irradiation, a "post-effect."

Monomer molecules are much more mobile than polymer radicals or growing grafted chains, and therefore the rate of grafting in any small-volume element within the polymer will depend on the local monomer concentration, (M). This generally leads to control of monomer diffusion and the local monomer diffusion coefficient, D, will be important. Due to the restricted reaction conditions, the propagation rate constant, k_p, may also be decreased below that expected for a homogeneous polymerization in solution or in bulk, especially at low degrees of swelling of the polymer substrate.

It is usually desirable that the polymer free radicals react as rapidly and efficiently as possible. This occurs if the availability of the macroradicals and the rate of monomer diffusion within the polymer matrix are both increased, for example, by adding substances that swell the polymer substrate; retard growing chain termination even further by causing coiling or precipitation of the grafted chains; and/or copolymerize with the original monomer with an exceptionally high cross-propagation rate. The net effect of most of these changes is to increase the grafting rate at first, but eventually to cause a decrease in the grafting rate due to competing effects. Table 1 summarizes these effects. One may also increase the temperature so that the monomer diffusion rate and k_p increase. However, as the mobility of the growing chains and the availability of the polymer radicals both increase, the rate of termination may increase faster than the propagation rate and the overall grafting rate may actually decrease.[16,17] The initiation step should be temperature-independent.

(DTIE: No hyphen)

Table 1. GENERAL KINETIC EFFECTS OF ADDITIVES IN GRAFTING MONOMERS TO POLYMER SUBSTRATES

Additive Miscible with Monomer	Additive Miscible with graft Polymer	Additive swells Substrate	Anticipated Major Kinetic Effects	Overall Result Expected	Examples
Substance X					
Yes	Yes	Yes	D, k_t, k_p increase; (M) increases, then decreases	Max. grafting with X	N-methylol acrylamide + water in cellulosic
Yes	No	Yes	D and / possibly k_p increase; k_t decreases; (M) increases, then decreases; G (radical) changes	Max. grafting with X	Styrene + alcohols in cellulosic[9]
Substances X and Y (Comonomer) Added					
Yes	No	Yes	k_p for cross propagation increases; (M), k_t, D, and G (radical) may also change	Max. grafting with X	Styrene + acrylonitrile (+ water) in rayon[10]
NO	No	Yes	(M) and k_t decrease; G(radical) may change	Max. grafting or continual decr.	Ethyl acrylate + water in wool or cellulosic [11-13]; Styrene + water in cellulosic [14]
Yes	No	No	(M) and k_t decrease; G(radical) changes	Max. grafting with X	Styrene + methanol in polyethylene[15]

Similar considerations apply to preirradiation techniques except that in this case the G value for radical formation depends only on the composition of the polymeric substrate and not on the monomer solution imbibed later. In addition, this technique does not tend to form homopolymer, as does the mutual irradiation technique.

It should also be recognized that in both mutual and preirradiation, the amount of graft (or homopolymer) deposited will vary across the cross-section of the fiber,[18] generally decreasing from the surface inward at a rate that depends on the relative rates of monomer diffusion and polymerization. The time of contact of a particular monomer solution with the fabric may determine the depth of penetration of the graft. Multiple steps involving contact of fiber with monomer followed by irradiation can significantly increase the total extent of grafting above that possible with a one-contact step, for any one total dose, especially for high-dose-rate electron irradiation. It is also possible to confine the graft to the core of the fiber by inhibiting surface reactions.

The graft copolymers are often distributed within a polymer substrate as a few long chains rather than as many short chains, reflecting the retardation of termination reactions within the narrow amorphous regions.[19-21] (Wool is an exception among the textile fibers, due presumably to the high concentration of -SH chain transfer sites on the wool backbone.[11]) It is also possible to chemically prereact a radiation-sensitive monomer to bond it to a fiber polymer backbone and later to irradiate. This will produce a completely different "molecular weight distribution" since the "graft" copolymer is now crosslinked to the substrate at many points along the grafted chain.

Textile Modification with Radiation (3)

Permanent Press (4)

The term "permanent press" signifies that a fabric may be subjected to many wash cycles and retain its smooth, wrinkle-free appearance without any ironing. It is quantitatively evaluated by two tests: (1) the Crease Recovery Angle, both wet (WCRA) and dry (DCRA), which measures the degree of recovery of a fabric sample when it is folded or creases; and (2) the Appearance Rating, which estimates the smoothness of a fabric specimen when viewed on a flat surface with a light at a fixed angle to the surface. Values of 300° or above for CRA and appearance ratings of 4 to 5 generally indicate acceptable permanent-press properties in a textile.

Fabrics made of 100% synthetics (e.g., polyester, nylon, or acrylic) usually do not require ironing when once pressed into shape. However, these textiles are not commonly used due to comfort problems. Certain fibers -- cotton, rayon, silk, and wool -- all tend to wrinkle when worn. Washing or dry-cleaning not only does not remove the wrinkles but may add new wrinkles. It is generally necessary to crosslink the polymer chains in these fibers* in order to ensure wrinkle-free performance. Cotton is commonly crosslinked by reaction with formaldehyde or formaldehyde-containing chemicals via reaction with the cellulose OH groups. The basis of the most widespread process used to accomplish this today (e.g., the Koratron process) is the reaction

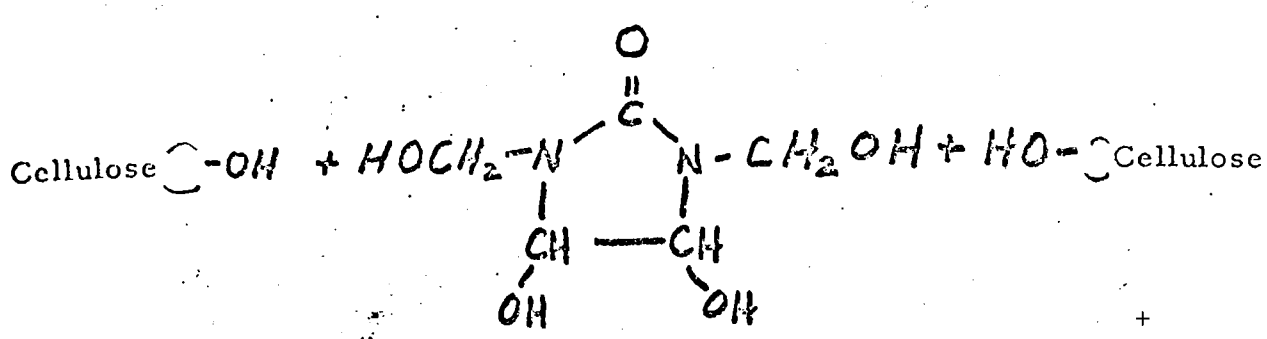

(Eq. cont'd on next p.)

---

* See also P. Roches, Textile Polymers: Effects and Application of Nuclear Radiation, Isotopes and Radiation Technology 6: 404-9 (1969).

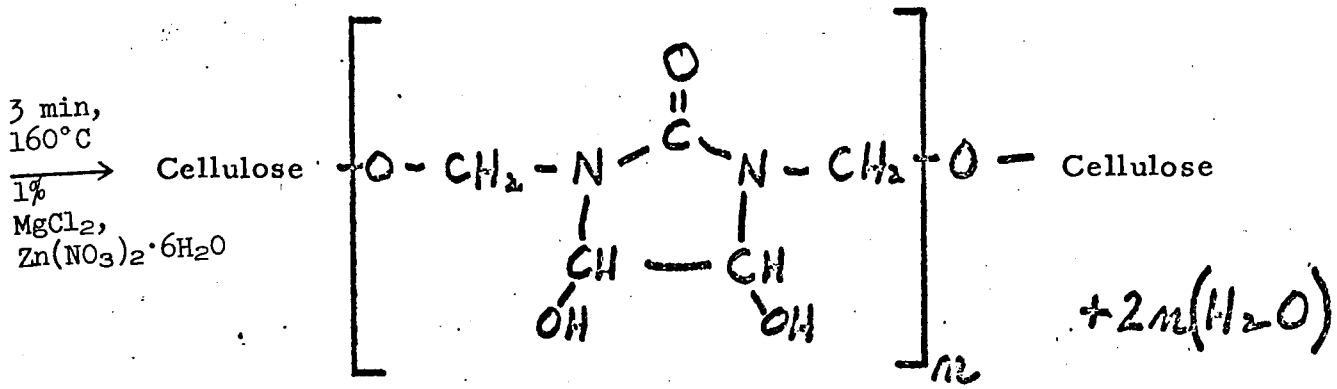

where n is probably[22] in the range of only 1 to 3. After sufficient cross-linking to yield satisfactory permanent-press appearance ratings, the cotton fabric has become weak and exhibits very poor tear strength, abrasion resistance, and wear resistance. It is therefore reinforced with a synthetic fiber, such as polyester; commercial blends contain between 50 and 65% polyester.

Radiation Processing (5) Obviously, a molecule which contains both $-CR = CH_2$ and $>NCH_2OH$ groups could be used to crosslink cotton by a process combining radiation and thermal-catalytic steps. One could synthesize such compounds, for example, by reacting one of the $>NCH_2OH$ groups on DHDMEU with a vinyl monomer containing a reactive side group such as an OH group. One such compound is already available commercially: N-methylolacrylamide (NMA) (e.g., "Radiac" of American Cyanamid Co.), $CH_2 = CH - CONH-CH_2OH$

The use of NMA to crosslink cotton has been studied by Gardon[23] using base-catalyzed Michael addition of the vinyl group to the cellulose OH, which may be preceded or followed by acid-catalyzed condensation of the methylol group with other cellulose OH groups. Hobart[24] has also studied this technique. Gardon[25] has patented the combined process of free-radical catalytically initiated polymerization of NMA (or copolymerization with other monomers) along with acid-catalyzed condensation of the methylol groups with cellulose OH groups—all within the cellulose substrate—to yield a crease-proof cellulosic fabric.

Four radiation-chemical processes that may be used to crosslink the cellulose chains in a textile are

Process A, Delayed Heat Cure with Mutual Irradiation

(1) Pad with NMA plus acid catalysts; dry

(2) Irradiate

(3) Make garment; press

(4) Heat to cure

Process B, Delayed Radiation Cure with Mutual Irradiation

(1) Pad with NMA plus acid catalysts plus free-radical polymerization inhibitor; dry

(2) Heat to condense; wash; dry

(3) Make garment; press

(4) Irradiate to cure

Process C, Delayed Heat Cure with Preirradiation

(1) Preirradiate fabric in air

(2) Pad with NMA plus acid catalysts; dry

(3) Make garment; press

(4) Heat to cure

Process D, Delayed Heat Plus Radiation Cure with Preirradiation

(1) Make garment; press

(2) Preirradiate garment in air

(3) Pad with NMA plus acid catalysts; dry

(4) Heat to cure; wash; dry

These processes should all produce a cross-linked cotton, although they will probably yield textiles having some physical properties different from each other and also different from those resulting from the conventional chemical process.

Deering Milliken Co. is using a continuous delayed heat cure process (similar to A) and is reported to have five ICT-500 electron accelerators of High Voltage Engineering Corp.[26] and to be processing millions of yards of textiles per year.[27]

No reports on this process have appeared in the technical literature, although some patents have been issued[28-30]; speculations on process details have also appeared in the nontechnical literature.[26,31] Cone Mills is developing a delayed radiation cure process (similar to B) based on the work of Walsh and Rutherford of North Carolina State University.[32,33] Processes similar to C and D are not being used, to the author's knowledge; the latter is no doubt impractical due to the undesirability of washing and drying a finished garment. Thus, the two mutual irradiation processes are being used, and the key kinetic factors (as discussed above) will be related to the swelling conditions in the cellulose substrate during the NMA pad step and then subsequently during curing or irradiation, whichever comes first.

Two Belgian patents[28,29] assigned to Deering Milliken Research Corp. describe the preferred use of NMA or di-NMA to crosslink cellulosics, and both delayed-heat-cure and delayed-radiation-cure processes are mentioned.

Preferred doses are 1 to 4 Mrads, resulting in 4 to 9% pickup of the grafted NMA. It is stated that the cellulosic fabric should be irradiated in a moisture-swollen condition, e.g., in a controlled humidity environment, in order to achieve good wet-crease recovery.

In U. S. Patent 3,337,249, issued to Marco and assigned to Deering Milliken Research Corp.,[30] a process is claimed in which a polyester-cellulose blended fabric is padded with three key ingredients (together, or in separate steps): (1) NMA, (2) an acid catalyst, and (3) a synthetic acidic emulsion polymer. The fabric containing NMA (± the other ingredients) is irradiated to polymerize the NMA and then the textile material containing the radiation-polymerized NMA, the acid catalyst, and the acidic emulsion polymer is oven-heated to effect the crosslinking between the methylol groups and the cellulose OH groups.

The emulsion polymer presumably forms a hydrophilic coating on the cellulose and polyester fiber surfaces and thereby confers soil release properties to the fabric. It is preferably a copolymer of various monomers which contains at least 20% acrylic acid. It may also incorporate acrylic monomers with pendant -OH, $-CONH_2$, $-CONHCH_2OH$, or $-\underset{O}{CH}-CH_2$ groups, all of which may be capable of reacting with the methylol groups of the radiation-polymerized NMA during the final acid-catalyzed heat-cure step. This is stated to yield a more durable soil-release coating on the fabric, which is unexpected. The NMA polymer is probably deposited only on and within the cellulosic fiber and should thus be able to react with the acrylic emulsion coating only on this fiber; yet, the most troublesome stains and soils are presumably located on and between the polyester fibers[30] although there is still some controversy in the literature over this question.[34-36] It should be noted that the process claimed in this patent does

not require the use of radiation to confer soil and stain-release properties to the treated cotton-polyester fabric.

The Walsh-Rutherford delayed-radiation cure process has been described in both the technical and patent literature.[32,33] The WCRA's and DCRA's increase with increasing add-on of NMA, but only a relatively minor improvement is noted in the absence of radiation. The CRA's increase with increasing dose, and at 8 Mrads the WCRA's level out at about 310°-320° while the DCRA's continue to increase above 320° (Fig. 2); these angles correspond to about 12% add-on of NMA. The Walsh patent states that a 2-Mrad dose yields "satisfactory" results. Increase in humidity during irradiation increases the WCRA, as expected.[13]

No significant difference in these results was noted for electron irradiation vs. ^{60}Co gamma irradiation.[32] However, the machine irradiation was stated to be the key to the feasibility of the process, since it can cure a pair of pants in 2 to 5 sec, roughly 8000 times as fast as the ^{60}Co source. New accelerator developments will shorten this time even further.[5]

Special advantages for this process are the lack of necessity to heat the garment in the final curing step, which leads to a more uniformly cured garment with less fading of dyes, and the removal of unreacted or incompletely reacted chemicals during the wash step which can yield a fabric less likely to irritate either the garment worker or the wearer. Widespread application of this process could require conveniently located irradiation facilities for garment manufacturers. A possible disadvantage to any process using NMA (i.e., both delayed-heat or radiation cure, process A or B) could be the reactivity of the N-hydrogen with chlorine bleaches, leading to fabric yellowing.[1,2] Radiation effects on the physical properties of

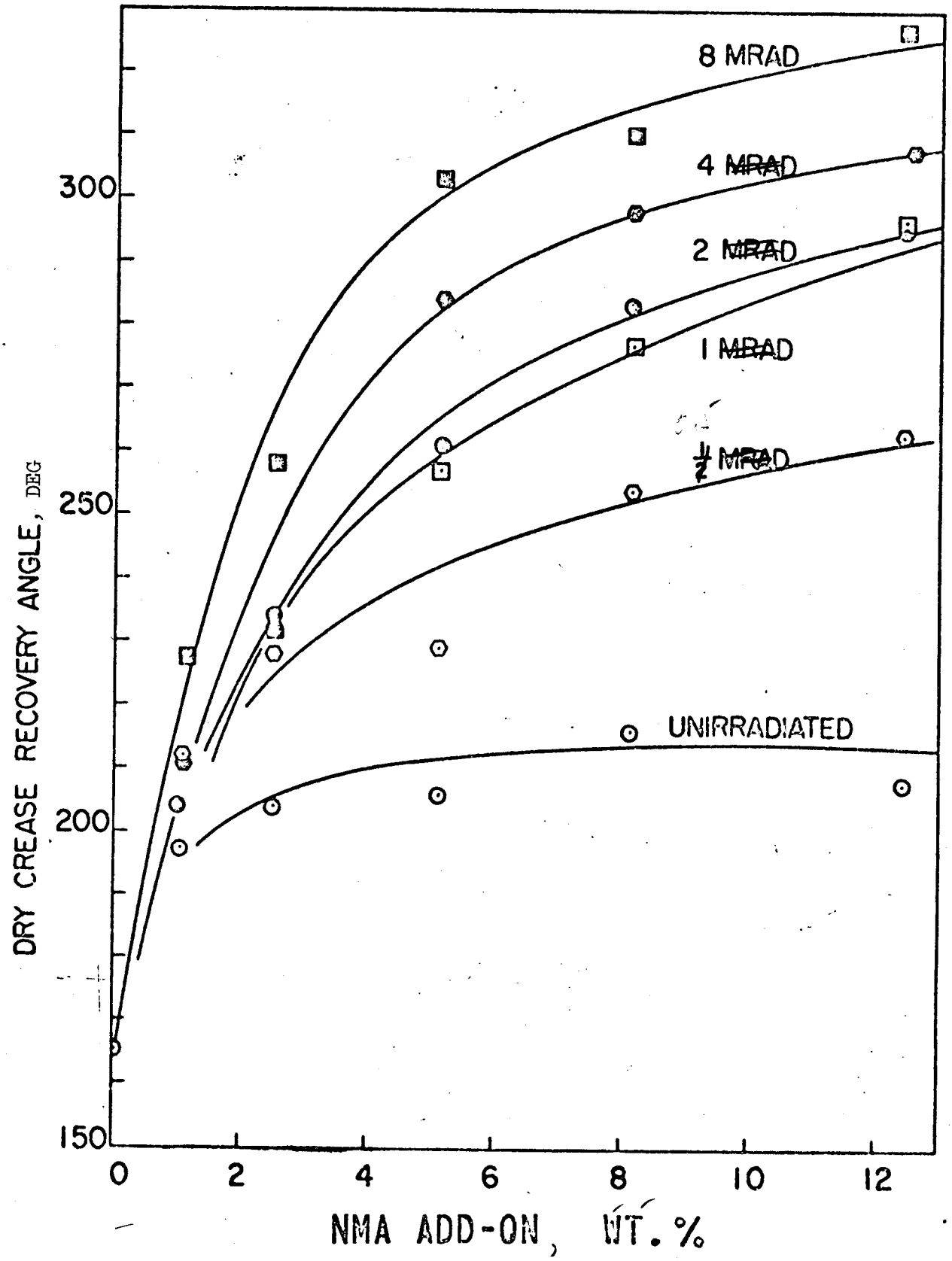

Fig. 2. Variation of dry crease recovery angle (warp plus fill) with NMA add-on for different doses, using an electron accelerator in a delayed radiation mutual irradiation process.[32]

cotton due to chain scission are relatively small and do not appear to result in any greater drop in tensile, tear, or abrasion strength than does a permanent-press process that does not use radiation.

Other work has been published on the improvement of crease recovery in textiles by radiation grafting. Walsh and coworkers[37] investigated other crosslinking agents for cellulosics, such as acrylic acid and glycidyl acrylate[33,37] and allyl acrylate[37], but none has appeared as promising as NMA.

DasGupta observed increased CRA's for cotton mutually grafted with styrene[38] or styrene-methyl methacrylate mixtures[39] using ^{60}Co radiation. This is in contrast with recent work of Walsh, Siahkolah, and Rutherford,[40] who radiation-polymerized a variety of monomers on and within a cotton fabric. They concluded that the greater the elasticity of the deposited polymer, the greater the improvement in CRA. Thus, both low glass transition temperature (T_G) and crosslinking or chain entanglements are deemed to be desirable for good crease recovery; glassy polymers improve CRA only if tested above their T_G and if the chains are crosslinked or highly entangled. Abrasion resistance of the cotton was improved most when the rubbery polymer was surface-deposited only. Earlier work of Prahl and coworkers[41] also showed that only the most flexible polymers (e.g., ethyl acrylate and n-butyl acrylate), which had been deposited in cotton, could improve crease recovery significantly before permanent press treatment. In this case the polymers were catalytically polymerized within the cotton, and this was followed by permanent-press treatment; the object was to improve the abrasion resistance of the final fabric.

Arthur and coworkers[42,43] have made significant contributions to the understanding of radiation effects on cotton. They irradiated bolts of

cotton with ^{60}Co, using either a mutual or preirradiation technique, and polymerized a wide variety of monomers within the cotton. Electron micrographs showed the polymers deposited across the cotton cross-section in layers, the extent of layering being related to the molecular weight of the polymer.[43] The abrasion resistance of these fabrics was measured to screen potential candidates for improving wear resistance of the cotton after permanent-press treatment.

Increased wet-crease recovery was noted by Magat and coworkers[44] in nylon fabrics grafted with monomers containing carboxylic acid — e.g., acrylic or maleic acid — converted to the Na+ form. This did not occur when the grafted chains were in the Ca++ form, and they concluded that the mutual repulsion of the $-CO_2^-$ groups along the backbone caused these chains to stiffen, yielding high wet-crease recovery angles.

Other Bulk Effects (4)

Williams and Stannett[12] reported recently that when wool was preirradiated with ^{60}Co and immersed in an aqueous emulsion of ethyl acrylate, the grafting continued to increase with time, up to almost 7000%. Above about 300%, the rate of grafting increased sharply, and the character of the fiber changed from wool-like to highly elastic, with excellent recovery properties. They speculated that since water is immiscible with ethyl acrylate, it remains at unit activity at all times and is therefore a most effective swelling agent. Water may also cause a precipitation of the growing chains, leading to a significant gel effect. Cotton showed the same behavior, and Stannett suggested that in such highly grafted fibers there must be a considerable disruption of the ordered

crystalline structure inside the fiber, with the resultant fiber being held together inside by the highly elastic polyethylacrylate and outside by the surface skin of the original fiber.[13]

Various Japanese laboratories have been very active in radiation modification of textiles. Danno of the Japan Atomic Energy Institute reported[45] that newly initiated pilot studies on acrylonitrile -- poly-(vinyl chloride) fiber graft copolymers (for improved heat resistance) were in an "advanced stage." He also noted, however, that a 5-year pilot plant study of styrene-cellulosic fiber grafts (for improved heat settability, dyeability, and hygroscopicity) was terminated in March, 1969, for economic reasons.

Principles of Textile Finishing (3)

Most textile fibers and fabrics are temporarily or permanently treated to make the fiber surfaces either more hydrophilic (higher surface energy) or more hydrophobic and/or oleophobic (lower surface energy). The changes in wetting characteristics resulting from such treatments will cause

1. Oily stain spreading and adsorption and release in detergent solutions
2. Soil deposition, release, and redeposition in detergent solutions
3. Static electricity buildup and dissipation
4. Water repellancy
5. Moisture transport and comfort
6. Wettability and adhesion
7. Wettability, chemical reactivity, and dyeability

Many textiles fibers have rough and/or chemically heterogeneous surfaces containing "islands" of deposited chemicals and resins left by the various finishing treatments, or simply dirty or oily areas. In addition, depending on the yarns and the weave, a fabric may contain crevices with capillary dimensions exhibiting a wide variety of shapes and sizes. Soil particles and oily stains entrapped in such regions may exclude water during the contact times normal for washing cycles. Thus, the surface phenomenons listed above may in some cases be dominated by dynamic rather than equilibrium considerations or by roughness or chemical heterogeneities on the surface.

Assuming that the intrinsic surface energy of the textile fiber is the most important factor to consider and that the surface of a textile fiber may be approximated as a plane, then surface free-energy equations may be formulated for the important liquid-solid wetting processes associated with these phenomenons. If we let γ be the surface tension or surface free energy per unit area and A, F, W, and O represent air, fiber, water, and oil, respectively, then wetting of "clean" fiber by water occurs if

$$\gamma_{F/A} - \gamma_{F/W} - \gamma_{W/A} > 0$$

← Wetting of "clean" fiber by oil or any low-surface-energy liquid occurs if

$$\gamma_{F/A} - \gamma_{F/O} - \gamma_{O/A} > 0$$

← Dewetting of oil from fiber when immersed in water occurs if (approximately)

$$\gamma_{F/O} - \gamma_{F/W} > 0$$

If the untreated fiber surface is both hydrophobic and oleophilic, then

$$\gamma_{F/W} > \gamma_{F/A} > \gamma_{F/O}$$

which favors wetting of the fiber surface by an oil (staining) and retarding dewetting of the oil under water (stain-release). Soiling or solid-particle adsorption may occur during use due to staining or to static charge buildup and would also therefore tend to redeposit during washing. Water wettability, moisture regain, and chemical reactivity will be low.

If the fiber is treated so that its surface becomes more hydrophilic, then $\gamma_{F/A}$ (especially) and $\gamma_{F/O}$ will increase while $\gamma_{F/W}$ will decrease significantly. These changes will favor wetting of the surface by water, moisture regain, and stain release during washing. Surface dyeing will be enhanced, and if ionized monomers are grafted, the fiber will be very sensitive to the charge on the molecules (e.g., dyes, stains) or particles (e.g., soil) to which the surface is exposed. Since soil particles are generally negatively charged, if monomers having negative groups (e.g., $-CO_2^-$ or $-SO_3^-$) are grafted, the sol should be repelled both in use and in the washing machine. A typical soil- and stain-release treatment involves padding the textile in a polymer emulsion (e.g., acrylic) followed by heating to form a tough, crosslinked film or coating with a hydrophilic character on the fiber surface.

Textiles may also be treated to render their surfaces more hydrophobic and oleophobic, e.g., by use of fluorinated or silicone-type compounds. Then staining will be retarded since most liquids are "repelled" from the surface, although soiling could be enhanced if static

charges build up. If stains or soil particles are adsorbed on such treated textiles, they would be difficult to release during washing.

Ideally, the textile should repel both soil and stains and also release these substances during laundering if they happen to have been adsorbed on the fabric during use. This requires an incompatible combination of surface energies. However, it is possible to achieve both low $\gamma_{F/A}$ and low $\gamma_{F/W}$ by treating the textile with a compound containing hydrophilic segments (e.g., polyethylene oxide) and oleophobic segments (e.g., fluorinated hydrocarbon) on the same molecule.[46] In air, the hydrophilic segment would be coiled up, exposing the low-energy oleophobic segments, which would repel stains, while in water the opposite should occur, releasing stains.

Radiation Modification of Surface Properties (4)

It is easy to envisage as a textile finishing operation the radiation grafting of hydrophilic, oleophilic, or oleophobic monomers within the surface regions of a fiber microstructure, resulting in changes in the fiber surface properties. There should be good wash-fastness of such a finish due to the possibility of chemical bonding to the substrate. It is beyond the scope of this review to cover extensive literature on radiation treatments of textiles to alter their surface properties, and the reader is referred to two recent reviews.[3,4] Instead, a brief summary of three systems for grafting of hydrophilic monomers on the surfaces of electron-preirradiated nylon and polyester substrates being investigated by the author will be presented:

System I: Acrylic acid (AAc) ($CH_2 = CHCO_2H$)

N-methylol acrylamide (NMA) ($CH_2 = CHCONHCH_2OH$)

Polyethylene glycol (PEG) [$HO(CH_2CH_2O)_nH$]

Sodium styrene sulfonate (SSNa) ($CH_2 = CH$- -$SO_3^- Na^+$)

Water (H_2O)

Dimethyl sulfoxide (DMSO) (CH_3SOCH_3)

System II: 2-Hydroxy-3-methacryloyl-oxypropyl trimethyl ammonium chloride (GMAC) $CH_2{=}C(CH_3)CO_2CH_2CHOHCH_2N(CH_3)_3^+ Cl^-$)

Dimethylformamide (DMF) [$(CH_3)_2NCHO$]

Water (H_2O)

System III: System II followed or preceded by sodium styrene sulfonate (SSNa) and water (H_2O)

<u>System I</u>. (5) In System I,[47,48] the AAc is present to swell the surface regions of the polymer substrate and to catalyze the condensation of NMA methylol groups with the end OH groups of PEG, leading to pendant polyethylene glycol chains,

$$-NHCH_2OH + HO(CH_2CH_2O)_nH \xrightarrow[-CO_2^-H^+]{heat} -NHCH_2O(CH_2CH_2O)_nH$$

The SSNa contributes strongly ionized sulfonate groups to repel soil particles, and the DMSO is used particularly with polyester substrates to help swell the surface regions.

Nylon and polyester films were preirradiated in air using an ICT-500 electron accelerator (High Voltage Engineering Corp.) and shortly thereafter were contacted with the treatment solution for different times and at different temperatures and then thoroughly washed and dried. To

estimate the increase in hydrophilic character of the film surface, the contact angle of water on the surface was determined. The results for nylon (Fig. 3) show that the combination of preirradiation and post-treatment with monomers is necessary for enhanced surface wettability. Release of a drop of a dispersion of carbon black in mineral oil was greatly enhanced on a radiation-treated nylon fabric when immersed in water. Polyester film and fabric behaved similarly, higher treatment temperatures and DMSO being used.

System II. (5) Nylon films were preirradiated[49,50] in air and then treated with aqueous GMAC solutions containing DMF to increase swelling of the surface regions. The results (Fig. 4) showed that the GMAC enhances surface wettability significantly. When increasing amounts of NaCl were added to the water droplet, the contact angle of the droplet (on one particular film surface) increased from 23° to 46° as the salt concentration was increased to 5N. This was not due to an increase in surface tension of the droplet, $\gamma_{L/A}$ / $\gamma_{L/A}$ cos θ actually decreases with increasing salt concentration) but rather to an increase in the interfacial tension at the polymer--salt solution boundary. It was concluded that the increased water wettability of such a polyelectrolyte-grafted surface is due mainly to the ability of the counterion (Cl^- here) to escape the field of the parent polyion, and that when salt ions are present in the water they compress the double layer created by escape of the counter-ions and force these ions back to the poly-ions on the surface.

System III. (5) The studies with System II were followed by experiments[51,52] in which a cationic monomer (GMAC) is adsorbed on a

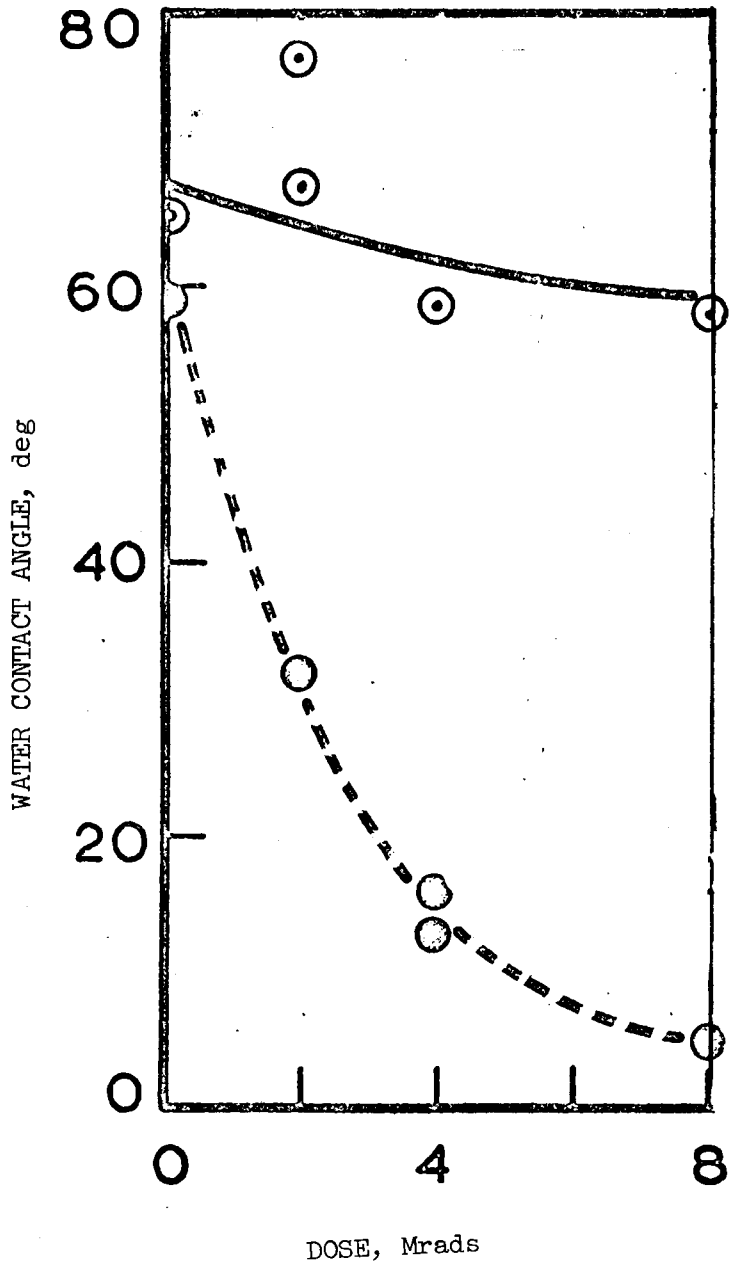

Fig. 3. Effect of dose and posttreatment on the water contact angles of preirradiated nylon substrates.[48] —— control; --- treated 5 min at 75°C under air in a solution of 5% AAc, 5% SSNa, 20% NMA, 20% PEG and 50% H_2O.

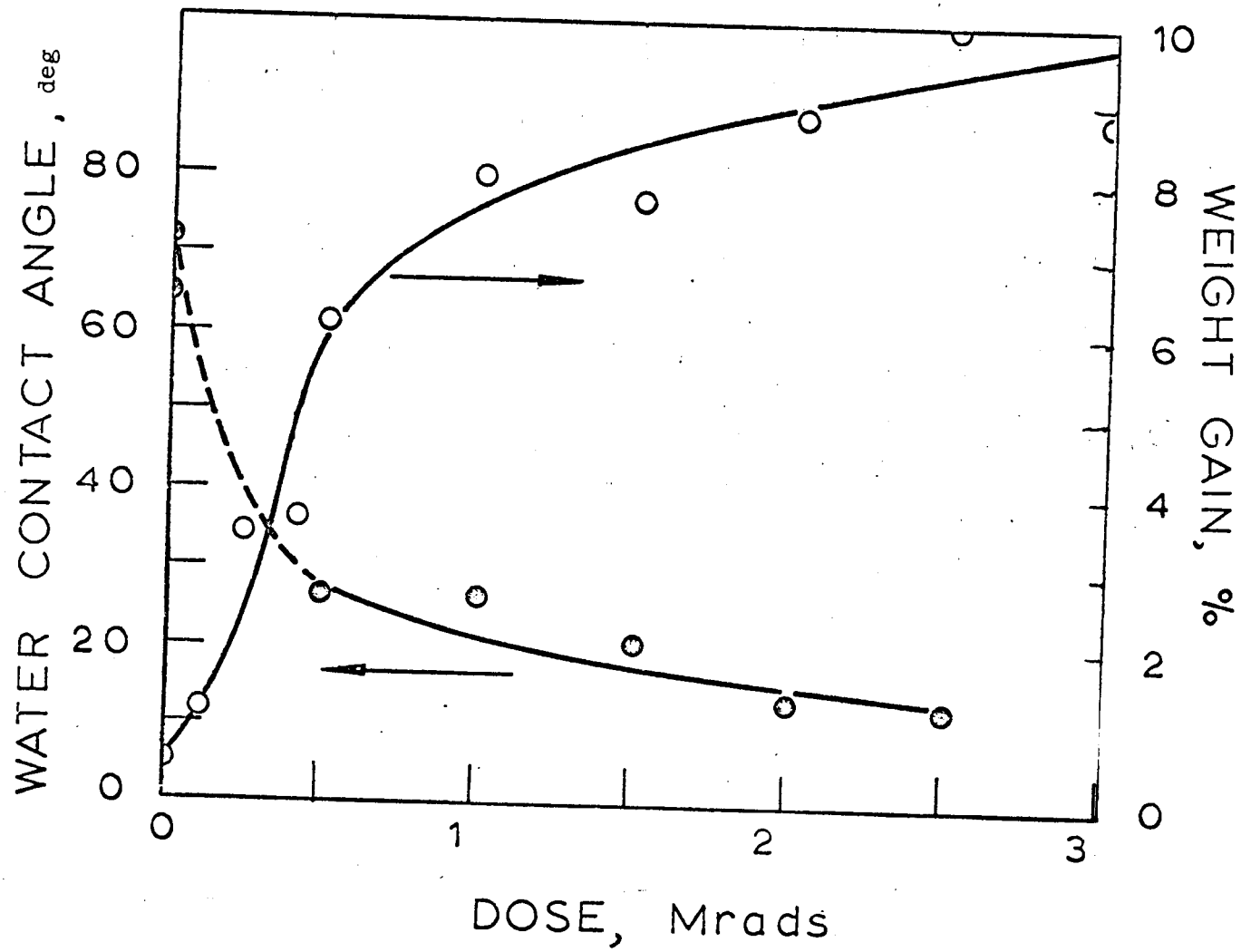

Fig. 4. Effect of radiation dose on weight, gain, and water contact angle in preirradiation grafting of GMAC poly-cation on nylon substrates.[50] Films treated 1 hr at 70°C under N_2 in a solution of GMAC/H_2O/DMF = 1/2/6.

grafted (SSNa) poly-anion and then radiation or catalytically polymerized to produce a grafted polyelectrolyte complex on the nylon surface (Fig. 5). These complexes are water insoluble and are both hydrophilic and hydrophobic at the same time --i.e., they exhibit abnormally high water fluxes as membranes but the surfaces tend to dewet water.[53] Thus, such a surface treatment might confer both a hydrophobic character to the surface in air and a hydrophilic character in water. Static dissipation in air should also be enhanced. Water contact angles may be increased or decreased after complexing the GMAC polymer on the poly(SSNa), depending upon the concentration of GMAC in the complexing solution.[52] These studies are continuing.

(MG)

Glossary

AAc	Acrylic acid
CRA	Crease recovery angle
DCRA	Dry crease recovery angle
DHDMEU	Dihydroxy dimethylol ethylene urea
DMF	Dimethylformamide
DMSO	Dimethyl sulfoxide
NMA	N-methylolacrylamide
SSNa	Sodium styrene sulfonate
GMAC	2-hydroxy-3-methacryloyl-oxypropyltrimethylammonium chloride
PEG	Polyethylene glycol
WCRA	Wet crease recovery angle

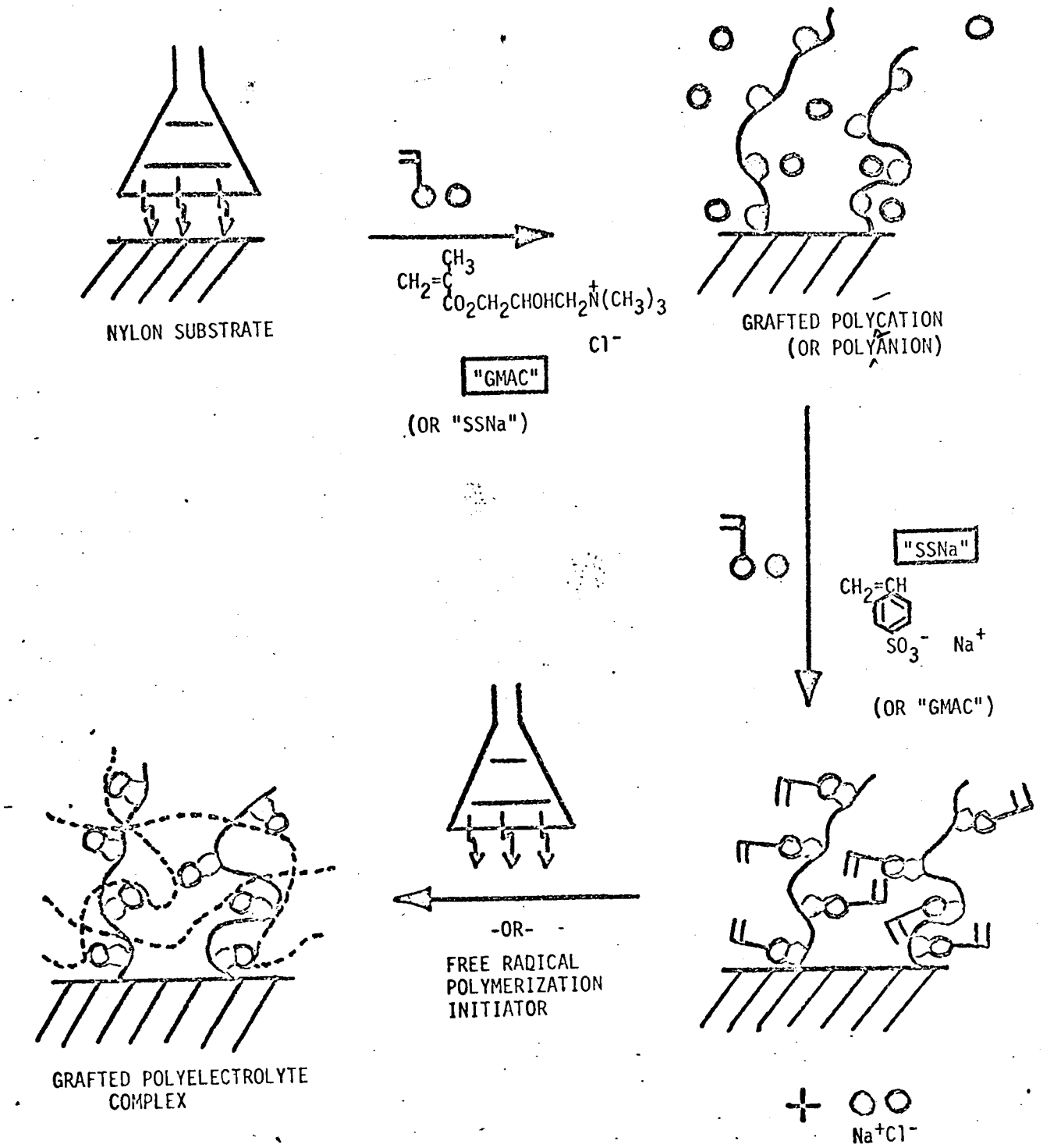

Fig. 5. Methods used to prepare radiation-grafted polyelectrolyte complexes on polymer substrates.[51,52]

References (3)

1. A. J. Hall, Textile Finishing, 3rd Ed., American Elsevier Publ. Co., London, 1966 .
2. J. T. Marsh, Crease Resisting Fabrics, Reinhold, 1962.
3. R. D. Gilbert and V. Stannett, Uses of High-energy Radiation for the Modification of Textile Fibers (Lit. rev. 1963-66), Isotopes and Radiation Technology 4: 403-25 (1967).
4.* V. Stannett and A. S. Hoffman, Amer. Dyestuff Rep. 57(25): 91 (1968).
5. D. A. Trageser, High Voltage Eng. Corp., personal communication, Apr. 1969.
6. Radiation Gives Permanent Press, Chem. & Eng. News 44(23): 19 (1966).
7. *High Voltage Eng. Corp., Sales Memo No. 46, Aug. 16, 1968.
8. A. Chapiro, Radiation Chemistry of Polymeric Systems, Interscience, N. Y. (1962).
9. R. Y.-M. Huang and W. H. Rapson, Grafting Polymers onto Cellulose by High-energy Radiation. II. Effect of Swelling Agents on the Gamma-ray-induced Direct Radiation Grafting of Styrene onto Cellulose, J. Polymer Sci. C2: 169-88 (1963).
10. W. H. Rapson and E. Kvasnicka, Grafting Mixtures of Vinyl Monomers onto Cellulose, Tappi 46: 662-4 (1963).
11. V. Stannett, K. Araki, J. A. Gervasi, and S. W. McLeskey, Radiation Grafting of Vinyl Monomers to Wool, J. Polymer Sci. A3: 3763-79 (1965).
12. J. L. Williams and V. Stannett, High-yield Preirradiation Grafting to Wool Leading to Highly Elastic Fibers, Textile Res. J. 38: 1065-6 (1968).
13. V. Stannett, Radiation Grafting to Cotton (and Other Textile Fibers), presented at First International Cotton Conf., Paris, April 24, 1969. (preprint)
14. R. E. Kesting and V. Stannett, The Preirradiation Grafting of Styrene onto Cotton Cellulose Using Gamma Rays, Makromol. Chemie 55: 1-14 (1962).
15. G. Odian, M. Sobel, A. Rossi, and R. Klein, Radiation-induced Graft Polymerization: the Trommsdorff Effect of Methanol, J. Polymer Sci. 55: 663-73 (1961).
16. J. A. Sykes and J. K. Thomas, The Radiation-induced Graft Copolymerization of 4-Vinyl Pyridine and Acrylamide to Nylon 6.6, J. Polymer Sci. 55: 721-9 (1961).

17. A. Chapiro and A. Matsumoto, Effect of Temperature on Grafting of Styrene to Polytetrafluoroethylene and Poly(Vinyl Chloride) Films by the Direct Radiochemical Method (French), J. Polymer Sci. 57: 743-61 (1962).

18. R. F. Stamm, E. F. Hosterman, C. D. Felton, and C. S. Hsia Chen, Grafting of Chloromethylstyrene to Polypropylene Fibers by the Use of Ionizing Radiation, J. Appl. Polymer Sci. 7: 753-82 (1963).

19. V. Stannett, J. D. Wellons, and H. Yasuda, Preparation and Characterization of Some Cellulose Graft Copolymers. II, J. Polymer Sci. C4: 551-62 (1964).

20. J. D. Wellons, A. Schindler, and V. Stannett, Molecular Weight Distributions of the Side Chains of Radiation-initiated Graft Copolymers, Polymer 5: 499-503 (1964).

21. R. Y.-M. Huang, B. Immergut, E. H. Immergut, and W. H. Rapson, Grafting Vinyl Polymers onto Cellulose by High-energy Radiation. I. High Energy Radiation-induced Graft Copolymerization of Styrene onto Cellulose, J. Polymer Sci. Part A,1: 1257-70 (1963).

22. E. Valko, personal communication, Spring 1968.

23. J. L. Gardon, A Quantitative Study of Crosslinking Cotton with N-Methylol Acrylamide, J. Appl. Polymer Sci. 5: 734-51 (1961).

24. S. R. Hobart, The Reversibility of N-methyloacrylamide Cross-links on Cotton, Textile Res. J. 37: 380 (1967).

25. J. L. Gardon (assignor to Rohm & Haas Co.), U. S. Patent 3,125,405, March 17, 1964 (Ger. 1,121,579; Brit. 955,088; Chem. Abs. 56: 13124G. Treatment of Cellulosic Textiles on Crease Resistance.

26.* Chem. & Eng. News 46(29): 41 (1968).

27. D. Gagarine, Deering Milliken Research Corp., personal communication, July 3, 1969.

28.* Belgian Patent 686,982 (to Deering Milliken Res. Corp.), March 16, 1967.

29.* Belgian Patent 686,987 (to Deering Milliken Res. Corp.), March 16, 1967.

30. F. W. Marco (assignor to Deering Milliken Res. Corp.), Soil Release of Polyester-containing Textiles, U. S. Patent 3,377,249, April 9, 1968 (Fr. 1,524,903; Chem. Abs. 68: 115656Q).

31.* Daily News Record, Jan. 12, 1967.

32. W. K. Walsh and H. A. Rutherford, Delayed Cure with Ionizing Radiation, Textile Res. J. 37: 89-93 (1967).

33. W. K. Walsh (assignor to Research Corp.), U. S. Patent 3,434,161, March 25, 1969.

34.* Stain and Soil Release Finishes, Mod. Textiles Mag. 48(12): 51 (1967).

35. R. Tsuzuki and N. Yabuuchi, Oleophilic Stain Release, Amer. Dyestuff Rep. 57: 472 (1968).

36.* S. Smith and P. O. Sherman, Amer. Chem. Soc. Abstracts 157th National Meeting, Minn., Minn. (April, 1969).

37. W. K. Walsh, C. R. Jin, and A. A. Armstrong, The Crosslinking of Cotton with Vinyl Monomers Using Radiation and Chemical Catalysis, Textile Res. J. 35: 648-54 (1965).

38. S. DasGupta, Modification of Cotton Fabrics by Graft Polymerization, Canadian Textile J. 81: 57-63 (1964).

39.* S. DasGupta, Amer. Dyestuff Rep. 55: 211 (1966).

40. W. K. Walsh, M. A. Siahkolah, and H. A. Rutherford, The Effect of the Glass Transition Temperature of Conventional and Radiation Deposited Polymeric Additives on Mechanical Properties of Cotton Fabric (preprint),

41. H. F. Prahl, H. Tovey, and C. E. Underwood, Short Investigation of Grafting as a Method for Improving Abrasion Resistance of Crosslinked Cotton, Textile Res. J. 36: 245-50 (1966).

42.* J. C. Arthur, Jr., J. A. Harris, and T. Mares, Textile Industries 132(9): 77 (1968).

43.* F. A. Blouin, A. M. Cannizzaro, J. C. Arthur, Jr., and M. L. Rollins, Vinyl-cellulose Copolymers. II. Fibrous Structure and Properties of Poly(Alkyl Methacrylate)-Cotton Copolymers Prepared by Radiation-initiated Reaction, Textile Res. J. 38: 811-6 (1968).

44. E. E. Magat, I. K. Miller, D. Tanner, and J. Zimmerman, Grafts of Nylon and Unsaturated Acids, J. Polymer Sci. Part C4: 615-29 (1963).

45. A. Danno, Technical Development of Radiation Chemistry in Japan, Ninth Japanese Conf. on Radioisotopes, Tokyo, May 13-15, 1969 (preprint).

46.* P. O. Sherman, S. Smith, and B. Johannessen, Amer. Chem. Soc. Abstracts, 157th National Meeting, Minn., Minn. (April, 1969).

47.* G. R. Berbeco, Radiation-Chemical Surface Treatments to Nylon and Polyester Substrates, S. M. Thesis, M. I. T. Chem. Eng. Dept., Cambridge, Mass., 1967.

48.* A. S. Hoffman, G. R. Berbeco, and R. Gomes-Casseres, Textil Veredlung 2: 6 (1967).

49.* R. Gomes-Casseres, Antistatic Nylon Surfaces Via Graft Copolymerization, S. M. Thesis, M. I. T. Chem. Eng. Dept., Cambridge, Mass., 1968.

50.* A. S. Hoffman, R. Gomes-Casseres, and G. D. Parfitt, Radiation-Grafted Polyelectrolytes on Polymer Surfaces, I. Water Contact Angles as a Function

of the Mobile Counter-Anion Species, to be published in Adv. in Chem. Series, "Polymerization and Polycondensation," A. C. S., Washington, D. C. (1969).

51.* E. Kiran, The Effect of the Formation of Polyelectrolyte Complexes Via Surface Polymerization on the Wettability of Nylon 6-6 and Mylar Films, 10.91, Experimental Research Project M. I. T. Chem. Eng. Dept., Cambridge, Mass, Feb. 10, 1969.

52.* M. Ostler, Contact Angles of Polyelectrolyte Complexes Bonded to Low Energy Substrates, S. B. Thesis, M. I. T. Chem. Eng. Dept., Cambridge, Mass, 1969.

53. A. S. Michaels, Polyelectrolyte Complexes, Ind. Eng. Chem. 57(10): 32-40 (1965).

V. ISOTOPIC HEAT AND POWER DEVELOPMENT

FRENCH ISOTOPIC POWER GENERATOR "MARGUERITE 20" (2)

Supplementary Key Words: (ENERGY SOURCE / CONVERSION, ELECTRIC / THERMOELECTRIC SYSTEM / INDUSTRY / INDUSTRY, PETROLEUM AND NATURAL GAS / STRONTIUM-90 / FRANCE)

The Marguerite 20, a 2500-kg generator, was developed in France to supply the power required to operate the remote controls and telemonitoring systems of a Zakum oil field wellhead in the Persian Gulf. It is an electric generator with a 780-W(th) heat source generated by a 130 thousand Ci ^{90}Sr source. The source is four strontium titanate cylindrical elements doubly encapsulated in Haynes 25 alloy. The biological shield is lead. The source is housed in a molybdenum heat collector sunk in a heat insulant through which germanium-silicon thermoelements pass. The whole forms part of the copper-block heat well. The assembly is housed in a stainless steel vessel. The thermopile has a power of 20 W with a 24-V output.

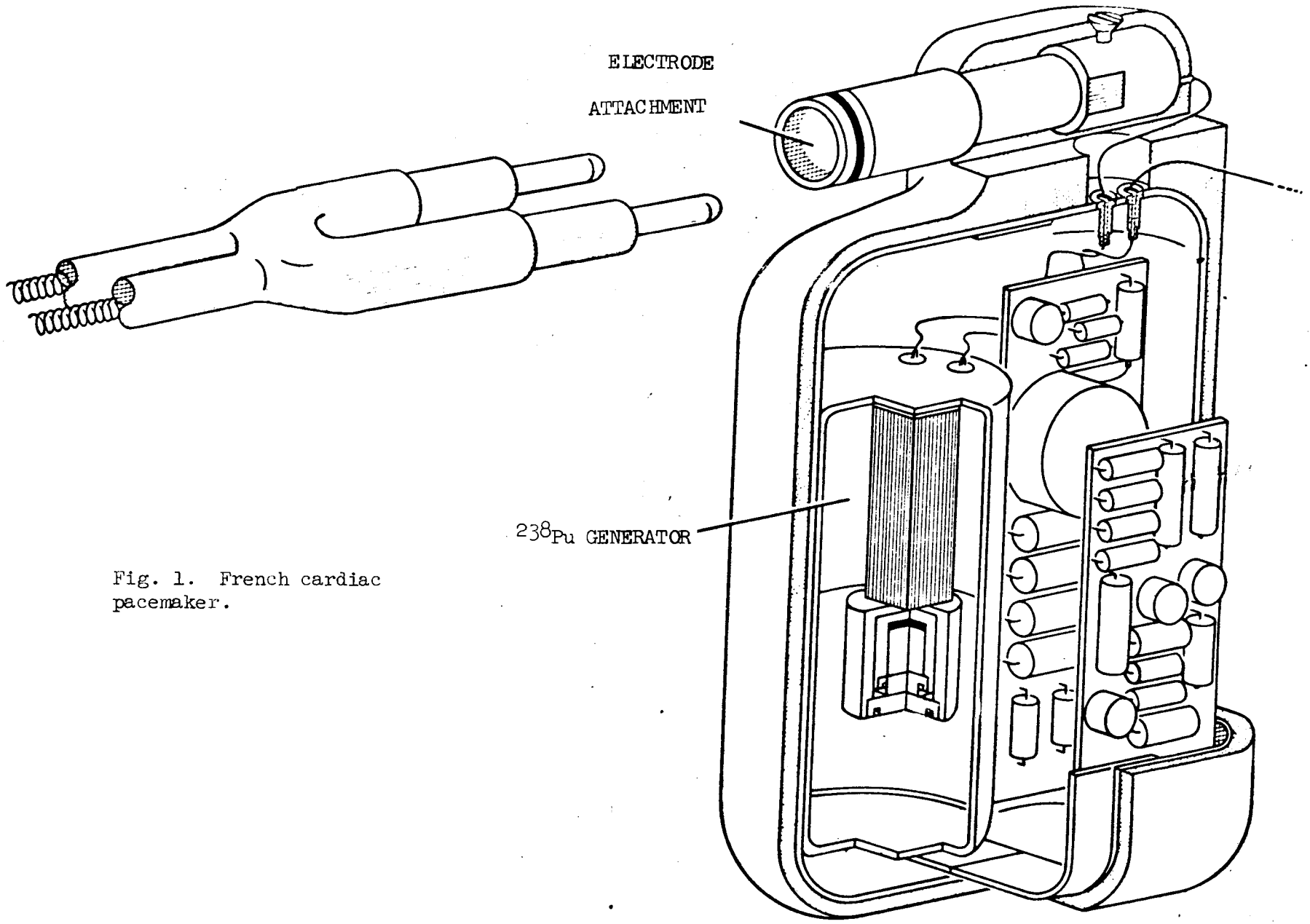

Fig. 1. French cardiac pacemaker.

VI. APPLICATIONS IN LIFE SCIENCES

RADIATION AND THE GREEN REVOLUTION* (2)

Supplementary Key Words: (MUTATION / AGRICULTURE / GRAIN / FLOWER / REVIEW, POPULAR / CONFERENCE / SPECIALTY FOOD / VEGETABLE / WORLDWIDE / FRUIT/ GROWTH IMPROVEMENT)

Abstract. Useful radiation-induced mutations in plants up to July 1, 1969 are summarized in a table, with a brief introduction.

(Introduction)

An important contribution to plant breeding is being made by researchers using radiation to induce mutations. Crop varieties have been improved, and shortages caused by disease have been averted. The technique is proving to be valuable to breeders of flowers and ornamental plants also. Some of the results achieved to date were reported at an IAEA/FAO symposium held in Pullman, Washington, in July 1969. Nearly 50 new varieties of plants have been released to growers in the last five years.

Sigurbjörnsson (United Nations) summarized progress since the last symposium on this subject. The efforts of scientists of the past 40 years are paying off in millions of hectares of superior crops throughout the world. Examples include Reimei, the highest-yielding rice variety in Japan. The protein content of rice has been doubled in one variety. The growing period of rice in Hungary has been shortened by three weeks. Radiation-induced mutant varieties of durum wheat have shown superior performance in so many countries that FAO is recommending that some countries replace their wheat acreage entirely with the new mutants. The contributions of radiation mutations to the "green revolution" have not only alleviated some problems of population growth, they have also called attention to the number of characteristics of even high-yielding varieties that need improvement.

---

*Slightly adapted from the original publication in the IAEA Bulletin 11(5): 16-27 (1969).

Swaminathan (India), one of the world leaders in this work, reported the solution to the problem of growing castor beans in India. Formerly, the plant took 270 days to mature and was thus at the mercy of changes in the rainy season. A new variety has been evolved by the use of radiation-induced mutations; it matures in 120 days. Farmers are now assured of a good crop each year, and they can use the soil during the saved 150 days to grow other crops.

Gardner (USA) announced the most important development with maize since the 1920's---an increase in yield beyond the highest known. This is the first example of using the method effectively on open-pollinated rather than self-pollinated crops.

One of the best-known flavors in the world, peppermint, might now be nonexistent except for a radiation-induced mutation, according to Murray (USA). Researchers have tried to fight a disease for 14 years with other mutations, but those that were disease-resistant tasted like spearmint. Only the radiation-induced mutation both resisted the disease and tasted like true peppermint.

The following table lists the new varieties in types of bread and durum wheat, barley, oats, rice, soybean, peas, beans, peanuts, rape, mustard, tobacco, peach, and flowers.

LIST OF PLANT MUTANTS RELEASED OR APPROVED AS OF JULY 1, 1969, PRODUCED WITH RADIATION-INDUCED MUTATIONS OR HAVING RADIATION-INDUCED MUTATIONS IN THEIR BACKGROUND

Name	Place, date*	Treatment	Improved attributes
BREAD WHEAT			
NP 836	India, 1961	Dry seeds (12%), 16 krad of X-rays	Fully awned; higher yield (10%); medium early maturity (140 days); high leaf rust resistance. Grows better than the parent in unirrigated areas.
Sharbati Sonora	India, 1967	Dry seeds (12%), 1 hour of 2600 A UV + 20 krad gamma rays from ^{60}Co	Amber grain color (preferred in India). Short straw, early maturity, high protein (16.5%) and high lysine/protein ratio.
Lewis	U.S.A., 1964	Thermal neutrons	Lodging resistance; early maturity; high yield.
Stadler	U.S.A., 1964	Thermal neutrons	Early maturity; strong straw; good yield; excellent soft quality grain; good disease resistance and winter hardiness.
Sinvalocho Gama	Argentina, 1962	20 krad of ^{60}Co gamma rays	More resistant to black stem rust and leaf rust.
Zenkouzi-Komugi	Japan, 1969	^{60}Co gamma rays	Earlier maturity (1 or 2 days); shorter culm (15-20 cm); higher yield (10-15%).

*The original table includes the researchers and their institutes. - Ed.

Name	Place, date	Treatment	Improved Attributes
Novo-sibir-skaia 67	USSR, 1969/70	^{60}Co gamma rays, 5 krad air-dry seeds	Lodging resistance; baking quality.
DURUM WHEAT			
Castel-porziano	Italy, 1968	Thermal neutrons dose of $8.38 \times 10^{12}/cm^2$	Lodging resistance; yielding ability.
Castelfusano	Italy, 1968	Thermal neutrons dose of $1.05 \times 10^{13}/cm^2$	Lodging resistance; yielding ability.
Castel del Monte	Italy, 1969	Fast neutrons, 100 reps	Lodging resistance; high yield.
BARLEY			
Vienna	Austria, 1959	9400 rad X-rays on dry seeds	High yield; high 1000-kernel weight; mildew resistance; lodging resistance.
Pennrad	U.S.A., 1963	Thermal neutrons (dosage to cause 50% germination)	Increased winter hardiness; awnleted, recessive gene mutant.
Jutta	Germany (Democr. Rep.), 1955	X-rays, 5000 r	Higher yield; lodging resistance; increased winter hardiness.
Milns Golden Promise	United Kingdom, 1966	Gamma rays, 6-24 krad	Shorter and stiffer straw with good grain yield and malting properties, but mildew-susceptible.
Midas	United Kingdom (to be released in 1970)	RM.759/10 × Miln Golden Promise	Short, stiff straw; erectoides habit; mildew resistance.
Luther	U.S.A., 1967	Seeds soaked in diethyl sulfate (dES) at .0038 M (conc.) for 3.5 hrs. at 30° C with solution changed every half hour	Shorter straw; increased grain yield and lodging resistance, especially with heavy fertilization.

Name	Place, date	Treatment	Improved Attributes
Diamant	C.S.S.R., 1965	Seeds (14% moisture) treated with 10 krad of X-rays	Very high yield; short stem; very good grain and malting quality; lodging resistance.
Hellas	Sweden, 1967	Selection from Pallas x Herta	Resistant to lodging and straw breakage; increased yield, especially with heavy fertilization; resists sprouting at harvest time.
Pallas	Sweden, 1960	Presoaked seeds X-rayed with 7350 rad	Stiff straw.
Mari	Sweden, 1962	Dry seeds X-rayed with 20 krad	Early maturity (by 8 days); stiffer straw.
Kristina	Sweden, 1969	Selection from Domen x Mari	Resistant to lodging and straw breakage; very high yield; outstanding malting quality.
OATS			
Florad	U.S.A., 1959	Thermal neutrons to seeds	Resistant to stem rust; superior grain quality and straw stiffness.
Alamo-X	U.S.A., 1961	Seeds X-rayed with 25 krad	Resistant to Victoria blight and crown rust.
Florida 500	U.S.A., 1965	Selection from Florad x Coker 58-7	Improved agronomic type combined with rust resistance of mutant Florad.
Florida 501	U.S.A., 1967	Selection from Florad x Coker 58-7	Improved agronomic plant and kernel type combined with crown rust resistance.
RICE			
SH 30-21	Rep. of China, 1957	X-rays	Higher yield; short growing period.

Name	Place, date	Treatment	Improved Attributes
KT 20-74	Rep. of China, 1957	X-rays	Higher yield; short growing period.
YH 1	Rep. of China, 1963	Selection from Taichung No.1 x SH 30-21	Higher yield; short growing period.
Reimei	Japan, 1966	Dry seeds treated with 20 krad of ^{60}Co gamma rays	Short straw; lodging resistance, especially with heavy fertilizer; less variation with location and year; tolerates lower temperatures, especially during germination and seedling stages.
SOYBEAN			
Tainung No. 1 (R)	Rep. of China, 1962	Thermal neutrons	Vigorous, dropping-resistant variety with the characteristics of long branches and higher yield.
Tainung No. 2 (R)	Rep. of China, 1962	X-rays	Vigorous, dropping-resistant variety with short internode, large seed, and adapted to acid or alkaline soil.
Raiden	Japan (Tohoku district), 1966	Dry seeds irradiated with 10 krad of ^{60}Co gamma rays	Earlier maturity; shorter stem (resists lodging); maintains high yield and nematode resistance of original variety.
Raiko	Japan (Tohoku district), 1969	Dry seed treatment with 10 krad of ^{60}Co gamma rays (originated from the same R_2 population which gave "Raiden").	Earlier maturity; shorter stem; resists lodging; higher yield; maintains nematode resistance of the original variety. (Raiden, Raiko and their original variety form a set of varieties of different maturities but of similar grain quality).
PEA			
Stral-ärt	Sweden, 1954	Presoaked seeds irradiated with 15 krad X-rays	Vigorous development; 2-6% higher seed yield; high regenerative capacity; stable yield.

Name	Place, date	Treatment	Improved Attributes
NAVY PEA BEANS			
Sanilac	U.S.A., 1956	X-rays	Bush type; early maturity; resistant to alpha, beta and gamma races of anthracnose and bean common mosaic virus 1 and 123; tolerant to wilt or white mold.
Seaway	U.S.A., 1960	X-rays	Short-season; upright bush-type; resistant to bean common mosaic races 1, 15, and 123.
Gratiot	U.S.A., 1962	X-rays	Same as for Sanilac except stiffer straw and added resistance to bean common mosaic 15; higher protein content than Sanilac.
Seafarer	U.S.A., 1967	X-rays	Very early maturity; bush-type; resistant to alpha, beta, and gamma races of anthracnose and bean common mosaic races 1, 15, and 123.
HARICOT BEAN			
Saparke 75	U.S.S.R., 1967	Seeds irradiated with 7 kRad of gamma rays	Surpasses the initial variety on average by 55 dt/ha in green pod yield and 5.2 dt/ha in seed yield; green pods are devoid of fibre and fixed on the stem 5-5 cm higher, making mechanical harvesting possible; improved resistance to bacterial diseases.
STRING BEAN			
Universal	Germany (Fed.Rep.), 1950	X-rays, 300 r	Early maturity; higher yield; good resistance to anthracnose.
Unima	Germany (Fed.Rep.), 1957	Selection from Granda x Universal	Immune against anthracnose; resistant to *Pseudomonas phaseolicola*.
PEANUT			
N.C.4-X	U.S.A., 1959	X-rays to dry seeds	Tougher hull (resists damage during harvest and transport); high yield; good quality.

Name	Place, date	Treatment	Improved ~~A~~ttributes l.c.
SPRING RAPE			
Regina varraps elite A	Sweden, 1953	Seeds X-rayed with 35 krad	Higher seed yield and percent oil.
Regina varraps elite F	Sweden, 1962	Seeds X-rayed with 45 krad	Higher seed yield and percent oil.
WHITE MUSTARD			
Svalöf's Primex	Sweden, 1950	Seeds X-rayed with 35 krad	Higher seed yield and percent oil.
CASTOR BEAN			
Aruna	India, 1969	Thermal neutrons, 1400 rad	Very early (120 days vs. 270 days for mother variety); ~~Y~~ield slightly higher. l.c.
TOBACCO			
Chlorina F_1	Indonesia, 1934	X-rays	Pale color; high quality of leaf.
PEACH			
Magnif 135	Argentina, 1968	Chronic irradiation in gamma field	Bigger fruits with deeper red skin color; 7 days earlier maturity.
LESPEDEZA			
Hi-way	U.S.A., 1970/71	Thermal neutrons, 2 hrs	Compact; fine-stem; leafy; good tillering and seedling vigor.
ROSE			
Desi	Germany (Democr.Rep.)	X-rays, 3000 r	Intensive colors; dark red stripes on yellow petals.

Name	Place, date	Treatment	Improved Attributes
CARNATION			
UConn White Sim No. 1	U.S.A., 1962	Gamma rays to rooted cuttings	Fewer ray flowers; "holds" longer after cutting.
CHRYSANTHEMUM			
Dr. X	U.S.A., 1966	Rooted cuttings X-rayed with 1200 rad	Darker purple-red flower color.
Izetka Köpenicker Bronce Vogue	Germany (Democr.Rep.), 1962	X-rays, 1000-2500 r	Red-bronze color; incurved type; 15 cm flower diameter.
Izetka Filmstar Bronce	Germany (Democr.Rep.), 1966	X-rays, 1000-2500 r	Bronze color; 6-8 flowers per stem; sturdy, dark green foliage.
Izetka Marienhain dunkelrosa	Germany (Democr.Rep.), 1966	X-rays, 1000-2500 r	Dark pink; 20 cm flower diameter; 6-8 flowers per stem; weather-resistant.
Izetka Marienhain cremeweiss	Germany (Democr.Rep.), 1966	X-rays, 1000-2500 r	Cream white; other attributes as above.
Izetka Marienhain hellgelb	Germany (Democr.Rep.), 1966	X-rays, 1000-2500 r	Bright yellow; other attributes as above.
Izetka ~~Herbstgold~~	Germany (Democr.Rep.), 1964	X-rays, 1000-2500 r	Yellow bronze; ray-shaped petals; sturdy stem; 20 cm diameter.
Izetka Köpenicker Barbarossa Goldkissen	Germany (Democr.Rep.), 1962	X-rays, 1000-2500 r	Bordeau-red with bright yellow center; windflower-shaped petals; good stem; slightly susceptible to sprays.

Name	Place, date	Treatment	Improved Attributes
Izetka Köpenicker Barbarossa Rotstern	Germany (Democr.Rep.), 1962	X-rays, 1000-2500 r	Dull-red with yellow center; other attributes as above.
DAHLIA			
Gracieuse	Netherlands, 1966	1-4 krad X-rays to dormant tubers	Violet mauve colored spider-cactus type.
Selection	Netherlands, 1966	1-4 krad X-rays to dormant tubers	Larger blooms and longer stems than its parent, but with the same flower color.
Rotonde	Netherlands, 1966	1-4 krad X-rays to dormant tubers	Vivid color-true pink flowering mutant with larger blooms than its parent.
Ornamental Rays	Netherlands, 1966	1-4 krad X-rays to dormant tubers	Apricot-colored mutant with larger blooms than its parent.
Holland Jubilee	Netherlands, 1967	1-4 krad of X-rays	Light orange throughout; blooms more firm and regular than the original cultivar.
Progression	Netherlands, 1967	1-4 krad of X-rays	Brick red throughout.
Rosy Mist	Netherlands, 1967	1-4 krad of X-rays	Empire rosé throughout.

Name	Place, date	Treatment	Improved Attributes
Autumn Harmony	Netherlands, 1967	1-4 krad of X-rays	Cadmium-orange with scarlet center.
Explosion	Netherlands, 1967	1-4 krad of X-rays	Bloodred with bright yellow center; massive bloom, full at center and having a very fine habit.
The Governor	Netherlands, 1968	2 krad X-rays to dormant tubers	Bloom 18 cm diameter; plant 150 cm tall; deep copper-red flower color.
Dutch Visit	Netherlands, 1968	2 krad of X-rays to dormant tubers	Orange-red flower color; bloom 30 cm diameter (rest of the genotype unchanged).
Temptation	Netherlands, 1968	2 krad of X-rays to dormant tubers	Dark lacquer-red color; giant flower.
STREPTOCARPUS			
Purple Nymph	Netherlands, 1969	X-irradiation, colchicine treatment and combined treatment of leaves	Larger flower and more purple flower color; plant more sturdy; Rest of the genotype unchanged.
Mini Nymph	Netherlands, 1969	X-irradiation of leaves	Compact growth; very free flowering; Rest of genotype unchanged.
Blue Nymph	Netherlands, 1969	X-irradiation of leaves	Light blue flower color; finer plant growth; Rest of genotype unchanged.
Netta Nymph	Netherlands, 1969	X-irradiation of leaves	Dark blue netted and picotee flowers; extremely free flowering.
Cobalt Nymph	Netherlands, 1969	Combined treatment of colchicine and X-irradiation	Compact plant; dark blue flowers; tetraploid.

(FEM)

FRENCH CARDIAC PACEMAKER (2)

Supplementary Key Words: (ENERGY SOURCE / CONVERSION, ELECTRIC / THERMOELECTRIC SYSTEM / MEDICINE / THERAPY / HEART/ PLUTONIUM-238 / FRANCE / PORTABLE)

A cardiac pacemaker (Fig. 1) using ^{238}Pu as the energy source, with thermoelectric conversion, has been developed in France. The source, 0.150 g of plutonium alloy, is doubly encapsulated in platinum-iridium, and the thermoelements, designed for minimum thermal power, are of Bi_2Te_3. The complete power pack — sealed source, thermoelements, insulation, and shielding — is 2.7 cm dia and 5 cm high. The microgenerator is designed to deliver 500 μW at 1 V for 10 years.

The French unit is described in more detail by R. Berger, R. Boucher, and P. Laurens in "^{238}Pu Energy Source for Medical Electric Stimulators" (in French), Bull. Sci. Tech. Info. (in press). U. S. developments in this field and a British unit were described in Isotopes and Radiation Technology 7(2).

(MG)

SOME USES OF ISOTOPES IN METABOLIC STUDIES WITH SOIL MICROORGANISMS (2)

P. E. Stanley and D. J. D. Nicholas*

Supplementary Key Words: (SOIL STUDY / MICROBIOLOGY / BIOCHEMISTRY / NUTRITION / ES NITROGEN-15 / NITROGEN-13 / SULFUR-35 /ES OXYGEN-18 / CARBON-14 / HYDROGEN-3 / IRON-59 / MOLYBDENUM-99 / COBALT-58 / COPPER-64 / PHOSPHORUS-32)

Abstract: The literature (18 references) on the use of isotopes in metabolic studies with soil microorganisms is reviewed.

Stable and radioactive isotopes have proved to be invaluable tools for unraveling metabolic events in biological systems. Indeed, without these tracer materials, the fate of compounds in bacteria, plants, and animals would be extraordinarily difficult to determine. Because of the specificity, sensitivity, and precision of tracer techniques, they are now in routine use in most chemical laboratories, and metabolic studies with soil microorganisms have benefited greatly from the use of tagged compounds. It is not the aim of this review to catalog all isotopes used in biochemical studies with soil microorganisms, but rather to give a few examples of their effective application to specific problems--- ^{15}N and ^{13}N in studies with nitrogen-fixing bacteria; ^{35}S- and ^{18}O-labeled inorganic sulfur compounds to follow oxidation of sulfide and reduction of sulfate; $^{14}CO_2$ for studying the fixation process in chemoautotrophic bacteria; ^{3}H, ^{14}C, and ^{32}P to follow the incorporation of nucleosides and nucleotides into nucleic acids; ^{32}P for studying the esterification of inorganic phosphate into adenosine triphosphate during respiration and ^{99}Mo, ^{59}Fe, and ^{58}Co for identification of these metals in enzymes.

Inorganic Nitrogen Metabolism (3)

The transformation of nitrogen and its compounds in nature is of vital importance to all living things since it maintains a balance and distribution of the element suitable for life on this planet. The nitrogen cycle is equal in importance to the photosynthetic system, which supplies the carbon required by plants and animals. The steps in the nitrogen cycle in nature,[1] mediated primarily by soil microorganisms (Fig. 1), can be conveniently considered as

*Department of Agricultural Biochemistry, Waite Agricultural Research Institute, University of Adelaide, Adelaide, Australia. This article is reprinted, by permission of the publisher, from Atomic Energy in Australia 12(3): 11-20 (July 1969) with some abbreviation.

(a) nitrogen fixation, in which N_2 gas is reduced to ammonia

(b) nitrification, involving oxidation of ammonia to nitrite and then to nitrate

(c) denitrification, in which nitrates are reduced to gaseous products, e.g., NO, N_2O, and N_2

(d) nitrate assimilation, involving its reduction to ammonia prior to incorporation into amino acids, proteins, and other cell constituents.

Nitrogen (4)

One of the basic reactions of the nitrogen cycle is activation of nitrogen gas followed by reduction to ammonia. This is done by various soil microorganisms, including bacteria, some yeasts, and blue-green algae (Table 1). In addition to these free-living forms there are microorganisms which live in association with higher plants. The *Rhizobia* bacteria, which invade the roots of legumes and form nodules that actively fix N_2 gas, are well known. In addition to these there are non-legume plants, e.g., the alder, which also have root nodules, but in this case the endophyte is probably an Actinomycete. Another unusual symbiosis is that of the *Klebsiella* bacteria, which reside in leaf-nodules in the *Psychotria* plants. The bacteria fix N_2 gas and supply the plant with all its nitrogenous diet.

Measurement of Nitrogen Fixation (5). The measurement of the N_2 fixed by microorganisms has posed many problems. Chemical methods lack sensitivity, with the micro-Kjeldahl procedure detecting about 10 μg of total nitrogen only. In 1942 the stable isotope of nitrogen (^{15}N) was first used to follow the fixation of nitrogen gas by bacteria.[2] This method detects a nitrogen gain of 0.01 to 0.02 μg. Values greater than 0.015 atom % ^{15}N excess are regarded as significant. The method is relatively independent of total nitrogen in the sample, provided, of course, that there is sufficient gas to analyze in the mass spectrometer (200 μg of N_2).

The method involves exposure of bacterial cells, or extracts prepared from them, to $^{15}N_2$ gas (33 atom % excess). The gas is prepared from $^{15}NH_4Cl$ by reacting

Table 1. BIOLOGICAL SYSTEMS THAT FIX ATMOSPHERIC NITROGEN

Free-living microorganisms		
Bacteria	Air, no light	Azotobacter vinelandii
	No air, no light	Clostridium pasteurianum
	Air and light	Rhodospirillum rubrum
Yeasts	Air	Rhodotorula
Blue-green algae	Air and light	Nostoc
Microorganisms in association with higher plants		
Bacteria in legumes	Root nodules	Rhizobium
Bacteria in nonlegumes (e.g., alder, Casuarina, Myrica)	Root nodules	Actinomycetes
Bacteria in Rubiaceae (e.g., Psychotria bacteriophila)	Leaf nodules	Klebsiella

it with alkaline hypobromite. It is usual to use a diluent gas, such as helium, to contain the $^{15}N_2$. A suitable gas mixture is 0.2 atm of $^{15}N_2$ and 0.8 atm of He. Flasks containing the appropriate reaction mixture are evacuated rigorously to around 10^{-7} mm Hg before the gas containing the tracer is introduced. The flasks are sealed and then incubated in a reciprocating unit for 60 min at 30°C. The material from each flask is transferred to a micro-Kjeldahl flask and digested in 36 N H_2SO_4 containing HgO catalyst, and the ammonia formed is distilled under alkaline conditions into boric acid. It is titrated against sulfuric acid to determine the total nitrogen. A suitable aliquot of this sample, containing about 200 μg of N_2, is put into one limb of a Rittenberg tube, with alkaline hypobromite in the other. The tube is affixed to the mass spectrometer vacuum system and rigorously evacuated to 10^{-7} mm Hg. The contents of the Rittenberg tube are then mixed to generate N_2 gas from ammonia, and the tube is immersed in liquid nitrogen to freeze out water vapor and nitrogen oxides. The gas is then introduced into an evacuated expansion flask and passed into the mass spectrometer for analysis. Masses 28, 29, and 30, representing ^{14}N-^{14}N, ^{14}N-^{15}N, and ^{15}N-^{15}N, respectively, are measured, and a check is made on mass 32, ^{16}O-^{16}O, to ensure that there is no oxygen. Some results of N_2 fixation studies on Azotobacter

vinelandii using this method are

	Excess ^{15}N, at. %
Whole cells	2.74
Cell extracts	1.18
Particles prepared by centrifuging cell extracts at 144,000 G for 2 hr in an ultracentrifuge	0.88
Supernatant fraction left after centrifuging	0.10

Since the ^{15}N method is time-consuming---some two days are required to complete an experiment from the initial exposure of the sample to the final analysis in the mass spectrometer---a technique using radioactive ^{13}N (1.24-Mev β^+, 10.05 min half-life) was developed.[3] The tracer was produced[4] continuously in a cyclotron by bombarding graphite with a deuteron beam current at 40 μA. The carrier-free gas product was swept from the target area in a stream of pure argon through small-bore polythene tubing to an adjacent laboratory. Since the target material was separated from the high-vacuum system of the cyclotron by a thin aluminum window, the active gas could be collected by blowing a suitable carrier gas (Ar or He) over the target.

Because of the short half-life of ^{13}N, this nuclide must be used adjacent to the cyclotron. In the procedure adopted, the gas was passed through Dreshel bottles containing sulfuric acid and alkaline sodium sulfite to remove any ammonia and NO, respectively, that might be present. The gas was either bled off into the reaction flasks, then into a Dreshel bottle containing water, and finally to the effluent line, or it was diverted to the effluent line before entry into the flasks. The flasks, which were contained in a reciprocating unit at 30°C, were tightly sealed. Some results obtained on Azotobacter vinelandii using this technique, with 10 min exposure to the tracer contained in helium as a carrier, are:

	^{13}N, cps (referred to standard time)
Whole cells	30,600
Cell extracts	24,500
Particles prepared by centrifuging cell extracts at 144,000 G for 2 hr in an ultracentrifuge	20,700
Supernatant fraction left after centrifuging	2,600

Nitrification and Denitrification (5). During the oxidation of ammonia to nitrite by the nitrifying bacterium *Nitrosomonas*[1,5] the reactions

$$NH_4^+ + 1/2\ O_2 \rightarrow NH_2OH + H^+ \quad \Delta F = -0.7 \text{ kcal}$$
$$NH_2OH + O_2 \rightarrow NO_2^- + H_2O + H^+ \quad \Delta F = -83.3 \text{ kcal}$$
$$NH_4^+ + 3/2\ O_2 \rightarrow NO_2^- + H_2O + 2H^+ \quad \Delta F = -84 \text{ kcal}$$

are known to occur.

Another nitrifying bacterium, *Nitrobacter*, oxidizes nitrite to nitrate:

$$NO_2^- + 1/2\ O_2 \rightarrow NO_3^- \quad \Delta F = -17.8 \text{ kcal.}$$

The stable isotope of nitrogen, ^{15}N, has been used to label NH_3, NH_2OH, NO_2^-, and NO_3^- to follow the fate of these in the presence of nitrifying bacteria. By using this technique it was shown that both oxidizing and reducing enzymes are present. In both *Nitrobacter* given $^{15}NO_3^-$ and *Nitrosomonas* given $^{15}NO_2^-$ or $^{15}NH_2OH$, the tracer was found in cell components.

Denitrification in bacteria involves[1] reduction of nitrate to nitrite and thence to gaseous nitrogen compounds, e.g., NO, N_2O, and N_2. By using $^{15}NO_3^-$ and $^{15}NO_2^-$, the conversion of these to the gaseous compounds can be readily followed with whole cells, extracts prepared from them, or purified enzymes of this sequence.

Inorganic Sulfur Metabolism (3)

Sulfur is found in living organisms in several oxidation-reduction states, from the highly oxidized sulfate to the completely reduced thiol groups of amino acids and proteins. There is an eight-electron difference between $SO_4^=$ (+6) and $S^=$ (-2), and the element is usually incorporated into organic form at its lowest

oxidation state. Some autotrophic bacteria, e.g., Thiobacilli,[6] that utilize carbon dioxide as the sole carbon source oxidize reduced forms of sulfur (e.g., sulfide to sulfate) to obtain their energy for growth. Other bacteria, fungi, and green plants reduce sulfate to sulfide prior to its incorporation into amino acids, e.g., cysteine, and then into proteins.

The oxidation and reduction sequences involved together with the energy yield per atom of sulfur are

	−2	0	+2	+4	+6
State of S:	$S^{=}$ ⇄	S ⇄	$S_2O_3^{=}$ ⇄	$S_4O_6^{=}$ ⇄	$SO_4^{=}$
Energy (kcal) during oxidation:	40	15	5	100	

The main features of the sulfur cycle in nature, mediated primarily by microorganisms, are illustrated in Fig. 2.

The radioisotope ^{35}S has been used to follow the reduction of $^{35}SO_4^{=}$, $^{35}SO_3^{=}$, and $^{35}S_2O_3^{=}$ by bacteria, fungi, and plants and the oxidation of $^{35}S^{=}$, $^{35}SO_3^{=}$ and $^{35}S_2O_3^{=}$ by Thiobacilli.

Reduction of Sulfate (5). The reduction of $^{35}SO_4^{=}$ involves[7] its activation by adenosine triphosphate (ATP) by the enzyme ATP-sulfurylase:

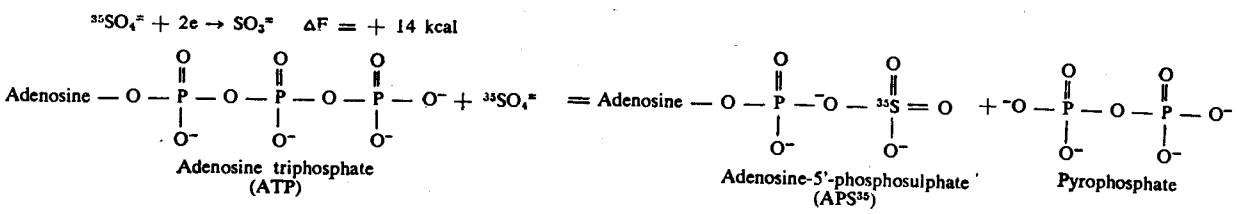

When ^{35}S-labeled sulfate is used, the formation of APS can be followed by separating the nucleotide from the reaction mixture by electrophoresis on Whatman 3MM paper (1.5 kV, 0.1 M sodium citrate, pH 5.0). The nucleotides, located with the aid of an ultraviolet lamp, are cut out and put into vials containing toluene, 2,5-diphenyloxazole, and 1,4-bis-2-(5-phenyoxazolyl)-benzene and counted on the liquid scintillation spectrometer.

A second enzyme phosphorylates APS in the 3' position to give adenosine-3'-phosphate-5'-phosphosulfate (PAPS):

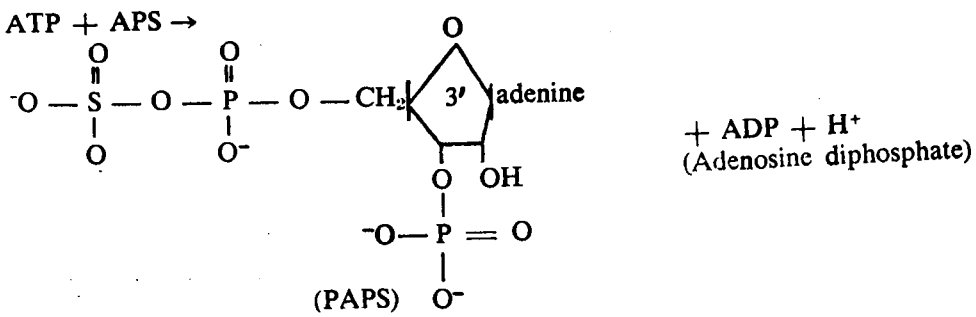

This labeled nucleotide can be separated from yeast by an electrophoresis technique. The tracer method is so sensitive that, although the nucleotide may be detected only as a faint spot under ultraviolet light, significant counts are obtained when the area is cut out and put into a scintillation vial and counted in a liquid scintillation spectrometer.

The reaction in which $^{35}SO_4^{=}$ is used may be summarized as follows:

$$\text{(1)}\quad ATP + {}^{35}SO_4^{=} \rightleftarrows AP^{35}S + PP_i \qquad \Delta F \text{ strongly positive}$$

$$\text{(2)}\quad ATP + AP^{35}S \rightleftarrows PAP^{35}S + ADP \qquad \Delta F \text{ strongly negative}$$

$$\text{(3)}\quad PP_i \rightleftarrows 2P_i \qquad \Delta F \text{ negative}$$

$$2\ ATP + {}^{35}SO_4^{=} \rightleftarrows PAP^{35}S + ADP + 2\ P_i \qquad \Delta F \text{ negative}$$

The further reduction of PAPS to sulfite is mediated by at least two enzymes as well as a protein factor:

$$\text{NADPH} + \text{PAP}^{35}\text{S} \rightarrow \text{NADP}^{+} + \text{PAP} + \text{SO}_3^{=} + 2\text{H}^{+}$$

(NADPH, reduced nicotinamide adenosine dinucleotide phosphate)

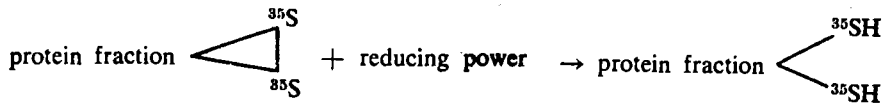

The reduced protein can then reduce disulfides.

The sulfonyl group of PAPS may be transferred to a thiol group of a protein:

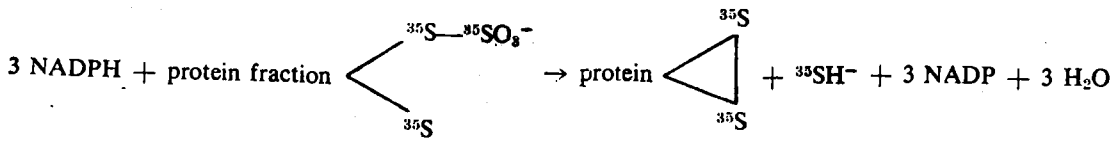

The S-sulfonyl compound is somewhat analogous, in chemical properties, to inorganic thiosulfate. The protein-bound mercapto group serves as a sulfonyl acceptor, and this may explain how inorganic sulfide, thiosulfate, and thionic acids serve as sulfur donors for the protein fraction. The reduction product of PAPS mediated by sulfite reductase from yeast is a bound intermediate, which is nondialyzable and has low electrophoretic mobility. The bound sulfide liberates inorganic ^{35}S sulfite to an acceptor to form a S-sulfonyl derivative. On adding reducing power, the bound sulfite yields labeled sulfite and sulfide. The evidence from tracer experiments suggests that no free intermediates can be detected between sulfite and sulfide.

Oxidation of Sulfide to Sulfate (5). The mechanism of sulfide oxidation to sulfate in bacteria, e.g., Thiobacilli, may involve elemental sulfur, thiosulfates, and polythionates as intermediates.[6] Compounds labeled with ^{35}S have been used to study their fate when added to cells or extracts prepared from them. Electrophoretic techniques similar to those described earlier have been used to separate the labeled products on cellulose paper. The labeled portions of the paper are cut out and put into vials for counting by liquid scintillation techniques. Thus the two sulfur nucleotides (APS and PAPS) have been found to be involved in some of the oxidative processes, and they have been identified by tracer techniques.

Labeled sulfide added to extracts of Thiobacillus concretivorus forms labeled polysulfides that have distinctive spectral properties and are bound to protein. These are then converted to elemental sulfur and to thiosulfates and sulfite and finally to sulfate.

A striking use for the tracer technique is the following of the fate of the two sulfur atoms in thiosulfate when they are oxidized by the bacteria to sulfate:

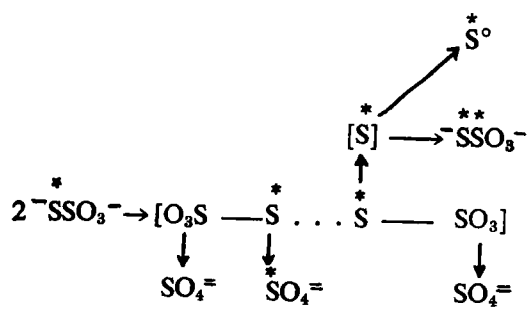

The tracer data suggest that, during thiosulfate oxidation in Thiobacillus neopolitanus, the ratio of sulfate formed from the hexavalent sulfur group to that formed from the divalent is 2:1; the remaining divalent sulfur is converted to elemental sulfur or to the hexavalent sulfur groups of thiosulfate and polythionates. There seems to be a 4-sulfur intermediate in thiosulfate oxidation, with two of the sulfur atoms that arise from the divalent groups of thiosulfate following

different paths to sulfate.

The stable isotope ^{18}O has been used to study the role of phosphate in the oxidation of thiosulfate to sulfate. Thus $S^{18}O_4^{=}$ was formed in this reaction from ^{18}O-labeled phosphate. Sulfite appears to be an intermediate, and labeled adenosine diphosphate (ADP) and adenosine monophosphate are formed:

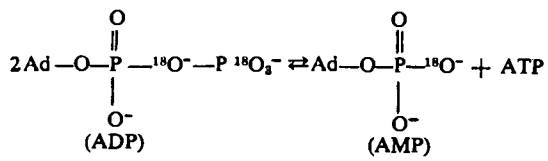

Subsequently ^{18}O is transferred to sulfate:

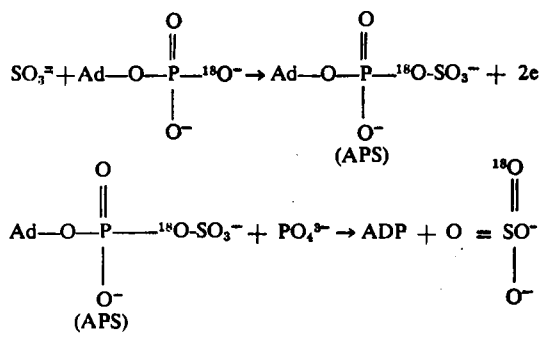

With infinite recycling, the specific activity of sulfate (atom percent excess ^{18}O) would be 25 percent of that of the phosphate added. A value of 22 percent for the sulfate formed by oxidation of thiosulfate was obtained by experiment, indicating that the major part of the sulfate arose from the intermediate containing the P-O-S linkage.

Carbon, Phosphorus, and Tritium Isotopes (4)

An important group of chemoautotrophic soil bacteria, the nitrifiers,[1,5] obtain their energy by oxidizing simple inorganic nitrogen compounds and derive their carbon from CO_2 without the aid of light energy. Other bacteria oxidize sulfide (Thiobacilli) or H_2 gas (Hydrogenomonas).

CO_2 Fixation Studies with ^{14}C (5). The pattern of CO_2 fixation has been studied in several of these bacteria, and it has been established that the reactions involved are very similar to those found in photosynthetic green plants.[8]

In the study of CO_2 fixation in Nitrosomonas (the bacterium that oxidizes NH_4^+ to NO_2^-), two different approaches to the problem have been made with the aid of ^{14}C-labeled materials. In the first, $^{14}CO_2$ incorporation into whole cells has been followed,[9] and in the second the enzymes responsible for the Calvin type cycle reactions have been investigated in cell-free systems using $^{14}CO_2$ and other ^{14}C-labeled intermediates.[10] A source of energy required for these reactions to proceed in whole cells is provided by ATP, which is produced when ammonia is oxidized to nitrite. However, in cell-free preparations, it is essential to add ATP. The use of $^{14}CO_2$ in these studies has been invaluable. After cells had been exposed to the tracer for 1 min, serine was found to be the most heavily labeled compound, followed by phosphopyruvic acid, phosphoglyceric acid, and sugar phosphates, in that order. Doubling the exposure time resulted in a higher labeling in phosphoglyceric acid and sugar phosphates. The labeled compounds produced in this sort of experiment can be separated readily and analyzed by paper chromatography followed by autoradiography. Some typical examples of autoradiograms are given in Fig. 3.

Phosphorylation Studies with ^{32}P (5). It has been established that the system responsible for CO_2 fixation is in the soluble fraction of the cell which is not sedimented in 2 hr of centrifuging of the cell extracts at 144,000 G. The pellet that is sedimented contains the respiratory system of the bacterium and is composed of small lipid-rich particles attached to membrane fragments.[1] The particles contain dehydrogenases and cytochromes, which are concerned with electron transfer and oxidative phosphorylation. The latter process involves the phosphorylation of adenosine diphosphate (ADP) with inorganic orthophosphate to form ATP. It has been shown that ^{32}P as inorganic orthophosphate can be used as a sensitive tool to detect oxidative phosphorylation. In this technique, the pellet fractions of the cells are incubated with unlabeled ADP and ^{32}P orthophosphate, and the nucleotides (ATP and ADP) are adsorbed on activated charcoal disks or separated by

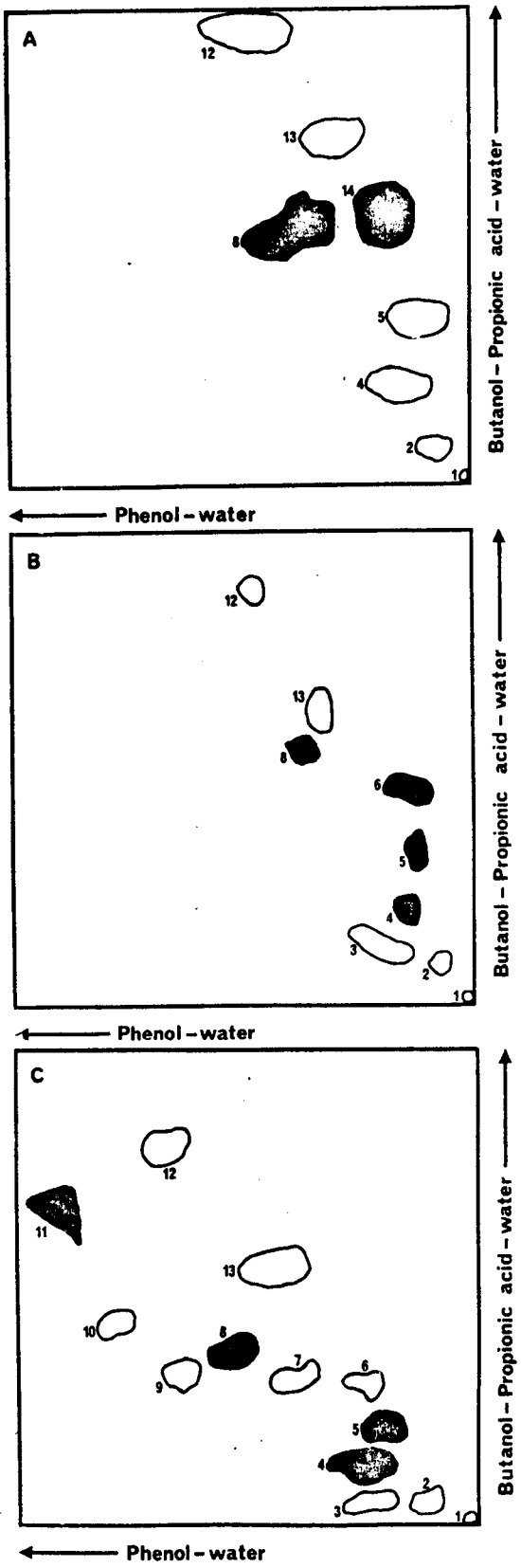

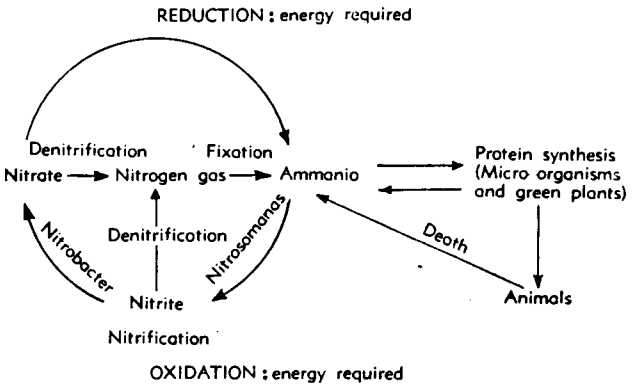

Fig. 1. Principal reactions in the nitrogen cycle in nature.

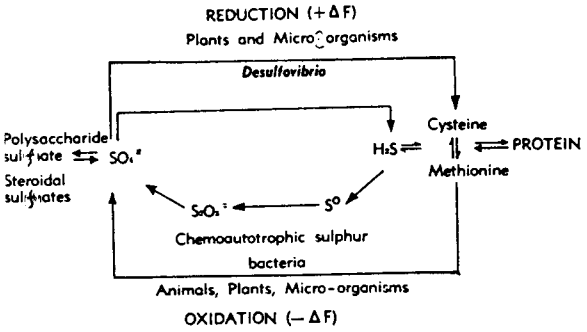

Fig. 2. Sulfur cycle in nature.

Fig. 3. Diagrams of autoradiographs of compounds produced by whole cells of Nitrosomonas *when exposed to* $^{14}CO_2$. *These were separated by paper chromatography. Cells utilising ammonia were exposed to* $Na_2{}^{14}CO_3$ *for (A) 1 min, (B) 2 min, (C) 4 min. Legend: 1, origin; 2, hexose diphosphate; 3, unknown; 4, sugar monophosphates; 5, phosphoglyceric acid; 6, phosphoglycollic acid; 7, unknown; 8, serine; 9, asparagine; 10, glutamine; 11, alanine; 12, succinic acid; 13, glutamic acid; 14, phosphoenolpyruvate. The blackened areas indicate the most heavily labelled compounds.*

paper chromatography and then counted. The amount of ^{32}P labeling in the ATP is a direct measure of oxidative phosphorylation, which can be related to the amount of oxygen utilized by the system. The P/O ratio, a criterion of oxidative phosphorylation, can then be calculated. Respiratory organelles (mitochondria) from animal cells give maximum P/O values of ~3. Particles from the chemoautotrophic bacteria appear to be less efficient since P/O values of ~0.2 are recorded.

Nucleic Acid Metabolism Studies with ^{14}C-, ^{32}P-, and ^{3}H-Labeled Compounds (5). The metabolism of nucleic acids has been studied extensively in microorganisms, but only a few soil types have been used. Thus Ochoa and his colleagues[11,12] have isolated two enzymes from Azotobacter vinelandii which are involved in the synthesis of ribonucleic acid (RNA). The enzyme polynucleotide phosphorylase was the first to be investigated, and, by the use of ADP labeled with ^{32}P and guanosine diphosphate, uridine diphosphate, and cytosine diphosphate, it was shown that this enzyme promoted synthesis of an AGUC* polymer, which, on hydrolysis with a diesterase enzyme from snake venom, gave adenosine-5'-monophosphate as the only labeled nucleotide. This indicated that during synthesis of the polymer the phosphorus ester linkage of the adenosine monophosphate (AMP) had not been broken. Further information was obtained by hydrolysis of the polymer with a spleen phosphodiesterase, which gave the four ^{32}P-labeled 3'-monophosphates. This indicated that polynucleotide phosphorylase had formed ApA, CpA, UpA, and GpA linkages. The true biological function of this enzyme and its importance in RNA metabolism is still obscure, but present evidence suggests that it may not be involved in RNA synthesis. The other enzyme from Azotobacter which appears to be directly involved in RNA synthesis is RNA polymerase, which catalyzes the polymerization of nucleoside triphosphates to RNA with the concomitant release of pyrophosphate. A primer of deoxyribonucleic acid (DNA) is required for this reaction, suggesting that it acts as a biological template. ^{14}C-, ^{3}H-, and ^{32}P-labeled nucleotides have

---

*A = adenylic acid; G = guanylic acid; U = uridylic acid; C = cytidylic acid.

been used for this assay, and it has been possible to follow the incorporation of two bases at the same time by labeling one with ^{3}H and the other with ^{14}C.

A simple technique for labeling the DNA of growing microorganisms has been to allow them to incorporate ^{3}H- or ^{14}C-labeled thymidine. This procedure has proved valuable for autoradiography as measured by electron microscopy and light microscopy[13] as well as for tracing in biochemical investigations. However, before the thymidine can be incorporated into DNA, it must be phosphorylated to thymidine monophosphate by the enzyme thymidine kinase. Recently it was shown that this enzyme is absent from the soil fungus Neurospora crassa.[14] The label from thymidine added to growing cultures was distributed in both DNA and RNA in the fungus, indicating that the thymidine molecule had undergone some modification prior to its incorporation into the nucleic acids. It is therefore important to check whether enzymes are present when doing tracer experiments of this kind.

Transition Metals (3)

Many of the proteins involved in biological oxidation-reduction processes contain transition metals.[15] However, frequently there is only one metal atom per protein molecule, or less than 0.1% metal by weight of the protein molecule. In studies of these proteins there is often only a limited amount of material available, and consequently there is a need for very sensitive methods for detection of the metal. By labeling the biological system with the appropriate radioactive metal, it has been possible to pinpoint and investigate the mode of action of various metallo-proteins. Thus ^{59}Fe has been used in studies of cytochromes and of non-heme iron compounds. The soft x-ray emitter ^{55}Fe, conveniently counted with a liquid scintillation spectrometer, may be used increasingly in the future because of its longer half-life and lower radiation dosage than ^{59}Fe.[16] The short-lived ^{99}Mo has been used in the study of proteins associated with gaseous nitrogen fixation in Azotobacter vinelandii, nitrate reductases, xanthine oxidase, aldehyde oxidase, and dihydroorotic acid oxidase.

Cobalt or vitamin B_{12} is required for nitrogen fixation in Azotobacter vinelandii and for the utilization of nitrates by a variety of microorganisms. Nitrate reductase formation in Azotobacter is dependent on cobalt or vitamin B_{12}. Isotopic ^{58}Co has been of value in this work since only 0.5 μg of cobalt per liter is required for growth.[17]

Metal ions such as these are often required by organisms in only submicrogram quantities, and thus the advantages of tracers are obvious. The limitation, of course, is the short half-lives of some isotopes, e.g., ^{64}Cu, since several days may elapse between growing the organism in the presence of the label and the isolation of the protein containing the metal. In these cases another procedure is of value---the technique of neutron activation. The gamma-emitting radioisotope components may be readily determined quantitatively using scintillation counting or semiconductor detectors followed by multichannel analysis or separation by chromatography.[18] The sensitivity of this method using neutron fluxes of 10^{14} n/cm^2·sec approaches 10^{-9} g. Consequently, it is necessary to have the metallo-proteins as free from contaminating materials as possible.

(MG)

References (3)

1. D.J.D. Nicholas, The Metabolism of Inorganic Nitrogen and its Compounds in Microorganisms, Biol Rev. 38: 530-68 (1963).

2. R. H. Burris, F. J. Epplyng, H. B. Wahlin, and P. W. Wilson, Studies of Biological Nitrogen Fixation with Isotopic Nitrogen, Proc. Soil Sci. Soc. Amer. 7: 258-62 (1942).

3. D.J.D. Nicholas, D. J. Silvester, and J. F. Fowler, Use of Radioactive Nitrogen in Studying Nitrogen Fixation in Bacterial Cells and Their Extracts, Nature 189: 634-6 (1961).

4. A.I.M. Ritchie, The Production of the Radioisotopes ^{11}C, ^{13}N and ^{15}O Using the Deuteron Beam from a 3 MeV Van de Graaff Accelerator, Nucl. Instr. Meth. 64: 181-4 (1968).

5. H. Lees, Biochemistry of Autotrophic Bacteria, Butterworth, London. 1955.

6. P. A. Trudinger, The Metabolism of Inorganic Sulphur Compounds by Thiobacilli, Rev. Pure Appl. Chem. 17: 1-24 (1967).

7. * D.J.D. Nicholas, Biological Sulphate Reduction, Mineralium Deposita 2: 169 (1967).

8. M. Santer and W. Vishniac, CO_2 Incorporation by Extracts of Thiobacillus thioparus, Biochim. Biophys. Acta 18: 157-8 (1955).

9. D.J.D. Nicholas and P. S. Rao, The Incorporation of Labelled CO_2 into Cells and Extracts of Nitrosomonas europaea, Biochim. Biophys. Acta 82: 394-7 (1964).

10. P. S. Rao and D.J.D. Nicholas, Studies on the Incorporation of CO_2 by Cells and Cell-free Extracts of Nitrosomonas europaea, Biochim. Biophys. Acta. 124: 221-32 (1966).

11. M. Grunberg-Manago and S. Ochoa, Enzymatic Synthesis and Breakdown of Polynucleotides; Polynucleotide Phosphorylase, J. Amer. Chem. Soc. 77: 3165-6 (1955).

12. J. S. Krakow and S. Ochoa, Ribonucleic Acid Polymerase of Azotobacter vinelandii, I. Priming by Polyribonucleotides, Proc. Natl. Acad. Sci. U. S. 49: 88-94 (1963).

13. A. W. Rogers, Techniques of Autoradiography, Elsevier, New York, 1967.

14. A. R. Grivell and J. F. Jackson, Thymidine Kinase: Evidence for its Absence from Neurospora crassa and Some Other Micro-organisms, and the Relevance of this to the Specific Labelling of Deoxyribonucleic Acid, J. Gen. Microbiol. 54: 307-17 (1968).

15. D.J.D. Nicholas, Minor Mineral Nutrients, Ann. Rev. Plant Phys. 12: 63-90 (1961).

16. S. E. Graber, L. C. McKee, and R. M. Heyssel, The Use of Benzene Phosphinic Acid to Prepare Mixed Samples of ^{55}Fe and ^{59}Fe for Liquid Scintillation Counting, J. Lab. Clin. Med. 69: 170-6 (1967).

17. D.J.D. Nicholas, M. Kobayashi, and P. W. Wilson, Cobalt Requirement for Inorganic Nitrogen Metabolism in Microorganisms, Proc. Natl. Acad. Sci. U.S. 48: 1537-42 (1962).

18. W. S. Lyon, Guide to Activation Analysis, Van Nostrand, Princeton, New Jersey, 1964.

FRENCH FACILITY FOR FABRICATION OF SEALED RADIOISOTOPIC SOURCES (2)

Supplementary Key Words:
(FACILITY DESCRIPTION/SOURCE PREPARATION/CESIUM-137/STRONTIUM-90/PROMETHIUM-147/RUTHENIUM-106/CERIUM-144/FRANCE)

The radioisotopic-source fabrication facility at Saclay, France, was designed for fabrication of radioactive sources from fission products---particularly ^{137}Cs, ^{90}Sr, ^{147}Pm, ^{106}Ru, and ^{144}Ce. Large amounts of radioactive material can be processed, e.g., 2 to 3 kg of ^{137}Cs, each radionuclide being processed in a separate cell. Equipment is available for a number of different techniques.

The facility, which is an integral part of the Radioelement Building, is divided into three zones:

Zone A---15 leaktight cells where radioactive material is processed

Zone B---a long corridor behind the cells from which the cells are reached; normally not contaminated

Zone C---a room in the front where instrument control panels are located; very unlikely to become contaminated

Air is renewed in the leaktight cells 30 times each hour (60 m^3/hr), the cells being kept at a negative pressure of 30 to 60 mm H_2O. The corridor is also ventilated and is kept at about -5 mm H_2O. The control room has no forced circulation of air, but it can be sealed and connected to the ventilation system if there should be leakage of radioactive material into it.

Ten of the processing cells (2 m high, 0.9 m deep, and 1 or 2 m wide) are constructed of stainless steel frames to which Plexiglas panels are clamped. The joints are sealed with rubber. In two of them a Plexiglas

*Summary of French report CEA-R-3622 (in French) by J. Fradin and C. Hayoun, January 1969 (190 pp.)

panel is fitted with gloves, and a conveyor belt connects these two to the others. Three of the processing cells (2.5 m high) are made of stainless steel with only the front and back panels of Plexiglas. The back panels are hinged, like doors, and the three are connected by a trolley that enters them through airlocks with inflatable joints. The last two cells are entirely of stainless steel except for a Plexiglas port in the front wall.

In Zone B there are two enclosed structures. One is a shielded hood, 1 m high by 1.5 m by 0.90 m. The other, 1 by 1 by 1 m, is not leaktight but is heavily shielded and used for source storage.

Material is transferred into and out of the processing cells on a conveyor belt that operates in a 16-m-long transparent (Lucoflex) tunnel and enters and leaves the cells through remotely controlled airlocks. The polyvinyl belt is reinforced with glass fiber and can support a load of about 5 kg. Objects are carried in smooth-bottom plastic containers to prevent damage to the belt. Source transport containers, because of their weight, are not carried on the belt but are introduced directly into the cells through an airlock. A grounding arrangement prevents buildup of static electricity on the belt. The tunnel is located in the rear passage, at working surface level, 0.9 m from the floor. It is leaktight and is under a slightly higher pressure than the cells so as to prevent its becoming contaminated when a port into a cell is opened. Airlocks at each end of the tunnel are opened and closed manually and are regulated so that they cannot be opened simultaneously. The space above the tunnel is used for storage.

Two liquid-waste systems are provided---one for radioactive effluent and one for material unlikely to be contaminated with radionuclides. Solid contaminated waste is removed to a bin, with built-in shielding, which can be transported without further handling of the waste. All conduits---for

liquids, gases, electric cables, and remote-control transmission rods---are leaktight.

After 6 years of operation, during which the levels of activity processed increased each year, all areas were in satisfactory condition. More than 8000 orders had been filled. The total downtime had been only a few months, the longest being 1 month for replacement of the master-slave manipulators with a better model.

The construction of the facility and the design of the equipment are described in minute detail in the original report.

(MG)

FRENCH X-RAY FLUORESCENCE ANALYZER

Supplementary Key Words: (FRANCE / IRON-55 / MEASUREMENT, COMPOSITION / MEASUREMENT AND CONTROL SYSTEM / INSTRUMENT / SOURCE, ALPHA / POLONIUM-210 / AMERICIUM-241/ CHEMISTRY, ANALYTICAL)

An x-ray-fluorescence analyzer, the ARIEL (Analyseur Radioisotopique d'Elements Legers) has been developed by the Radioisotope Applications Section of the CEA Radioelement Department (France) for determination of light elements. The analyzer is based on the principle of excitation of characteristic x rays of an element by the radiation from a radioactive nuclide and is particularly suitable for determining elements from carbon (Z = 6) to calcium (Z = 20).

The instrument (Fig. 1) includes a radioactive source chamber, a simple and inexpensive proportional counter (with a resolution of 36 to 40% for the aluminum K x ray), and four sample chambers that can be moved into the irradiation position without polluting the detector gas with atmospheric oxygen. The circulating-gas proportional counter is windowless, which offers maximum geometrical excitation and detection yield, with no solid barrier in the path of the low-energy x rays. Electronic equipment is standard, pulse heights being analyzed by a multi- or single-channel analyzer.

Radioisotope source strengths range from 0.1 to 5 mCi. The source used most frequently is ^{55}Fe, with a 2.7-year half-life, which decays by electron capture with emission of the manganese K x-ray lines (about 5.9 keV). Its field of application extends to determination of elements down to about magnesium in the periodic table. Alpha excitation is especially effective for the second-period elements---B, C, N, O, and Ne. At present, the alpha sources being used are ^{210}Po and ^{241}Am,

*Based on P. Martinelli, Radioisotopic Apparatus for X-ray Fluorescence Analysis Determination of Low Atomic Number Elements, translation No. 69-6/B of French report 69-6 PM/JJ (announced September 1969). A portable instrument based on this principle, developed by J. B. Rhodes and co-workers, was described in Isotop. Rad. Technol. 5: 280-4 (1968).

ISOTOPES IN AUSTRALIA, JULY 1, 1968--JUNE 30, 1969 (2)

Supplementary Key Words: (ECONOMICS / REVIEW, TECHNICAL / WORLDWIDE / PRODUCTION, RADIOISOTOPE)

Summarized by Martha Gerrard

The total income from sales of Australian-produced radioisotopes was $236,039 in FY69 (Table 1), more than double that of the previous year (see Isotopes and Radiation Technology 7: 111-3 (1969)), according to the Australian Atomic Energy Commission's annual report for FY69. Demand has increased particularly for medical products, teletherapy ^{60}Co, and ^{192}Ir radiography sources. Total imports were 2281 shipments, twice as many as in the previous year, but a large proportion of the rapidly rising demand for radioisotopes in Australia has been met by production at the Commission's Research Establishment. The Isotope Division has continued to concentrate on production of two general types of radioisotopes---those with a short half-life, and thus difficult to import in the Australasian area, and those with very high activities, such as teletherapy ^{60}Co.

Radioisotope shipments now average more than 400 per month, and more than half of these are very short-lived products, which are delivered to all major centers in Australia. The most extensively used radiopharmaceuticals---those containing ^{99m}Tc with a half-life of 6 hr---are delivered daily to seven Sydney hospitals, and there are plans to extend this service to other cities. At present, cities other than Sydney are supplied with the conventional $^{99}Mo/^{99m}Tc$ generators. Extensive research has been undertaken on production of biologically specific pharmaceuticals containing ^{99m}Tc, and two new products are now in routine production---a new form of ^{99m}Tc-S colloid that is free from the occasional patient sensitivity found in earlier foreign preparations and ^{99m}Tc-labeled macroaggregates of ferrous hydroxide. Production of fission product ^{99}Mo for ^{99m}Tc generators increased, and new equipment now being installed will allow a 10-fold increase in production. The shortest lived radioisotope in regular supply for medical use is 110-min ^{18}F, which is being delivered daily in Sydney, weekly to Adelaide, and

occasionally to Melbourne. A very high specific activity ^{131}I is being produced which shows high protein-labeling efficiency. This ^{131}I is dry-distilled from irradiated presintered TeO_2.

In addition to sales in Australia and New Zealand, one ^{60}Co source was supplied to a Japanese teletherapy-equipment manufacturer. Cobalt-60 sales have equaled about half the total sales for the previous eight years. Iridium-192 radiography sources are widely used for nondestructive testing in Australia, especially in oil- and gas-pipe-line construction, and have also been sold to New Zealand, Singapore, and Papua.

Table 1. PRODUCTION OF RADIOISOTOPES BY THE AAEC, JULY 1,1968--June 30, 1969

Use	Product	Total No. of items	Value
In Australia			
Industrial	^{60}Co and ^{192}Ir radiography sources	226	$35,435
	Other encapsulated sources	8	287
	Miscellaneous	371	4,027
		605	39,749
Research (non-medical)	^{60}Co radiation sources	4	3,142
	Service irradiations	188	3,347
	Miscellaneous	533	7,994
		725	14,483
Medical	Implants	555	1,556
	$^{99}Mo/^{99m}Tc$ generators and solutions	1,382	39,743
	^{18}F and other solutions (^{24}Na, ^{131}I, ^{32}P, etc.)	874	20,703
	Teletherapy sources	5	53,131
		2,816	115,133
Other	Teaching and calibration sources	391	2,812
		4,537	172,177
Exports	^{192}Ir radiography sources	12	2,300
	Medical, implants and solutions	368	1,188
	Teletherapy sources	4	60,147
	Research	11	227
		395	63,862
GRAND TOTAL		4,932	236,039

The irradiation facilities of the Research Establishment are available as a service to outside organizations, and materials irradiated on behalf of commercial organizations included plastic drive belts for record player turntables to prevent stretching in long-term use and certain Australian gemstones to improve their quality. Gamma-sterilization, besides being used for routine sterilization of pharmaceutical products and soil, were also used for heart valves, bone grafts, and other surgical and orthopedic materials. Some types of transistors were irradiated to improve switching time. Australian gamma-irradiation facilities were augmented substantially by the addition of 100 thousand Ci of ^{60}Co at the Westminster Carpets Pty. Ltd. in Dandenong, Victoria.

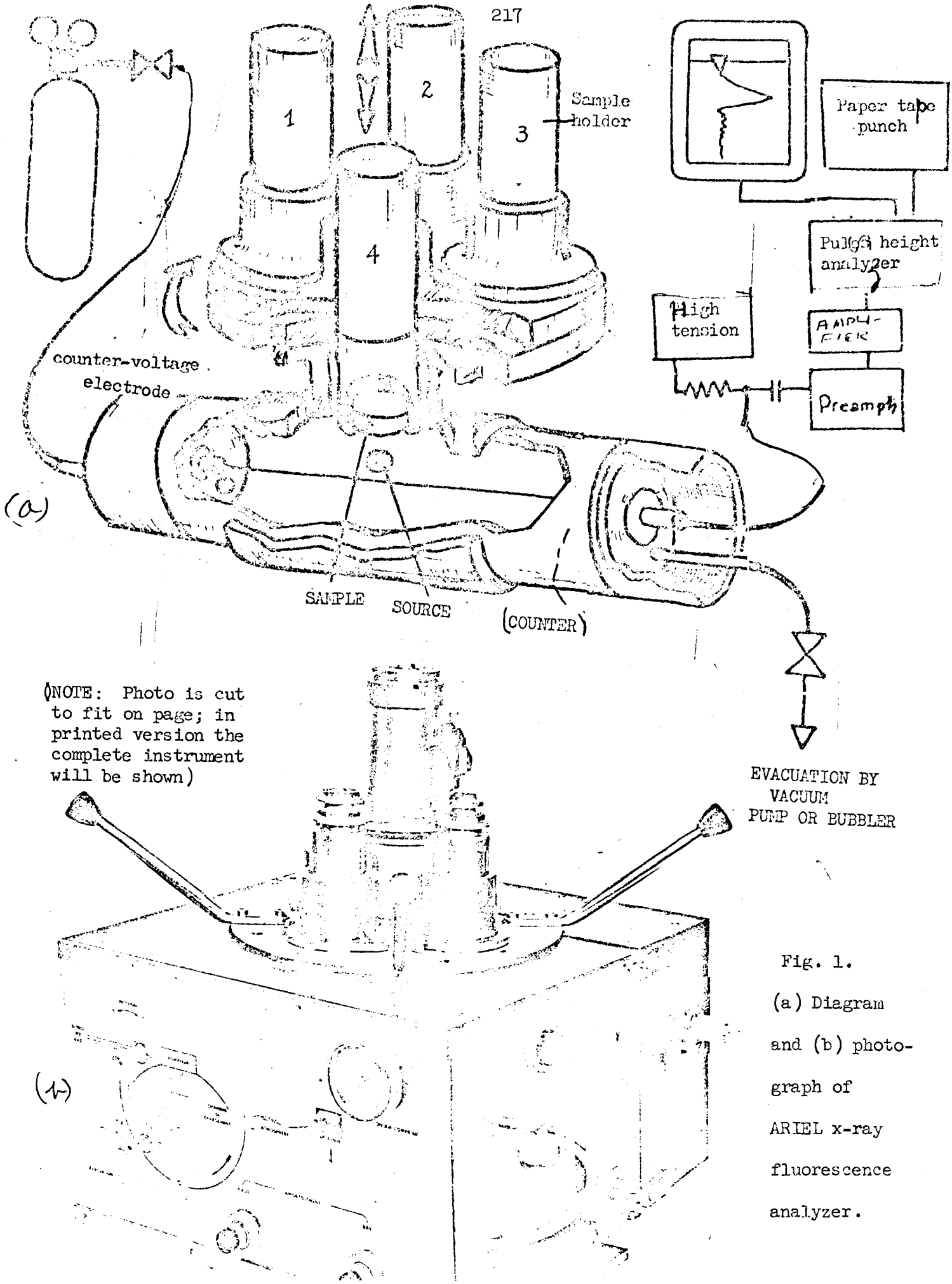

Fig. 1.
(a) Diagram and (b) photograph of ARIEL x-ray fluorescence analyzer.

with half-lives of 138 days and 458 years, respectively. Alpha excitation differs from x-ray excitation in that the alpha-particle cross-section for interaction with electronic layers increases as the atomic number of the excited element decreases.

In use of the instrument, silicon has been determined with a precision of ±0.06% in white cast iron and to better than ±0.8% in soluble alkaline silicates. Sulfur has been determined in hydrocarbons with an absolute error of 500 ppm in the 1 to 5% concentration range and with a standard error of 7 ppm in the 0- to 250-ppm range. Sodium has been determined in glass, and starch in synthetic mixtures of starch plus magnesia. Both liquids and solids (32-mm-dia pellets) have been found to be satisfactory samples, and the instrument can be adapted to continuous monitoring of liquid and gas streams. Filters may be added if desired, and source changing is a simple procedure.

(MG)

DTIE: No abstract

ACTIVATION ANALYSIS WITH CHARGED PARTICLES AND GAMMA PHOTONS*

Supplementary Key Words: (CHEMISTRY, ANALYTICAL / ACTIVATION, CHARGED PARTICLE / ACTIVATION, PHOTON / ACCELERATOR / CARBON-11 / NITROGEN-13 / FLUORINE-18 / OXYGEN / OXYGEN-15/ COMPARISON / BORON / HYDROGEN / HELIUM-3 / FRANCE)

An analytical technique being widely used by the French Atomic Energy establishment at Saclay is activation analysis with charged particles and gamma photons. The activation analysis laboratory at Saclay, one of the best equipped in the world, is connected by pneumatic tubes with two cyclotrons and two accelerators:

Fixed-energy cyclotron: 44-MeV α, 22-MeV d, and 11-MeV p

Variable-energy cyclotron: 3- to 25-MeV p and 3- to 35-MeV ^{3}He

Linear accelerator: bremsstrahlung gamma radiation of maximum energy varying from 25 to 45 MeV

Van de Graaff accelerator: 2 MeV, particularly useful for surface analyses and for measurements of diffusion of light elements

Despite the extensive facilities, the laboratory operates near capacity most of the time because of the usefulness and popularity of the technique.

Many elements can be determined by charged-particle or gamma-photon activation.

The chief application of such analytical methods is to light

---

*Extracts from a paper (in French) by Ch. Engelman (C.E.N., Saclay, France), Bull. Inform. Sci. Tech. No. 140, pp. 65-70 (Sept. 1969) (English: ORNL-tr-2265 by Martha Gerrard).

elements---boron, carbon, nitrogen, oxygen, and fluorine---for which they are specific and which can be determined in concentrations as small as 1 part (by weight) in 10^9. Activation analysis is suitable as a nondestructive testing technique. Further, when necessary, the sample may be scraped to a controlled depth after irradiation to eliminate any risk of contamination. Thus these methods are of considerable interest for analyzing very pure materials.

The charged-particle technique is generally more sensitive than the gamma activation, but the particles must be used with great care. The effect of competitive nuclear reactions (Table 1) is important, and, whereas gamma photons are very penetrating, the path length of charged particles is limited. When gamma activation is used, the extraneous reactions can be eliminated by proper choice of the maximum energy of irradiation (compare the thresholds in Table 1). With charged particles, this discrimination is not so easy. However, there are cases---with oxygen, for example---where the determination can be made without interference by activation with protons of energy less than 9 MeV. This is also true when deuterons are used to determine nitrogen and boron. With regard to other reactions, study of the activation curve usually allows selecting the energy to be used as a function of the degree of purity of the material analyzed.

The sensitivities shown in Table 2 take into account chemical separation of the isotopes. However, numerous nondestructive determinations are also possible with these two types of activation.[1]

Recently, a method for separation of ^{11}C and ^{13}N by oxidizing fusion has been studied.[2] The two elements producing these isotopes can thus be determined with a single irradiation. Oxygen-15 can

Table 1. NUCLEAR REACTIONS USED FOR DETERMINING B, C, N, AND O BY ACTIVATION WITH CHARGED PARTICLES AND GAMMA RADIATION AND CHIEF COMPETING REACTIONS*

Element	Reaction used	Threshold, MeV	Chief competing reactions	Threshold, MeV	Product half-life, min
			Charged-particle Activation		
B	$^{11}B(p,n)^{11}C$	3.02	$^{12}C(p,d)^{11}C$ $^{14}N(p,\alpha)^{11}C$	18 3.12	20.3 20.3
	$^{10}B(d,n)^{11}C$ + $^{11}B(d,2n)^{11}C$	Q >0 5.9	$^{14}N(d,\alpha n)^{11}C$ $^{12}C(d,t)^{11}C$	5.9 14.5	20.3 20.3
C	$^{13}C(p,n)^{13}N$ $^{12}C(p,\gamma)^{13}N$	3.2 Q >0	$^{14}N(p,d)^{13}N$ $^{16}O(p,\alpha)^{13}N$	8.9 5.5	10 10
	$^{12}C(d,n)^{13}N$	0.3	$^{14}N(d,t)^{13}N$ $^{16}O(d,\alpha n)^{13}N$	4.9 8.4	10 10
	$^{12}C(^{3}He,\alpha)^{11}C$	Q >0	$^{10}B(^{3}He,pn)^{11}C$ $^{9}Be(^{3}He,\alpha n)^{11}C$	Q >0 Q >0	20.3 20.3
	$^{12}C(\alpha,\alpha n)^{11}C$	25	$^{9}Be(\alpha,2n)^{11}C$ $^{10}B(\alpha,t)^{11}C$ $^{11}B(\alpha,tn)^{11}C$	18.8 15.6 30.8	20.3 20.3 20.3
N	$^{14}N(p,\alpha)^{11}C$	3.12	$^{11}B(p,n)^{11}C$ $^{12}C(p,d)^{11}C$	3.02 18	20.3 20.3
	$^{14}N(d,n)^{15}O$	Q >0	$^{16}O(d,t)^{15}O$	10.6	2.1
O	$^{18}O(p,n)^{15}F$	2.6	$^{19}F(p,d)^{18}F$	8.6	110
	$^{16}O(^{3}He,p)^{18}F$	Q >0	$^{19}F(^{3}He,\alpha)^{18}F$	Q >0	110
	$^{16}O(\alpha,d)^{18}F$	20.4	$^{19}F(\alpha,\alpha n)^{18}F$ $^{15}N(\alpha,\alpha n)^{18}F$	12.6 8.1	110 110
			Gamma Activation		
C	$^{12}C(\gamma,n)^{11}C$	18.7	$^{14}N(\gamma,\alpha t)^{11}C$ $^{16}O(\gamma,\alpha\alpha n)^{11}C$	22.7 26	20.3 20.3
N	$^{14}N(\gamma,n)^{13}N$	10.5	$^{16}O(\gamma,\alpha t)^{13}N$	25	10
O	$^{16}O(\gamma,n)^{15}O$	15.7	$^{19}F(\gamma,\alpha tn)^{15}O$ $^{20}Ne(\gamma,\alpha\alpha n)^{15}O$	27.4 20.4	2.1 2.1
F	$^{19}F(\gamma,n)^{18}F$	10.5	$^{20}Ne(\gamma,\alpha d)^{18}F$ $^{23}Na(\gamma,\alpha\alpha n)^{18}F$	21.1 21	110 110

*There are other reactions, but they produce the same isotope as that on which the measurement is based.

also be separated in a few minutes with a reducing fusion in a graphite crucible.[3] Thus, nitrogen and carbon can be determined in 20 to 30 min and oxygen in less than 10 min by the gamma-activation technique.

Activation with charged particles and gamma photons has been used for determining the light elements mentioned in high-purity materials---silicon, germanium, iron, nickel, and niobium. Lowest concentrations determinable with the activation technique, as found at Saclay, are shown in Table 3. Other laboratories have also determined concentrations as low as 10^{-9}—e.g., Nozaki et al.[4] for O, C, and N in silicon by ^{3}He and p activation and Ph. Albert et al.[5] for O by ^{3}He and α activation in numerous materials—or 10^{-8}—e.g., Revel et al. for C in pure iron by photon activation.[6]

Among the other analytical applications of charged particles and gamma photons are

1. Analysis of thin layers using low-energy (less than 3 MeV) charged particles. The method is nondestructive and very sensitive. For example, Barrandon and Albert estimate that with tritons one can determine oxygen in amounts of 10^{-3} $\mu g/cm^2$ on metal surfaces.[7] Amsel and Samuel[8] developed a method with which they can detect 10^{-6} μg of ^{18}O.
2. Localization of impurities in a monocrystal by the intermediate effects of channeling of the charged particles in the crystals.[9]
3. Determination of the distribution of an impurity on the surface of a sample by charged-particle activation followed by autoradiography.[10]

Table 2. MINIMUM AMOUNTS OF C, N, O, AND F DETERMINABLE BY ACTIVATION WITH CHARGED PARTICLES AND ALPHA RADIATION WITH A 100-μA BEAM INTENSITY

Element	Wt. Concentration, ppm						
	p 10-15 MeV	d 10-15 MeV	^{3}He 10-20 MeV	α 40 MeV	γ* 30 MeV	γ* 40 MeV	γ* 50 MeV
B	0.001	0.0001			0.05	0.02	0.007
C	0.01	0.001	0.001	0.01	0.04	0.01	0.005
N	0.0005	0.0002			0.02	0.005	0.002
O	0.01		0.001	0.001	0.01	0.002	0.001

* 2.1 min for O, 10 min for N, 2.3 min for C, and 110 min for F.

Table 3. EXAMPLES OF CONCENTRATION DETERMINED BY GAMMA-PHOTON AND CHARGED-PARTICLE ACTIVATION (AT SACLAY)

Material	Impurity determined	Concentration, ppm	Type of activation	Observations
Si	O N B F	0.2 < 0.001 < 0.001 < 0.01	α p p (γ,n)	Nondestructive
Fe	O C N	0.6 0.4 0.04	^{3}He (γ,n) p	Nondestructive
Ge	C N	< 0.05 < 0.05	(γ,n) (γ,n)	
Nb	O C N	0.6 0.6 0.8	^{3}He (γ,n) (γ,n)	Nondestructive
Ta	C N	0.8 1.1	(γ,n) p	

4. Determination of hydrogen in very low concentrations (10^{-6} to 10^{-8}) without interference by triton activation—$^{1}H(t, \gamma)^{4}He$—in which the very-high-energy (about 20 MeV) radiation emitted during the irradiation is measured.

5. Nondestructive determination, using gamma photons of energy lower than 10 MeV, of a dozen or more elements---Se, Br, Sr, Y, Ag, Cd, In, Ba, Hf, W, Ir, Pt, Au, and Hg---by (γ,γ') reactions.[11] The analysis is very simple, is free of interference, and should be very useful for systematic determinations on a number of samples---geological, biological, and others of the same type. It is not a method for determining trace amounts, the concentrations determinable being from 10^{-6} to 10^{-4}, but the simplicity of its use and the speed with which it can be carried out should ensure its use.

(MG)

References

1. C. Engelmann, Use of Gamma Photons and Charged Particles for Determining Very Small Traces of B, C, N, and O (French), Bull. Soc. Chim. France 1967: 2316-20; Activation Analysis with Gamma Photons (French), French Report CEA R-3307 (1967).

2. C. Engelmann, J. Gosset, M. Loeuillet, A. Marschal, P. Ossart, and M. Boissier, Examples of Determinations of Light Elements in Various High-purity Materials by Gamma-photon and Charged-particle Activation, pp. 819-28 of Proc. Internatl. Conf. on Modern Trends in Activation Analysis, Gaithersburg, Md., Oct. 7-11, 1968. (CONF-681003)

3. C. Engelmann, B. Fritz, J. Gosset, P. Graeff, and M. Loeuillet, Determination of Small Amounts of Oxygen and Carbon by Gamma-photon and Alpha-particle Activation (French), pp. 319-50 in Proc. of the 2nd Conf. on Practical Aspects of Activation Analysis with Charged Particles, Liege (Belgium), Sept. 21-22, 1967 (EUR 3896 d.f.e).

4. T. Nozaki, Y. Yatsurugi, N. Akiyama, and I. Imai, Charged-particle Activation Analysis of C, N, and O in Semiconductor Silicon, Proc. Internatl. Conf. on Modern Trends in Activation Analysis, Gaithersburg, Md., Oct. 7-11, 1968, pp. 842-6 (CONF-681003).

5. J.-L. Debrun, J. N. Barrandon, and P. Albert, Contribution to Activation Analysis by Charged Particles, Determination of C and O in Pure Metals, Possibilities of S Determination, Ibid. pp. 774-84.

6. G. Revel, T. Chaudron, J.-L. Debrun, and P. Albert, Determination of C in High-purity Iron by Irradiation in Photons, Ibid. pp. 838-41.

7. J. N. Barrandon and P. Albert, Determination of Oxygen in Surface Layers by Irradiation with 3-MeV Tritons (French), Rev. Phys. Appl. 3: 111-5 (June 1968)(Paper by same name in English in CONF-681003, pp. 794-801).

8. G. Amsel and D. Samuel, Microanalysis of the Stable Isotopes of Oxygen by Means of Nuclear Reactions, Anal. Chem. 39: 1689-98 (1967).

9. L. Eriksson, J. A. Davies, J. Denhartog, H. J. Matzke, and J. L. Whitton, Proton and Alpha-particle Channeling as a Tool for Locating Foreign Atoms in Crystals, Canad. Nucl. Technol. 5(6): 40-3 (1966).

10. D. M. Holm, J. A. Basmajian, and W. M. Sanders, Observation of the Microscopic Distribution of O and C in Metals by ^{3}He Activation, USAEC rpt LA-3515, Los Alamos Scientific Laboratory (1966).

11. C. Engelmann and D. Y. Jerome, Application of Nuclear Isomerism to Nondestructive Determination of Some Elements by Activation with 4- to 8-MeV Photons (French), pp. 119-45 in Proc. 2nd Conf. on Practical Aspects of Activation Analysis with Charged Particles, Liege (Belgium), Sept. 21-22, 1967 (EUR-3896 d.f.e).

VIII. MISCELLANEOUS

AVAILABILITY OF ISOTOPES AND SERVICES (2)

ORNL Enriched Stable Isotope Inventory (3)

Recent additions to the Oak Ridge National Laboratory (ORNL) enriched-stable-isotope saleable inventory include the following:

Isotope	Purity, %	Amount Available, g
^{33}S	90.8	0.08
^{64}Ni	97.9	5.00
^{78}Se	86.8	7.14
^{82}Se	56.5	6.27
^{108}Cd	82.3	0.47
^{113}Cd	96.3	18.56
^{114}Cd	99.2	80.39
^{161}Dy	95.9	10.00
^{163}Dy	93.1	10.58
^{164}Dy	95.7	24.02

In addition to the regular inventory, ORNL maintains a rather large research-materials collection; for further information regarding availability from this inventory, write Isotopes Sales Department, Oak Ridge National Laboratory, P. O. Box X, Bldg. 3037, Oak Ridge, Tenn. 37830.

(PSB)

Patent Search Capability (3)

The Isotopes Information Center has now added extensive computer search capability to its routine information retrieval service through the purchase of IFI/Plenum Data Corporation's Uniterm Index Magnetic Tape, with AEC funds. More than 11 thousand keywords (or terms) have been used to index the more than 200 thousand chemical and chemically related U. S. patents from 1950 through 1968. Searches are being made using one or more of the keywords, assignees, Patent Office class and code numbers, or patent numbers. Search terms can be assigned an arbitrary weight value for identification of the term or terms used to retrieve a particular patent. (This is particularly helpful when one or a few terms may be used to recover a patent when many search terms are involved.) ¶ In a typical printout of a search for patents relevant to a given question, the following information, in addition to the patent number is given: the total weight which indicates the specific terms used in the recovery of that patent; the accession number; the assignee; the Chemical Abstracts reference number; the patent title, together with a short designation of the major chemical company assignees, e.g., Carbide, Dow, Du Pont; and the total number of patents that satisfied the request. This patent search program has been extremely valuable in the recovery of patents for a process radiation review now in preparation at the Isotopes Information Center.

R. E. Greene

Industry Expands Cobalt-60 Irradiation Facilities (3)

A report by the Atomic Industrial Forum on nuclear industry developments in 1969 indicates that commercial irradiation facilities have expanded extremely rapidly. The acceptance of radiation-hardened wood plastics (primarily flooring products), the use of radiation in production of chemicals and plastics, and radiation sterilization of medical products have been so widespread that some feared a temporary shortage of ^{60}Co, according to Carl Goldstein, who prepared the news release for AIF.

Radioisotope Instrument for In-Vitro Diagnosis (3)

Picker Nuclear (1275 Mamaroneck Ave., White Plains, N. Y. 10605) is marketing its Hemolitre, a precision instrument for use with isotopes in in-vitro measurements of blood volume and for such tests as the Schilling for primary pernicious anemia (^{57}Co-labeled vitamin B_{12}), thyroid tests using ^{125}I or ^{131}I, plasma disappearance, red cell survival, fat metabolism, iron-binding capacity, and body-water measurement. The use of in-vitro tests eliminates exposure of a patient to radiation.

U. S. NBS Reference Standards (3)

Supplementary Key Words: /(MERCURY-203 / YTTRIUM-88 / COBALT-60 / SODIUM-22 / NICKEL-63 / PLUTONIUM-238)

Four gamma-ray point-source standards have recently been issued by the U. S. National Bureau of Standards especially for the calibration of Ge(Li) detectors. The standards, which consist of the radionuclide between two 0.006-cm-thick layers of polyester tape, are:

^{203}Hg (SRM 4208, $83), 6 x 10^5 dis/sec in June 1969

^{88}Y (SRM 4209, $77), 4 x 10^5 dis/sec in May 1969

^{60}Co (SRM 4210, $86), 2 x 10^6 dis/sec in April 1969

^{22}Na (SRM 4996-B, $79), 3 x 10^5 dis/sec in April 1969

Three additional gamma-ray point-source standards have been reissued:

^{203}Hg (SRM 4995-C, $83), 1.5 x 10^5 dis/sec in June 1969

^{88}Y (SRM 4998-E, $77), 1 x 10^5 dis/sec in May 1969

^{22}Na (SRM 4991-C, $79), 6 x 10^4 dis/sec in April 1969

Two other standards issued are:

^{63}Ni (SRM 4226, $148.50), 1.5 x 10^6 dis/sec per gram of solution on May 27, 1968. It is supplied as a glass ampule containing 4.1 g of a solution, in 1 M HCl, of 84 mg of carrier plus ^{63}Ni.

^{238}Pu (SRM 4906, $158), 1.4 x 10^3 to 3.4 x 10^4 dis/sec at time of calibration. These are practically weightless alpha-particle sources of ^{238}Pu electroplated on a 0.010-cm-thick foil cemented to a 2.5-cm-dia, 0.16-cm-thick monel disk.

The standards may be purchased from the Office of Standard Reference Materials, Rm. B308, Chemistry Bldg., National Bureau of Standards, Washington, D. C. 20234.

New Laboratory-scale Cesium-137 Irradiator Design (3)

Radiation Machinery Corporation is offering a series of gamma irradiators — the Gammators — which provide exposure rates up to 150 thousand rads/hr, with even higher rates available in custom installations. The gamma radiation source is ^{137}Cs as the chloride.

The Gammator B (Fig. 1), which provides an irradiation rate of 35 thousand R/hr, contains a 400-Ci source. Material is irradiated in a plastic container, which is placed on a turntable and rotated 180° to position it in front of the source for full exposure. For lower dose rates, the turntable is rotated less than 180°.

The radioisotopic source is completely contained in two concentric stainless steel capsules, which are locked in a third cavity by a shielding plug.

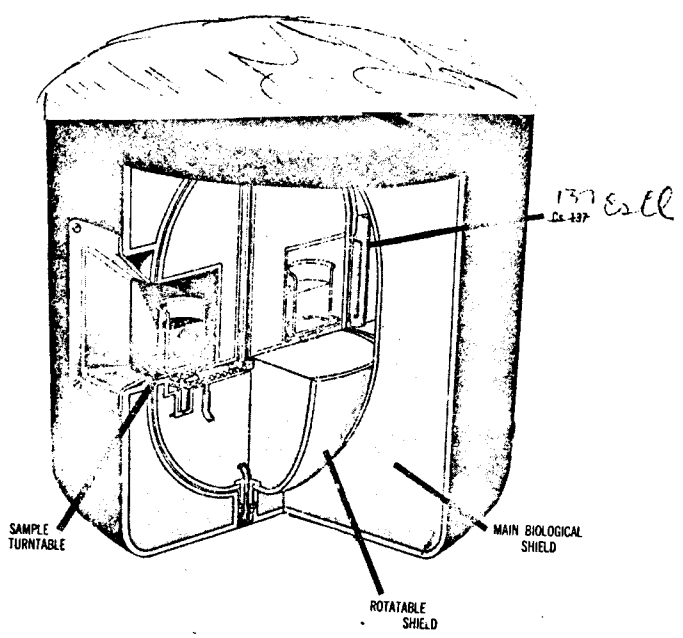

Fig. 1. Gammator B — Radiation Machinery's ^{137}Cs 35 thousand R/hr gamma irradiator.

Standard Luminescence Regulations (3)

The British Standards Institution (2 Park St., London, W.1) has issued a booklet (6 pages of text) stating requirements for instruments having hands and/or dials bearing radioactive luminous substances. It is entitled "Specifications for Radioluminous Time Measurement Instruments. Part 1. Instruments Bearing Radioactive Luminous Materials" (BS 4333: Part 1: 1968, 6 shillings). Radionuclides permitted are ^{3}H, ^{147}Pm, and ^{226}Ra. Permissible levels of these nuclides, casing requirements, luminosity requirements, and certain test methods are included.

International Nutronics Has Sterilization Contract (3)

Supplementary Key Words: (SOURCE, GAMMA / POLLUTION / INDUSTRY, PHARMACEUTICAL / INDUSTRY / PILOT PLANT SCALE)

International Nutronics Inc. (IN), at its new Palo Alto, Calif., plant will terminally sterilize for Smith Kline Instruments sealed plastic tubes of distilled water in an enzyme blood-test kit. IN is the only commercial isotopic gamma irradiator on the West Coast and is considering expanding into gamma irradiation of enzymes for the detergents market. It has installed a pilot plant for sewage processing for the town of Menlo Park, Calif.

Cobalt-60 Source Available on Loan (3)

The Atomic Energy Commission will lend high-specific-activity ^{60}Co heat sources to industrial firms, research organizations, and educational institutions for research and development use. Further information concerning the program is available from the Manager, Savannah River Operations Office, U. S. Atomic Energy Commission, P. O. Box A, Aiken, S. C. 29801.

Portable Accelerator for Activation Analysis (3)

A 30-lb unit for use in activation analysis has been developed at Texas A&M University in cooperation with Sandia Corp. A 14-MeV generator with a 28-V power supply provides a flux of about 10^8 n/cm^2·sec. The instrument is designed for analysis to a few tenths of a per cent of major elements in the moon and other solar bodies.

Gamma-Irradiation Facility Expansion (3)

Radiation Technology, Inc., has reported that its Canadian subsidiary, Radiation Technology (Canada) Ltd., plans to double its St. Hilaire, Quebec, radiation processing capability. Full-scale production is expected to begin by June 1970. The new installation will use a processing approach that will permit annual production of over 350,000 square feet of Radwood wood plastic composite floor tiles along with over 100,000 square feet of Radstone concrete polymer decorative tiles. The pilot facility is to serve as a basis for a major production facility to be constructed later this year in order to meet growing demand. The U. S. and Canadian market for wood parquet flooring has been estimated at about $40 million per year, while the terrazzo market has been placed at over $400 million. Tests have been made on another product expected to be produced in quantity, Radcrete, for structural items such as building blocks and architectural facade, water and drainage pipe, and railroad ties. The properties most important for use in railroad ties include a factor of 4 increase in tensile strength, a doubling of the modulus of elasticity, and virtual inertness to atmospheric and brine corrosion coupled with an extreme resistance to freeze-thaw damage.

Radiation Technology is also beginning to sell a new research facility aimed at university and industrial research markets. The Radtank will be provided by the Company in a number of interchangeable configurations at prices ranging from $25 thousand to more than $100 thousand and will use ^{60}Co or ^{137}Cs as the source.

In the 9-month period from mid 1969 to early 1970, the number of RTI's customers for enzyme sanitization and for disposable medical product sterilization each increased 66%; for cosmetic product sterilization, 300%; and for miscellaneous service irradiations, which often becomes the big business of tomorrow, 60%. The increase in sterilization is related to recent Food and Drug

Administration's and industry's comments on the potential hazards of residual ethylene oxide gas now used for sterilization, as well as to the deeper sterilization possible with radiation and the feasibility of sterilizing in the final package.

A spin-off from the RTI permanent press process, which may have been given added glamour due to the wash results, is the development of a permanent wave and/or hair-straightening formula based on existing process technology. RTI is seeking suitable partners to exploit this development.

RTI has also developed a new family of products which they expect to market nationally early in 1970. These Radfast products include polymer fasteners, rivet devices, and joiners made from crosslinked thermoplastic, semicrystalline materials, such as polyethylene, which are given the so-called "memory" effect by either electron or gamma irradiation. The material of these devices is similar to the shrinkable tubing or shrink-film products. Another interesting process developed is one for selectively or totally removing dye colors from polyester or acetate materials (Chameleon Process). This process is being marketed by Scientific Textiles Systems, Inc.

AEC ACTIVITIES (2)

Argonne Uses Activation Analysis to Analyze Fish for Pollution Control (3)

As part of the nation's overall pollution-control problem, the AEC's Argonne National Laboratory is analyzing fish from various regions of the Great Lakes, using thermal neutron activation analysis, to determine the types and amounts of metals present. The metals may come from industrial waste or from chemical fungicides and pesticides used in agriculture. The analyses are conducted on ashed fish, and the data are processed by a computer to give an overall picture of the dispersion and types of metallic-element pollution.

Cobalt-60 Made Available for Food Preservation Research (3)

Fifty thousand Ci of ^{60}Co is being loaned by the USAEC to the Univ. of Mass. for use in basic and applied research on the preservation and public health aspects of food and food products. Studies will be conducted on the foods themselves, their individual components, and organisms that cause spoilage.

Californium-252 Progress (3)

Supplementary Key Words: (PLANT SCALE / BIBLIOGRAPHY / MEDICINE / THERAPY / RADIOGRAPHY / INDUSTRY / INDUSTRY, MINING)

The second issue of this publication [see Isotopes and Radiation Technology 7(4) p. for announcement of 1st issue], January 1970, includes papers on the use of ^{252}Cf in radiotherapy, neutron radiography, natural resources exploitation, and process control and news items related to ^{252}Cf development. The publication may be obtained from Manager, Savannah River Operations Office, USAEC, P. O. Box A, Aiken, S. C. 29801.

Californium-252 Used Needles to be Loaned to Universities (3)

In addition to loans already made to commercial and research institutes (Isotopes and Radiation Technology 7: 245,), the AEC is making available to educational institutions on an extended loan basis small quantities of ^{252}Cf. The material to be loaned is currently at The M. D. Anderson Hospital and Tumor Institute, Brookhaven National Laboratory, and the Hospital of the University of Pennsylvania, where its effectiveness, as an implanted source, for cancer therapy is being studied.

The needles will be returned around 1971, when they will contain less than 1 μg of californium, whose recovery would be uneconomic.

Because of the potential benefit to educational institutions and the AEC's californium market evaluation program, these sources will be made available under an existing loan program offering a wide variety of nuclear material to universities. The opportunity will thus be provided for students to become familiar with the handling, features, and applications of this isotope. In addition, other uses of the material may be found.

In addition to loaned californium sources, direct sale of 1 μg or less of the isotope may be arranged with Oak Ridge National Laboratory for $100 per 0.1 μg.

The Savannah River Operations Office will coordinate the loan of the needles. Representatives of universities interested in the program should write to the Manager, Savannah River Operations Office, P. O. Box "A," Aiken, South Carolina 29801, or to the Director, Division of Nuclear Education and Training, U. S. Atomic Energy Commission, Washington, D. C. 20545.

Integrated Waste Management — Water Recovery System for Pollution Control (3)

An integrated waste management — water recovery system using radioisotopes for thermal energy is the subject of a joint AEC/NASA and AF study expected to last about 3 years and to cost about $750 thousand for the total government effort. About 2 years of work will probably be done with General Electric Co. for building the system, with another year of testing. The leading radioisotope so far is ^{238}Pu, whose decay heat would be used to incinerate waste. Water would be reprocessed, along with human and solid wastes (food containers, etc.).

Energy Source Development (3)

Hittman Associates, Inc., has been given two multiyear contracts from the AEC for over $750 thousand to pursue development of materials for nuclear and aerospace applications. One material under development would provide protection from reentry heating for radioisotope fuel capsules used in aerospace nuclear power systems; the other program is on development of materials and devices to vent helium, which is generated in decay of alpha-emitting radioisotope fuels.

TRW, Inc., has a $9.4 million contract from AEC for final design and development of a radioisotopic thermoelectric generator (RTG) for use on the Navy's advanced Transit navigation satellite. The power supply will be a ^{238}Pu fuel capsule and a thermoelectric energy-conversion system. The Transit RTG (Fig. 1) will be designed for a 5-year operating life, with 30 W of power, and will weigh less than 30 lb.

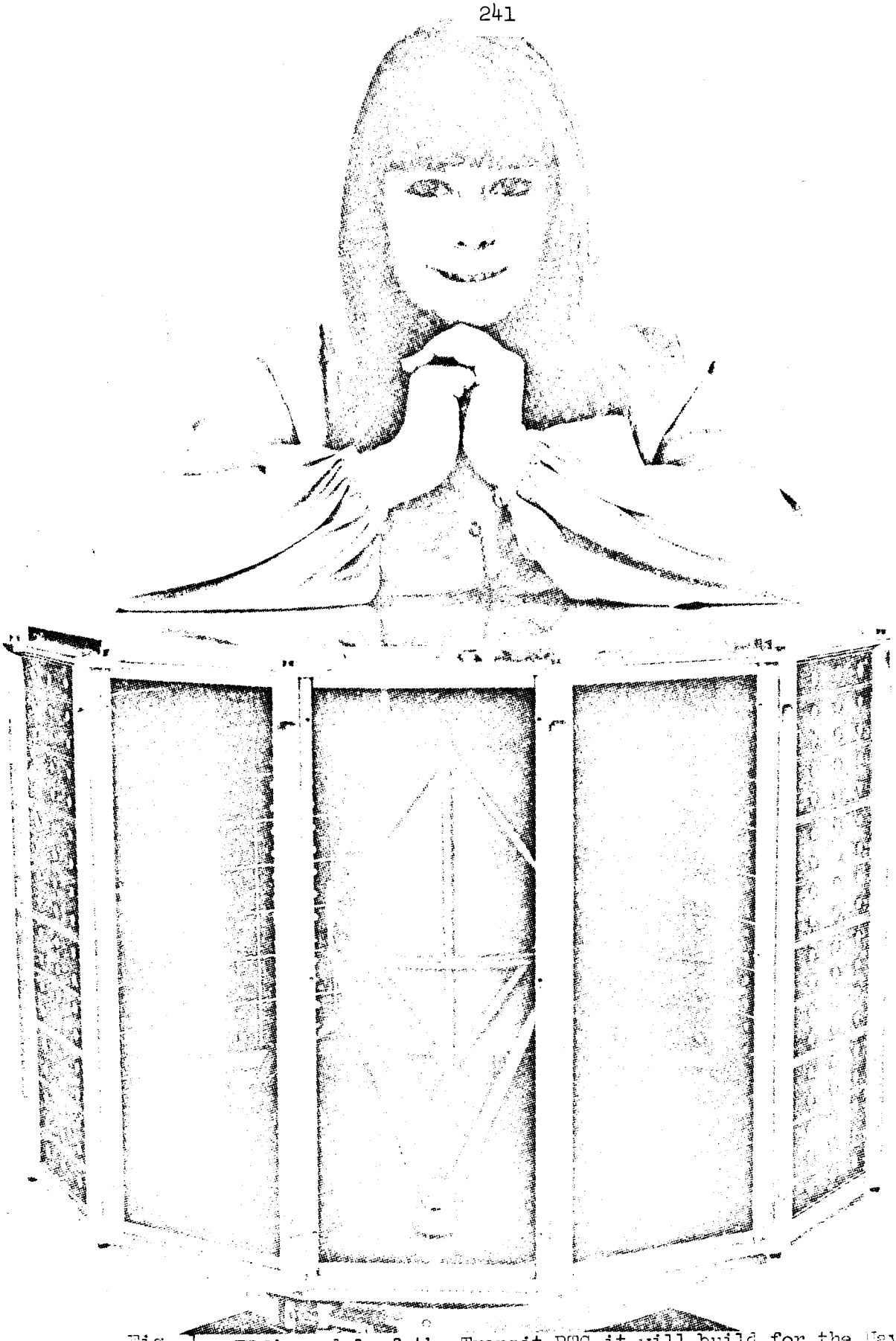

Fig. 1. TRW's model of the Transit RTG it will build for the Navy's navigation satellite.

GENERAL (2)

New Neutron Radiographs Technique for Locating Hydrogen in Low Concentrations (3)

Hydrogen concentrations as low as 150 ppm (Fig. 1) can be pinpointed with Hysen Service, a new nondestructive testing technique offered by General Electric Company's Irradiation Processing Operation in Pleasanton, Calif. A Hysengraph increases nondestructive hydrogen inspection capabilities by a factor of 10 to 20 over that of neutron radiography records, where about 1500 ppm had been the smallest concentration that could be inspected.

Hysen Service, in which a reactor neutron beam passes through the object examined and forms an image of it on a photographic plate, can be particularly valuable in work with such materials as titanium, zirconium, and steel. For instance, airframe welds and zirconium-clad reactor fuel can be inspected for hydriding and hydrogen embrittlement with a Hysengraph.

Additional information may be obtained from Hysengraph, General Electric Company, Irradiation Processing Operation, Pleasanton, California 94566 or telephone (415) 862-2111, ext. 4224.

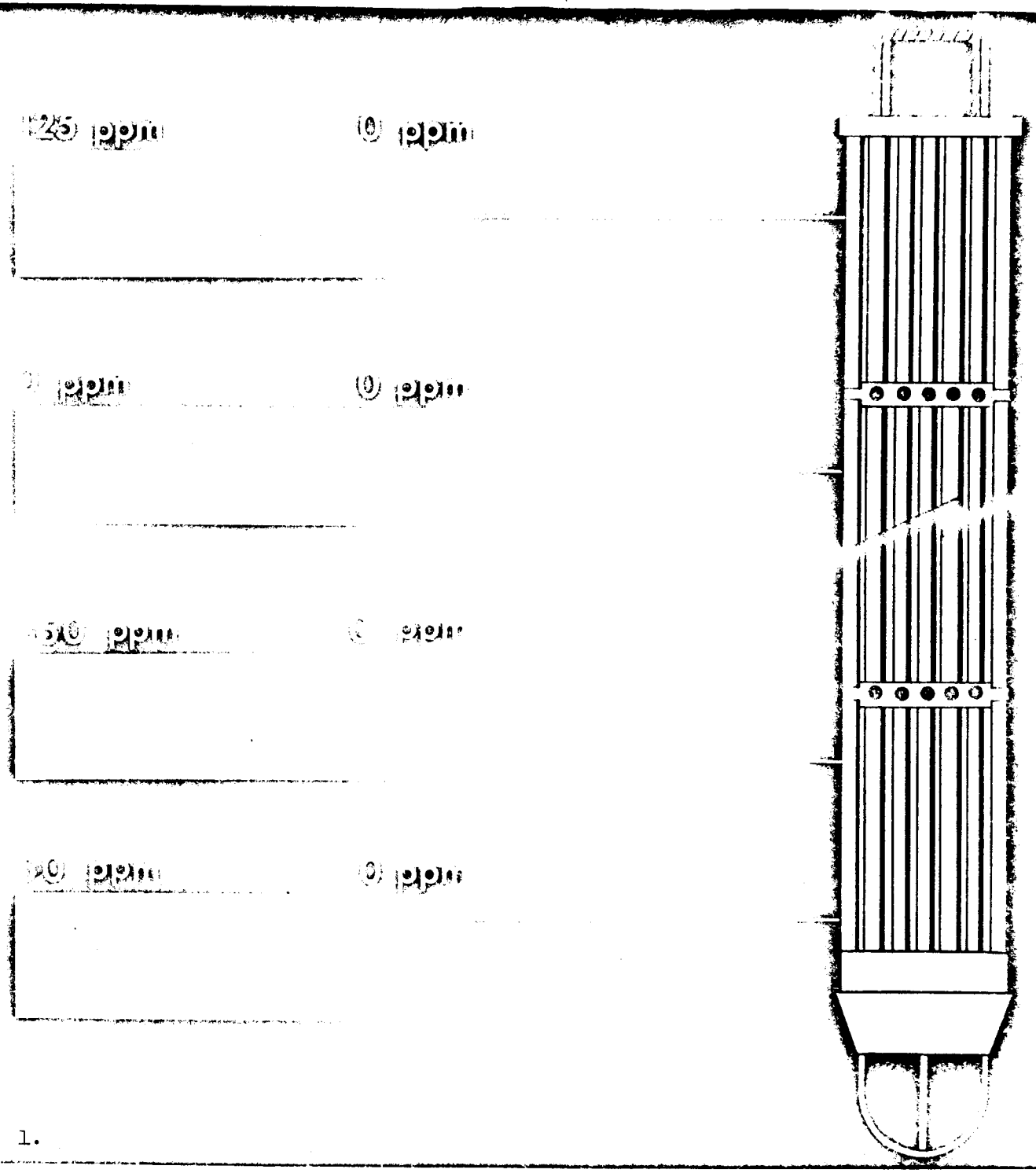

Fig. 1.

Cosmetic Sterilization (3)

Purchase by Gamma Process Company, Inc., of Dunn Laboratories, a cosmetics manufacturer, will bring together the know-how of the two companies to produce bacteria-free cosmetic products. Sidney Oscar Dunn, President of the Laboratories, became concerned about FDA findings of bacterial contamination in cosmetics — 61 contaminated products in 250 tested. Dunn stated, "There is only one solution to this problem and that is to sterilize the finished product, after it has been sealed. Since sterilization by conventional means is impractical, the only possible way to sterilize the finished product is by radiation processing."

Energy Source for Highway Deicing (3)

Dynatherm Corp., Cockeysville, Md., has received a $96 thousand contract from the Federal Highway Administration for a comparison of the use of nuclear wastes and other heat sources for deicing bridges, ramps, and pavements. The project is expected to take about a year. Dynatherm specializes in heat transfer systems and is working in new technologies, such as the "heat pipe." Its president, Milton Prayda, and other company officials are from the former Martin Co.'s Nuclear Division.

Isotopic Analysis in Space (3)

NASA has awarded a $37 thousand contract to the University of California, Berkeley, for isotopic analysis of lunar samples.

European Sterilization Plants (3)

Atomic Energy of Canada Limited (AECL) has orders for two irradiation plants in Europe — one from Gammaster for a facility in Utrecht, Netherlands, and one from Johnson & Johnson for a plant in Stockholm, Sweden.

Brown Engineering Studying (n,γ) Reaction Theory (3)

Brown Engineering Co. has a continuation contract with the Marshall Space Flight Center for calculations of secondary gamma production by neutron interactions with materials.

Strontium-90 Acoustical Beacon for Ocean Installations (3)

Nuclear Materials & Equipment Corp., subsidiary of Atlantic Richfield Co., has developed a long-lived underwater acoustical beacon. The beacon is powered by ^{90}Sr and is designed to operate for up to 10 years without refueling at depths down to 15,000 ft, delivering an ultrasonic signal with a peak acoustic output of 2 W about every 2 sec. One of the $10 thousand devices has been delivered to the Navy and a second is to be anchored off the Washington coast at Project Sea Use (Cobb Seamount), a joint government-industry underwater research program.

Fundamentals of Radiation Protection, H. F. Henry, 485 + xvii pp. $17.50. New York, Sept. 1969.

Supplementary Key Words: (TEXTBOOK / EFFECT OF RADIATION ON MATERIAL / EFFECT OF MATERIAL ON RADIATION / DOSIMETRY / PHYSICAL PROPERTY / SAFETY / ISOTOPE USE / ISOTOPE DETECTION AND DETERMINATION / STATISTICS / ISOTOPE USER / HISTORY)

Fundamentals of Radiation Protection has been written to introduce the reader not only to the technical aspects of radiation protection (including its physical and biological bases) but also to describe briefly the principles that will guide the implementation of a radiation-protection program and to help the novice understand some of the implications of actions taken with respect to matters of national and international concern as they are presented in the public press and elsewhere. The author hopes that the treatise will help to place in proper perspective the actual impact of radiation on society—somewhere between promises, on the one hand, of a utopian tomorrow, and a danger so great, on the other hand, that it menaces any kind of tomorrow. Hopefully the reader will be able to make his own reasonable evaluations of the future, which is clouded by apparently contradictory data and suffers from the voicing of the opinions and recommendations of the whole gamut of political, sociological, economic, and other self-interest groups.

The contents of the text include a short introduction that comprises background material—history of radioactivity, dangers of radioactive material, current radiation protection activities, etc. This is followed by two sections that deal primarily with physical data: Atomic Structure and Nuclear Transformations, Radioactivity and Fission. Next come discussions of General Effects of Radiation on Cells, Physical Aspects of Radiation Exposure, Background and Other Radiation Exposures, Effects of Acute Total-Body Radiation Exposures, Long-Term Somatic Effects of Radiation, and Genetic Effects of Radiation.

The next several units cover Permissible Exposure Limits, Internal-Exposure Evaluation, Radiation Detection and Measurement, Principles of Personnel Monitor-

ing, Principles of Environmental Monitoring, and Fundamentals of Radiation Intensity Reduction.

The last chapters include four that discuss Guides to Practical Protective Measures, Offsite Monitoring and Surveys, Plant Emergencies, and Administration (i.e., basic aspects of a health-physics program, general activities of a health-physics group, records, etc.), and two entitled Nuclear Weapons and Benefits of Radiation. Of particular note in connection with the discussion of radiation effects is the statement (and warning) in Chapter 9 that "It is thus a not illogical position that the conclusions, frequently so glibly stated, which imply that all radiation is harmful to the individual or to the human species simply have not been validated.----------Extrapolation of data can give results, but this does not mean that a fact has necessarily been discovered. Failure or refusal to consider data that disagree with some predetermined concept is a cardinal sin." As a matter of fact, in an earlier chapter the author indicates that he does not agree with the widely stated conclusion that all radiation is genetically bad, suggesting that extrapolation of experimental data from high-dose effects to (unsupported by data) low-dose effects cannot be conclusive.

All in all, Fundamentals of Radiation Protection contains a tremendous wealth of detailed information and appears to have accomplished what the author set out to do. Dr. Henry, incidentally, is presently Chairman of the Department of Physics, DePauw University, Greencastle, Indiana, but for more than 10 years was head of the Radiation Hazards and Safety Department at the USAEC's Oak Ridge Gaseous Diffusion Plant, operated by Union Carbide Corp.

(PSB)

(DTIE: Please get Supplementary Key Words from following page.)

Handbook of Radioactive Nuclides Published by Chemical Rubber Company. 960 + xlll pp. $27.50; The Chemical Rubber Company, Cleveland, Ohio.

An addition to CRC's long list of "Handbooks" is the recently published Handbook of Radioactive Nuclides, edited by Yen Wang, Director, Department of Radiology, Homestead (Pa.) Hospital. The 960-page compendium includes ten chapters, starting out with Nuclear Data and finishing with a section on Reference Data, which cover such items as signs and symbols of interest in radiation and radioactivity, fundamental constants, the standard man, radioactive decay, a comparison of lead and concrete as gamma-ray absorbers, and decay curves for radioactive materials.

In between are units on Essential Physics Data (radiation interaction with matter and statistical aspects of nuclear counting); Nuclear Instrumentation (radiation detectors and equipment, radioisotope counting and calibration, personnel monitoring, whole-body counter systems, radioisotope cameras, etc.); Radiation Dosimetry (radiation absorbed-dose calculations for biologically distributed nuclides, radiation doses from administered radionuclides, and dose from ingestion or inhalation of soluble radionuclides); Biochemistry (standards of activity, isotope dilution analysis, sample preparation for liquid scintillation counting, and synthesis, stability, and storage of labeled compounds); Radionuclides for Medical Application (measurement of cerebral blood flow, brain scanning, endocrine studies, investigation of cardiovascular disease, respiratory studies, gastroenterologic diagnosis, studies of the osseous and cartilagenous systems, and techniques as applied to the hematopoietic and genitourinary systems); Radionuclides for Industrial Applications (characteristic effects of radionuclides, availability of isotope, and applications in numerous industries, agriculture, and aerospace); Radiation Protection and Regulations (basic units of radiation measurement, radiation protection guides, methods for estimating exposure, facilities required for various types of operating personnel dosimetry,

transportation of radioactive materials, radioactive-waste disposal, and emergency planning and procedures. Also included are 10 appendixes dealing with procedural items); Radiation Injury and its Management.

The writing and editing were done by more than 30 acknowledged experts in the various areas covered. It is hard to imagine anything that has been left out of this comprehensive document.

(PSB)

Supplementary Key Words: (DATA COMPILATION / MEDICINE / INDUSTRY / REVIEW, TECHNICAL / BIBLIOGRAPHY / ISOTOPE USE / ISOTOPE USER / MATERIAL PROPERTY / SAFETY / IDC PUBLICATION/ EFFECT OF RADIATION ON MATERIAL / EFFECT OF MATERIAL ON RADIATION / DOSIMETRY)

[redacted]

INTERNAL DISTRIBUTION

1- 4. P. S. Baker
5. F. R. Bruce
6. J. H. Gillette
7. D. S. Napolitan (K-25)
8-10. C. P. Keim
11. H. G. MacPherson
12. A. F. Rupp
13. M. J. Skinner
14. Laboratory Records (RC)
15. Central Research Library

EXTERNAL DISTRIBUTION

16. Roland A. Anderson, Asst. General Counsel for Patents, USAEC, Washington, D. C. 20545.
17-22. H. B. Atkinson, DTI, USAEC, Washington, D. C. 20545
23. Battelle Memorial Institute, Pacific Northwest Laboratory, P. O. Box 999, Richland, Washington 99352.
24. B. F. Boardman, Idaho Nuclear Corp., P. O. Box 1845, Idaho Falls, Idaho 83401.
25-27. E. T. Bond, DTIE, AEC, P. O. Box 62, Oak Ridge, Tenn. 37830.
28. R. W. Dayton, Battelle Memorial Institute, 505 King Ave., Columbus, Ohio 43201.
29. W. E. Dreeszen, Ames Laboratory, Iowa State University, Ames, Iowa 50010.
30-31. Alvin Glassner, Argonne National Laboratory, 9700 S. Cass Ave., Argonne, Ill. 60440.
32-33. John C. Dempsey, DID, USAEC, Washington, D. C. 20545.
34. John A. Koch, Savannah River Patent Group, SROO, USAEC, P. O. Box A, Aiken, S. C. 29801.
35. Stephen Lawroski, Argonne National Laboratory, 9700 S. Cass Ave., Argonne, Ill. 60440.
36. George H. Lee, Chicago Patent Group, Chicago Operations Office, USAEC, 9800 S. Cass Ave., Argonne, Ill. 60439.
37. Los Alamos Scientific Laboratory, P. O. Box 1663, Los Alamos, N.M. 87544.
38. S. W. O'Rear, SRL, E. I. Du Pont de Nemours, Inc., Aiken, S. C. 29801.
39. H. S. Potter, New York Patent Group, Brookhaven National Laboratory, Upton, L.I., New York 11973.
40. Dennis Puleston, Head, Information Div., Brookhaven National Laboratory, Upton, L.I., New York 11973.
41. F. A. Robertson, California Patent Group, USAEC, San Francisco Operations Office, Livermore, Calif. 94550.
42. H. M. Roth, USAEC, ORO.
43. C. G. Stevenson, Manager, Technical Information, Battelle-Northwest, P. O. Box 999, Richland, Washington 99352.
44. D. S. Zachry, Jr., USAEC, ORO.

[redacted]